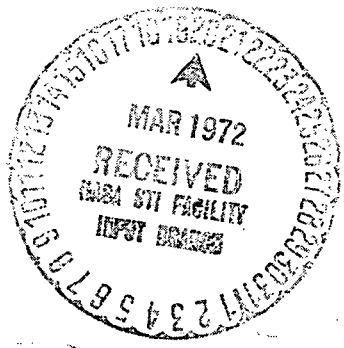

SD 71-770

THE EFFECTS OF RADIATION ON THE OUTER PLANETS GRAND TOUR

JET PROPULSION LABORATORY
CALIFORNIA INSTITUTE OF TECHNOLOGY
PASADENA, CALIFORNIA

SD 71-770

THE EFFECTS OF RADIATION ON THE OUTER PLANETS GRAND TOUR

November 1971

Contract 953295

Prepared For

Jet Propulsion Laboratory
California Institute of Technology

Space Division
North American Rockwell

Page Intentionally Left Blank

FOREWORD

This handbook was prepared to accompany the oral presentation on the effects of radiation on an Outer Planets Grand Tour (OPGT) spacecraft. The presentation and handbook were prepared for Jet Propulsion Laboratory (JPL) of California Institute of Technology, under JPL Contract 953295, by the OPGT Program of Space Division (SD) of North American Rockwell Corporation (NR).

Mr. T. R. Gavin of JPL was Technical Monitor of the contract. Dr. J. B. Weddell of NR-SD was Presentation Coordinator and technical editor of this handbook. The following NR personnel prepared and conducted the presentation: Dr. J. W. Haffner (SD); Dr. G. Gigas (Atomics International Division); J. E. Bell, D. T. Butcher, Dr. R. A. Kjar, C. T. Kleiner, and G. C. Messenger (Autonetics Division).

CONTENTS

INTRODUCTION

This handbook is designed to accompany an oral presentation on the effects of radiation on the Outer Planets Grand Tour (OPGT). The presentation begins with a summary of OPGT radiation environments expected from natural sources and the radioisotope thermoelectric generators. Basic radiation effects and processes are reviewed, and ionization and displacement effects are examined in some detail. Before turning to electronics, the presentation summarizes the effects of radiation on miscellaneous spacecraft materials and devices. The annealing and hardening (i.e., the radiation-resistant design) of electronics are then described. Special emphasis is placed on microcircuits because of their importance and newness. Mathematical modeling of circuits affected by radiation and radiation environmental testing are discussed. The presentation concludes with a review of means of evaluating the performance and correcting failures of irradiated devices.

The presentation is limited to forms and levels of radiation expected in OPGT missions, and to materials and devices appropriate to an OPGT spacecraft. Other information, for example the effects of transient bursts of radiation, is presented only where necessary to indicate the limits of its applicability to OPGT. It is hoped that this handbook will prove useful both as an introduction to further study in this area and as a working tool for the spacecraft/instrument engineer.

ERRATA

THE EFFECTS OF RADIATION ON THE OUTER PLANETS GRAND TOUR

Page 19. The gamma ray dose rate from 0.5 to 1.0 MeV is 2.4×10^{-2} rad/hr.

Page 27. The unit of carrier mobility is

$$\frac{\text{cm/sec}}{\text{volt/cm}}$$

The mobility degradation coefficient is $d\mu/d\phi$.

Page 29. In the second line of the illustration, replace E_d by E_a.

Page 35. The horizontal axis should be labelled: Angle from Initial Direction (Degrees).

Page 36. In the third column from the left, the proton energy is 20 MeV.

Page 41. The potential $\phi_b = E_F - E_i$. The letter i above ϕ_b should be deleted. The first sentence should read "...electrons are attracted from the silicon..."

Page 46. Commercial MOS should be added to the list of vulnerable devices.

Page 47. The list of slightly vulnerable devices includes hardened MOS but not commercial MOS.

Pages 84, 95. The curve for neutrons is a plot of the reciprocal of the normalized damage constant ($1/k_n$) vs. energy. The curves for protons and electrons on page 95 are correct.

Page 100. k_p refers to P-channel, k_n to N-channel.

Page 113. The last line in the table applies to commercial MOS FETs. The assessments for hardened MOS FETs are:

Neutrons, 1
Protons, 5
Electrons, 3
Gamma rays, 1

Page 121. The ordinate is $k_p \dot{\gamma}^{\Delta}$.

Page 133. The current is 200 μamp.

Pages 139, 140. The solid points are for neutron irradiation following the electron irradiation. The open points are for proton irradiation following the electrons.

Page 142. The ordinate is h_{FE}, not per cent gain.

Page 147. The number of device hours is 200,000. "Epitaxial" should be read for "expitaxial."

Page 148. "Evacuated" should be read for "evaculated."

Page 149. These data apply to P-channel MOS.

Page 157. Uni-junction transistors should be listed as minority carrier parts.

Page 158. In the figure for the Ebers-Moll model, the term $\alpha_n I_{ce}$ should be $\alpha_n I_{ef}$. The term $\alpha_I I_{ce}$ should be $\alpha_n I_{cf}$.

Page 160. I_{EF} and I_{CF} should be replaced by I_E and I_C, respectively.

Page 186. The formulas on the graph should read as in the text.

Page 189. Delete "101PD111050" which is a drawing identification number.

Page 193. The curves should be labelled with the gate voltage: 10, 8, 6, and 4 volts (from top to bottom).

Page 197. The terminal at the top of the digram should be labelled: $-V_{DD}$.

Page 198. The output voltage (ordinate scale) is negative.

Page 205. The lowest curve should be labelled: Clean Cr Doped Oxide.

Page 213. The currents are given in micro-amperes.

Page 227. The current flowing through R_L should be labelled I_C.

Page 235. The curve labelled 0547 is for both 2N2907 and 2N3265 transistors, but not for the 0547.

Page 239. The base of the transistor at the upper left is connected to the collector of the transistor to its lower right, and also to resistor above that collector. There is no connection to the emitter of the transistor below the V_{CC} terminal.

Page 248. The curve labelled 0547 is for both 2N2907 and 2N3265 transistors, but not for the 0547.

Page 256. The ordinate should bear the additional label: Range (g/cm^2).

Page 264. In the left-hand box under "Electrical Testing," F/T should be replaced by FT.

Page 278. The unit of cross section is 10^{-30} cm^2 (i.e., microbarn).

Page 302. The title should read: Image Dissector Star Tracker Damage.

Pages 305–308. These pages have been deleted.

Pages 309, 310. N and P designate N-channel (i.e., negatively-charged majority carrier channel) and P-channel (i.e., positively-charged majority carrier channel), respectively, either alone or in combinations such as NMOS, PMOS, NPN, etc.

NATURAL SPACE RADIATION

- SOLAR FLARES
- SOLAR WIND
- GALACTIC COSMIC RAYS
- TRAPPED PARTICLES

RADIOISOTOPE RADIATION

- GAMMA RAYS
- NEUTRONS

OPGT RADIATION ENVIRONMENT

The Outer Planets Grand Tour missions involve both natural and artificial sources of nuclear radiation which can affect the performance of spacecraft components and materials. Natural sources include solar flares (high-energy protons and other charged particles), the solar wind (low-energy charged particles), cosmic rays originating outside the solar system (very energetic charged particles), and high-energy protons and electrons trapped in the magnetic fields of Jupiter and possibly other planets.

The OPGT spacecraft will derive its electric power from radioisotope thermoelectric generators. These emit gamma rays and energetic neutrons throughout the mission.

NEUTRON	NO CHARGE MASS ~ 1 AMU (1.6×10^{-24} G) ATTENUATED EXPONENTIALLY MEAN FREE PATH OF FISSION NEUTRONS ~ 10 CM IN WATER
PROTON	+e CHARGE (1.6×10^{-19} COULOMB) MASS ~ 1 AMU DEFINITE RANGE 30 MeV — 1 G/CM^2 100 MeV — 10 G/CM^2
ELECTRON	-e CHARGE MASS ~ 1/1836 AMU DEFINITE RANGE 1.7 MeV — 1 G/CM^2 19 MeV — 10 G/CM^2
PHOTON (X & γ RAYS)	NO CHARGE RELATIVISTIC MASS = ENERGY/(LIGHT VELOCITY)^2 ATTENUATED EXPONENTIALLY

PARTICLE TYPES AND CHARACTERISTICS

The nuclear radiation environments for outer planet missions will consist of fluxes of four distinct types of particles. Protons and electrons constitute the bulk of the solar, galactic, and Van Allen radiations while the Pu^{238} radioisotope thermoelectric generators emit neutrons and gamma rays. These particles differ in charge and mass, which determines the mechanisms by which they interact in matter. Uncharged radiations (neutrons and photons) are attenuated exponentially because they can be absorbed in one or a few atomic collisions. Charged radiations (protons and electrons) exhibit fairly definite ranges in matter because it usually takes thousands of atomic collisions to stop them. Neutrons can produce gamma rays, and electrons can produce X-rays as secondary radiations. The attenuation of electrons and protons is relatively insensitive to material composition, being primarily a function of mass per unit area (g/cm^2) of the shield. Neutrons are best attenuated by hydrogenous material (e.g., H_2O, LiH) while photons are best attenuated by materials of high atomic number (e.g., W, Pb, U).

FLUX	$\frac{\text{PARTICLES}}{\text{AREA X TIME}}$
FLUENCE	$\frac{\text{PARTICLES}}{\text{AREA}}$
DOSE	MEASUREMENT OF EFFECT OF GIVEN FLUENCE
ROENTGEN (R)	1 ESU/CM^3 = 83 ERGS/GRAM
RAD	100 ERGS/GRAM
REP	SAME PHYSICAL EFFECT AS 1 R OF X-RAYS
REM	SAME BIOLOGICAL EFFECT AS 1 R OF X-RAYS
DOSE RATE	$\frac{\text{DOSE}}{\text{TIME}}$

FLUX AND DOSE UNITS

Nuclear radiation is quantified by the particle type (neutron, electron, proton, or photon), particle energy, and flux (particles per unit area per unit time). The usual unit of flux is particles/cm^2-sec. The time integral of particle flux is the fluence, or particles/unit area (usually particles/cm^2).

In order to compare radiation effects produced by different types, energies, or fluxes of particles, dose units are used. The dose measures the energy deposited by the radiation in the absorber, or its physical or biological effect on the absorber. The effects of a given dose depend on the kind of particle and the nature of the absorber. The basic dose unit is the rad (100 ergs/gm). Older units were the roentgen (83.8 ergs/g in air) for ionizing radiations and the roentgen-equivalent-physical (rep) (93 ergs/g) for neutrons in tissue. Radiation effects in tissue are measured in rem (roentgen-equivalent-man) which is related to the rad by a multiplicative factor (the quality factor or the RBE). For doses in silicon the symbol (Si) is often placed after the dose unit rad.

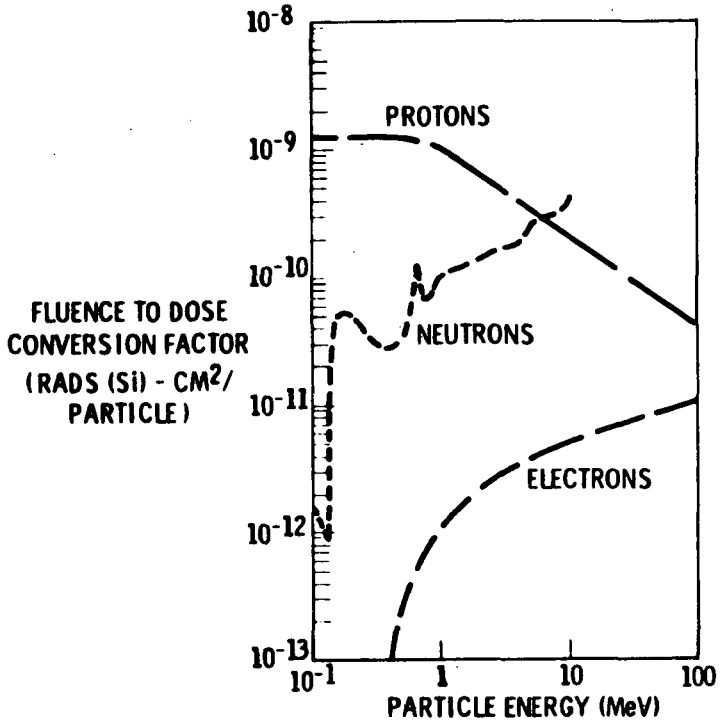

FLUENCE TO DISPLACEMENT DOSE (Si) CONVERSION FACTORS

In many situations, it is desirable or necessary to compare radiation damage produced by particles of one type and energy with that produced by particles of a different type and/or energy. This is often difficult to do since some radiations (e.g., electrons, gamma rays) produce chiefly ionization effects while others (e.g., neutrons) produce chiefly displacement effects. However, where steady state (as contrasted to transient) radiation effects are of interest (as is the case for an OPGT spacecraft) it is possible to obtain semi-quantitative fluence-to-dose conversion functions. These curves are approximate, as n-type and p-type silicon react differently to the same type and energy of particle. This graph presents proton, electron, and neutron displacement dose vs. fluence for silicon or aluminum.

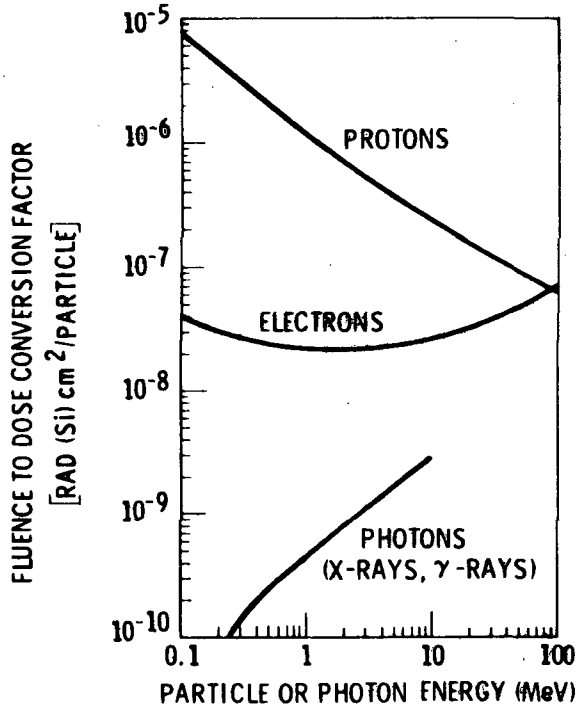

FLUENCE TO IONIZING DOSE (Si) CONVERSION FACTORS

These curves show the relationship between proton, electron, and gamma ray fluences and the corresponding ionizing doses in silicon. The curves are based on radiative plus collisional ionization energy loss rates in silicon.

SOLAR WIND	MOSTLY PROTONS AND ELECTRONS LOW ENERGY (<10 keV) AFFECTS $\lesssim$ 1 MICRON BENEATH SURFACES FLUX $\lesssim 10^9/R^2$ PROTONS/CM^2-SEC CONTINUOUS FLOW
SOLAR FLARE PARTICLES	90% PROTONS, 10% ALPHAS, FEW ELECTRONS ENERGY 1 MeV TO >100 MeV PENETRATING FLUX $\lesssim 10^5/R^2$ PROTONS/CM^2-SEC GRAND TOUR DOSES SMALL 1977 LAUNCH ~50 RADS 1979 LAUNCH ~200 RADS

SOLAR PARTICLE RADIATION

The sun emits a semi-continuous flux of low energy (< 10 keV) protons (called the solar wind) and sporadically a flux of high energy (MeV) protons (90%) and alpha particles (10%) associated with large solar flares. Both types of radiation are assumed to have enough low-energy electrons to be electrically neutral and to decrease inversely with the square of the sun-spacecraft distance.

The solar wind particles are stopped in the first micron of most materials and affect spacecraft surfaces only. Many solar flare particles can penetrate >1 gm/cm^2 and are preferentially emitted when the sun is active (1968-1972, 1979-1983, etc.) Because the OPGT spacecraft will be going away from the sun, these particles will produce doses of only ~50 rads (1977 launch) to ~200 rads (1979 launch).

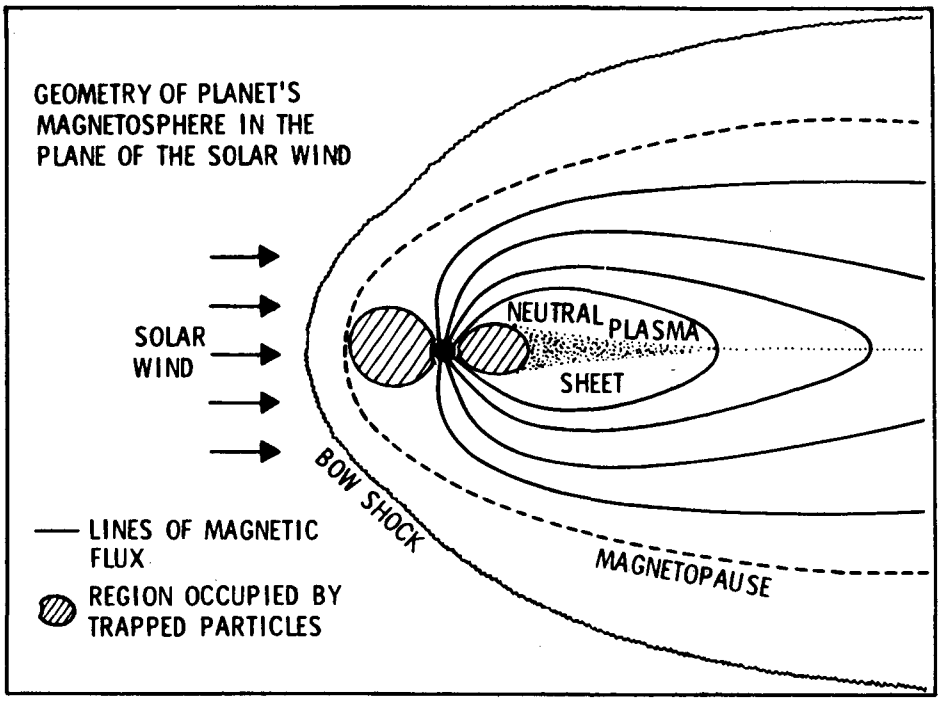

JUPITER'S MAGNETOSPHERE

A planet with a significant magnetic field (e. g., earth, Jupiter) is surrounded by a teardrop-shaped cavity called the magnetosphere. Within the magnetosphere the planetary magnetic field is dominant and the solar magnetic field is excluded. The figure shows a cross-section of the earth's magnetosphere. The earth has an approximate dipole field of 0.3 gauss at the equator, producing a magnetosphere extending ~10 R_e in the sunward direction, ~60 R_e wide, and having a tail of ~200 R_e. (R_e = radius of the earth). Jupiter's magnetic field at its visible surface is believed to be an order of magnitude larger than that of the earth. Consequently, Jupiter's magnetosphere is expected to have sunward radius of ~50 R_J, a width of ~ 250 R_J, and a tail length of ~1000 R_J. Since Jupiter's radius (R_J) is ~ 11 times that of earth, the Jovian magnetosphere (including its Van Allen belts) is ~ 50 times larger than that of earth.

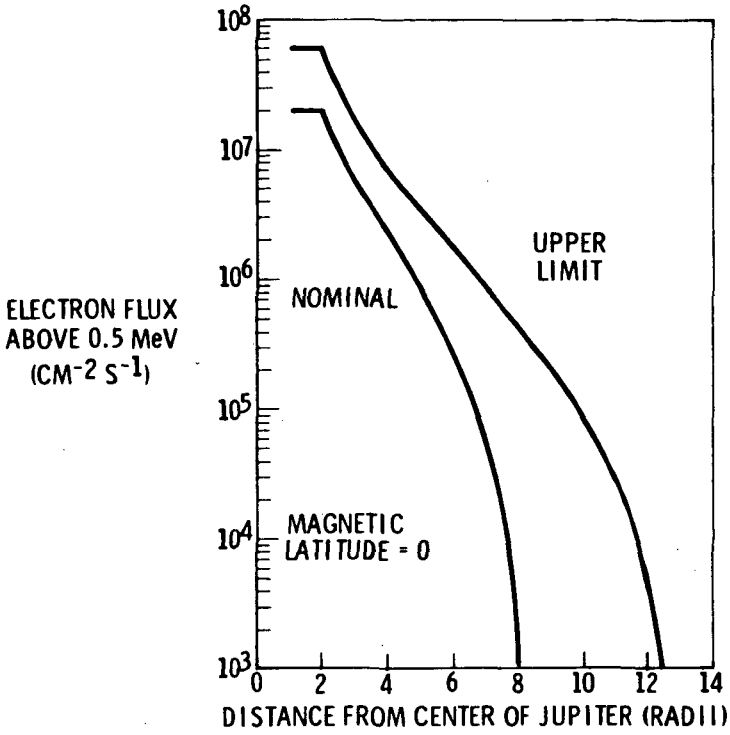

JUPITER ELECTRON FLUX

The electron fluxes in Jupiter's Van Allen belts are relatively well known because they emit rf (decimetric) radiation. This decimetric radiation is emitted continuously and has been mapped out to ~3 R_J (Jupiter radii) on each side of the planet. The radiation is believed to be due to synchrotron emissions from relativistic (>0. 5 MeV) electrons trapped in Jupiter's dipole magnetic field. Based upon the characteristics of the decimetric radiations, estimates of the electron fluxes, electron energies ($\lesssim$ 300 MeV) and Jupiter's surface magnetic field strength (6 to 48 gauss) have been obtained. Unknown factors relating to the effects of Jupiter's large size (~11 times the diameter of the earth) and rapid rotation rate (~ 9 hrs 55 minutes/revolution) remain, however. Therefore, both nominal and upper-limit models are presented (the "JPL Workshop" models).

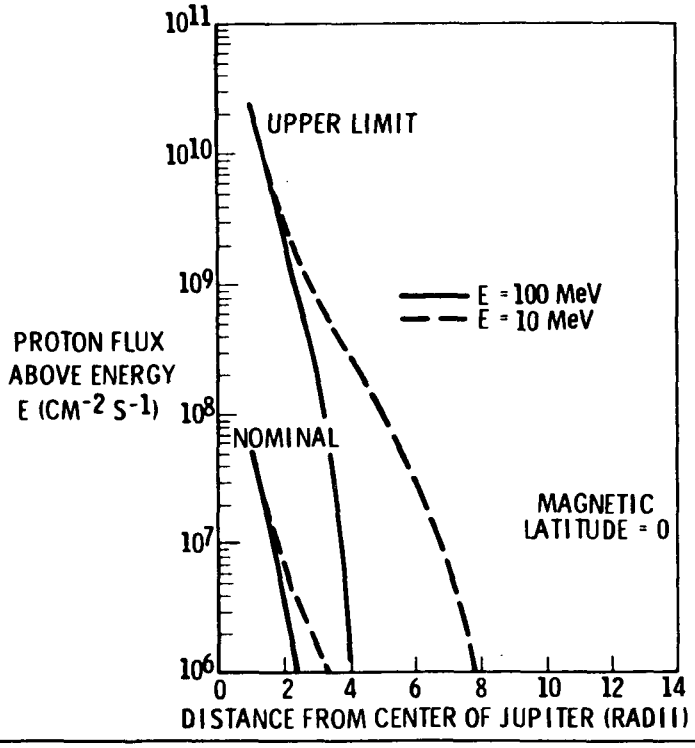

JUPITER PROTON FLUX

The proton fluxes in Jupiter's Van Allen belts are not well known, since the protons do not emit detectable radiation (as far as we know). There are at least three schools of thought on the Jovian proton fluxes. One school of thought is that because the protons do not radiate their fluxes may be near the stability limit ($\sim 10^{3}$ times the electron flux which is at $\sim 10^{-3}$ times the stability limit). A second school of thought is that proton and electron fluxes may be comparable (as in the earth's Van Allen belts). A third school of thought is that the large Galilean satellites of Jupiter (Io, Europa, Ganymede, and Callisto) will preferentially remove the protons as they orbit through the Jovian Van Allen belts. Consequently, two proton flux models are presented (the "Workshop" models). Proton energies are not well known either, but may become >1000 MeV close to the planet.

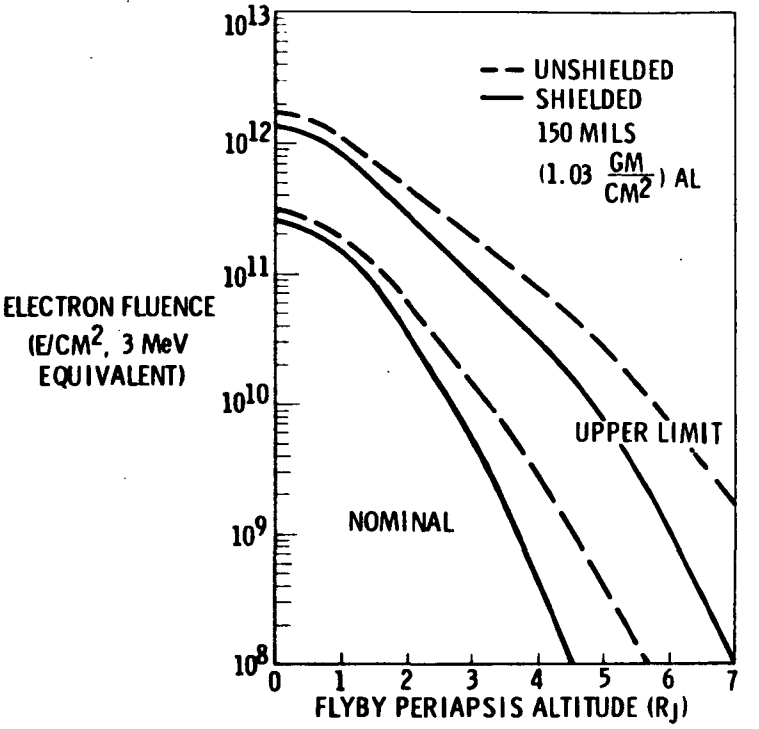

JUPITER FLYBY ELECTRON FLUENCE

The flux of trapped electrons at Jupiter is low compared to fluxes at which rate-dependent effects become important. Therefore, the radiation effects are dependent on the fluence. The unshielded electron fluence during flyby is the time integral of the electron flux along the trajectory. Now the spacecraft scalar velocity (speed) near periapsis (i.e., in the region of highest flux) is nearly independent of the asymptotic approach velocity, and is governed by the periapsis altitude. The flyby fluence is, then, determined to a first approximation by the periapsis altitude or distance of closest approach. In order to eliminate consideration of the spatial variation of the electron energy distribution, the fluences are given for 3-MeV equivalent electrons for both nominal and upper-limit "Workshop" models. If 150 mils (1.03 g/cm^2) aluminum shielding is present, electrons below 1.7 MeV will not penetrate, 5-MeV electrons will be slowed to ~3.2 MeV, and electrons above 10 MeV will be virtually unaffected.

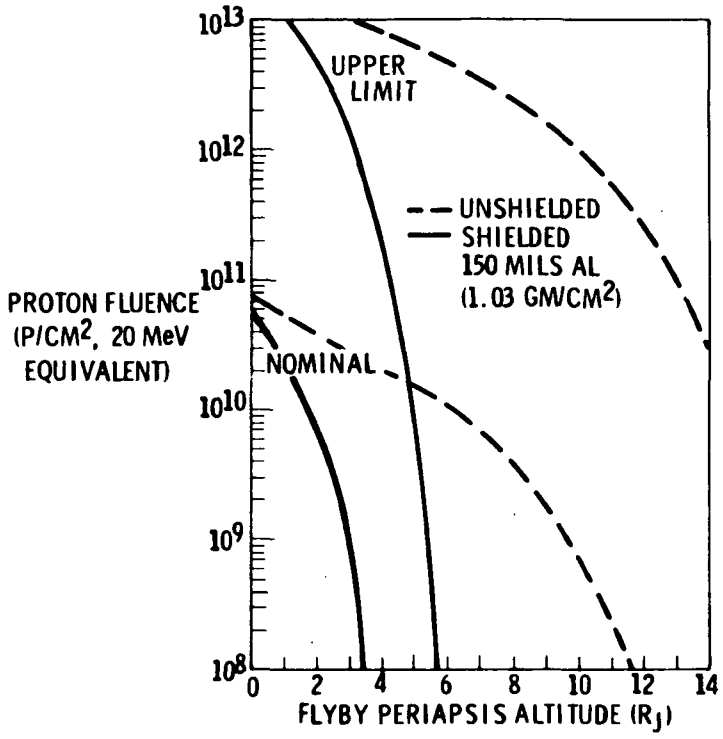

JUPITER FLYBY PROTON FLUENCE

The flyby proton fluences are (to a first approximation) a function of periapsis altitude (distance of closest approach). Due to the greater uncertainties in Jupiter's Van Allen proton fluxes, the flyby proton fluences are correspondingly uncertain. The differences between the unshielded fluences for the nominal and upper-limit "Workshop" models reflect this uncertainty.

The incorporation of 150 mils (1.03 g/cm^2) of aluminum reduces the flyby proton fluence (in units of p/cm^2 for 20-MeV equivalent protons). It will be noted that this reduction becomes quite large as the flyby periapsis increases. This is due to the reduction in particle energy as distance from the planet increases and the magnetic field strength decreases. This effect, which is much greater for protons than for electrons, is aided by the shorter ranges of protons in matter (1.03 g/cm^2 will stop 28-MeV protons).

- 86.8-YEAR HALF-LIFE

- PRODUCES GAMMA RAYS
  - FUNCTION OF
    - FUEL AGE
    - Pu-236 IMPURITY
    - CONTAINER

- PRODUCES ALPHA PARTICLES
  - SHORT RANGE < 0.01 GM/CM^2 (DO NOT ESCAPE)
  - SOURCE OF HEAT

- PRODUCES NEUTRONS
  - Pu-238 SPONTANEOUS FISSION
  - ALPHA PARTICLE CAPTURE
  - FUNCTION OF
    - FUEL AGE
    - LOW-Z IMPURITIES
    - GEOMETRY

Pu^{238} RADIOISOTOPE FUEL

In addition to the natural nuclear radiations (solar, galactic, and Van Allen), an outer planet spacecraft will have to operate in the nuclear radiations produced by its on-board power sources. Pu^{238} is the preferred radioisotope power source because of its large half life (86 yr), relative absence of penetrating radiation emission, low weight (~ 0.5 watt/g), and availability. Radioisotope power is independent of distance from the sun, is smaller and lighter than alternate systems (for sizes up to tens of kilowatts), and is essentially infallible (it can't be turned off).

Because more than 99% of the radiation produced by Pu^{238} is in the form of alpha particles of energy < 10 MeV, shielding is simple (< 1 g/cm^2 stops all of them). However, in addition to emitting spontaneous fission neutrons and gamma rays ($\sim 2,100$ n/g sec) Pu^{238} will form critical (reactor-like) assemblies if sufficiently concentrated. In the oxide form ($Pu^{238}O_2$) it produces secondary neutrons from (α, n) reactions in O^{18} and impurities). The isotopic impurity Pu^{236} also emits a significant decay gamma-ray flux.

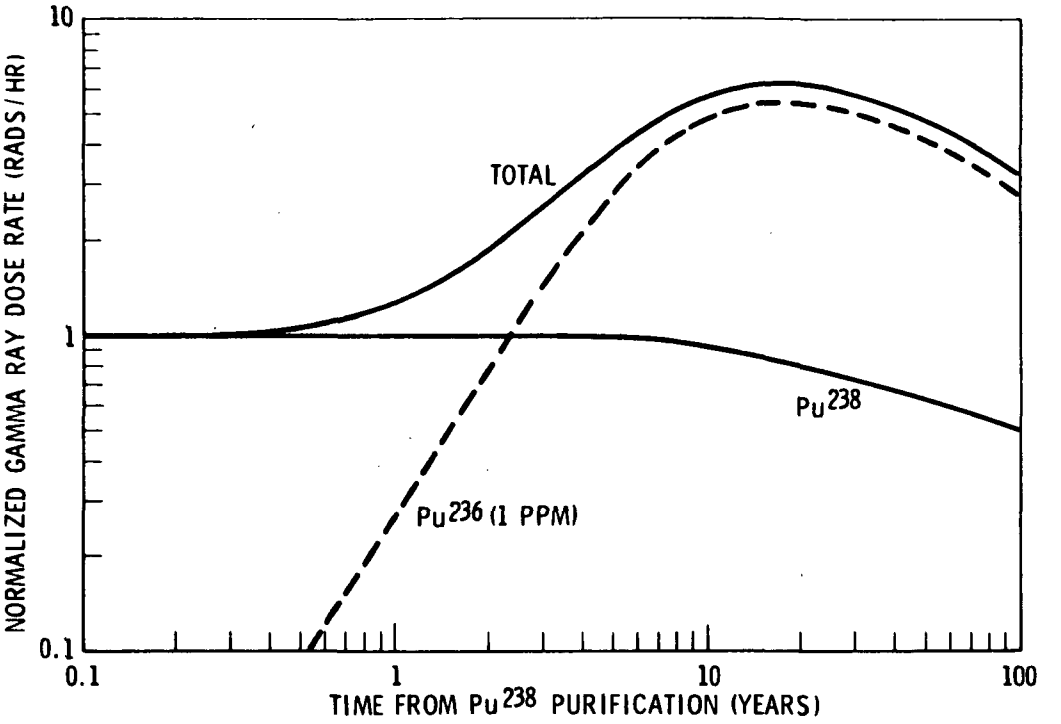

Pu^{236} IMPURITY INFLUENCE ON Pu^{238} DOSE RATE

As produced commercially, Pu^{238} contains ~1 ppm (part per million) of Pu^{236}. This Pu^{236} decays with a 2.7-year half life with Th^{228}, a member of the decay chain, being a particularly notable source of gamma rays. Consequently, the gamma ray output of a Pu^{238} source continues to increase for the first 18 years until the effect of the Pu^{236} daughter has passed its peak. Consequently, the gamma ray dose rate for new fuel ($\sim 100/X^2$ r/hr watt, where X is the distance from the source in cm) must be multiplied by the gamma ray dose rate impurity factor. While it is desirable to use fuel as soon after purification as possible, safety and operations considerations usually impose 1 to 3 years from purification to launch.

PHOTON ENERGY INTERVAL	0 YRS	1 YR	5 YRS	10 YRS	18 YRS
0.04-0.5 MeV	0.12	0.16	0.56	0.90	1.0
0.5 -1.0 MeV	0.23	0.25	0.30	0.33	0.35
1.0 -2.0 MeV	0.096	0.096	0.096	0.096	0.096
2.0 -3.0 MeV	0.003	0.018	0.18	0.32	0.37
3.0 -5.0 MeV	0.0003	0.0003	0.0003	0.0003	0.0003
5.0 -7.0 MeV	0.00003	0.00003	0.00003	0.00003	0.00003

NORMALIZED Pu^{238} GAMMA RAY SPECTRUM VS. FUEL AGE

The effects of the Pu^{236} impurity on the gamma ray output of a $Pu^{238}O_2$ source are not independent of gamma ray energy. While the spectral table does not show all the detail inherent in the gamma ray energies, it is seen that the effects of the Pu^{236} lie below 1 MeV (except for a band of energies between 2 and 3 MeV). These low-energy gamma rays (especially ~0.3 MeV) are of interest because they are relatively damaging to electronics and they are attenuated more by materials of high atomic number (e.g., tungsten, lead, uranium). Thus, some shielding to protect sensitive space components from these low-energy gamma rays can be effected for only a small weight penalty.

NEUTRON SOURCE	NEUTRON YIELD (N/GRAM Pu^{238} -SEC) NOMINAL	MAXIMUM
SPONTANEOUS FISSION	2,100	2,100
O^{18} (α, n) Ne^{21} REACTION	11,300	11,300
IMPURITY REACTIONS		
BORON	4,100 (100 PPM)	262,000 (6400 PPM)
SODIUM	1,300 (600 PPM)	16,700 (7600 PPM)
MAGNESIUM	200 (100 PPM)	18,000 (9000 PPM)
ALUMINUM	100 (100 PPM)	3,500 (3500 PPM)
TOTAL	19,100	313,600

NEUTRON YIELD FROM $Pu^{238}O_2$ FUEL

$Pu^{238}O_2$ radioisotope fuel will be the source of neutrons from several different types of nuclear reactions. First will be the spontaneous fissions, which will be responsible for ~2100 n/g-sec. If the fuel is sufficiently large and compacted (e.g., >1 kw thermal and quasi-spherical) the neutron multiplication rate may not be negligible. In this case the spontaneous fission rate must be multiplied by this neutron multiplication factor and added to the 2100 n/g-sec.

There will be a number of impurities of low atomic number in the fuel which will produce neutrons via (α , n) reactions. The practical maximum and nominal neutron outputs per gram of Pu^{238} are listed along with their totals. Typical total neutron outputs of 20,000-40,000 n/g-sec are expected.

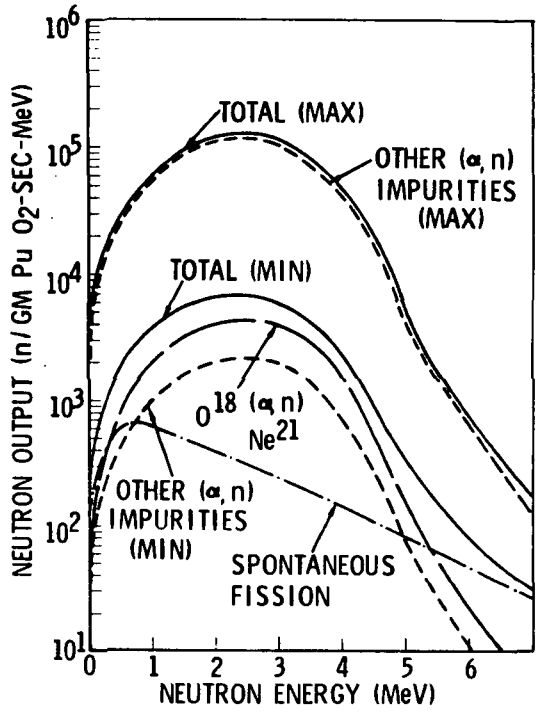

$Pu^{238}O_2$ NEUTRON SPECTRUM

The neutron spectra due to the various nuclear reactions in $Pu^{238}O_2$ fuel are shown. It is seen that the (α , n) neutrons have an appreciably different spectrum from the spontaneous fission neutrons. If neutron multiplication is a factor, such induced fissions will produce a neutron spectrum essentially the same as the spontaneous neutron spectrum.

Unless there is considerable neutron multiplication, which is undesirable because the fission gamma ray as well as the fission neutron output increases, the total neutron spectrum is dominated by the (α , n) neutrons. Since the half-life of the Pu^{238} alpha emission controls the fission and (α , n) neutron emissions, the neutron spectrum does not change with time.

JUPITER TRAPPED PARTICLES (5×10^3-KM APPROACH)

ENERGY (MeV)	ELECTRON FLUENCE (/CM^2)	PROTON FLUENCE (/CM^2)
1-3	4.9×10^{10}	8.9×10^{11}
3-10	1.1×10^{11}	1.7×10^{12}
10-30	2.4×10^{11}	3.3×10^{12}
30-100	2.0×10^{11}	6.9×10^{12}
100-300	1.1×10^{10}	1.5×10^{13}
300-1000	2.7×10^{5}	2.8×10^{13}
10^3-10^4	0	2.0×10^{13}
$>10^4$	0	4.7×10^{5}
(EQUIVALENT)	2×10^{12} (3 MeV)	3×10^{13} (20 MeV)

Pu^{238} RADIOISOTOPE THERMOELECTRIC GENERATOR (1.5 M = 5 FT)

NEUTRONS		GAMMA RAYS	
ENERGY (MeV)	FLUX (/CM^{2}S)	ENERGY (MeV)	DOSE RATE (RAD/HR)
< 0.5	3.7×10^{2}	0.2-0.5	7×10^{-3}
0.5-1.5	8.7×10^{2}	0.5-1.0	$2.4 \times 10^{-}$
1.5-2.5	1.2×10^{3}	1.0-2.0	1.7×10^{-2}
2.5-3.5	8.7×10^{2}	2.0-3.0	5.0×10^{-2}
>3.5	1.3×10^{2}	>3.0	2.0×10^{-3}
TOTAL	3.5×10^{3}	TOTAL	1.0×10^{-1}

TOPS RADIATION DESIGN CONSTRAINTS

For design work it is necessary to specify constraints to which the practicing engineer can refer. One such set of design constraints is presented here for the TOPS spacecraft. It consists of the maximum flux rate as well as the mission integrated fluence for electrons and protons in each of several energy bands. For neutrons (as well as sometimes for electrons and protons) a single flux and a single fluence (in terms of particles of some equivalent energy) is often specified. For neutrons 1 MeV equivalent is fairly common. 3-MeV equivalent electrons and 20-MeV equivalent protons are sometimes used for these particles. Gamma ray environments are often specified directly in rad/sec and rad.

EARTH'S VAN ALLEN BELTS

ELECTRONS		PROTONS	
ENERGY (MeV)	FLUENCE (/CM^2)	ENERGY (MeV)	FLUENCE (/CM^2)
> 0.25	6×10^{10}	> 4	9×10^{8}
> 1	1.8×10^{10}	> 15	5×10^{7}
> 3	1.5×10^{9}	> 34	8×10^{6}
> 7	1.5×10^{7}	> 50	2×10^{6}

SOLAR FLARE PROTONS

ENERGY (MeV)	FLUX (/CM^{2}S)	FLUENCE (/CM^2)
> 5	1.15×10^{6}	1.6×10^{11}
> 10	4.5×10^{5}	4.8×10^{10}
> 30	1.15×10^{5}	8×10^{9}
> 100	1.0×10^{4}	8×10^{8}

SOLAR WIND PROTONS

~ 3 keV	1.2×10^{8}/CM^{2}S	5×10^{15}/CM^2

GALACTIC (COSMIC) RADIATION FLUX (/CM^{2}S)

ENERGY (MeV)	PROTONS	ALPHAS	$Z \geq 3$
> 100	5.5	0.56	0.077
> 500	4.2	0.40	-
> 10^3	3.4	0.27	-
> 10^4	0.44	0.015	-

TOPS RADIATION DESIGN CONSTRAINTS

The above table lists TOPS design constraints for minor sources of radiation: the earth's Van Allen belts, solar flare protons, solar wind protons, and protons, alpha particles (helium nuclei), and heavy nuclei in the galactic radiation (cosmic rays). For lack of information, no constraints are given for other types of particles (e.g., solar wind electrons) or the trapped radiation at planets beyond Jupiter.

MICROSCOPIC PROCESSES

DISPLACEMENT EFFECTS

IONIZATION EFFECTS

SUSCEPTIBILITY LEVELS

BASIC RADIATION EFFECTS

This section gives an overview of the physical basis of radiation effects from the microscopic (single-atom, single-particle) standpoint. Displacement effects result mostly from protons and neutrons, and cause disordering of the lattice structure of insulators and semiconductors. Ionization produced by charged particles and gamma rays introduces electrons into conduction and trapping levels, and otherwise alters the electrical properties of the absorbing material. The section concludes with a summary of the radiation susceptibility levels of various materials and devices.

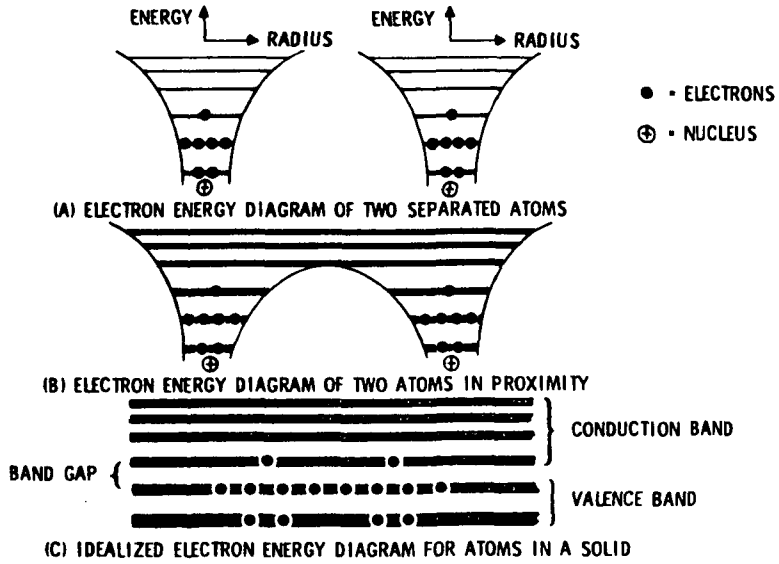

ELECTRONIC BAND STRUCTURE

An electron energy diagram for two separated atoms is similar to diagram A; with two electrons on the lowest energy level, four electrons on the next energy level, and one electron on a third (loosely bound) level. At some separation distance it is possible for the most loosely bound electron to migrate from one atom to the other (see diagram B). For many atoms in close proximity, the idealized electron energy diagram consists of one or more valence bands (occupied by electrons that are bound to one nucleus) and one or more conduction bands (electrons in the conduction band are free to move from atom to atom), as shown in diagram C. Insulators are materials with a wide band gap and no conduction electrons. Conductors are materials with many conduction electrons in the conduction band. Semiconductors are materials with small band gaps and some electrons in the conduction band.

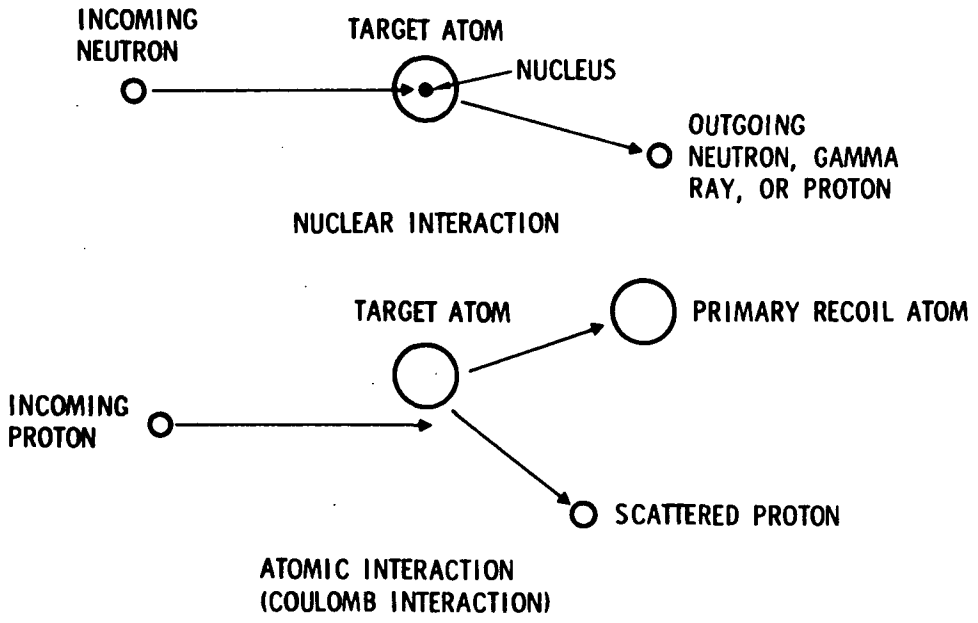

ATOMIC AND NUCLEAR INTERACTIONS

Energetic particles known as nuclear radiation interact with matter in two general ways: nuclear interactions and atomic interactions. Nuclear interactions result when the incoming particle path is altered in some way by fields characteristic of the nucleus. Atomic interactions result when the incoming particle path is altered by fields characteristic of the whole atom. The probability of an atomic interaction is greater than the probability of a nuclear interaction and nuclear interactions are generally ignored when the effects of radiation on macroscopic material properties are considered.

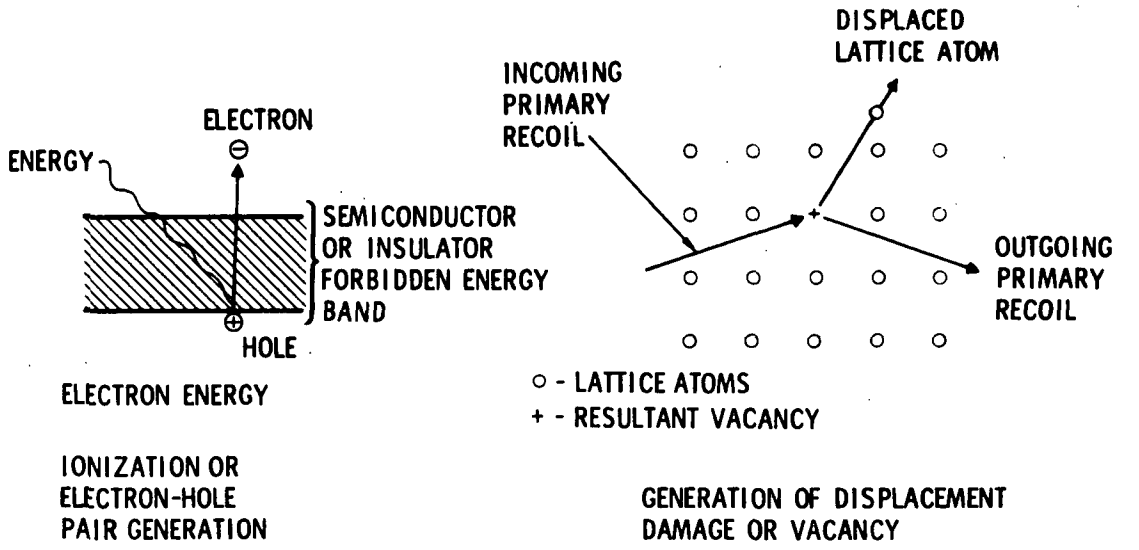

IONIZATION AND DISPLACEMENT

Atomic interactions result in the transfer of energy from the incoming energetic particle to either a lattice atom or electron. The energetic lattice atom (primary recoil) or electron is then able to travel through the lattice, ionizing and displacing atoms. In an insulator or semiconductor ionization of atoms results in the generation of excess electron-hole pairs. The displacement of atoms results in the production of defects in the lattice. At room temperature these defects generally consist of the absence of atoms in a periodic lattice, called vacancies. It is also possible to have more than one vacancy act as a single defect. These vacancy complexes are termed divacancies.

INCIDENT RADIATION IONIZES ATOMS OF ABSORBER

- ELECTRIC FIELD INTERACTION
- COLLISON (RECOIL PRIMARY PARTICLE)
- PHOTOELECTRIC EFFECT
- COMPTON EFFECT
- ELECTRON - POSITRON PAIR PRODUCTION

DETACHED ELECTRONS

- CONDUCTION BAND - CARRY CURRENT
- TRAPPED - CHANGE ELECTRIC PROPERTIES

IONIZED ATOMS

- SERVE AS TRAPPING CENTERS

IONIZATION DAMAGE

Ionization damage results when incident radiation ionizes atoms of the absorber material. This electric field interaction requires an incident charged particle (electron, proton, recoil primary, etc.) or photon. Incident photons can ionize by the photoelectric effect, the Compton scattering effect, or electron-positron pair production; the last two processes require photon energies in the gamma-ray region.

The detached electrons may be raised to the conduction band of an insulator or semiconductor, providing current carriers and lowering the resistivity. Or, they may be trapped at impurity or vacancy levels and alter electric properties that depend on these levels being empty. The ionized atoms can also serve as trapping centers.

INCIDENT RADIATION DISLODGES ATOM FROM LATTICE

- INTERSTITIAL ATOM
- VACANCY
- TRAPPING CENTERS

INCIDENT NEUTRON CAPTURED BY ATOM IN LATTICE

- RADIOACTIVE DECAY PRODUCES NEW ELEMENT (SUBSTITUTIONAL DEFECT)
- TRAPPING CENTER

DISPLACEMENT DAMAGE

Displacement damage results when incident radiation dislodges an atom from its place in the crystalline lattice. Because this process requires considerable momentum transfer from the incident particle which is much lighter than the atom, most displacement damage results from protons and neutrons. Energetic electrons can also displace atoms, but they cause mostly ionization damage.

The displaced atom occupies a position between normal crystalline sites. This interstitial atom and the vacancy it left behind both form defect centers that alter electric properties of the absorber. Incident neutrons captured by absorber atoms can cause radioactive transmutations, with a defect center resulting at this substitutional site. This last process is not important at OPGT neutron fluences.

$$\Delta\left(\frac{1}{\tau}\right) = k_n \phi$$

τ = MINORITY CARRIER LIFETIME IN SEC

ϕ = NEUTRON FLUENCE IN NEUTRONS/CM^2

k_n = DAMAGE CONSTANT $\simeq 6 \times 10^{-7}$ CM^2/NEUTRON SEC IN Si

$$\Delta n = \left(\frac{dn}{d\phi}\right)\phi$$

n = MAJORITY CARRIER CONCENTRATION IN CARRIERS/CM^3

$\frac{dn}{d\phi}$ = CARRIER REMOVAL RATE $\simeq 1$ CARRIER/NEUTRON-CM IN Si

$$\Delta\mu = \left(\frac{d\mu}{d\phi}\right)\phi$$

μ = CARRIER MOBILITY IN (CM/SEC)(VOLT/CM)

$\left(\frac{du}{d\phi}\right)$ = MOBILITY DEGRADATION COEFFICIENT

DISPLACEMENT DAMAGE IN SEMICONDUCTORS

In semiconductors displacement damage introduces additional energy levels in the forbidden band. These additional energy levels enhance minority carrier recombination reducing minority carrier lifetime, decrease majority carrier concentration (known as carrier freeze-out) and decrease carrier mobility. Minority carrier lifetime reduction is the most sensitive change and will be of primary interest for OPGT consideration.

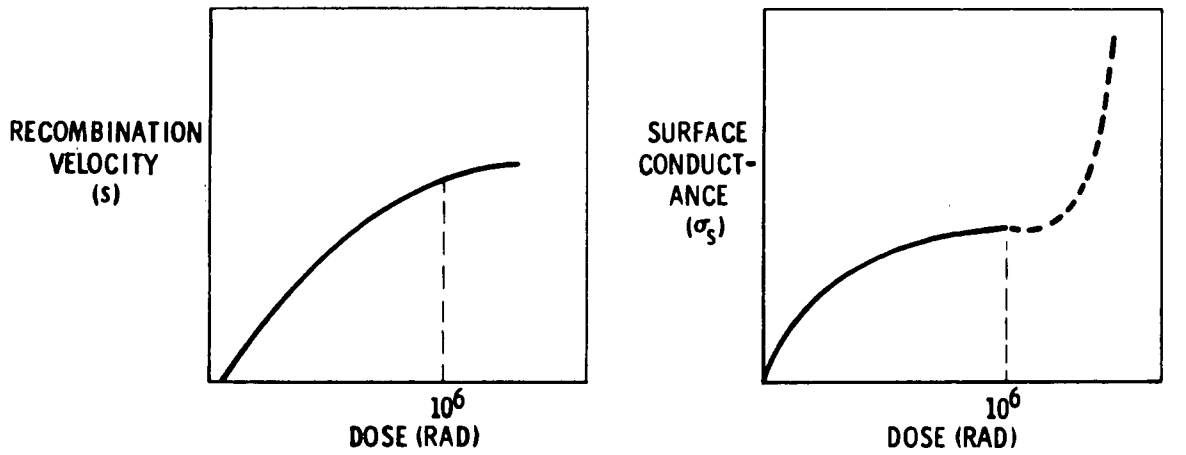

CHARGE TRAPPING

Charge trapping increases positive charge density on the oxidized surface of semiconductors or within the gate insulator. Consequently, surface recombination velocity and surface conductance increase.

Both effects tend to saturate at about 10^6 rads, although if surface inversion occurs, a near short circuit can develop between semiconductor regions.

$n_{e\text{-}h} \simeq E_a/\epsilon$

$\simeq gD$

$n_{e\text{-}h}$ = NUMBER ELECTRON-HOLE PAIRS GENERATED/cm^3

E_d = ENERGY DEPOSITED IN MATERIAL/cm^3

g = CARRIER GENERATION CONSTANT$\simeq 4.2 \times 10^{13}$ e-h PAIRS/RAD(Si)

D = ABSORBED RADIATION DOSE IN RADS (Si)

$\dot{D}$ = ABSORBED RADIATION DOSE RATE

$i_{pp} \simeq q\, g\, V\, f(t,\tau)\dot{D}$

i_{pp} = JUNCTION PRIMARY PHOTOCURRENT

q = ELECTRONIC CHARGE

V = JUNCTION CHARGE COLLECTION VOLUME

$f(t,\tau)$ = COMPLICATED FUNCTION OF TIME AFTER START OF RADIATION AND MINORITY CARRIER LIFETIME

IONIZATION IN SEMICONDUCTORS AND INSULATION

Energetic particles impinging on matter give up most of their energy in the form of ionization. This is manifested in semiconductors and insulators by the creation of electron-hole pairs. In semiconductors this results in additional leakage currents known as photocurrents. Because photocurrents are dose-rate dependent, their magnitudes in conventional semiconductor devices will be much lower than normal leakage currents for the OPGT environments. In insulators it is possible that one or both kinds of carriers will be trapped and a charge buildup in the insulator will occur. This effects is most often dependent on the integrated dose and will be of primary interest for the OPGT environments.

- STIMULATED CHEMICAL REACTIONS

  RADIATION + $H_2O \rightarrow H_2O^+ + e^-$

  $H_2O^+ \rightarrow H^+ + OH$

  $H^+ + H^+ + 2e^- \rightarrow H_2 \uparrow$

  $OH + OH \rightarrow H_2O_2$

- ORGANIC REACTIONS

  POLYMER CROSS-LINKING CHANGES

- NUCLEAR TRANSMUTATIONS

  $S^{32}(n, p)P^{32}$

CHEMICAL EFFECTS

Chemical reactions can be stimulated by energetic radiation. These reactions can release gases (maybe corrosive), solidify liquids (such as hydralic fluid), or change the mechanical properties of polymers (particularly Teflon). These effects can usually be avoided by choosing a proper insensitive alternative substance that can do the same job.

Capture of slow neutrons or bombardment by high energy particles can result in nuclear transmutations. These are seldom directly important in OPGT environment but form the basis of neutron dosimetry used for simulation testing.

Chemical reactions induced by radiation are important for thermal control coating and optical films. A simple reaction is shown above which produces both H_2 and H_2O_2.

$$N_D = N_A \int_{E_T}^{E_N} \int_{E_D}^{E_{pmax}} \phi(E)\sigma(E, E_p)\, N_S(E_p) dE_p dE$$

$$N_D = N_A \Phi \sigma_D \bar{n}$$

GENERAL DISPLACEMENT DAMAGE INTEGRAL

Displacement damage results when radiation disrupts the lattice structure on an atomic basis. Since electrical properties of semiconductors depend strongly on the degree of lattice perfection, damage thresholds are relatively low.

The damage is proportional to the density of atoms in the lattice, the radiation fluence striking the lattice, and the cross section for producing displacements. Since atoms which receive large amounts of energy from the incident radiation can produce additional displacements as they come to rest in the crystal, the damage is also proportional to the number and energy of recoil atoms, resulting in the multiplication factor $\bar{n}$. The cross section depends on the energy, charge state, and mass of the incoming particle and is quite different for neutrons, protons, electrons, and γ radiation. The displacement damage produced by γ radiation is usually negligible.

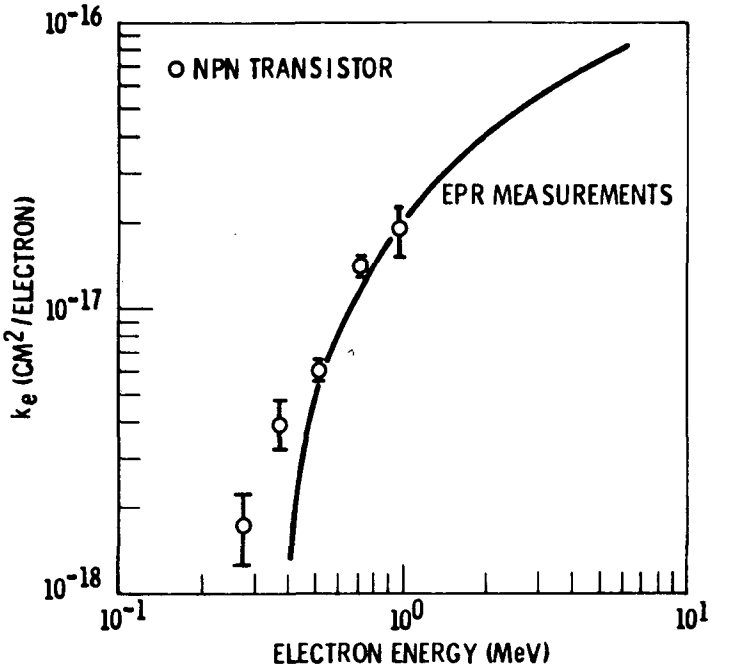

ELECTRON DISPLACEMENT DAMAGE

The threshold energy for electron displacement damage is approximately 0.3 MeV, primarily reflecting its relatively small mass. The scattering process is subject to a screen potential (Rutherford scattering) and the scattering cross section is proportional to 1/E. However, the electron mass must be corrected for relativistic effects at energies above 1 MeV. Thus, the damage threshold is above 0.3 MeV and increases at first linearly with increasing energy and then approaches a saturated value above about 30 MeV. Below 1 MeV shielding effects are very important and even the device package can produce significant shielding effects. The electron damage curve is fitted here to electron paramagnetic resonance data.

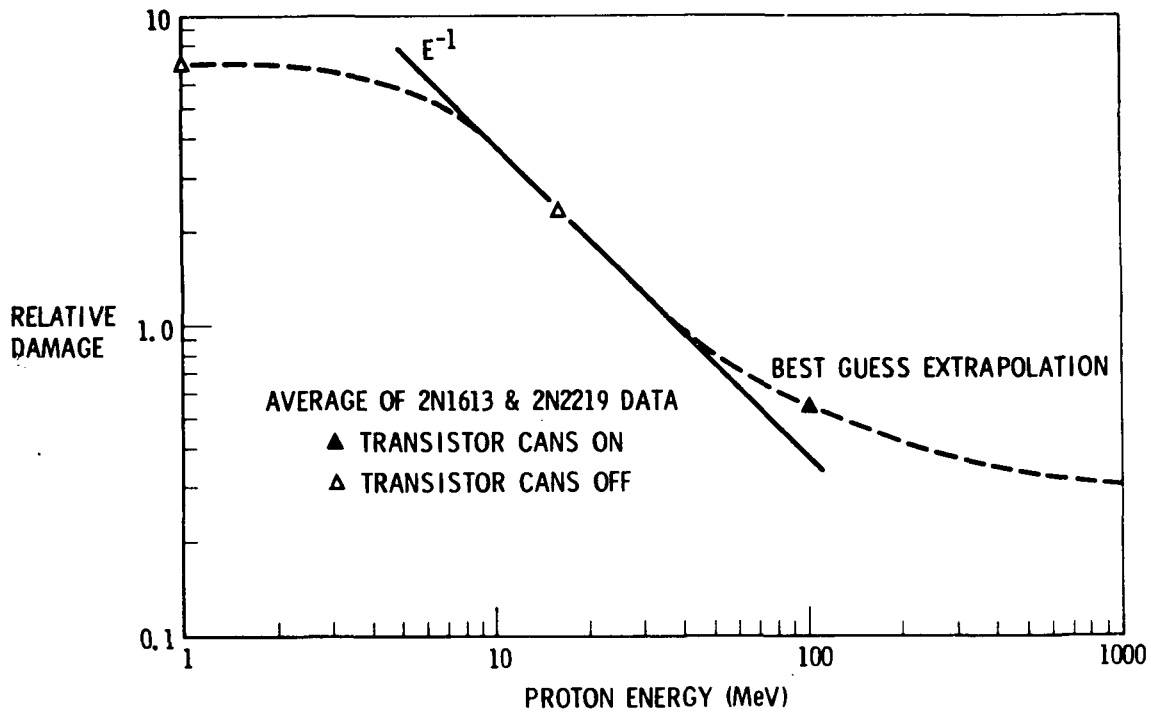

PROTON ENERGY DEPENDENCE OF DISPLACEMENT DAMAGE

Rutherford scattering also governs proton displacement damage, but no relativistic corrections are required below 1000 MeV since the mass of the proton is so much larger than the mass of the electron. The threshold for displacement damage is ~ 200 eV; however at energies below 10 MeV self-shielding effects are very important. That is, the damage produced is near the surface of the device and is not uniform throughout the bulk of the device.

Above 10 MeV the displacement damage curve approaches the same energy dependence as the cross-section, 1/E. High-energy (> 100 MeV) proton damage data are not available and the curve represents a best guess estimate after considering the dE/dx and damage processes.

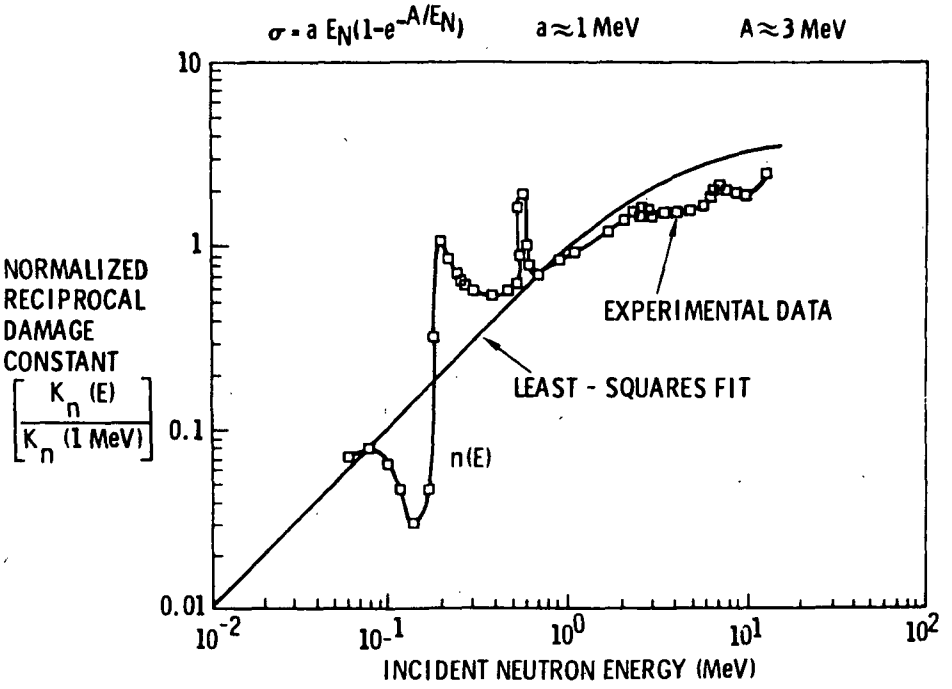

NEUTRON DAMAGE

Neutron damage is produced by a hard sphere scattering process involving direct nuclear collisions. The cross section is very small and nearly energy independent above 1 MeV. Most of the damage is done by high-energy recoil primaries resulting in cluster defects. As a consequence of the small cross section, the range is quite long, ~ 7 cm. The average number of displacements per neutron collision is quite large, ~500. The saturation observed in the damage curve above 1 MeV results from a higher percentage of recoil primary energy going into ionization effects.

The energy going into atomic processes contains several resonance peaks. The average curve is usually easier to use when dealing with a fission spectrum.

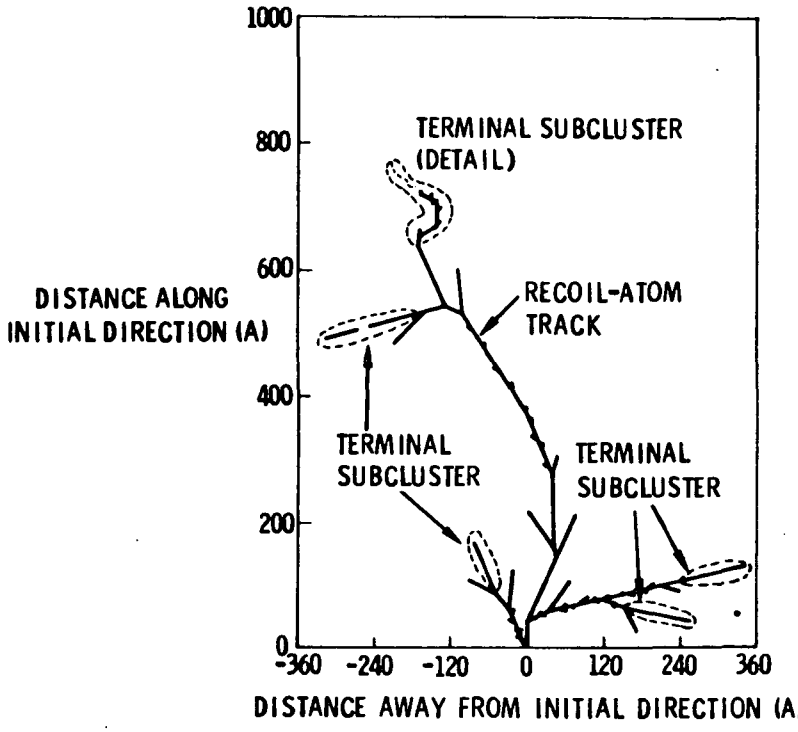

CLUSTER DEFECTS

The production of point defects and clusters can be understood by looking at a "typical" 1-MeV neutron collision. This initial collision occurs at the bottom center of the plot. The recoil atoms travel relatively large distances, giving up a significant amount of energy to ionizing other atoms in the lattice. The collision cross section increases as the recoil energy decreases until finally a large sequence of displacement collisions occurs as the primary comes to rest creating a cluster. A number of point defects are created along the paths. The final catastrophic collision leading to a cluster releases large amounts of energy in a small lattice volume. During the cooling process, substantial annealing occurs, thereby reducing the total number of displacements to a net of ~50 at room temperature, for 1-MeV neutrons.

PARTICLE TYPE AND ENERGY	ALPHA* 5 MeV	PROTON 15 MeV	NEUTRON TRIGA REACTOR	ELECTRON 1.3 MeV	GAMMA RAYS COBALT-60
ALPHA* (5 MeV)	1	4.1	1.4×10^{2}	3.75×10^{3}	3.75×10^{5}
PROTON 20 MeV	2.5×10^{-1}	1	3.3×10^{1}	9.0×10^{3}	9.0×10^{4}
NEUTRON (REACTOR)	7.1×10^{-3}	3.1×10^{-2}	1	2.8×10^{1}	2.8×10^{3}
ELECTRON 1.3 MeV	2.7×10^{-4}	1.1×10^{-3}	3.6×10^{-2}	1	1.0×10^{2}
GAMMA RAYS COBALT-60	2.7×10^{-6}	1.1×10^{-5}	3.6×10^{-4}	1.0×10^{-2}	1

*TRANSISTOR CANS OFF FOR 5-MeV ALPHA PARTICLES

EXPERIMENTAL DAMAGE CONSTANTS

An overall summary of displacement damage effects oriented toward device effects by using Δh_{FE}^{-1} is provided above. Because transistor can shielding effects are important for charged particles, a 0.17-gm/cm^2 shielding factor has been used.

Protons are the most damaging radiation particles encountered in space. A 1-MeV proton is approximately 40 times as damaging as a 1-MeV neutron, 2,000 times as damaging as a 1-MeV electron, and 43,000 times as damaging as Co^{60} gammas.

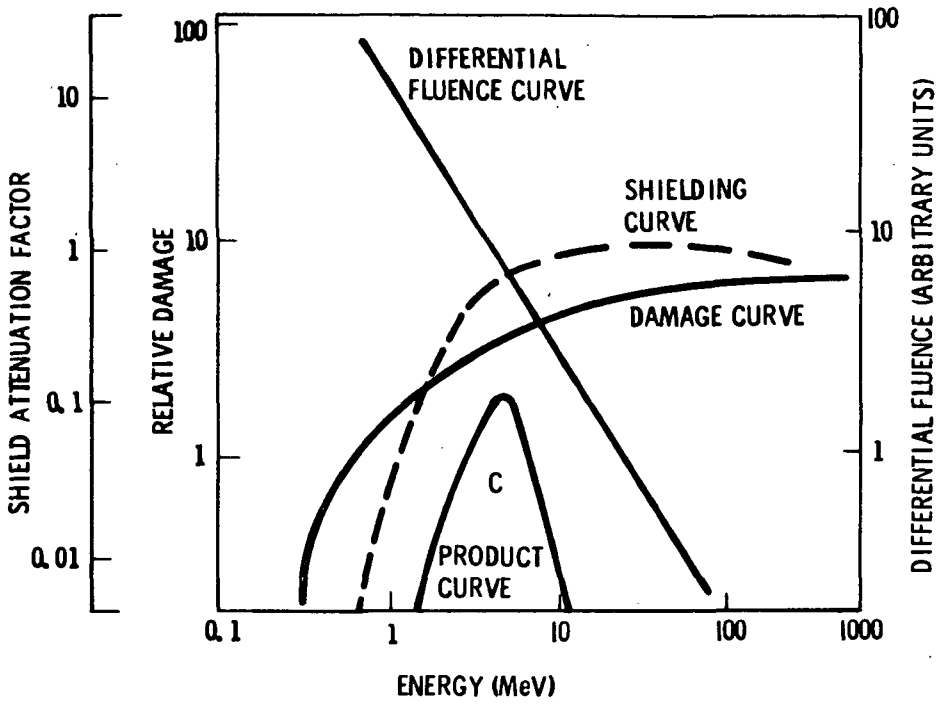

ENERGY DEPENDENCE

The overall effect on the electron energy spectrum is qualitatively illustrated above. The product curve which determines the semiconductor device damage is proportional to

$$\int_{E_T}^{E_{max}} A(E)\, \emptyset\,(E)\, \sigma\,(E)\, dE.$$

This can be closely approximated by taking all the electrons in the 2.5-MeV to 7.5-MeV interval, and multiplying by the 5-MeV relative damage and the 5-MeV attenuation. Although these curves have been selected to be representative of the space environment problem, differences in the shielding could significantly affect the product curve. A similar argument applies to protons.

PHOTON IONIZATION

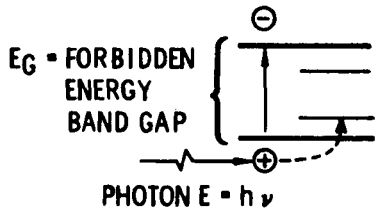

IF $h\nu \geq E_G$ WILL GENERATE 1 ELECTRON-HOLE PAIR

ENERGETIC PARTICLES

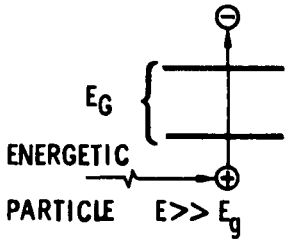

IF ENERGY ABSORBED $E_a >> E_g$

THEN TOTAL NUMBER OF ELECTRON-HOLE PAIRS GENERATED IS

$$n_{e-h} = E_a/\epsilon$$

WHERE $\epsilon \sim 3E_G$

IONIZATION IN SEMICONDUCTORS AND INSULATORS

Ionization in semiconductors and insulators can occur when the energy of the incident photon exceeds the band gap. For highly energetic particles, the excited electron can produce further ionization in a cascade process. However, the excited electron or electrons will give up much of their energy to phonons (in the form of heat). For high energy particles about 2/3 of the energy ends up as heat and 1/3 as hole-electron pairs. For silicon, 4×10^{13} hole-electron pairs are produced per rad of absorbed radiation.

The hole-electron pairs disappear by recombination. A small percentage may disappear by trapping. Hole trapping is the phenomenon responsible for degradation in conventional MOS devices. The holes are trapped in the insulator layer (SiO_2) under the gate electrode.

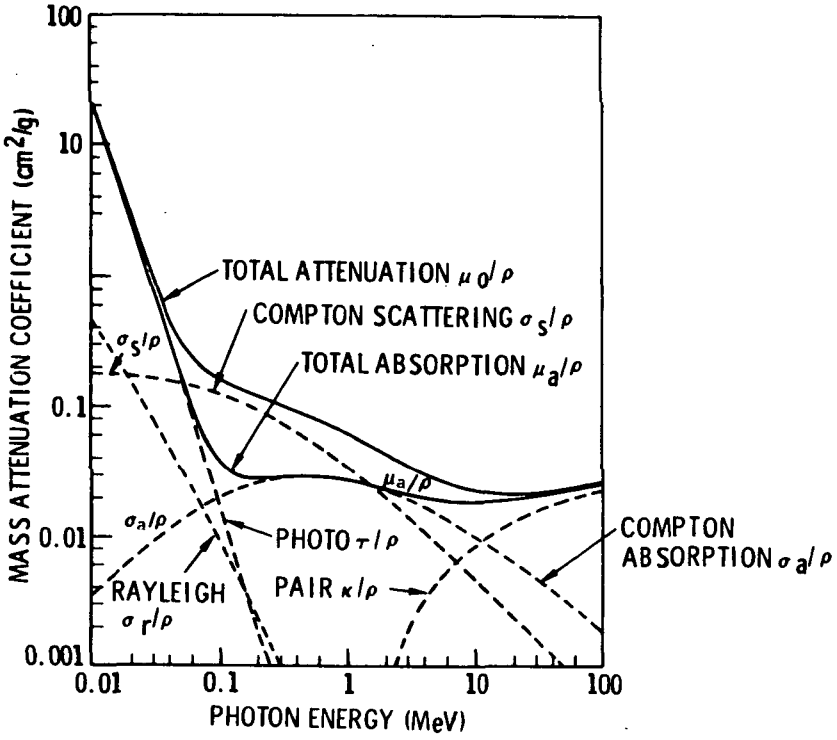

BASIC PHOTON CROSS SECTIONS

At high photon energies, the first interaction may be photoelectric, Compton, or electron-positron pair production. These cross sections depend on the atomic number of the material. Photoelectric interaction leads only to hole-electron pair production and trapping. Compton interaction produces electrons energetic enough to produce displacement effects. Electron-positron pair production is usually negligible for radiation effects considerations.

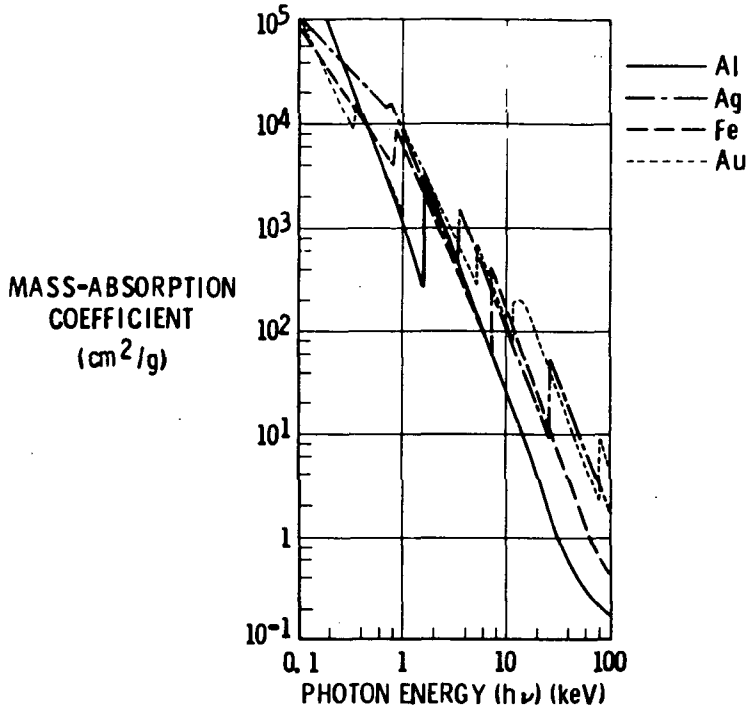

PHOTOELECTRIC MASS ABSORPTION COEFFICIENT

Photons interact with electrons in the various electron shells (K, L, M, ...) leading to mass absorption coefficients which decrease rapidly with increasing energy. The discontinuities are caused by resonances with the K, L, and M electron shells. An understanding of this phenomenon is basic to shielding considerations.

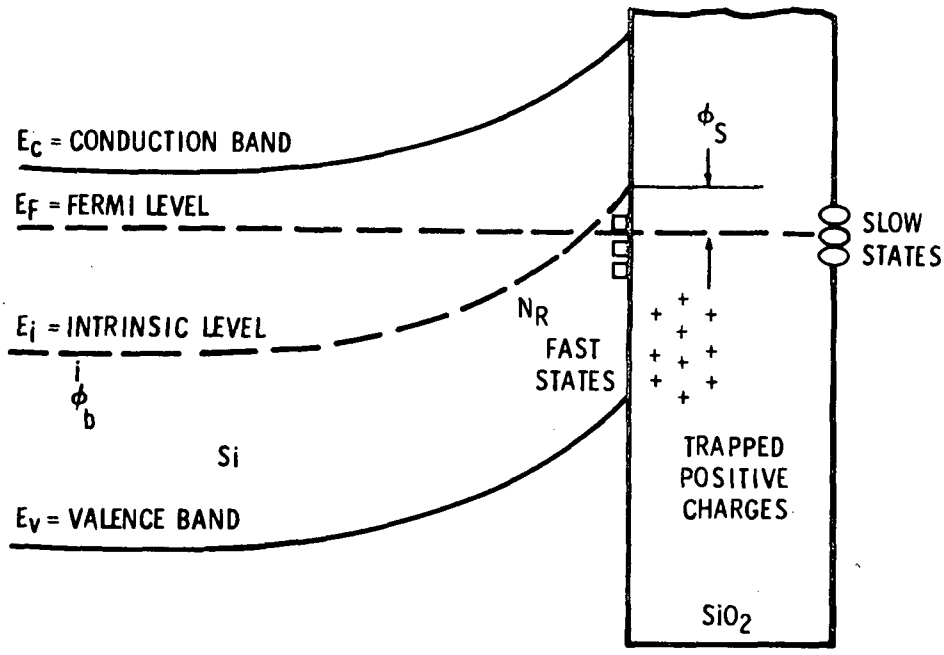

CHARGE TRAPPING

When positive charge is trapped in the SiO_2 layer on the surface of silicon or beneath the gate electrode in MOS devices, electrons are attached from the silicon to the surface to produce local neutralization. This forces a readjustment of the surface potential, leading to device degradation effects. Interface states reduce channel mobility and transconductance in MOS devices. Trapped charge produces shifts in threshold voltages for MOS FETs and decreases in gain in bipolar devices.

The superior performance of conventional PMOS as compared to NMOS in a radiation environment is based on the fact that SiO_2 contains a preponderance of hole traps. Hardening of MOS devices is accomplished by introducing compensating electron traps (Cr) or reducing the hole traps (pure oxide). Annealing of surface damage is caused by thermal de-trapping of the holes in SiO_2.

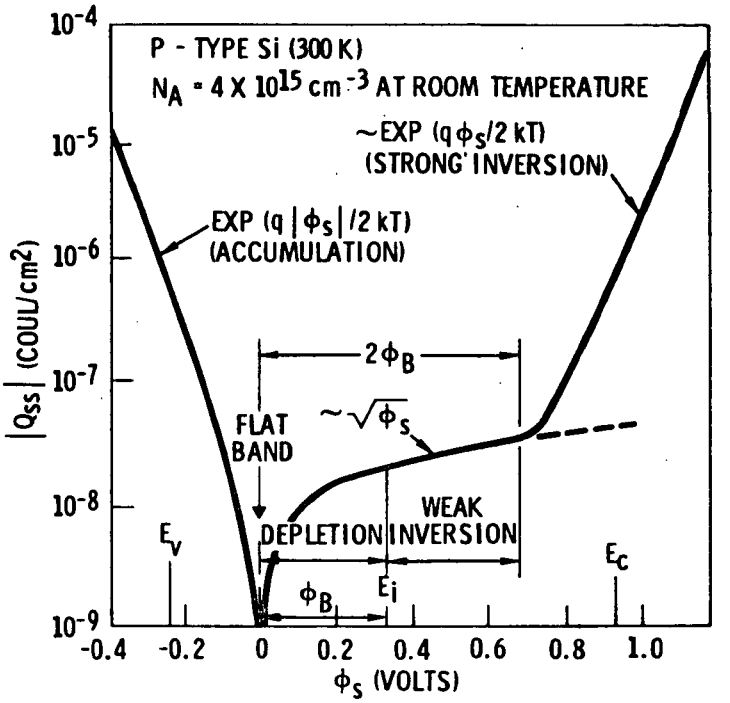

SURFACE POTENTIAL

The trapping of charge changes the surface potential as indicated. Negative charge produces surface accumulation, whereas positive charge results in inversion. Most surfaces are initially depleted, and the change in trapped charge with potential is usually relatively small. In the accumulation or inversion region, surface potential changes logarithmically with surface charge. In the depletion region, surface potential changes quadratically with surface charge.

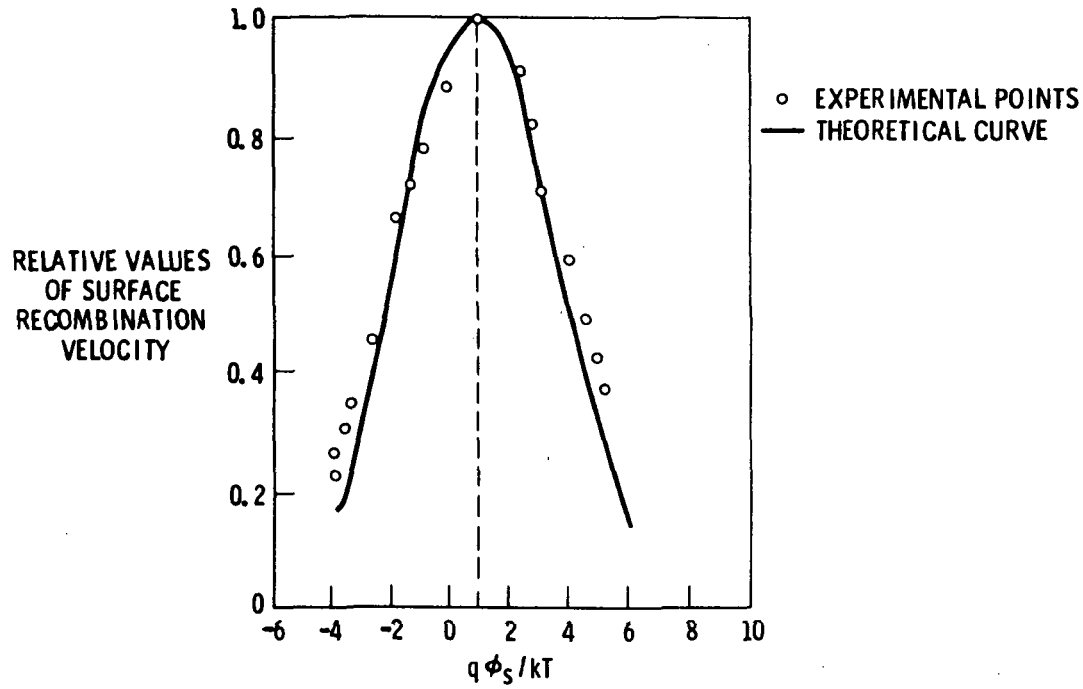

SURFACE RECOMBINATION VELOCITY

Surface recombination velocity is determined by Shockley-Read statistics. The effect maximizes when the surface potential is approximately zero. This usually occurs in bipolar transistors at a forward bias of 0.3 volt corresponding to the energy level of the recombination centers.

The effect of ionizing radiation is not to increase the number of recombination centers but rather to change the occupation probability and reinforce the effect of the existing centers by changing the surface potential. Thus, there is reasonable hope of using device parameters such as current gain measured at about 0.3 V as an electrical screen to eliminate radiation-sensitive devices.

- REDUCTION OF DISPLACEMENT EFFECTS

- REDUCTION OF IONIZING EFFECTS

SHIELDING CONSIDERATIONS

The OPGT environments include electrons, protons, gamma rays, and neutrons, and shielding compromises must be evaluated.

Shielding can very easily increase the displacement damage effectiveness of protons by reducing their energy. Some shielding is useful because it reduces the displacement damage effectiveness of electrons.

Shielding reduces ionization damage very effectively up to about 2 gm/cm^2. Above this thickness bremsstrahlung effects predominate, and a point of diminishing returns is reached for the space environment.

COMPOSITION

- PROTONS - DEFINITE RANGE, ALMOST INDEPENDENT OF Z
- ELECTRONS - DEFINITE RANGE, ALMOST INDEPENDENT OF Z
  - BREMSSTRAHLUNG X-RAY FLUX ~ Z
- GAMMA RAYS - EXPONENTIAL ATTENUATION FACTOR ~ Z
- NEUTRONS - EXPONENTIAL ATTENUATION
  - SLOWED BY COLLISIONS WITH LOW-Z ATOMS
  - CAPTURED BY H, B, Li, Cd, ETC.
  - SECONDARY GAMMAS

GEOMETRY

- FLAT PLATES - MASS ALMOST INDEPENDENT OF Z
- CURVED PLATES - LOWEST MASS FOR HIGH Z
- OPENINGS UNDESIRABLE

SHIELDING DESIGN CONSIDERATIONS

The effectiveness of shielding materials depends on their composition and the radiation to be stopped. Protons and electrons have definite ranges which vary as E^n and are almost independent of the shield's mean atomic number, Z. Electrons, however, produce bremsstrahlung X-rays at a rate proportional to Z. Gamma and X-rays are exponentially attenuated with a factor roughly proportional to Z. Fast neutrons are also attenuated exponentially by scattering which reduces the neutron energy at a rate roughly proportional to $1/Z$. The slow neutrons may be captured in certain low-Z and medium-Z elements such as H, B, Li, Cd, etc.; some of these elements (e.g., B, Cd) then emit gamma rays.

Shields of a given stopping power with flat geometry weigh the same regardless of density, but weight can be saved by using high-density materials in curved shields. Openings, thin spots, and curved ducts admit radiation out of proportion to their area.

VERY VULNERABLE (AVOID IF POSSIBLE)

- SCRs (UNPREDICTABLE RESPONSE)
- UNIJUNCTION DEVICES
- OPTICAL SENSORS

VULNERABLE (ALLOW GAIN MARGIN AND/OR SHIELD)

- POWER TRANSISTORS
- LOW FREQUENCY TRANSISTORS (<1 MHz)

GENERAL SUSCEPTIBILITY LEVELS FOR ELECTRONICS

The general susceptibility of electronics for an OPGT-type environment may be broken down into several categories, although accepting these categories without appropriate qualification introduces some element of decision risk. Primarily there are devices that, for the present state-of-the-art, should be categorically rejected. These include SCRs whose performance is unpredictable and unijunction devices which are relatively very vulnerable. Optical sensors are also in the very-vulnerable class. Devices which are graded as vulnerable are power transistors and low-frequency transistors which, if their use is required, should be screened by statistical, electrical, and radiation test response.

SLIGHTLY VULNERABLE (SHOULD CHARACTERIZE)

- INTEGRATED CIRCUITS
- HIGH-FREQUENCY TRANSISTORS
- REFERENCE DIODES
- MICROWAVE DEVICES (NEWER SOLID-STATE DEVICES)
- MOS
- QUARTZ CRYSTAL UNITS

BASICALLY UNAFFECTED

- SIGNAL DIODES
- TUNNEL DIODES
- RESISTORS
- CAPACITORS (WITH QUALIFICATIONS)
- TRANSDUCERS
- MAGNETICS

GENERAL SUSCEPTIBILITY LEVELS FOR ELECTRONICS (CONT)

Slightly vulnerable devices should be usable with slight parameter degradation. These slightly vulnerable devices are the state-of-the-art higher frequency devices, including integrated circuits, reference diodes, MOS devices, and quartz-crystal oscillator units. Finally, basically unaffected, although appropriate precautionary qualifications should be made, are signal diodes, tunnel diodes, resistors, capacitors and magnetics. It must be mentioned that the data on proton effects are sparse and the combined or synergistic effects of total environments are, as yet, essentially uninvestigated.

FILM (TYPICAL)	5 rads
MAN	500 rads
SOLAR CELLS	10^{10} n/cm^2
THERMAL COATINGS	10^{14} p/cm^2
SEMICONDUCTOR POWER DEVICE	10^{11} n/cm^2

GENERAL SUSCEPTIBILITY THRESHOLDS

A number of items are extremely susceptible to radiation and provide special shielding problems if they are to be used.

Film is used as a dosimeter to measure minute quantities of radiation. Its great susceptibility to damage makes it unusable for most radiation environments.

Man must be protected at all stages of a radiation effects program because the lethal whole-body radiation dose is about 500 rads.

Thermal control coatings undergo chemical changes produced by ultraviolet radiation as well as the proton and electron environments. Much research has gone into stable thermal coatings.

SURFACE PHYSICS

FIELD EFFECT DEVICES

BIPOLAR DEVICES

IONIZATION EFFECTS

This and the Displacement Effects section are device-oriented in their presentation of radiation effects. To understand ionization effects, the surface physics of semiconductors is reviewed. Emphasis is then placed on field effect and bipolar devices. Numerous examples based on current technology are presented, together with data on some older devices that more clearly exhibit these effects.

- TRANSIENT DAMAGE EFFECTS
- SURFACE DAMAGE EFFECTS

TYPES OF IONIZATION EFFECTS

The changes in the electrical characteristics of semiconductor devices are the result of two basic effects of the radiation inside and on the surface of the semiconductor material: ionization and displacement. Ionization effects may be further broken down into transient damage effects and surface damage effects. Transient damage effects are temporary changes in the electrical characteristics as a result of ionization in the bulk lattice material. This ionization, or alternately the production of electron-hole pairs, creates photocurrents at semiconductor junctions. For the OPGT, the transient damage associated with steady-state photocurrents during radiation exposure times that are very long compared with the minority carrier lifetime, is the significant mechanism. Surface damage effects are semipermanent changes in the electrical characteristics as a result of charge distributions near the surface or the passivating layer. Because ionization is an intermediate process, and because either effect is proportional to the absorbed dose, the effects per unit of energy absorbed are identical.

- TRAPPED RADIATION BELTS
- RTG GAMMA-RAYS
- SOLAR FLARE PARTICLES
- COSMIC RAYS

SOURCES OF IONIZING RADIATION

The sources of ionizing radiation for OPGT are the trapped radiation belts of the earth and Jupiter, the leakage radiation from the radioisotopic thermoelectric generators, large-scale solar events, and galactic cosmic radiation. These sources have been described in Section I. For the purposes of effect calculations, these sources have been combined into maximum design particle fluence and fluence spectra and gamma ray absorbed dose. The OPGT could experience (1977 JSP mission) an unweighted fluence of 1.0×10^{11} e/cm^2 and 1.0×10^{13} p/cm^2. For equivalent damage one translates these numbers into 3.3×10^{11} e/cm^2 (3 MeV) and 4×10^{12} p/cm^2 (20 MeV). The RTGs produce 1.0×10^{12} n/cm^2 and 1.0×10^4 rads (Si) of gamma rays.

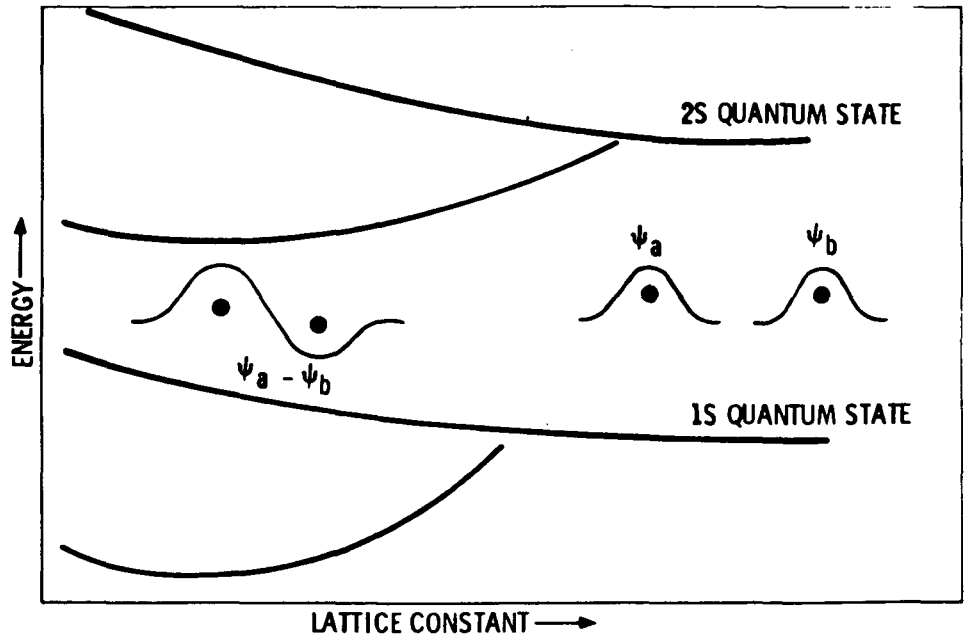

ENERGY BANDS VS. ATOMIC SEPARATION

In the concept of the monoatomic linear lattice and the idea of nearly free (ionization) electrons, the electron motion is perturbed by the periodic potential of the crystal lattice. The solutions to the Schrödinger electron wave equation is a series of standing waves, differing in energy by the interaction of the electron wave function with the positive ion core field. An alternate way to view this situation is to consider two hydrogen atoms in the ground state, initially separated, being brought closer together. As the atoms are brought closer, their wave functions overlap and one has an admixture of states $\psi_a \pm \psi_b$. In the case of $\psi_a + \psi_b$, the electron has a probability of being between the two atoms, increasing the binding energy and depressing the energy level. In the case $\psi_a - \psi_b$, the probability vanishes for the midway position, raising the energy level. Two single discrete levels are split into two energy bands or allowed zones with a forbidden zone, the energy gap, between.

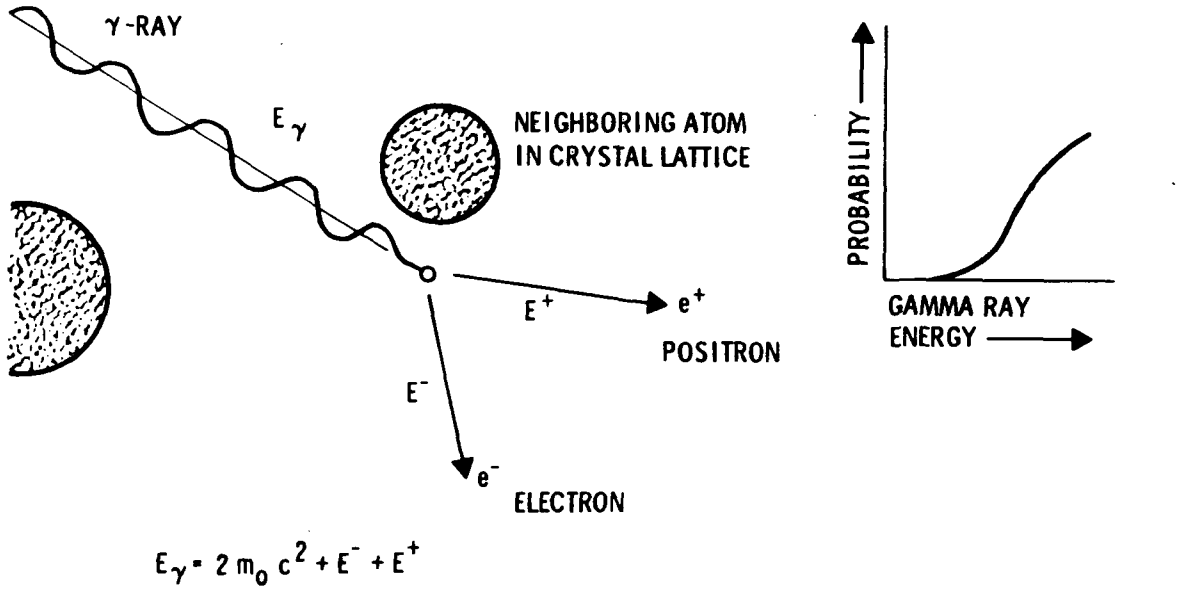

CREATION OF ELECTRON-POSITRON PAIRS

From the operational point of view, the interaction of charged nuclear radiations and photons with matter is the basis of the hypothesis of the existence of the particles. The nature of the interaction depends upon the type of particle and the target as well as the relative kinetic energy. When moving charged paricles interact with matter they lose energy by excitation and ionization of the absorber atoms. Interactions with nuclei are not an important flux-reducing mechanism. Gamma rays are conveniently defined as the electromagnetic radiations that appear following nuclear transitions. Gamma rays interact with matter via three photon absorption processes. These are: 1) the photoelectric effect in which a photon ejects an orbital atomic electron; 2) Compton scattering in which a photon is degraded in scattering by a free electron; and 3) pair production in which the photon is annihilated and a positron-negatron (electron) pair is created.

- ELECTRIC FIELD APPLIED TRANSISTOR-TO-CAN
- CHARGE MIGRATION ACROSS SiO_2
- JUNCTION POTENTIAL PROVIDES STRONG FIELD
- POSITIVE CHARGE BUILDUP AT SiO_2 INTERFACE, INVERTS BASE

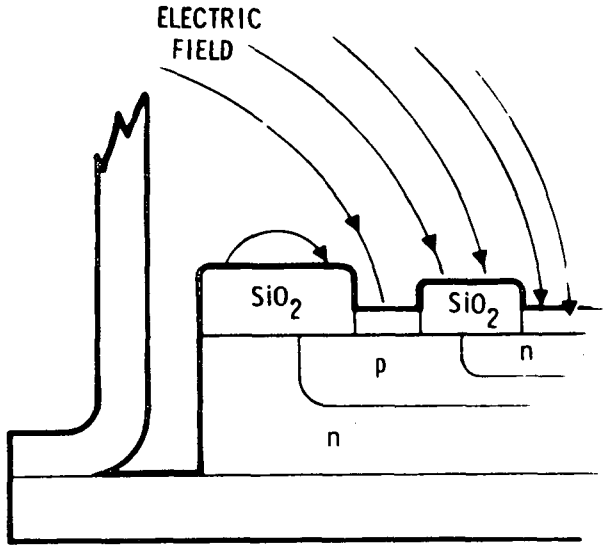

POSITIVE CHARGE DEPOSITION ON SILICON DIOXIDE SURFACE

The failure of several satellites following the Starfish nuclear explosion in July 1962 was related to surface damage effects in transistor collector-base leakage. It was later found that the increase in the collector-base reverse current I_{CBO} was a function of the collector potential. It was also determined that the damage was only semipermanent and that the effect of residual gas in the transistor can was important. Electrical charges in the can are influenced by the existing electrical fields due to junctions and the transistor-to-can field. It is theorized that charge accumulation can invert the silicon in a surface layer. As a result of this a channel is created for junction leakage to increase. For passivated surfaces gain change is found to be more significant than change in collector-base leakage; the effects are more gradual but persist for longer periods of time.

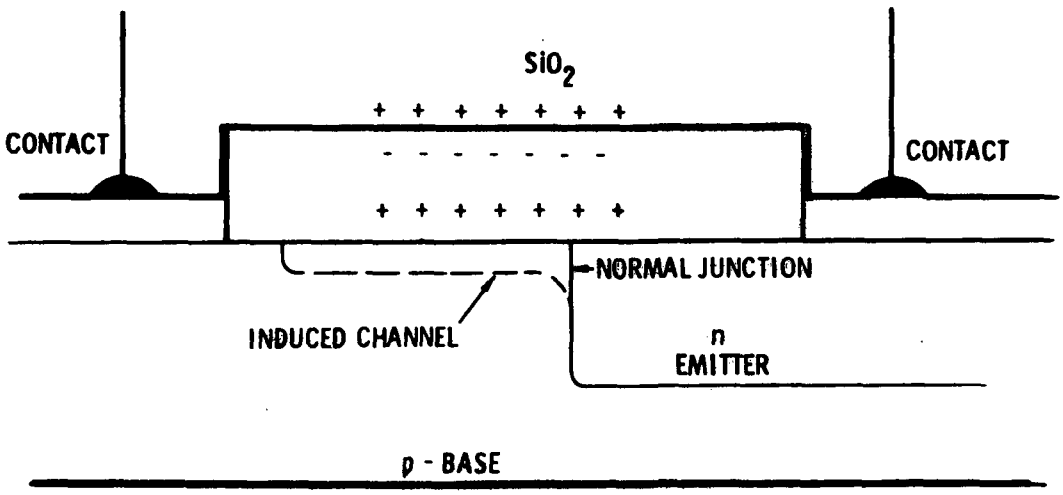

CHANNELING IN BASE

For many devices the transistor can is connected to the collector; therefore, the can-to-base and can-to-emitter voltage differential is about equal to the collector-to-base reverse bias voltage. These fields, together with the junction field, will cause charge migration or electrophoresis toward the base region (NPN configuration).

Accumulation of charge on the surface, limited by the collector-base potential, creates an inversion layer channel which experimentally shows up on some devices at V_{CB} = 6 volts. The assumption is that the surface positive charge has by electrophoresis produced a change in potential at the interface. At this point, a channel has been formed in the base.

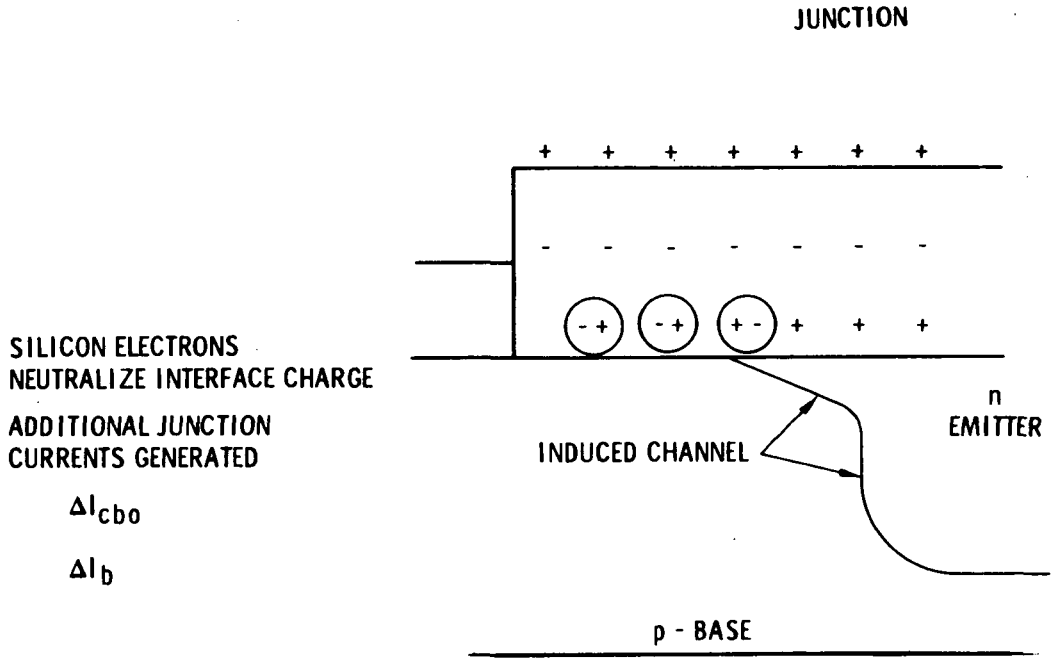

CHANNEL RECESSION

The effect of the channel is modified by the action of electron-hole pairs created in the bulk silicon by the radiation source. The migration of these electrons, whose kinetic energy is sufficient to cross the interface, allows recombination with the positive charge resident on the surface. The effect of this charge neutralization is to allow the channel to recede.

The effects described result in additional base current terms which have at low currents the form

$$I_{BASE} = I \exp (q V/\eta kT)$$

A large increase in junction capacitance is observed when a channel is formed.

$$S = \frac{\text{RECOMBINATION RATE}}{\text{AREA}} \Big/ \text{EXCESS CONCENTRATION ADJACENT TO SURFACE}$$

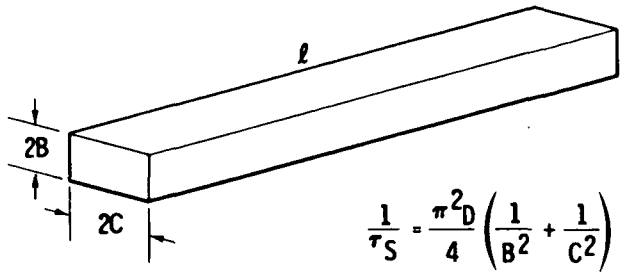

$$\frac{1}{\tau_S} = \frac{\pi^2 D}{4}\left(\frac{1}{B^2} + \frac{1}{C^2}\right) \qquad S \to \infty$$

- HIGHEST S FOR SANDBLASTED SURFACES
- LOWEST S FOR ETCHED SURFACES

SURFACE RECOMBINATION VELOCITY

Experimentally it has been determined that recombination occurs both in the volume and on the surface of the crystal. These terms are combined to yield an observed lifetime τ as follows:

$$\frac{1}{\tau} = \frac{1}{\tau_V} + \frac{1}{\tau_S}$$

The surface recombination is understandably especially sensitive to chemical treatments or mechanical operations. Since carriers must reach the surface to recombine there, the surface lifetime is a function of the geometry of the specimen. The surface velocity of recombination is a convenient quantity inasmuch as it is independent of sample configuration. Shockley has derived equations relating lifetime and surface velocity of recombination for long rectangular rods. The quantity D appearing in the equations is the diffusion constant for the minority carrier which may be obtained from the mobility by Einstein's equation $\mu = kT/eD$.

$$S = \frac{\text{RECOMBINATION RATE}}{\text{AREA}} \Big/ \text{EXCESS CONCENTRATION ADJACENT TO SURFACE}$$

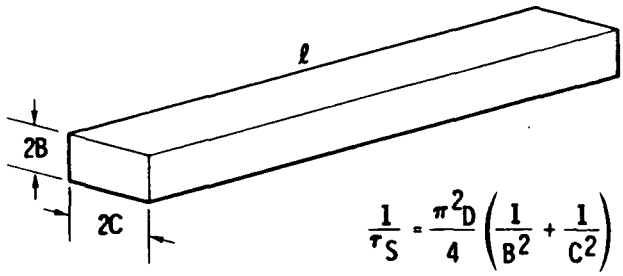

$$\frac{1}{\tau_S} = \frac{\pi^2 D}{4}\left(\frac{1}{B^2} + \frac{1}{C^2}\right) \qquad S \to \infty$$

- HIGHEST S FOR SANDBLASTED SURFACES
- LOWEST S FOR ETCHED SURFACES

SURFACE RECOMBINATION VELOCITY

Experimentally it has been determined that recombination occurs both in the volume and on the surface of the crystal. These terms are combined to yield an observed lifetime τ as follows:

$$\frac{1}{\tau} = \frac{1}{\tau_V} + \frac{1}{\tau_S}$$

The surface recombination is understandably especially sensitive to chemical treatments or mechanical operations. Since carriers must reach the surface to recombine there, the surface lifetime is a function of the geometry of the specimen. The surface velocity of recombination is a convenient quantity inasmuch as it is independent of sample configuration. Shockley has derived equations relating lifetime and surface velocity of recombination for long rectangular rods. The quantity D appearing in the equations is the diffusion constant for the minority carrier which may be obtained from the mobility by Einstein's equation $\mu = kT/eD$.

$$\mu = \frac{\text{DRIFT VELOCITY}}{\text{UNIT ELECTRIC FIELD}}$$

HIGH MOBILITY ⟶ SMALL ENERGY GAP

LOW MOBILITY ⟶ COMPLEX DEGENERATE FORMS OF ENERGY SURFACES

- IN AN IDEAL INTRINSIC SEMICONDUCTOR MOBILITY IS DETERMINED BY LATTICE SCATTERING
- ACTUAL SPECIMENS CONTAIN IMPURITY ATOMS THAT DOMINATE SCATTERING AT LOW TEMPERATURES
- ELECTRON AND LATTICE WAVES INTERFERE

MOBILITY AND ENERGY GAP

A highly purified semiconductor may exhibit intrinsic conductivity in a temperature range in which the electrical characteristics of a semiconductor are not influenced by impurity atoms in the crystal lattice. At temperatures lower than the intrinsic range, the electrical characteristics are determined by the impurities present, a condition referred to as extrinsic conductivity. Intrinsic conductivity is expressed in terms of equilibrium concentrations of carriers and their mobilities

$$\sigma = (n_e \mu_e + n_h \mu_h) |e|$$

By convention, mobilities of electrons and holes are positive with the drift velocities opposite. In a real intrinsic sample some impurity atoms are always present that dominate electron scattering at low temperatures when the crystal thermal vibrations (lattice waves) are minimal. A review of experimental energy gaps shows that small energy gaps are associated with high mobility and small effective masses. Low mobilities are characteristic of holes associated with energy surfaces near the top of the valence band.

- FABRICATION PROCEDURES
- OPERATE DEVICE IN SATURATION MODE
- MODIFY BIASING OF JUNCTIONS
- PERFORM ELECTRICAL SCREENING TESTS
- INTRODUCE DOPING INTO SiO_2
- USE SPECIAL DIELECTRIC MATERIALS

DEVICE HARDENING

Some general hardening principles applicable to bipolar devices have been determined. Operation of devices near their h_{FE} and collector current peak helps the process of radiation annealing by emptying, through thermal dislocation, shallow traps that act as recombination centers for minority carriers. The use of high-frequency devices is effective in that the base transit time is shorter, with less probability of carrier loss. Electrical screening tests on devices in the avalanche breakdown mode have determined that microplasma noise is an effective screening criterion. Noisy NPN and quiet PNP devices are found to be more resistant than their counterparts. Preirradiation exposure to Co^{60} gamma rays, together with screening and annealing, has proven to be effective. Evacuation of transistor cans reduces ionization damage as has been mentioned. The introduction of dopants and the use of special dielectric materials has been found effective.

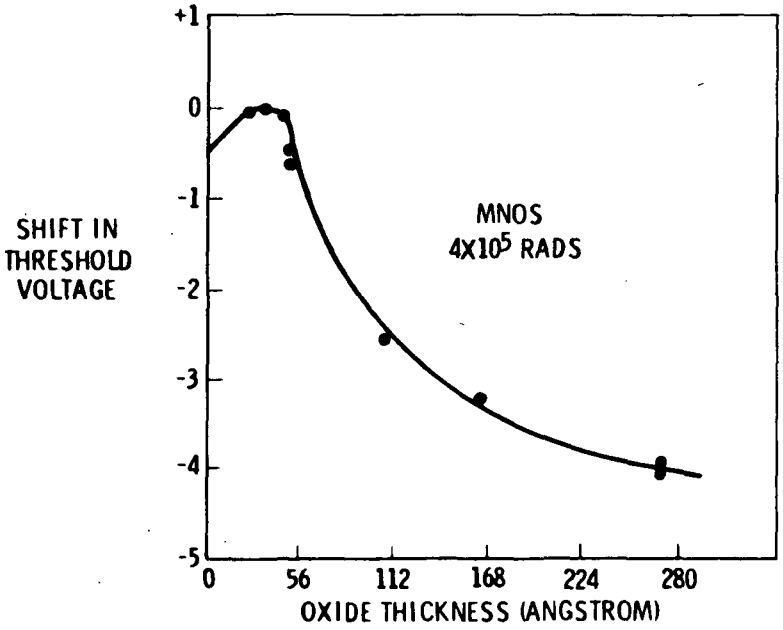

THRESHOLD VOLTAGE SHIFT VS OXIDE THICKNESS

For insulated gate field effect transistors, at the present state-of-the-art, the most significant damage mechanism to metal-oxide-semiconductor field effect transistors is ionization in the oxide. The most sensitive parameter is the gate threshold voltage which often shifts several volts for doses of 10^4 to 10^5 rads (Si) depending on the applied gate bias. Experimentally, several hardening mechanisms have been found such as changing the oxide thickness according to gate bias, or the addition of elemental doping, particularly phosphorus or chromium.

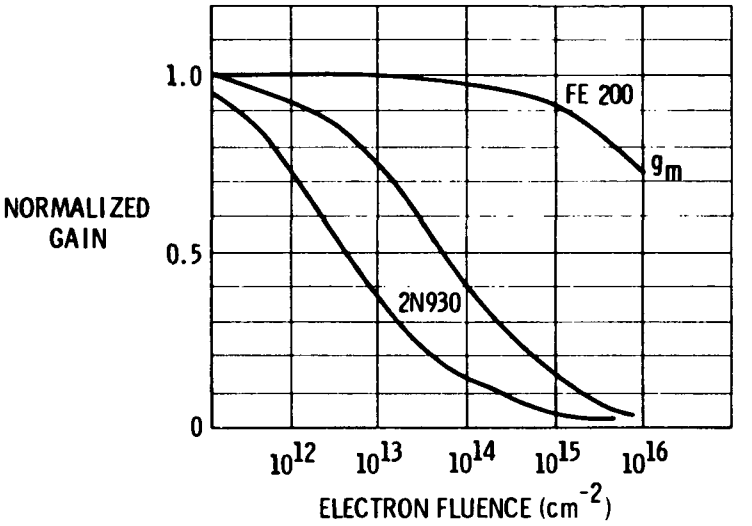

DEGRADATION COMPARISON JFET VS BIPOLAR FOR 1-MeV ELECTRONS

A comparison of the relative tolerance of bipolar and field effect transistors to 1-MeV electrons has been made. Sample lots were 40 units of each field effect silicon transistor and NPN bipolar units with similar low-power, high-gain characteristics. The devices selected were the field effect FE 200 and the bipolar 2N930. Parameters measured included saturation voltage, gain, and reverse-biased junction current. The gain degradation was determined by the measurement of transconductance for the FE 200 and the current transfer ratio for the bipolar. The results demonstrated that the FE 200 was operable at an exposure level 10^3 times that which rendered the 2N930 unusable.

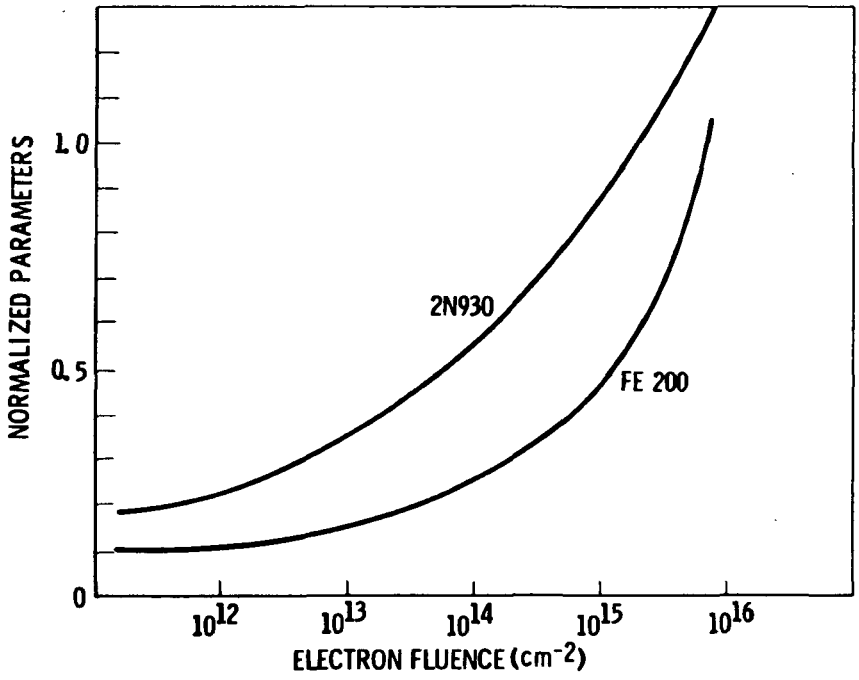

I_{SGO} VS. I_{CBO} FOR 1-MeV ELECTRON IRRADIATION

The 2N930 group tolerated more dose at high collector current but the high input impedance was lost in this operational mode. The increased gate current of the FE/200, assumed due to an increase in recombination states in the reverse-biased junction, was greater than the reverse current of the bipolar. However, the input impedance of the FET-200 was still operationally high. The increase in saturation voltage $V_{CE(SAT)}$ is similar to the decrease of the transconductance of the FET. This may indicate a single operational mechanism, reduction in majority carrier conductivity. As to proton damage, a 2N2497 silicon FET lost only 25 percent of its drain current at fixed voltage after 3.4×10^{13} p/cm^2 whereas bipolar devices with $F_T > 50$ MHz are severely degraded at 10^{12} p/cm^2 at 20 MeV.

- I_{GS} MOST SENSITIVE PARAMETER WITH RAPID DEGRADATION $>10^6$ RADS

- P-CHANNEL JFETs MORE RESISTANT THAN N-CHANNEL DEVICES

JFETS IONIZATION DAMAGE

Current state-of-the-art JFETS are comparable or superior to the best high-frequency (150-MHz) bipolars in radiation sensitivity. P-channel JFETS are more resistant to ionization damage than N-channel units. For displacement damage the opposite is true, so a design decision based on the anticipated environments must be made. The selection of P-channel vs. N-channel JFETs is dependent to some extent on the degree of confidence in estimates of Jupiter's trapped proton environment.

- CHARGE ACCUMULATION IN THE PASSIVATION OXIDE BUILDS UP INVERSION LAYERS IN P MATERIAL
- INVERSION LAYERS CAUSE CHANNEL FORMATION OVER JUNCTIONS
- CHANNEL FORMATION PRODUCES LEAKAGE PATHS
- P-CHANNEL JFETs ARE MORE RESISTANT TO THIS MECHANISM

STANLEY THEORY OF INVERSION LAYERS

A. G. Stanley has theorized that the greater sensitivity of N-channel devices is due to the build-up of inversion layers on the high resistivity P-type material in these devices. Electrophoresis causes charge buildup in the passivation oxide layer. As has been seen, the inversion layers result in channel formation with attendant leakage. This mechanism is less effective in inverting P-type silicon of low-resistivity. As a result, P-channel devices are more resistant to ionization-induced damage. Surface effects are not amenable to prediction, but a general threshold is approximately 10^6 rads (Si), or 10^5 rads for high input impedance functions.

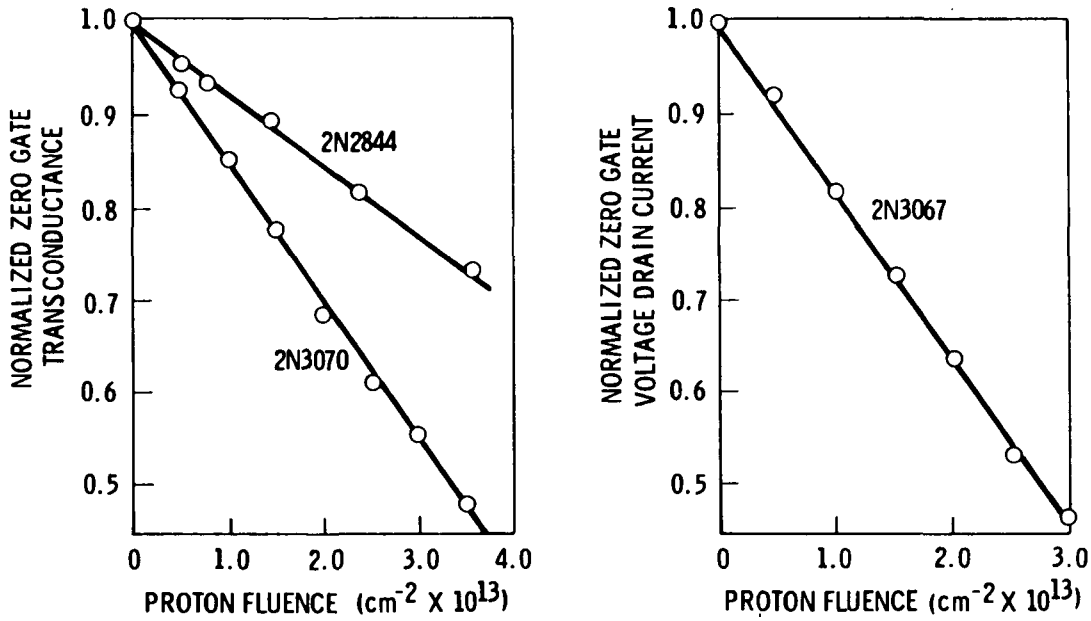

PROTON EFFECTS

In their interaction with matter, protons produce both damage by displacement and ionization. The ratio of damage attributable to each mechanism is a function of the proton energy. At 20 MeV the relative damage displacement to ionization is taken to be 3:1. At 200 MeV this same ratio becomes 5:1, favoring displacement. At 20 MeV, however, a proton is four times as damaging as at 200 MeV. The foregoing data are for germanium. Protons damage JFETs by lowering the transconductance and the drain current. Nominally, a decrease of 30 per cent in these parameters occurred after fluence of 10^{13} p/cm^2 at 22 MeV. A suggested damage model contains a constant showing extensive variation between device types, presumably due to impurities.

- IONIZATION DAMAGE IS THE MOST IMPORTANT DEGRADATION MECHANISM IN MOS FETs

- MOST SENSITIVE PARAMETER IS V_{GT}. SEVERAL VOLT SHIFT AT $\sim 10^4$ - 10^5 RADS FOR COMMERCIAL DEVICES

- DEGRADATION IS A FUNCTION OF APPLIED GATE BIAS DURING IRRADIATIONS

INSULATED GATE FIELD EFFECT TRANSISTORS

It has been found that the damager to MOS FET devices is due almost entirely to ionization. For these devices, damage correlation using stopping power tables has shown that by converting exposures of particles (fluence) to absorbed dose (rads) moderate agreement can be found for different particulate radiations. Degradation of biased units shows saturation properties at high radiation levels $> 10^6$ rad. Further damage can be related to bias level during the duty cycle.

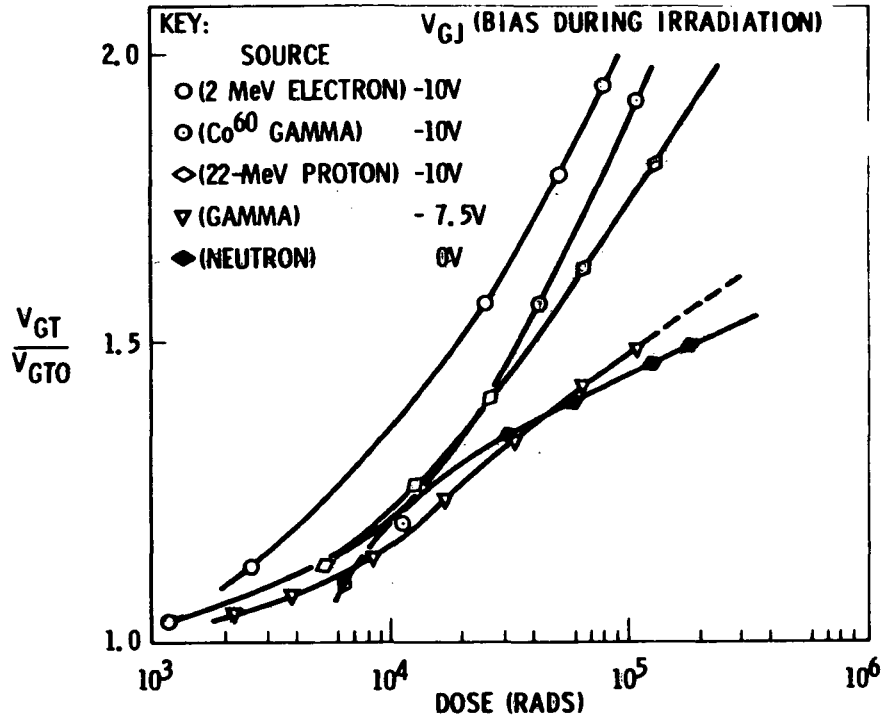

RELATIVE EFFECTIVENESS OF RADIATION FOR DAMAGE TO MOS FET DEVICES

By converting charged particle fluence to absorbed dose by use of the stopping power tables, and converting neutron fluence for typical reactors from the gamma dose to absorbed dose, damage to the gate threshold voltage for some older MOS FETs is seen to be nominally specific to dose. In fact, the curves are ordered exactly according to the ionization/displacement effects ratio, that is, electrons, gamma rays, protons, and neutrons in order of decreasing effect on the MOS FET threshold voltage.

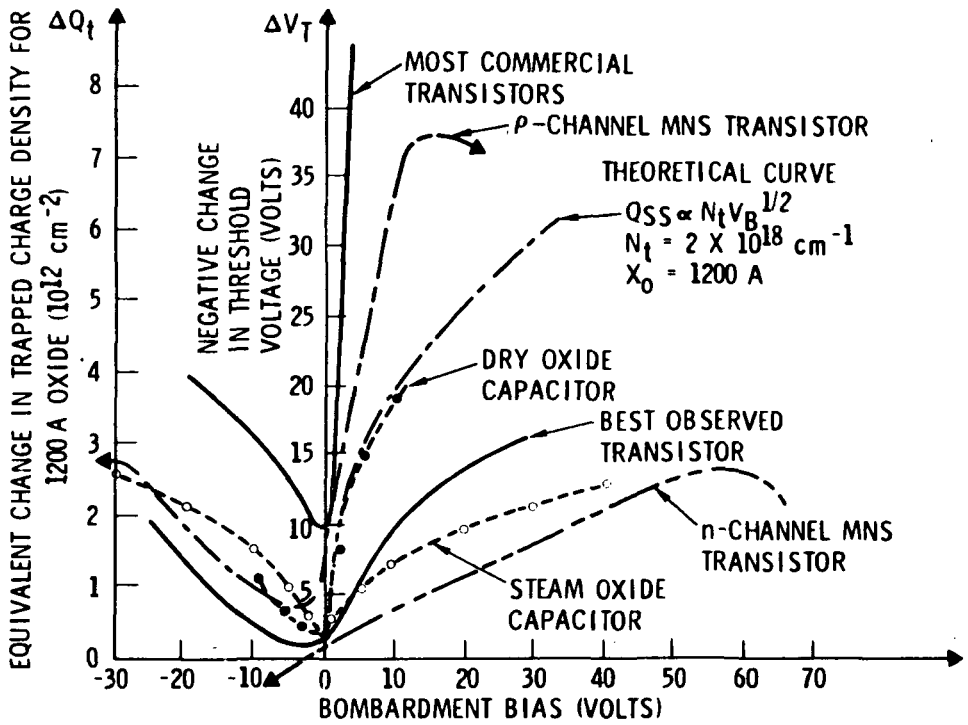

THRESHOLD VOLTAGE SHIFT VS. BOMBARDMENT BIAS

The change in trapped charged density and gate threshold voltage for MOS transistors is dependent on the insulator material, construction technique, thickness, and voltage bias during irradiation. Most commercial devices enhibit unacceptable parameter changes at low levels of ionizing radiation. Recent advances in construction processes and materials have resulted in significant hardness advances. The threshold voltage shift and the equivalent change in trapped charge density (in a 1200-A oxide thickness) are plotted here vs. bombardment bias for several transistors and capacitors.

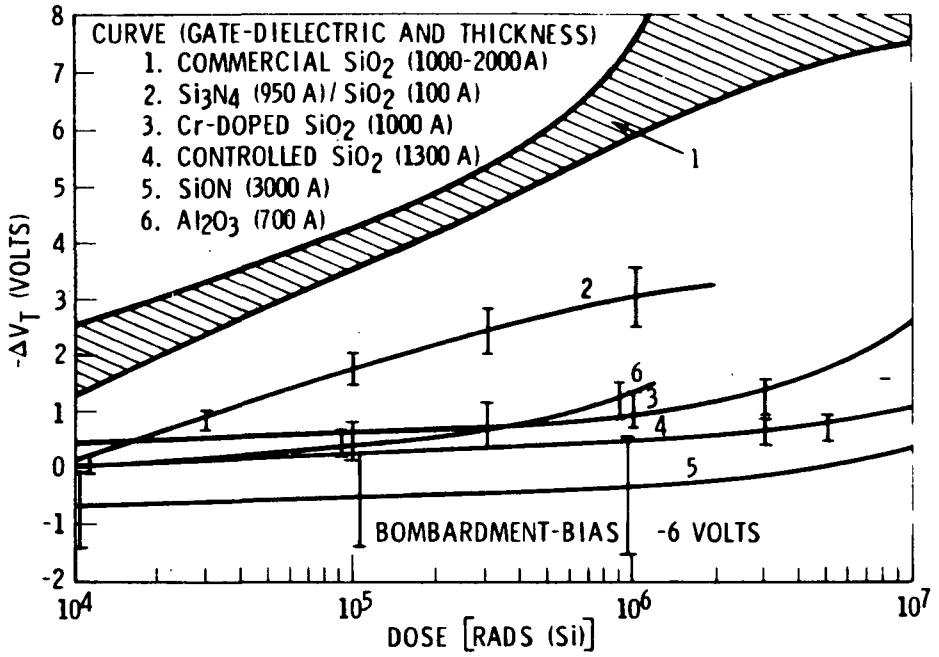

THRESHOLD VOLTAGE SHIFT VS. IONIZING DOSE

Commercial MOS devices with silicon dioxide gate dielectric thicknesses from 1000 to 2000 A (shaded region) exhibit unacceptable threshold voltage shifts (in excess of about 3 volts) at ionizing radiation doses from 10^4 to 10^5 rads (Si). Other dielectric materials and doped SiO_2, as well as SiO_2 deposited under carefully controlled conditions, limit the voltage shift to acceptable values at doses as high as 10^7 rads.

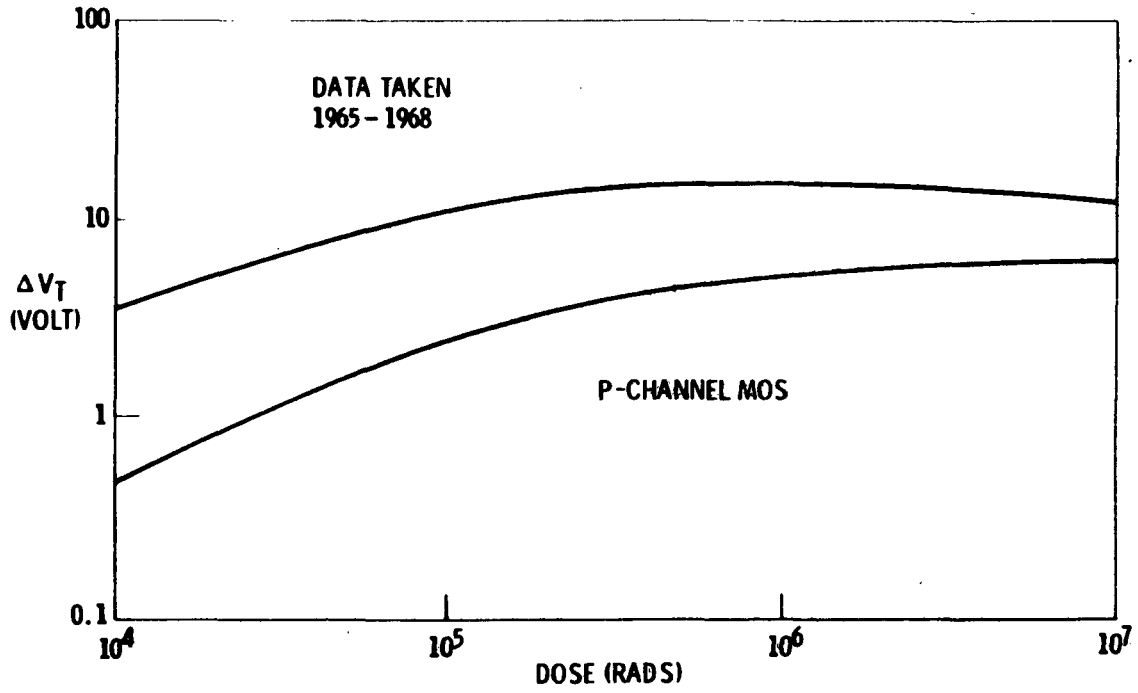

RANGE OF THRESHOLD VOLTAGE SHIFT VS. RADIATION

An interesting plot of experimental data on threshold voltage shift vs.dose for ten P-channel MOS transistors with SiO_2 insulators, taken between 1965 and 1968, shows upper and lower limits for the shift. At an absorbed dose of one megarad, a factor of two exists between upper and lower limits. At lower exposures the spread is greater, and at higher dose the spread decreases. The data were taken with a gate bias (i.e., oxide field) applied during the course of the radiation. Above the 1×10^6-rad-level the upper-limit damage level is slightly decreasing. Data for more recent MOS devices will be presented in the Hardening section.

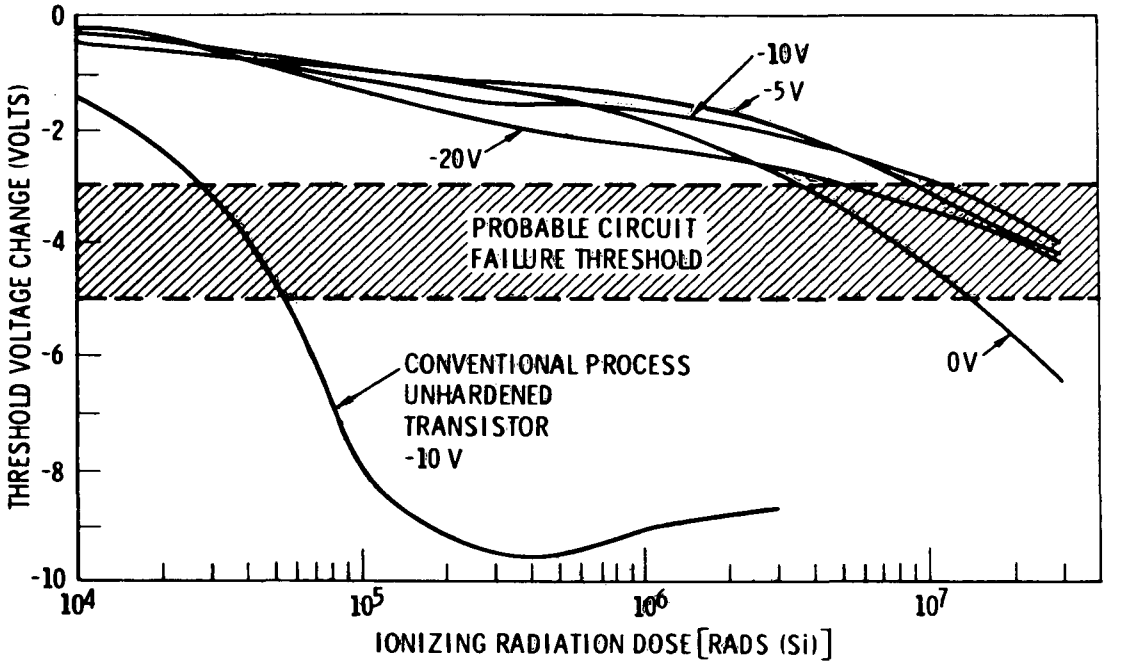

THRESHOLD VOLTAGE SHIFT VS. GAMMA RAY DOSE

Fabrication techniques that appear to increase the ionizing radiation resistance of insulated gate devices to Co^{60} gamma rays, have led to improvements over commercial devices. Assuming a circuit failure threshold of ΔV_T = -3 volts, commercial device failure occurs at a level of about 2 x 10^4 rads (Si). Improved devices show a shift of about -3 volts at an absorbed dose near 10^7 rads (Si), with greatest radiation resistance being achieved at intermediate gate bias voltages (-5 to -10 volts).

- THERMALLY GROW CLEAN SiO_2
- DOPE SiO_2 WITH Cr
- Si_3N_4 DIELECTRIC
- Si_3N_4-SiO_2 SANDWICH
- SiON

RADIATION HARDENING OF IG FETs

Various methods have been tried in order to improve the radiation performance of IG FETs. Some of these methods are (1) growing clean silicon dioxide by thermal process, (2) doping SiO_2 with chromium, (3) using a silicon nitride dielectric, (4) using a sandwich construction of silicon nitride and silicon dioxide, and (5) using silicon oxynitride.

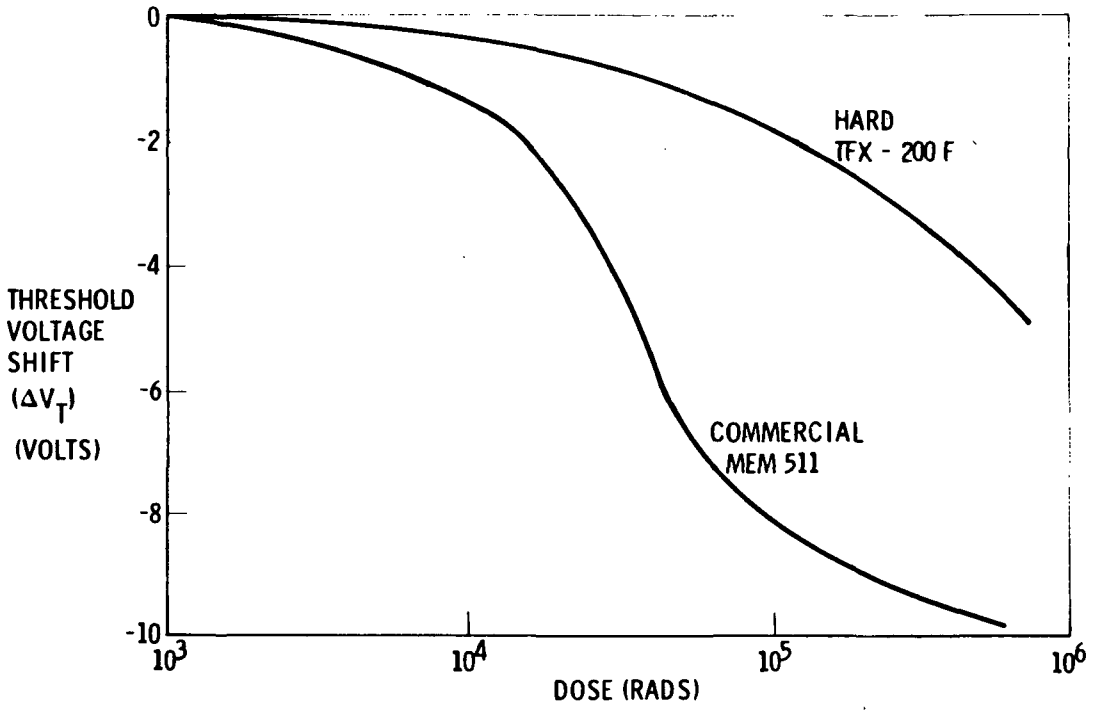

HARDENED MOS FET THRESHOLD VOLTAGE SHIFT

It appears that the introduction of phosphorus into the insulator has a significant hardening effect on MOS FETs. Although the effect is not explainable at the present time, it is theorized that the role of the phosphorus may be to act as a getter for impurities in the oxide that contribute to charge trapping. Composite dielectric structures that resist the devitrification-compaction-bond-breakage chain leading to interface states have been suggested. Silicon nitride with chromium doping is one scheme that has been proposed. Hardening of TFX-200F devices produced significantly harder devices than those commercially available; however, a duplicate process failed to reproduce the initial results by a wide margin, although the duplicate MOS FETs were somewhat superior to commercial devices.

- BIPOLARS SENSITIVE TO IONIZING RADIATION
- CURRENT GAIN h_{FE} DECREASES
- JUNCTION LEAKAGE CURRENTS INCREASE
- SATURATION VOLTAGE $V_{CE(SAT)}$ INCREASES
- BREAKDOWN VOLTAGE BV_{CBO} INCREASES

BIPOLAR DEVICE EFFECTS

Transient ionization damage effects of concern to OPGT are the steady-state photo-currents created for exposure times long compared with the minority carrier lifetime. The carrier generation rate in silicon may be determined from the radiation rate and the effective volume as

$$I = q\,g\,\frac{d\gamma}{dt}\,V = GV$$

Here g is the radiation carrier generation constant which in silicon is 4×10^{13} carriers/cm^3-rad, and G is the generation rate of bulk current equal to 6.4×10^{-6} A/cm^3 - rad/sec. It is only necessary to determine the effective volume over which all carriers generated can diffuse to the junction before recombining. Under irradiation, free electrons and holes are liberated within the semiconductor material. While majority carriers are trapped by the junction fields, the minority carriers are carried across the emitter-base or collector-base junctions creating a primary photocurrent. Any additional current due to transistor action is called secondary photo-current.

EXACT MECHANISM OF SURFACE DAMAGE IS NOT WELL UNDERSTOOD

MODEL:

- IONIZATION PRODUCES RECOMBINATION SITES AND TRAPPING CENTERS AT INTERFACES
- RADIATION BREAKS CHEMICAL BONDS AND DEVITRIFIES SILICON DIOXIDE
- BROKEN BONDS BECOME SITES TO HOLD POSITIVE CHARGE
- POSITIVE CHARGE MODIFIES SURFACE POTENTIAL
- MODIFIED POTENTIAL AFFECTS SURFACE RECOMBINATION

MECHANISM OF IONIZATION EFFECTS IN BIPOLAR DEVICES

It has been noted that ionization effects on current gain are a function of the operating conditions of the transistor during irradiation. Although protons produce primarily displacement damage, protons are also strongly ionizing leading to significant surface damage. The approximate ionization dose in silicon can be determined from

$$1 \frac{\text{proton}}{\text{cm}^2} \text{ (8 to 17 MeV)} = 5 \times 10^{-7} \text{ rads}$$

$$1 \frac{\text{proton}}{\text{cm}^2} \text{ (100 MeV)} = 1 \times 10^{-7} \text{ rads}$$

Some measurements indicate that proton irradiation causes anomalously high damage in NPN transistors, as compared with equivalent dose damage from gamma rays or electrons. In passivated silicon devices leakage current changes are usually not significant as compared with changes in gain.

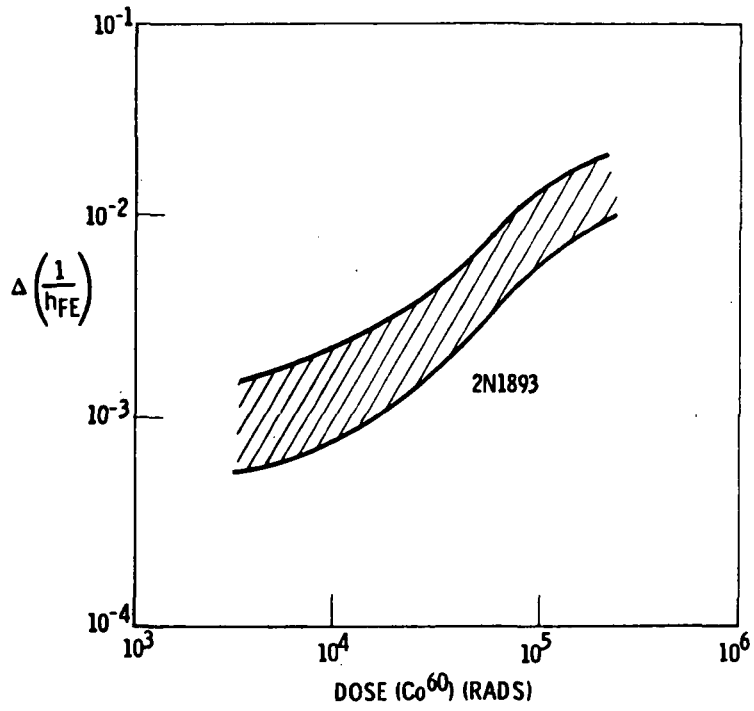

TRANSISTOR IONIZATION DAMAGE

A typical gain shift curve for soft transistor ionization damage vs. radiation dose shows a one-decade increase in $\Delta(1/h_{FE})$ for an increase in dose from 10^4 to 10^5 rads (Si) from a Cobalt-60 gamma source (data for 2N930, 2N1893, 2N2946). For these devices, if one considers the envelope formed by device-to-device variation for the same transistor, then it appears immaterial whether or not the device is passive or has collector bias and is drawing current. This is true because the variation due to operating condition is within the envelope limits of device variability.

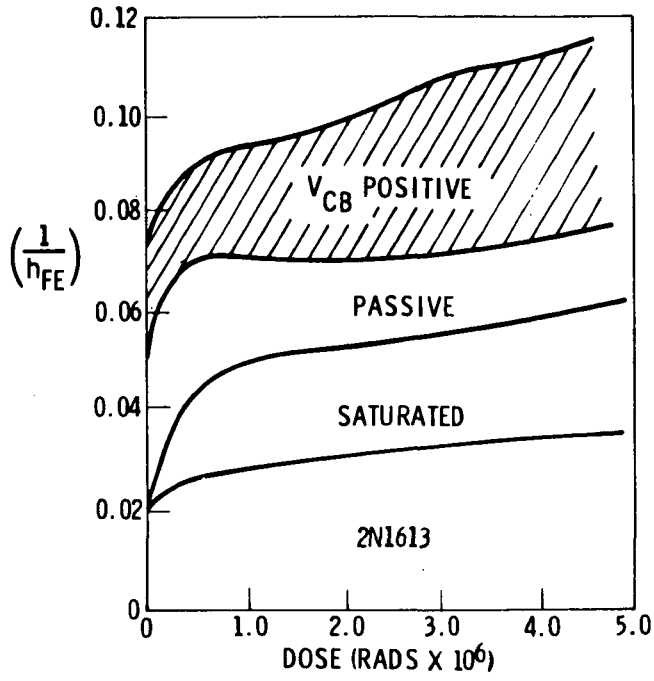

TRANSISTOR SURFACE DAMAGE VS. OPERATING CONDITION

The loss of gain for silicon dioxide passivated transistors is a most important surface damage effect. A detailed view of damage vs. operating conditions should reveal the damage to be a function of the base junction voltages. It has been reported that the change in gain decreased with forward biasing and increased with reverse biasing either junction. The maximum effect is observed with a collector-base reverse bias of approximately 12 volts for a 2N1613 transistor. The operation of a transistor with a high duty cycle for saturation conditions will show less damage than a similar device operating as cutoff or active. The gain change for the 2N1613 occurs at $<10^6$-rad dose, leveling out significantly thereafter.

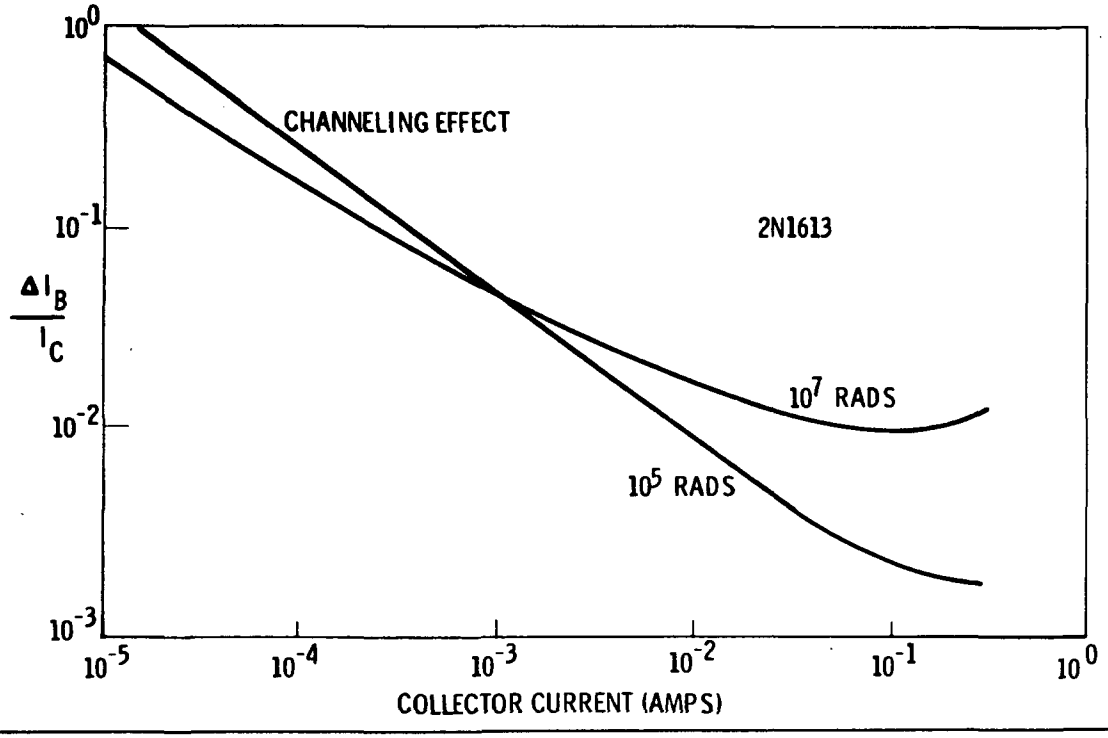

CHANNELING EFFECTS IN SURFACE DAMAGE

The effect of a channel on the gain of a device may be significant at low levels, maximizing for a dose of about 10^5 rads, but at higher radiation levels the channel will recede. For circuits operating at low collector currents, the gain at low exposure could be quite different if channeling were present, whereas at higher exposure the response would be nearly independent of channeling. At high collector currents there is an increase in damage from a base current due to holes from the base injected into the emitter (NPN) near the passivation interface. This source of base current is called the inverse diffusion component.

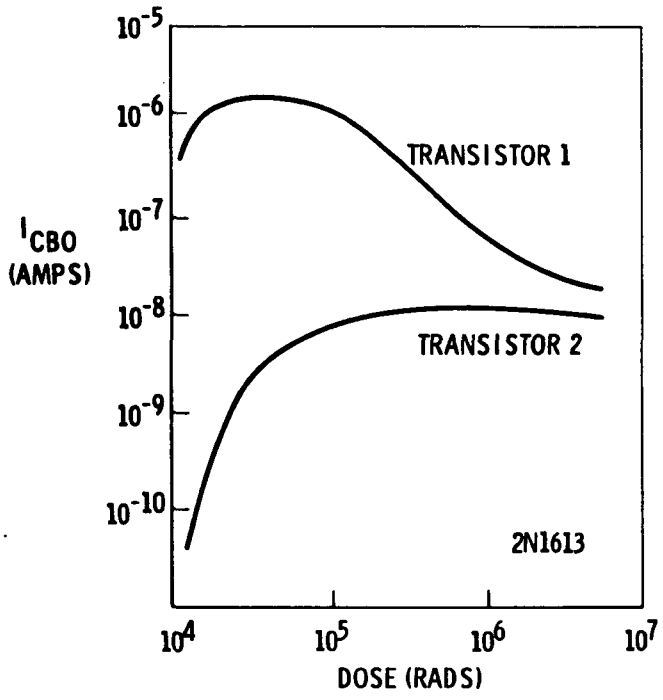

DEVICE ITEM VARIABILITY FOR TWO 2N1613 TRANSISTORS

On an absolute current basis, the effect of ionizing radiation on the junction leakage of a transistor is very small, although the effects are very large relative to the initial leakage. Two specimens of the same transistor device may show very different leakages at low exposures, presumably due to local defect sites contacted by the channel. The effect on circuit design is probably insignificant inasmuch as must devices show typical leakages $\sim 10^{-8}$ ampere.

Mesa transistors are particularly variable and show unpredictable response to ionizing radiation, and should not be used where surface damage effects must be considered.

"Page missing from available version"

CURRENT GAIN REDUCTION

FIELD EFFECT DEVICES

BIPOLAR DEVICES

DISPLACEMENT EFFECTS

The predominant effect of radiation-induced lattice displacements is a reduction in current gain in active semiconductor devices. This and other displacement effects are illustrated by examples from current and--where necessary to show the effects--earlier device technology. Both field effect and bipolar devices provide such examples.

SIMPLE DEFECTS

- INTERSTITIAL ATOMS
- VACANCIES - DIVACANCIES
- FRENKEL DEFECTS

DEFECT CLUSTERS

- SEVERAL HUNDRED ATOMS MAY BE INVOLVED

GENERAL TYPES OF DEFECTS

The general types of displacement defects have been examined in Section II, but are listed here for review; they include interstitial atoms, vacancies, and combinations (e.g., Frenkel defects). All of these involve only a few atoms and are described as simple or point defects. In addition, defect clusters, which may involve several hundred atoms in a highly disordered region, result from thermal or displacement spikes. If an atom is "placed" at one of the interstices of a silicon crystal lattice the energy of the crystal is increased by the energy of formation of the interstitial atom. Similarly, removal of an atom from the lattice raises the energy of the crystal, usually by a lesser amount. For any real crystal, at any temperature, an equilibrium concentration of defects exists and is determined by the energy of formation. Point defects are usually mobile. An interstitial atom sits in a potential well of depth w and executes thermal vibrations. The frequency with which an interstitial jumps to another site is $\sim 10^{-13} \exp(-w/kT)\ \text{sec}^{-1}$.

- CREATION OF NEW LEVELS IN THE FORBIDDEN ENERGY GAP
- NEW LEVELS AS RECOMBINATION AND GENERATION SITES
- EFFECTS ON THERMAL CONDUCTIVITY, CARRIER MOBILITY, MINORITY CARRIER LIFETIME

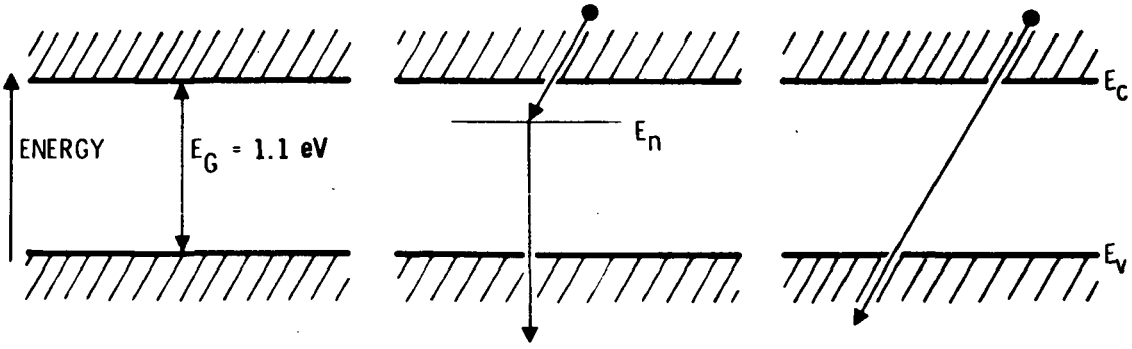

EFFECTS OF DISPLACEMENT DAMAGE

The creation of new energy levels in the forbidden energy gap modifies the electronic properties of the conductivity, carrier mobility, and minority carrier lifetime of a semiconductor material. This is true because an electron can now be liberated from the valence band into the conduction band via the defect level in two small energy steps, rather than one large one. The exponential form of the electron energy distribution implies that the former event is much more probable than the latter. Thus, the rate of generation of electron-hole pairs is directly proportional to the number of defects in the crystal. The reverse process (recombination) shows a similar effect. Therefore, at thermal equilibrium the minority carrier concentration will not change. The evaluation of the non-equilibrium behavior of minority carriers will illustrate the effect of displacement radiation on carrier lifetime and recombination.

$$\frac{\text{RECOMBINATION RATE}}{\text{CARRIER}}: R = R_0 + k\phi$$

IMPURITY CONCENTRATION: $N = N_0 - \left(\frac{dN}{d\phi}\right)\phi$

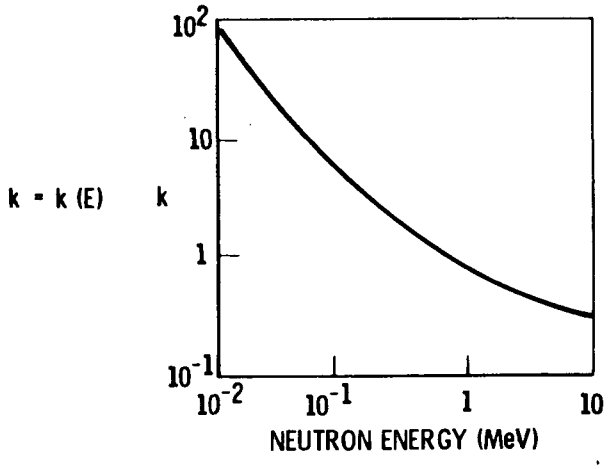

NEUTRON DISPLACEMENT DAMAGE

Inasmuch as the defect damage production is proportional to the radiation exposure, the recombination rate per carrier can be expressed as $R = R_o + \Delta R = R_o + K\phi$ where K is a so-called radiation damage constant. In reality, it is a function depending on particle type and energy, time, temperature, carrier concentrations, etc. For typical transistor doping levels, operating conditions, and neutron exposures, $K = 10^{-6}$ cm^2/n-sec. For a fluence of 10^{12} n/cm^2, one may calculate the increase in recombination rate for silicon transistors

$$R = R_o + K\phi = 1 \times 10^7 \text{ sec}^{-1} + (10^{-6} \text{cm}^2/\text{n-sec})\,(10^{12} \text{ n/cm}^2)$$
$$= 1.1 \times 10^7 \text{ sec}^{-1}$$

i.e., the neutrons have increased the recombination rate by 10 per cent and decreased the minority carrier lifetime by the same factor.

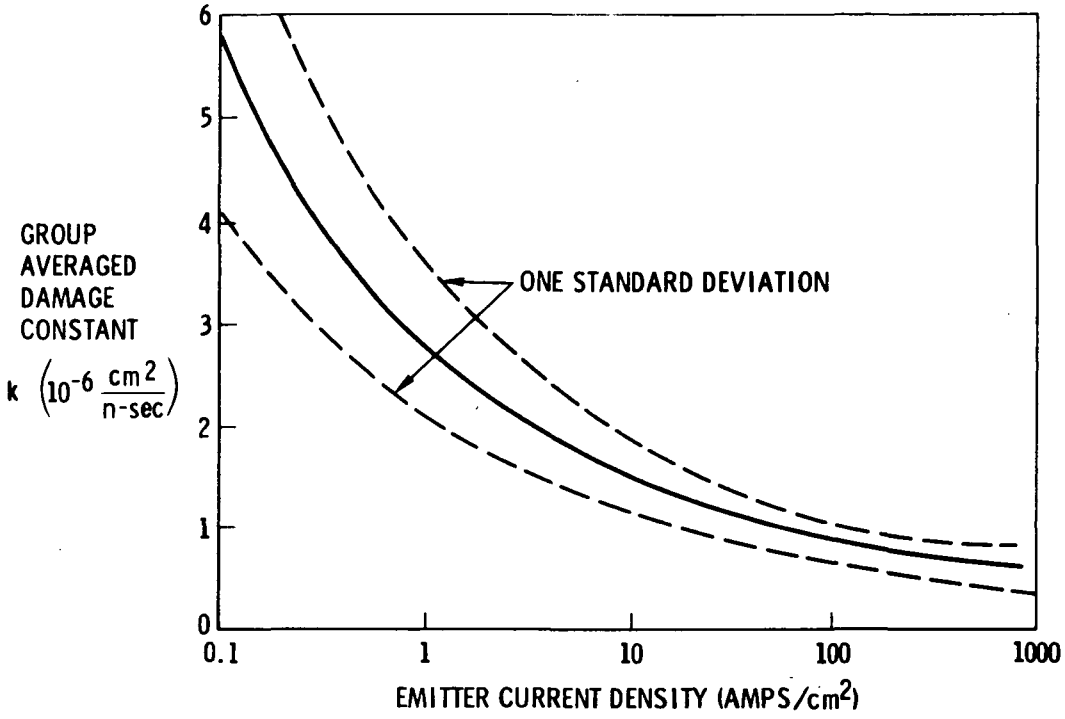

AVERAGE DAMAGE CONSTANT FOR NPN TRANSISTOR TYPES

A composite damage constant for NPN transistors (for seven manufacturers) with large difference factors in transit times (70), and emitter areas (1400), has been formulated as a function of current density (emitter current divided by the physical area of the emitter). The same curves can be used for PNP transistors by increasing the NPN values by a factor of approximately 1.4. The decrease of K at higher emitter current densities is due to thermal annealing effects.

I (mA)	$1/h_{FEO}$	K (10^{-6} cm^2/n-s)	$tk\phi$	$1/h_{FE}$
100	0.020	0.9	0.001	0.021
10	0.020	1.6	0.002	0.022
1.0	0.033	2.9	0.004	0.037
0.1	0.062	5.9	0.007	0.069

CALCULATION OF NPN TRANSISTOR GAIN DEGRADATION AFTER EXPOSURE TO 10^{12} n/cm^2

Using the data of damage constant variation vs. current density the degradation from a exposure of 10^{12} n/cm^2 may be determined for various emitter current densities. The gain degradation equation may be expressed as

$$\frac{1}{h_{FE}(\phi)} = \frac{1}{h_{FE}(0)} + tK\phi$$

For a 1-ma collector current $K = 2.9 \times 10^{-6}$ cm^2/n-sec and, assuming a base transit time of $t = 1.2 \times 10^{-9}$ sec,

$$\frac{1}{h_{FE}(\phi)} = 0.037$$

This represents a gain change from an initial value of 30 to 27.

I (ma)	$1/h_{FEO}$	$1/h_{FE}$
100	0.020	0.030
10	0.020	0.040
1.0	0.033	0.073
0.1	0.062	0.132

NPN TRANSISTOR GAIN DEGRADATION AFTER 10^{13} N/CM^2

A standard radiation testing procedure is to expose certain samples to ten times the expected fluence. The degradation of NPN transistors after exposure to 1×10^{13} n/cm^2, ten times the expected OPGT fluence, is indicated here.

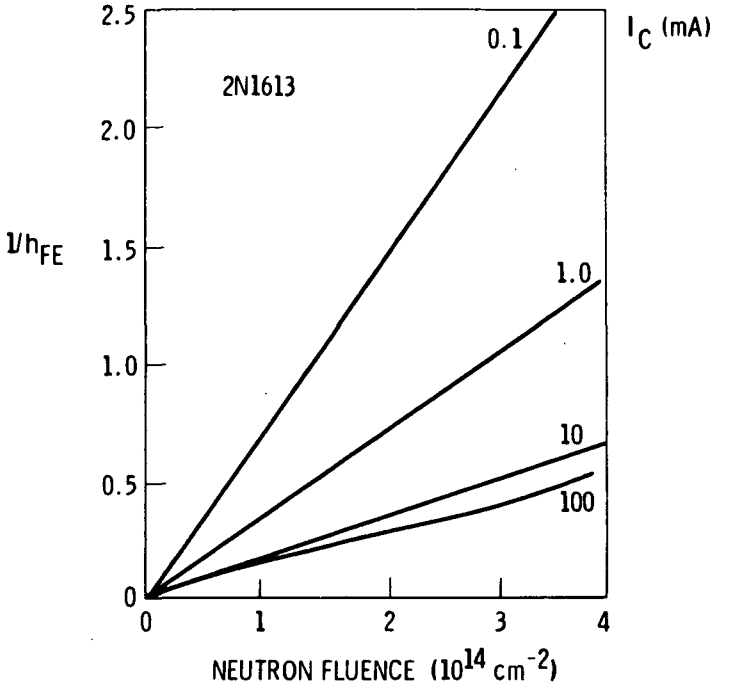

TRANSISTOR GAIN AND NEUTRON EXPOSURE FOR VARIOUS COLLECTOR CURRENTS

Experimental data on transistor gain vs. neutron fluence for the 2N1613 transistor show strong dependence on collector current. For a radiation exposure of 2×10^{14} n/cm^2, operating at a collector current of 10 mA, the residual gain is approximately 3. Transistors that have a lower base transit time and higher current density should show superior radiation resistance. The 2N914 transistor, under the same neutron exposure as the 2N1613, would have a residual gain of about 6 for the same collector current. Superior in resistance to either of the above is a 2N709, a fast switching transistor for microelectronic digital circuits, with a base transit time of 0.2 ns and a gain-bandwidth product of about 800 MHz. The 2N709 has a residual gain of about 20 after 2×10^{14} n/cm^2 and still has tolerable gain (about 6) after 10^{15} n/cm^2.

- COST AND TIME CONSIDERATIONS LIMIT THE AMOUNT OF USEFUL TEST INFORMATION

- SMALL SAMPLE STATISTICS (STUDENT'S t DISTRIBUTION) CAN BE USED TO MAKE STATISTICAL INFERENCES

- THE DISTRIBUTION OF THE TEST STATISTIC

$$t = \frac{\bar{y} - \mu}{S/\sqrt{n}}$$ IS APPROPRIATE

GAIN DEGRADATION AND SMALL SAMPLE STATISTICS

It is frequently the case that considerations of cost, available time and other factors limit the size of a test sample. Statistical inference concerning population parameters for small sample sizes (N = 30 is the usual dividing line between large and small sample sizes) requires a special test statistic, t, known as Student's t distribution. The Student's t is the arithmetic mean of a set of n measurements minus the population mean, divided by the ratio of the sample standard deviation to $\sqrt{n}$. Critical values of t which separate the acceptance and the rejection regions for the statistical test at various confidence levels have been extensively tabulated. The risk for making an incorrect decision for the hypothesis to be tested may be evaluated. A decision table may be made and two types of errors may arise. Type I errors, or rejecting the hypothesis when it is true, are readily calculable. Type II errors, or accepting the hypothesis when it is false, are very difficult to calculate.

$$X = \frac{\text{STANDARD DEVIATION OF k}}{\text{MEAN VALUE OF DAMAGE CONSTANT}}$$

GAIN DEGRADATION AT CONFIDENCE LEVEL t MAY BE EXPRESSED

$$(1/h_{FE} - 1/h_{FEO}) < t_b \bar{k} \phi (1 + tX)$$

WHERE

N	t*
4	1.48
5	1.44
6	1.42
8	1.38
10	1.36
20	1.32
30	1.31

*t FOR 90% CONFIDENCE LEVEL

COEFFICIENT OF VARIATION

Small sample methods may be used to calculate the gain degradation for a transistor at a given confidence level. If a coefficient of variation is defined as the ratio of the standard deviation of the damage constant to its mean value, then the gain shift must be less than the $t_B K\phi$ damage term augmented by the damage term times the coefficient of variation times the test statistic. In a particular example of a lot size of ten NPN transistors, the gain degradation at the 90-per cent confidence level would be given by

$$(1/h_{FE}) = t_B K\phi (1 + tX) = 0.14$$

This is the reciprocal gain change for NPN transistors operating at an emitter current density of 100 A/cm^2 after a neutron exposure of 10^{14} n/cm^2.

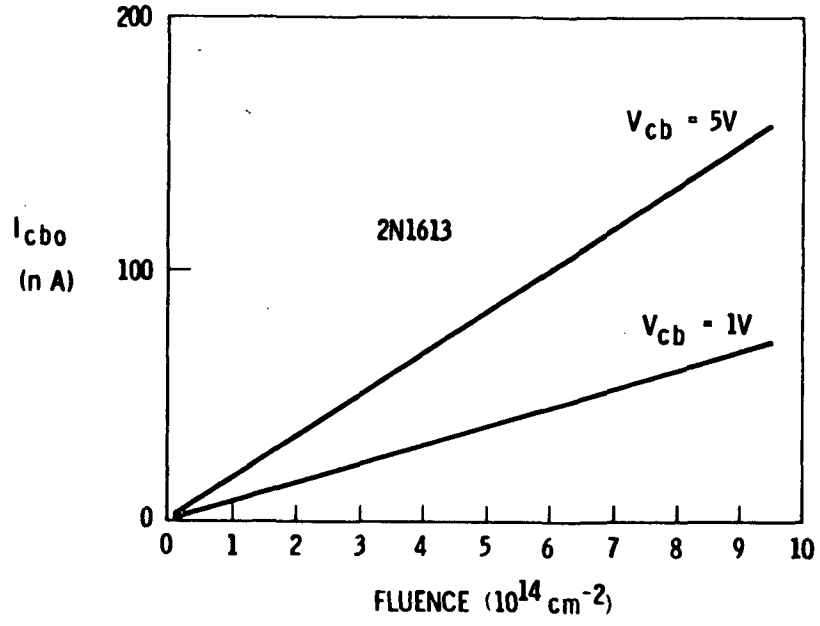

COLLECTOR BASE REVERSE CURRENT LEAKAGE VS. NEUTRON FLUENCE

Carrier generation in the depletion layer of a transistor is taken to be a source of junction leakage. Defects created by displacement damage in the junction increase the leakage. As has been noted, the collector base junction leakage may be calculated directly using the junction volume and the generation rate. The generation rate is obtained from the damage coefficient and exposure fluence. The results of calculation are nearly correct for mesa transistors but a leakage correction factor as a function of collector voltage for planar transistors is required. Plotting experimental data for I_{CBO} as a function of neutron fluence gives a linear relationship with exposure, indicating that the radiation damage is a displacement effect rather than surface damage. Most accurate predictions are for larger transistors operating at higher operating currents.

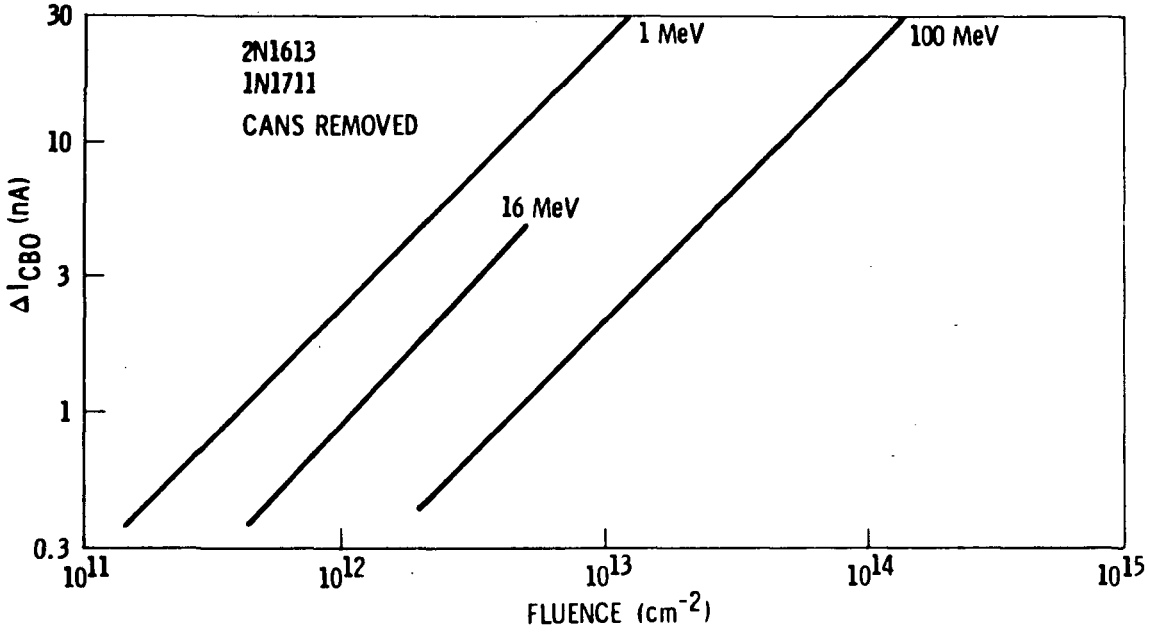

LEAKAGE CURRENT VS. PROTON FLUENCE

Leakage currents are not readily predicted since the leakage is strongly influenced by surface effects. Data on ΔI_{CBO}, as a function of proton fluence, plots reasonably linearly on log-log paper for a given V_{CB} even for some different devices. Tests with 2N1613, 2N1711, and 2N2219 show almost identical leakage current slope vs. proton fluence, as well as the same energy dependence at three different proton energies (1, 16, and 100 MeV). An interesting observation for proton damage, made during studies with solar cells, is that 100-MeV protons and fission neutrons cause about equivalent damage.

$$I = q\,[\text{VOLUME OF JUNCTION}] \times [\text{GENERATION RATE}]$$

$$R = R_0 + \Delta R = R_0 + k\phi$$

FOR OPGT $\phi = 10^{12}$ n/cm^2

$$I = a\,[AX]\,[n_i(R_0 + k\phi)]$$

$$I = 0.7 \text{ nA}$$

CALCULATION OF JUNCTION LEAKAGE

The calculation of junction leakage is readily accomplished for the 2N1613 transistor for any exposure and any collector to base potential. For 10^{12} n/cm^2 the result is 0.7 nA which, for a reverse bias of 5 volts, should be multiplied by 1.3 as a planar correction factor. At higher exposure, say a fluence of 10^{15} n/cm^2, the leakage, after correction, is about 100 nA. The problem of junction leakage at this level is probably not a serious one to circuit operation.

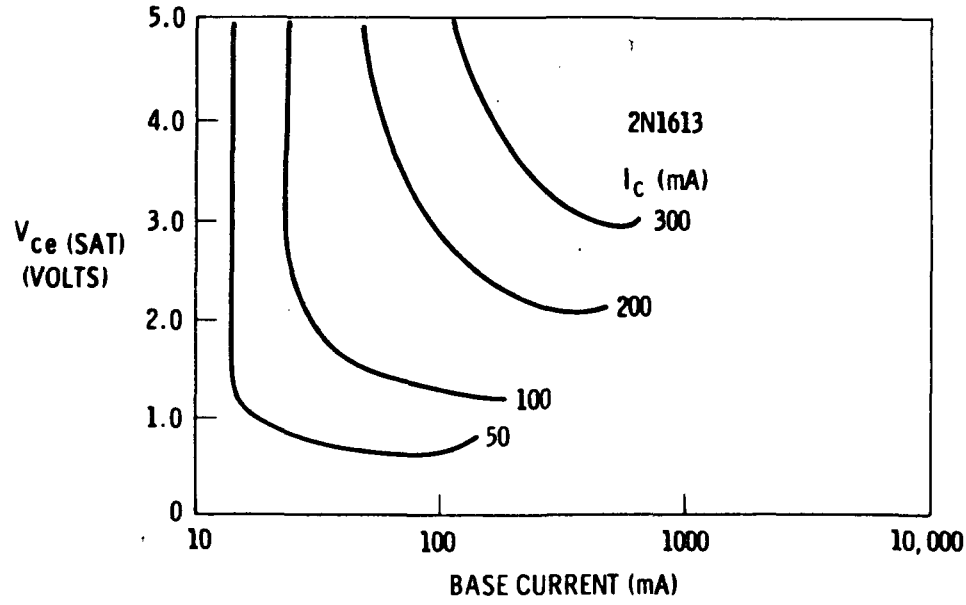

SATURATION VOLTAGE AFTER 10^{14} N/CM^2 VS. COLLECTOR CURRENT

For power transistors operating in a neutron environment the change of the saturation voltage is the most significant radiation effect. The lifetimes in the base and collector regions are reduced and an increase of base current is required to drive a transistor into the saturation region. As the carrier lifetime in the collector is diminished, and the rate of recombination increased, then for the same collector body resistance an increased current is needed to maintain the same carrier concentration in the collector. For nonepitaxial transistors, with lightly doped bases, a large increase in saturation voltage is typical. The increased base current to drive into saturation is seen to increase as a function of the collector current.

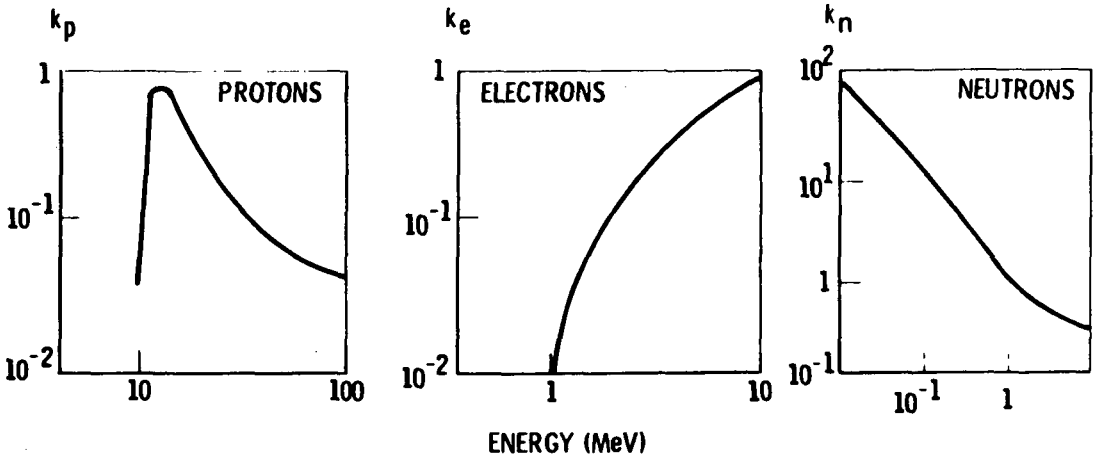

NORMALIZED DAMAGE CONSTANTS

A very significant point in equivalencing damage is that the primary effect of the damage must be identical for both radiation sources to allow a valid comparison. It is to be noted that the damage effect is a function of semiconductor quality, level of doping, carrier concentration during irradiation and measurement, temperature, and level of impurities, particularly oxygen. Damage equivalence may vary widely for different experimental parameters. Nevertheless, as a practical matter, it is convenient to plot normalized damage constants to determine the effectiveness of a given particle in causing, for example, displacement damage. Protons and neutrons of less than the OPGT maximum energies are more effective for producing displacement damage. This point has particular significance for the designing of shielding for spacecraft.

DISPLACEMENT:

k_p (MEDIUM-ENERGY PROTONS) = 30 k_n

k_p (HIGH-ENERGY PROTONS) = 10 k_n

IONIZATION:

5×10^{-7} RADS/(MEDIUM-ENERGY PROTON/CM^2)

1×10^{-7} RADS/(HIGH-ENERGY PROTON/CM^2)

EQUIVALENCES FOR COMBINED ENVIRONMENTS

If estimates for damage are to be made for a situation of combined enfironments, e.g., RTG plus trapped belt radiation, it is found that protons of 8 to 17 MeV (medium energy) are equivalent to 33 neutrons, and protons of 100 MeV (high energy) are equivalent to 8 neutrons. One would assume (incorrectly) that defects produced would not interact to a first approximation, and find a total damage by simple linear superposition. It is emphasized again, however, that the equivalences of two disparate radiations in producing displacement damage cannot be given by a single number. For charged particles which produce both displacement and ionization damage, that fraction of the damage related to ionization damage is a function of the particle's energy. At high energy (100 MeV) the absorbed dose per particle in silicon is only one-fifth that at medium energy (8-17 MeV).

FUNDAMENTAL EQUATIONS SOLVED BY THE COMPUTER:

- CONTINUITY EQUATION FOR ELECTRON CONCENTRATION
- CONTINUITY EQUATION FOR HOLE CONCENTRATION
- POISSON'S EQUATION

COMPUTER MODELING OF RADIATION EFFECTS

The calculation of primary and secondary photocurrents is difficult because of a lack of a detailed description of currents as a function of time since voltages, and capacitances are all varying with time. Even simplified models are not practical for hand computation, and digital computer codes are used to calculate photocurrents. An equivalent circuit is set up to represent the response of the transistor during the pulse. One difficulty in modeling a transistor as an equivalent circuit is the storage of minority carriers in the collector and base regions. Also, in calculating the secondary photocurrent it is assumed that the primary photocurrent can be given as a function of time using an appropriate equation as a current generator. The calculations assume that the net effect of all radiation sources is the creation of an excess number of hole-electron pairs, together with displacement atoms to act as carrier recombination centers.

- EBERS-MOLL - REDUCES TRANSISTOR TO FOUR-TERMINAL BLACK BOX
- CHARGE CONTROL - REVEALS ROLE OF TOTAL MINORITY CHARGE OF BASE
- LINVILL - GIVES INSIGHT INTO LUMPED PARAMETERS

ALL MODELS USE THE SAME FOUR PHYSICAL MEASUREMENTS AS INPUT

SIMPLE MODELS

Computer modeling will be dealt with in detail in Section simple models and their main features will be mentioned here. The Ebers-Moll model describes a transistor as various resistances and capacitances in a versatile arrangement where the collector and emitter current generators can be detailed prescriptions of these currents as a function of junction voltages. The transistor capacitances can likewise be functions of time. The Ebers-Moll model will represent cutoff, active and saturation modes. A second model not basically different from the Ebers-Moll circuit, except in nomenclature and in the way of representing charge stored in the collector and base, is the charge control model. Depending on programming, diffuse capacitance or storage is used and the equivalent circuits are the same. In the Linville model the collector is subdivided into a number of regions and the currents flowing into and out of each region are determined. Each computer equation has the form of Kirchoff's law. The coefficients of the difference equations for lumped circuit parameters are the minority carrier concentrations.

- JFETs COMPARABLE TO BEST BIPOLARS
- JFETs HAVE POTENTIAL FOR HARDNESS IMPROVEMENT
- SENSITIVE PARAMETERS ARE:
  - g_m: TRANSCONDUCTANCE
  - I_{DSS}: DRAIN SOURCE CURRENT
  - V_p: PINCH-OFF VOLTAGE

DISPLACEMENT EFFECTS IN JFETS

Displacement damage to JFETs affects primarily the transconductance, the drain to source current and the pinch-off voltage. The normal radiation effect is typical for FETs: a delayed onset with little damage at 10^{13} n/cm^2, and then rapid damage for higher levels, 10^{14}-10^{15} n/cm^2. Some recent evidence indicates that JFETs can be improved to tolerate 10^{15}-10^{16} n/cm^2 by special heavy doping. For a JFET, a thin channel allows this heavy channel doping without degradation of electrical properties. Contrary to ionization damage results, N-channel devices are harder than P-channel devices.

MECHANISM: ATOMIC DISPLACEMENTS

EFFECT: CARRIER REMOVAL IN CHANNEL

DEGRADATION: $g_m(\phi) = g_m(0) \exp(-\phi/k)$

WHERE:

$k_p = 398\ P_0^{0.77}$

$k_n = 93\ N_0^{0.82}$

NEUTRON EXPOSURE DISPLACEMENTS IN JFETs

The predominant basic process of JFET damage from neutron irradiation is the production of cluster atomic displacements. Carrier removal in the channel region is the most significant displacement effect since JFETs are majority carrier devices. The theory of displacement effects in JFETs shows the usual exponential dependence of degradation (transconductance decrease) on neutron fluence. The damage constants indicate N-channel devices are more radiation resistant than P-channel devices, in agreement with experimental findings. Level data show that JFETs tolerate 10^{13} n/cm^2 with little damage, but show marked effects at 10^{14} n/cm^2 and may be rendered useless by a fluence of 10^{15} n/cm^2.

DEGRADATION:

- g_m AND I_{DSS} DEGRADED 30% AT 10^{12} - 10^{13} p/cm^{2*}
- V_p SHOWED DEGRADATION AT 10^{10} - 10^{11} p/cm^{2*}

MODEL:

$$I_{DSS}(\phi) = I_{DSS}(0)(1 + \gamma\phi)^2$$

$$g_{mo}(\phi) = g_{mo}(0)(1 + \gamma\phi)$$

WHERE

$$\gamma = \frac{1}{N_0 (dN/d\phi)_0}$$

*22-MeV PROTONS

PROTON EXPOSURE DISPLACEMENTS IN JFETS

Data on proton exposure displacements in JFETs are very sparse. Protons are a source of both ionization and displacement damage, the ratio depending on the proton energy. Significant damage to transconductance and drain-to-source current has been found as a result of proton irradiation. A 30-per cent degradation in the above parameters was observed for a 22-MeV proton fluence range of 10^{12}-10^{13} p/cm^2. A model for damage has been proposed in which the damage term involves a damage constant γ which exhibits a high variability to device type, presumably due to material impurities. A restriction on the theory of proton damage is that it is restricted to a condition of zero gate voltage.

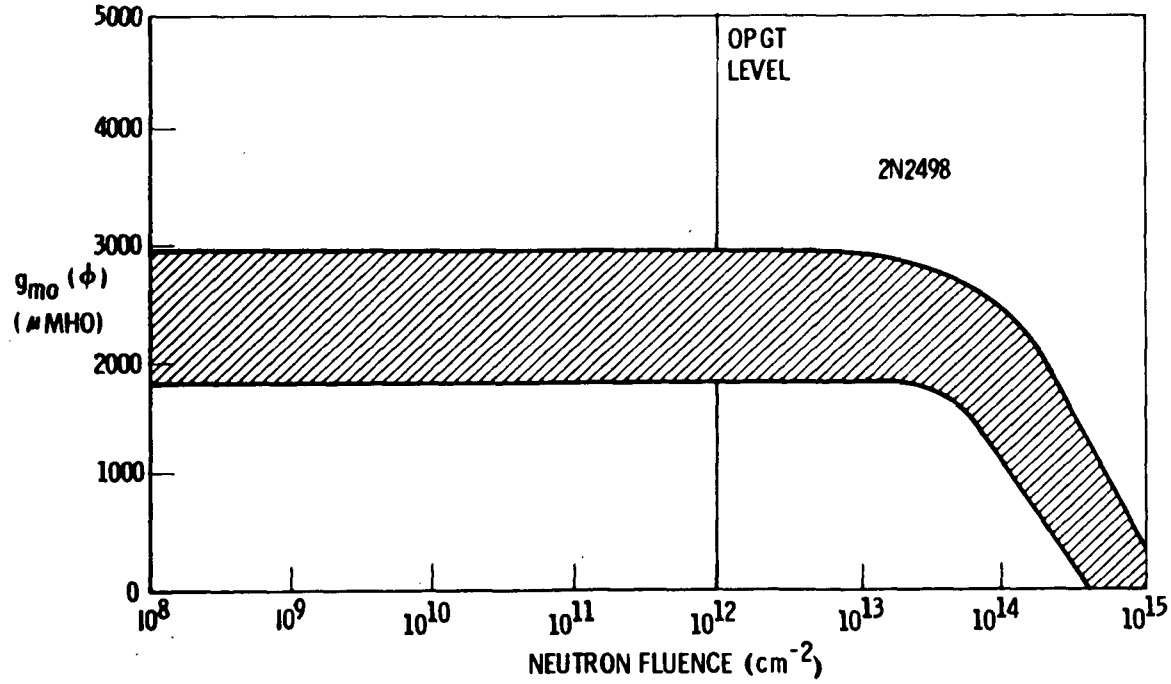

TRANSCONDUCTANCE VS. NEUTRON FLUENCE

The extent of the radiation degradation of transconductance as a function of neutron fluence again exhibits the FET characteristic; that is, little or no damage up to a particular level, followed by a rather rapid change with additional exposure. Tests with LiH shields show little or no difference compared to the unshielded 2N2498. If a failure criterion of a reduction of transconductance to one-half of its initial value is established, then for the 2N2498 a fluence of 5×10^{14} n/cm^2 at room temperature determines a 50-per cent failed level for a large number of devices with little data dispersion.

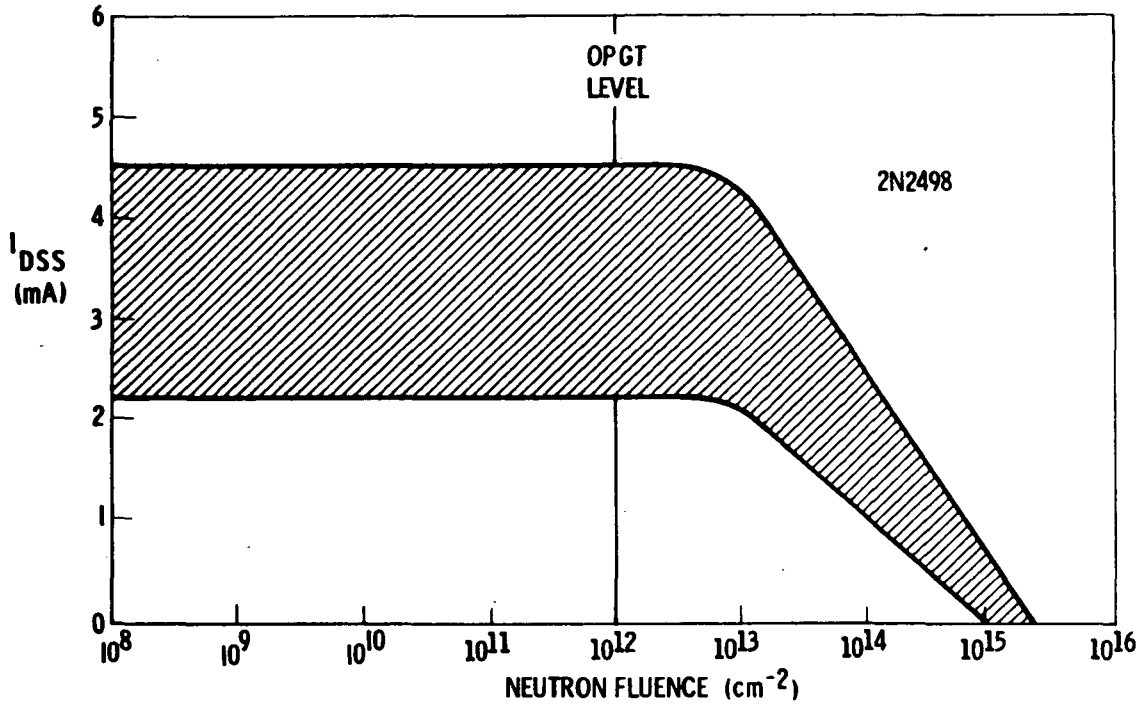

DRAIN-TO-SOURCE CURRENT VS. NEUTRON FLUENCE

For JFETs the drain-to-source current is a neutron fluence sensitive parameter. The typical FET performance behavior may be noted. Some neutron rate effects have been observed, but only at very high fluences and in conjunction with very high gamma ray fields. As with change in transconductance, the presence of a LiH shield appears to have little effect on the damage.

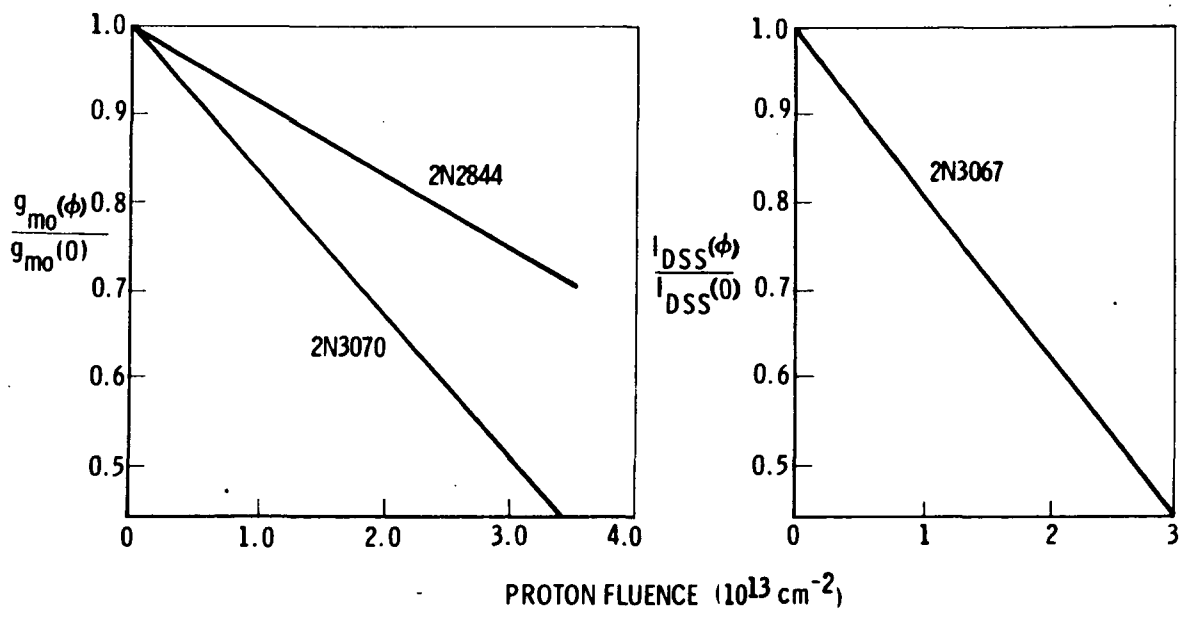

ZERO GATE TRANSCONDUCTANCE AND ZERO GATE DRAIN CURRENT VS. PROTON FLUENCE

If the data for zero-gate transconductance and zero-gate drain current are normalized at zero fluence for 22-MeV proton irradiation, some device-dependent results are apparent. If again the criterion of transconductance to one-half of its initial value is used then a 2N3070 has failed at about 3.5×10^{13} p/cm^2, whereas a 2N2844 would not have failed at twice this level. Experimental data for both parameters show relatively little dispersion.

- ≲25% DEGRADATION
- 22-MeV PROTONS

TYPE	ΔI_{DSS}	Δg_m
2N2497	25%	15%
2N3085	10%	7%

TRANSISTOR TYPES TESTED TO SURVIVE 2×10^{13} P/CM^2

Experimental tests with groups of transistors including 2N3067, 2N3386, 2N2344, 2N3089, 2N3070, 2N3086, 2N3088, 2N2497, 2N3085 have shown an order of magnitude difference in the proton fluence (22 MeV) to cause a 30-per cent degradation in drain current and almost the same factor for 30-per cent degradation in transconductance. Of those tested the performance of the 2N2497 and the 2N3085 appeared best, surviving 2×10^{13} p/cm^2 with 25-per cent or less degradation in either parameter. This information illustrates the need for experimental test data as a screening procedure for transistors.

PARTICLE	FLUENCE (CM^{-2})	PARAMETER	DEGRADATION (%)
FISSION NEUTRONS	10^{14}	g_m	-10
	10^{14}	I_{DSS}	-15
	10^{14}	V_p	-25
22-MeV PROTONS	10^{13}	g_m	-15
	10^{13}	I_{DSS}	-20
	5×10^{10}	V_p	+100
1.5-MeV ELECTRONS	10^{12}	I_{GS}	+300
Co^{60} GAMMA RAYS (1.25 MeV)	10^5 RADS (Si)	I_{DSS}	+250
	10^5 RADS (Si)	V_p	0
	10^5 RADS (Si)	I_{GS}	>+2800

JFET DEGRADATION FACTORS

The sensitive parameters for JFETs, the transconductance, the drain-to-source current and the pinch-off voltage may be listed vs. radiation type, that is, fission energy neutrons, medium energy protons (22 MeV), electrons (1.5 MeV), and gamma rays (Co^{60}) for various appropriate levels of fluence. Very large changes ($\sim$100 per cent) are exhibited for protons on pinch-off voltage at 5×10^{10} p/cm^2, gate-to-source current for electrons at 10^{12} e/cm^2, gamma rays on drain-to-source and gate-to-source current at 10^5 rads (Si). At high fluences, 10^{15} n/cm^2, 3×10^{13} p/cm^2, 10^{13} e/cm^2, or 10^6 rads the degradation factors are all considerable, except perhaps pinch-off voltage in a gamma radiation field.

- DISPLACEMENT EFFECTS ARE MINOR RELATIVE TO IONIZATION
- SENSITIVE TO IONIZATION IN THE OXIDE
- V_{GT} MOST SENSITIVE PARAMETER

INSULATED GATE FETs

As has been mentioned previously, the degradation mechanism for IGFETs is ionization damage and displacement effects are only secondary in importance. It has been shown previously that if particle fluences are converted to ionization absorbed dose in rads, a somewhat reasonable agreement may be achieved for different particle types. A strong dependence on operating parameters makes a tabulation of damage factors for IGFETs impractical. Some long term annealing of damage has been observed and damage does tend to saturate at high dose levels, i.e., in excess of 1×10^6 rad.

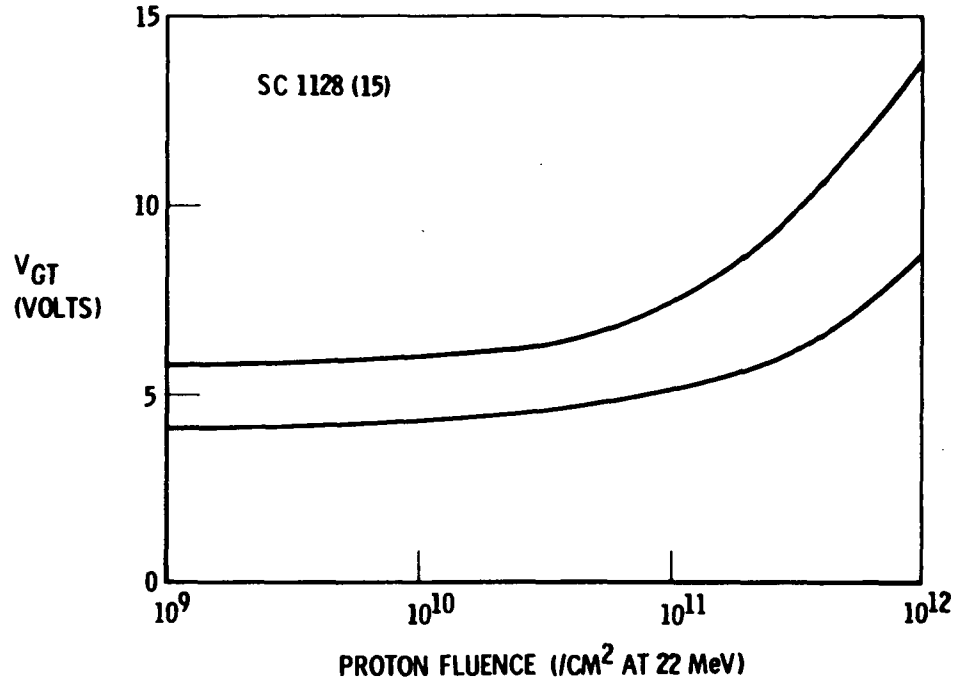

SHIFT AND SPREAD OF GATE THRESHOLD VOLTAGE VS. PROTON FLUENCE

For medium energy (22 MeV) proton irradiation, the shift in gate threshold increases rapidly above a fluence of about 10^{11} p/cm^2 for SC 1128 units with a gate voltage of -20 volts during the irradiations. The spread for 5 each SC1128 (15 individual devices) is nominal at lower fluences, but increases with increasing proton fluence, reaching about an 8-volt spread at 10^{12} p/cm^2.

MECHANISM:

- REDUCTION OF MINORITY CARRIER LIFETIME IN BASE REGION
- INCREASE OF RECOMBINATION-GENERATION CURRENTS IN THE EMITTER BASE JUNCTION

MODEL:

$$h_{FE}(\phi) = \frac{h_{FE}(0)}{1 + h_{FE}(0)\, tk\phi}$$

NEUTRON EFFECTS IN BIPOLAR TRANSISTORS

The mechanisms for neutron damage to transistor current gain is effected by a reduction of minority carrier lifetime in the base region. For operation with currents greater than a few milliamperes this is the most important mechanism. A second effect is recombination-generation current increase in the emitter-base space charge region. In an analytic representation of the current gain, the damage term is directly proportional to the fluence. The proportionality constant K is the damage factor term which is a function of operating conditions and the incident neutron energy spectrum. For an RTG spectrum it is approximately constant. Estimates of damage may be more easily made when the device is operating at the gain vs. collector current peak, for here the base transit time appearing in the damage equation may be taken to equal the reciprocal of the cutoff frequency.

- PROTONS PRODUCE IONIZATION AS WELL AS DISPLACEMENT
- FEASIBLE TO ESTIMATE BULK DISPLACEMENT DAMAGE ONLY
- PROTONS CAUSE ANOMALOUSLY HIGH DAMAGE IN NPN TRANSISTORS

PROTON EFFECTS IN BIPOLAR TRANSISTORS

The effects of proton irradiation on transistors are complicated by the fact that protons produce displacements as well as intense ionization. An equation of the form given for neutron damage to gain may be used to make a first-order estimate of proton damage in silicon transistors by an appropriate choice for an equivalent proton damage constant. The term constant here is a misnomer inasmuch as it is a function of the proton energy. These relations have been given before; they are:

$$K_p = 33\ K_n \qquad 8 < E_p < 17\ \text{MeV}$$

$$K_p = 8\ K_n \qquad E_p = 100\ \text{MeV}$$

Displacement damage to bipolar transistors may be estimated using these "constants". For critical applications, however, recourse should be had to actual experimental data.

- MAKE BASE WIDTH THIN
- OPERATE DEVICES NEAR PEAK CURRENT
- KEEP EMITTER PERIPHERY SMALL
- METALLIZE THE OXIDE ON THE EMITTER BASE JUNCTION
- EXERCISE MANUFACTURING QUALITY CONTROL

RADIATION HARDENING OF BIPOLAR TRANSISTORS

A few general principles for hardening bipolar transistors to radiation exposure damage have emerged from an analysis of relevant test data. The principles are divided into general areas of device geometry, device operating conditions, construction materials and doping, and quality control procedures on the manufacturing process. Examples of the foregoing are thin base widths to minimize carrier transit time, small emitter periphery, metallization of the oxide, operating near peak collector current, and the utilization of PNP construction for surface effects environments.

- IRRADIATE DEVICES IN Co^{60} ENVIRONMENT
- TEST ELECTRICALLY
- ELIMINATE LOW-CUTOFF FREQUENCY DEVICES
- ANNEAL SCREENED DEVICES BY BAKING AT 150 C

RADIATION SCREENING

Those bipolar transistors to be subjected to a radiation environment should be screened first by electrical testing, and second, by ionization radiation screening.

Electrical testing should include microplasma noise in the avalanche breakdown mode, and screening by a measurement of cutoff frequency. Devices with low cutoff frequencies or equivalently large transit times should be eliminated.

Radiation testing would involve exposuring the devices to the 1-MeV gamma rays from Co ^{60} and subsequently making an assessment of their relative radiation sensitivity. The more sensitive devices would be eliminated. The remainder would be damage annealed at elevated temperatures (~ 150 C) to return the devices to their original response characteristics.

DEVICE TYPE \ SOURCE	NEUTRONS	PROTONS	ELECTRONS	GAMMA RAYS
SILICON CONTROLLED RECTIFIERS	4	5	4	4
UNIJUNCTION TRANSISTORS	4	5	4	1
POWER TRANSISTORS (LOW FREQUENCY)	4	5	4	2
POWER TRANSISTORS (HIGH FREQUENCY)	4	5	4	2
TRANSISTORS (LOW FREQUENCY)	3	5	3	1
TRANSISTORS (HIGH FREQUENCY)	1	4	4	2
INTEGRATED CIRCUIT AMPLIFIERS	3	4	4	2
INTEGRATED CIRCUIT LOGIC	1	3	3	1
JUNCTION FIELD EFFECT TRANSISTORS	2	3	3	2
MOS FIELD EFFECT TRANSISTORS	1	5	4	3

1 = NO PROBLEMS ANTICIPATED
2 = SLIGHT DEGRADATION POSSIBLE
3 = USABLE; SLIGHT TO MODERATE DAMAGE
4 = MODERATE TO SEVERE DAMAGE
5 = FAILURE ANTICIPATED

RADIATION VULNERABILITY ASSESSMENT

The level of vulnerability of typical OPGT candidate parts is indicated for each type of radiation encountered. Ionization and displacement damage are not separated here. The flux, fluence, and energy distribution of each type of radiation are appropriate to OPGT. The fluences are:

Neutrons	$1.0 \times 10^{12}/cm^2$
Protons	$7.5 \times 10^{13}/cm^2$
Electrons	$6.1 \times 10^{11}/cm^2$
Gamma rays	1.0×10^{4} rads (Si) (dose)

DEVICE TYPE \ SOURCE	NEUTRONS	PROTONS	ELECTRONS	GAMMA RAYS
THIN FILM CIRCUITS	1	-	-	-
SIGNAL DIODES	1	4	1	1
ZENER DIODES	3	4	1	1
TUNNEL DIODES	1	4	1	1
POWER DIODES	2	5	3	1
SOLID STATE CHOPPERS	3	-	-	-
RESISTORS	1	3	1	1
CAPACITORS	1	4	1	1
MAGNETICS	1	3	1	1

1 • NO PROBLEMS ANTICIPATED
2 • SLIGHT DEGRADATION POSSIBLE
3 • USABLE; SLIGHT TO MODERATE DAMAGE
4 • MODERATE TO SEVERE DAMAGE
5 • FAILURE ANTICIPATED

RADIATION VULNERABILITY ASSESSMENT (Cont'd.)

The vulnerability levels of candidate OPGT parts are continued here. The environments are the same as indicated on the preceding page.

RESISTORS

CAPACITORS

INSULATORS

CABLES

CRYSTALS

OPTICAL COMPONENTS

MAGNETIC DEVICES

FLUIDS

BONDING MATERIALS

COATINGS

LUBRICANTS

MISCELLANEOUS DEVICES

The main emphasis in this handbook is on radiation effects in semiconductor devices. Effects, damage modes, and susceptibility levels in other electrical and mechanical parts and materials that are candidates for use in an OPGT spacecraft or in radiation testing should also be described. Parts of interest include resistors, capacitors, insulators, cables, crystal oscillators, optical lenses and mirrors, and electro-mechanical and magnetic devices. Materials susceptible to radiation damage include fluids, bonding materials, thermal coatings, and lubricants.

ITEM	THRESHOLD	MODERATE DAMAGE	SEVERE DAMAGE
CARBON RESISTORS	10^7 rads	10^8	10^9
	10^{14} n/cm^2	10^{15}	10^{16}
SUBMINIATURE VACUUM TUBES	5×10^7 rads	3×10^8	2×10^9
	5×10^{14} n/cm^2	3×10^{15}	2×10^{16}
SOLAR CELLS	10^{10} n/cm^2	10^{11}	10^{12}
SEMICONDUCTOR DEVICES	10^3 rads	10^5	10^7
	10^{11} n/cm^2	10^{13}	10^{15}
MAN	20 rads	100	500

QUALITATIVE SUMMARY OF RADIATION EFFECTS ON MISCELLANEOUS ITEMS

Radiation damage effects span many orders of magnitude and all aspects of a space system must be reviewed from a radiation damage standpoint. This section will review many miscellaneous devices most of which are quite unaffected by OPGT levels of radiation. A radiation program must necessarily concentrate on semiconductor devices, but must be alert not to overlook occasional exceptions which are even more susceptible to radiation damage.

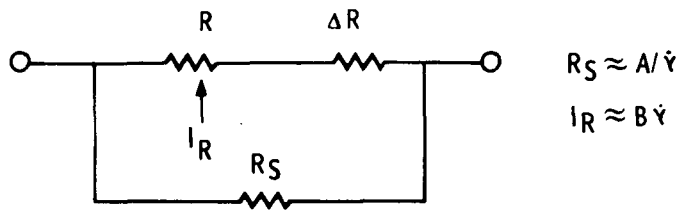

EQUIVALENT CIRCUIT OF RESISTOR

Radiation effects on resistors are generally much smaller than on semiconductor components. Transient effects are produced by:

(1) Leakage in surrounding insulating medium.
(2) Current flow resulting from net absorption or emission of electrons.
(3) Conductivity modulation of bulk resistor material

These effects increase with magnitude of applied voltage and can be minimized by proper thickness of potting material and use of miniaturized resistors. Values of empirical constants A and B for many resistor types are given in the TREE Handbook.

Permanent effects are caused by displacement damage and are usually negligible below 10^7 rads or 10^{13} n/cm^2.

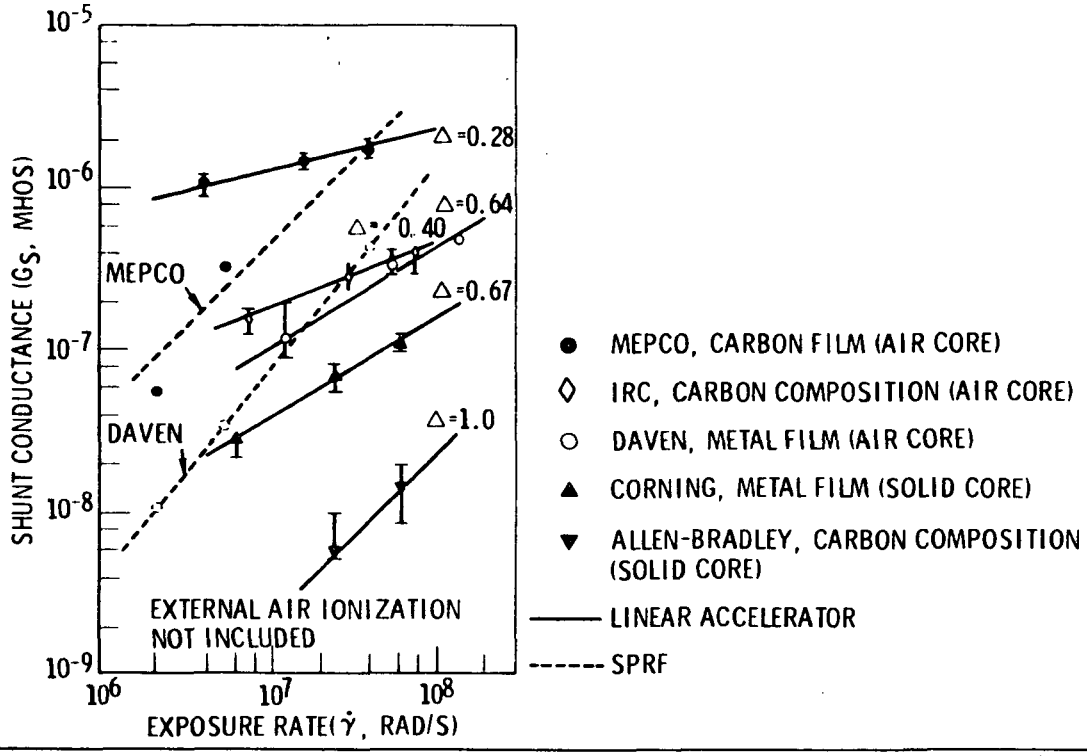

RESISTOR EXPOSURE RATE DEPENDENCE

These data show typical resistor response to exposure rate. Notice that $R_S = A/\dot{\gamma}^{\Delta}$ is a general formulation which encompasses all of the data. The basic physics is not well understood; especially the necessity of using values of Δ less than one. Some resistors such as the Mepco carbon film (air core) could show significant shunt conductance effects in high impedance circuits at the dose rates characteristic of Jupiter's radiation belts. Air core resistors are generally about an order of magnitude more sensitive to ionizing dose rate effects than solid core resistors.

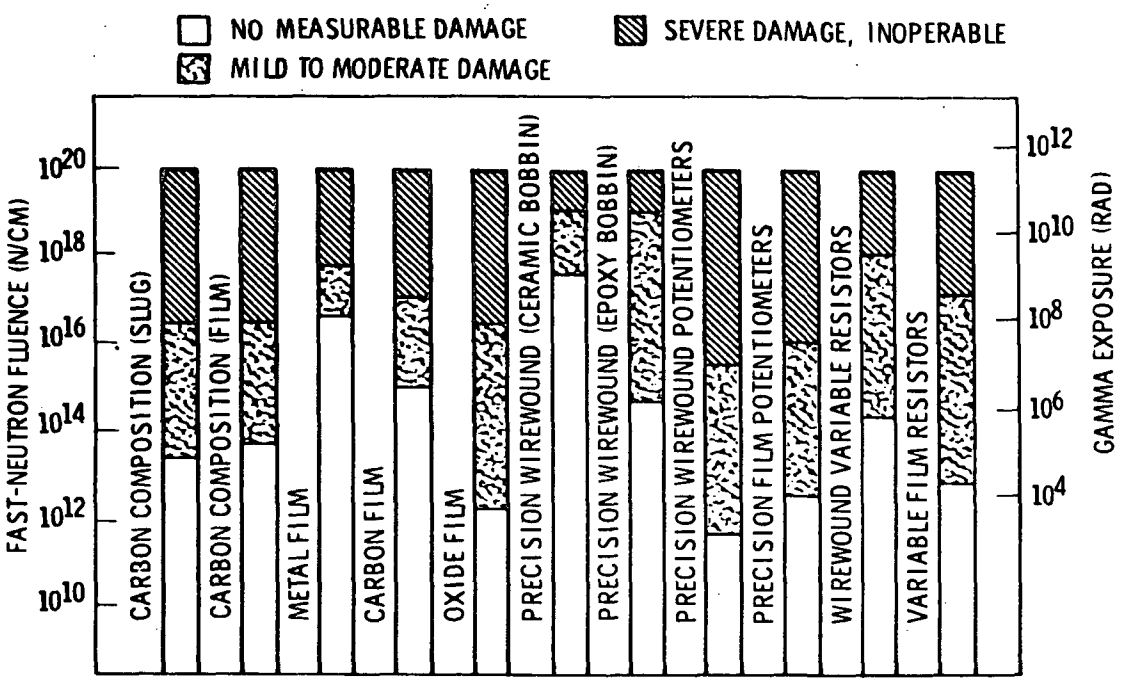

RESISTOR PERMANENT DAMAGE

The resistor permanent damage problem is of little concern in most applications; consequently, it has received very little experimental attention. Qualitatively, ΔR is usually negative although positive values have been observed in wire-wound resistors. The data shown above was obtained in steady-state reactors during the early 1960's and is intended only as a qualitative summary of permanent damage effects.

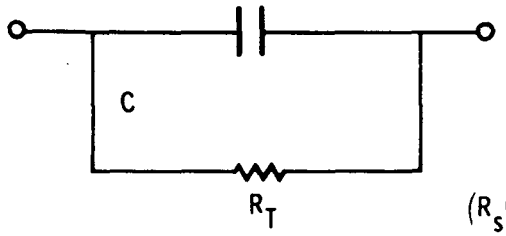

$$R_T^{-1} = R_0^{-1} + R_S^{-1}$$

$$R_0 = \epsilon\epsilon_0 / \sigma_0 C$$

$$R_S = \epsilon\epsilon_0 / (\sigma - \sigma_0) C$$

$$(R_S C)^{-1} = K_p \dot{\gamma}^{\Delta} + Kd_1 \int_{-\infty}^{t} e^{-\frac{t-t'}{\tau d_1}} (t')^{\Delta_1} dt'$$

$$+ Kd_2 \int_{-\infty}^{t} e^{-\frac{t-t'}{\tau d_2}} \dot{\gamma}(t')^{\Delta_2} dt'$$

EQUIVALENT CIRCUIT OF CAPACITOR

Radiation effects on capacitors are caused almost entirely by changes in conductivity of the dielectric. The mathematical model shown above is adequate for most radiation applications. The conductivity change is determined by a prompt component and two or more delayed components. For space applications consideration of the prompt component is sufficient. The delayed components are caused by electron trapping in the dielectric. For application where conductivity changes must be minimized, capacitors with low values of K_p should be chosen. Conductivity changes should be negligible in the radiation environments of interest to the OPGT.

Permanent damage is caused by displacement effects but the threshold is above 10^{15} n/cm^2 or 10^8 rads. This effect is negligible for OPGT environments.

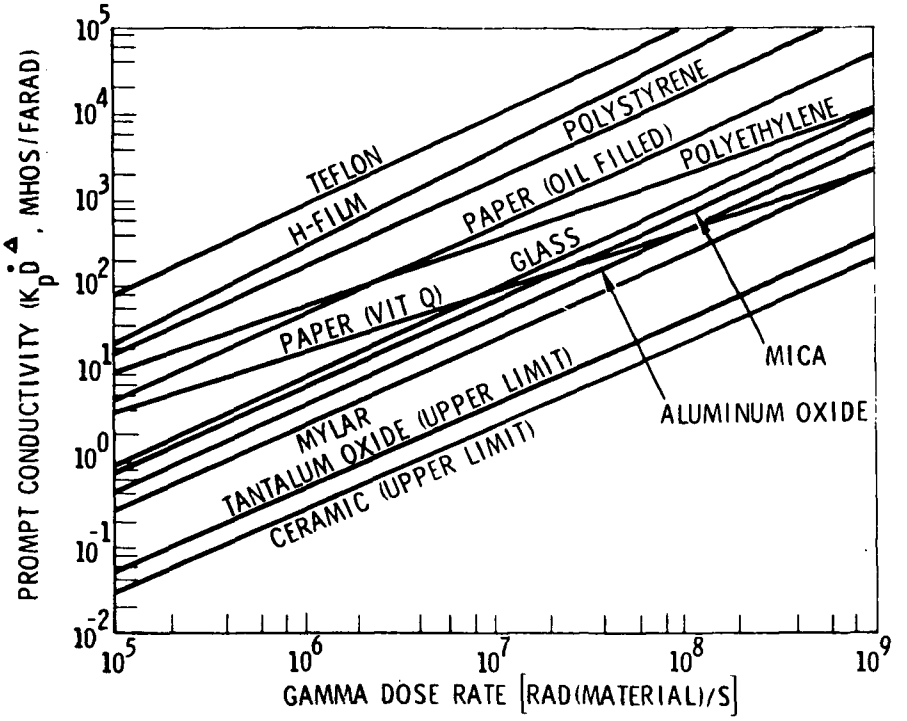

PROMPT CONDUCTIVITY AS A FUNCTION OF DOSE RATE

Experimental data for several common capacitor types are shown above. Extrapolation to the low dose rates characteristic of OPGT Missions shows that the effect can be neglected. For most capacitors the value of Δ is approximately one. The Nichols-Van Lint model, based on a detailed analysis of the ionizing tracks produced by the incident radiation, explains deviations of Δ from unity and introduces a dependence on dose as well as dose rate.

For some zero-voltage applications, the ability of the capacitor to act as a battery for short periods of time after irradiation can be important. Basically, this is caused by emptying of the electron tracks and produces millivolts after the irradiation.

RADIATION COMPONENT	AVERAGE RADIATION RATE	RESPONSE	SATURATION EXPOSURE	REPLACEMENT CURRENT	INDUCED CONDUCTANCE
	rad/s		rad	$\frac{A}{cm}\left(\frac{s}{rad}\right)$	$\frac{mho}{cm}\left(\frac{s}{rad}\right)$
GAMMA	3×10^4	SATURATED		$+4 \times 10^{-14}$	5.3×10^{-17}
	3×10^4	INITIAL	50	$+4 \times 10^{-14}$	$\sim 10 \times 10^{-17}$
	50	SATURATED		$+4 \times 10^{-14}$	4.7×10^{-16}
	$n/(cm^2\ s)$		n/cm^2	$\frac{A}{cm}\left(\frac{cm^2\ s}{n}\right)$	$\frac{mho}{}\left(\frac{cm^2\ s}{n}\right)$
THERMAL NEUTRONS	3×10^{13}	SATURATED		-1.3×10^{-23}	$\lesssim 2 \times 10^{-26}$
	3×10^{13}	INITIAL	10^{12}	-1.3×10^{-23}	2×10^{-25}
	5×10^{10}	SATURATED		-1.3×10^{-23}	$\approx 10^{-25}$
FAST NEUTRONS (E>10keV)	2×10^{14}	SATURATED		-1.4×10^{-24}	$\lesssim 10^{-26}$
		INITIAL	10^{13}	-8×10^{-23}	2×10^{-25}

RESPONSE OF RG-58U COAXIAL CABLES TO RADIATION

The dielectric material in cables reacts to radiation in the same way as it does in capacitors. For very high impedance circuits, connected by long lengths of cable, problems can conceivably arise even at the low ionizing dose rates encountered in space. The experimental information above is typical of most cables; further data is available in the TREE Handbook.

Permanent damage effects in cables are completely negligible for radiation levels of interest to the OPGT.

COMPOUND	APPROXIMATE DAMAGE THRESHOLD (rads)
ELASTOMERS	
POLYURETHANE RUBBER	7×10^6
NATURAL RUBBER	2×10^6
SILICONE RUBBER	1×10^6
THERMOSETTING RESINS	
PHENOLIC, GLASS LAMINATE	8×10^9
PHENOLIC, ASBESTOS FILLED	3×10^9
EPOXY, AROMATIC CURING AGENT	2×10^9
POLYURETHANE	1×10^9
SILICONE, GLASS FILLED	9×10^8
SILICONE, MINERAL FILLED	9×10^8
SILICONE, UNFILLED	1×10^8
PHENOLIC, UNFILLED	3×10^6
TEFLON	1×10^6

RADIATION THRESHOLDS FOR VARIOUS INSULATING MATERIAL AND POTTING COMPOUNDS

Most insulating materials have thresholds above the radiation levels of interest for OPGT missions. However, some materials such as silicone rubber and teflon are unsuitable for application above 10^6 rads. A hardened form of teflon is available with a threshold of about 10^8 rads.

RATED FREQUENCY (MHz)	ELECTRODE MATERIAL	FREQUENCY CHANGE (10^{-8} $\Delta f/f$)	POST-IRRADIATION AGING (10^{-8}/wk) ($\Delta f/f$)	GAMMA EXPOSURE (10^4 rads)	FAST-NEUTRON FLUENCE (10^{12} n/cm^2)
16	Au-Ni-Au	-183	+8.1	8.6	1.4
16	Au-Ni-Au	-165	+20.6	8.6	1.4
16	Au-Ni-Au	DEAD	DEAD	8.6	1.4
16	Au-Ni-Au	-337	+7.5	8.6	1.4
16	Au	-870	+54.3	8.6	1.4
16	Au	-447	+28.8	8.6	1.4
16	Au	-970	+8.1	8.6	1.4
19	Au-Ni-Au	-17.0	+1.05	0.85	0.46
19	Au-Ni-Au	-37.0	0	0.85	0.46
19	Au-Ni-Au	-26.0	-0.53	0.85	0.46
19	Au	-25.8	+0.53	0.85	0.46
19	Au	+8.4	-3.2	0.85	0.46
19	Au	+39.0	-2.6	0.85	0.46
19	Au	-35.0	+1.6	0.85	0.46

RADIATION EFFECTS FOR MODERATE-PRECISION CRYSTAL UNITS

The effects of radiation on crystal controlled oscillators can be very significant at total dose levels above 10^4 rads or neutron fluence levels greater than 10^{12}n/cm^2. The above data was obtained during weapons tests and the gamma-to-neutron ratio is much higher than for a typical reactor test. The effects can be reduced about an order of magnitude by using "swept" synthetic crystals.

Tests on high precision units have resulted in oscillation stoppages at levels of approximately 10^{12}n/cm^{2}or 3,000 rads. If oscillation resumes after minutes of dead time it is at reduced frequency and drive current.

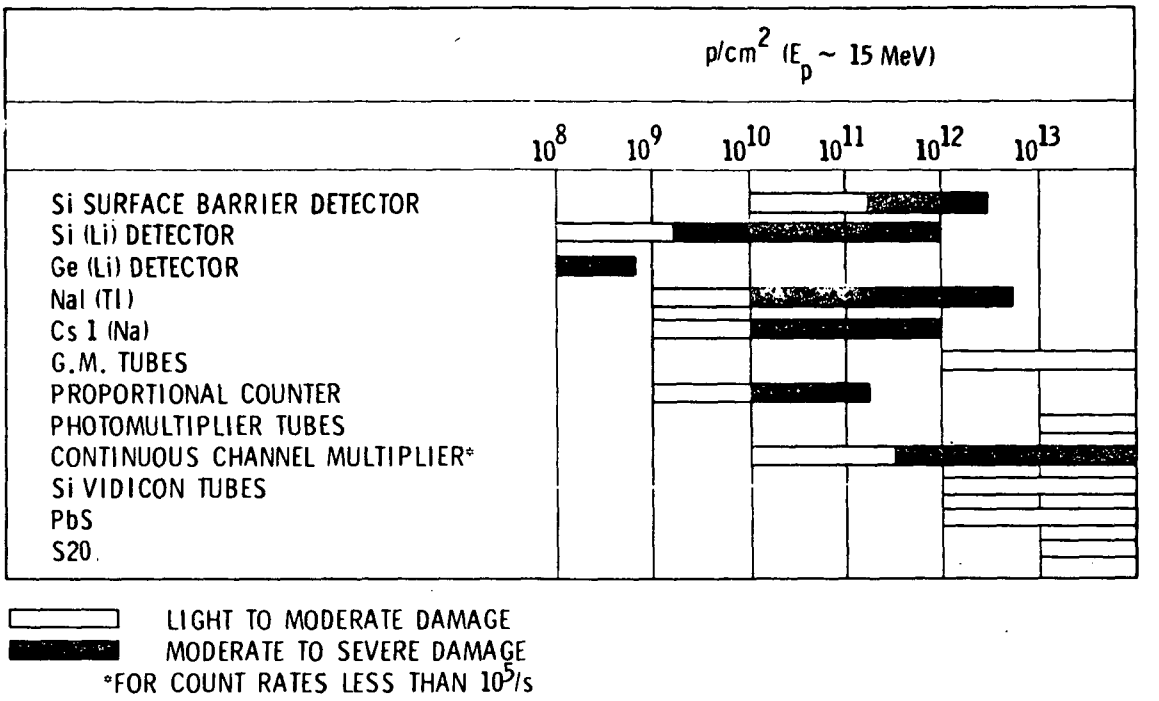

TYPICAL PROTON DAMAGE FOR SCIENCE INSTRUMENT COMPONENTS

Science instruments typical of those considered for OPGT missions use a number of special components which are readily damaged by protons. The actual thresholds are strongly influenced by experimental objectives and requirements. Interference with experiment operation may occur at low fluxes of protons and other radiation. Trapped electrons in the channel multiplier detectors of an ultraviolet spectrometer is an example.

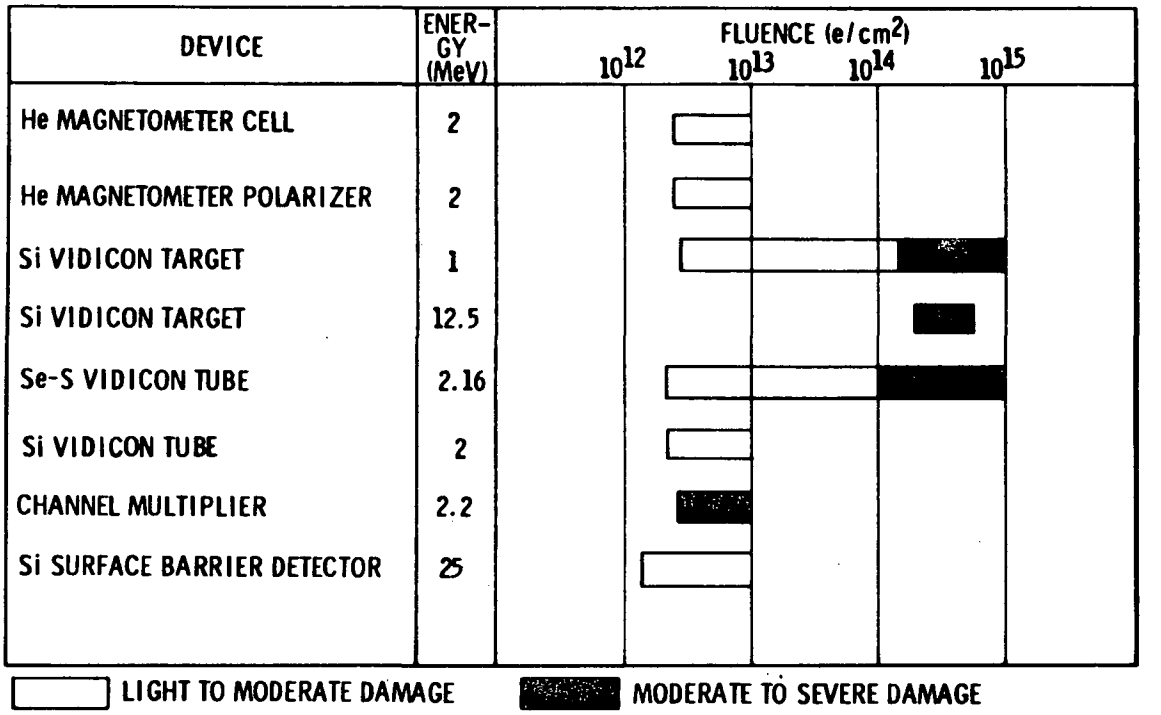

SCIENCE COMPONENT ELECTRON DAMAGE

This chart shows some electron damage data for representative OPGT science sensor components. The effect in some cases (e.g., the channel multiplier) is interference with response to the environment to be sensed, i.e., a lower signal-to-noise ratio.

In addition to the proton and electron data, some fission neutron and gamma ray (Co^{60}) damage thresholds are:

Si Vidicon Targets	10^{11} - 10^{12} n/cm^2; 10^6 - 10^7 rads
Geiger-Mueller Tube	Interference at 10^3 rads

NO PROBLEM	USUALLY NO PROBLEM	SERIOUS PROBLEM
RESISTORS	INSULATORS	PHOTOGRAPHIC FILM
MAGNETIC DEVICES	SENSING DEVICES	CRYSTAL OSCILLATORS
CAPACITORS	MICROWAVE DEVICES	SOME SCIENCE SENSORS (INTERFERENCE)
CABLES		
WIRING		
BATTERIES		

MISCELLANEOUS DEVICE SUMMARY
(OPGT Environment)

Some representative miscellaneous devices and materials are categorized with respect to OPGT radiation environments. This is a qualitative summary for guidance purposes and should not be rigidly applied since specific usage, shielding, and other factors will influence the magnitude of the radiation problem.

"Page missing from available version"

ANNEALING PROCESS

RAPID ANNEALING

SHORT-TERM ANNEALING

LONG-TERM ANNEALING

DEPENDENCE ON INJECTION LEVELS

DEVICE DATA

ANNEALING

The annealing process is the restoration of radiation-damaged components by heating or passage of an electrical current. Annealing returns trapped electrons to the atoms from which they were ionized, and can cause diffusion or migration of interstitial atoms back to lattice vacancy sites. Some rapid and short-term annealing processes are insignificant in OPGT environments, but long-term annealing processes may be feasible. The rate and amount of annealing depends on temperature, current, voltages, and on carrier injection-energy levels in semiconductors. Data on device annealing are presented.

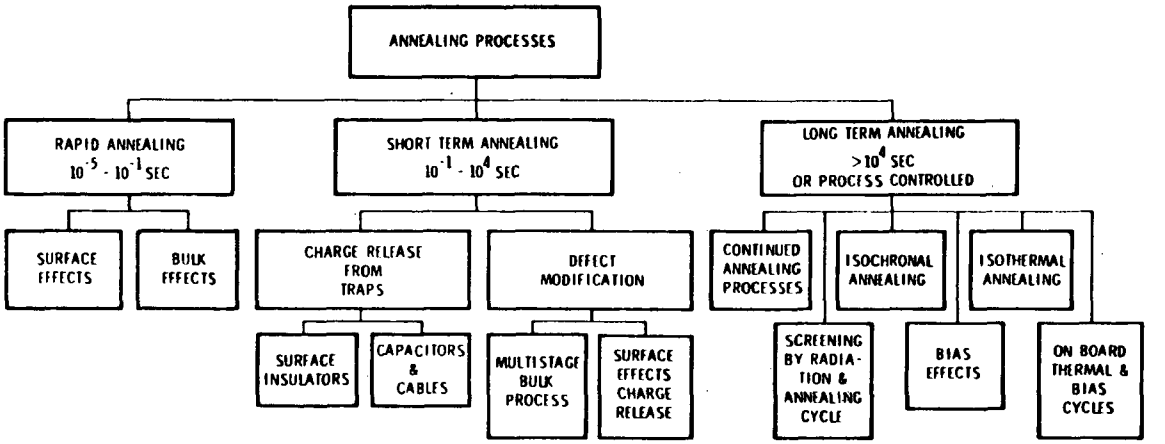

ANNEALING PROCESSES

Annealing processes involve the relaxation of defects introduced by displacement processes and release of charges trapped as a result of ionizing radiation. Defect modification is a bulk semiconductor process very important for bipolar devices. Charge detrapping is an insulator process very important for capacitors, cables and semiconductor device surfaces. Subsequent to irradiation, there is a very rapid change to a quasi-equilibrium situation; this occurs in a 10^{-5}-to 10^{-1}-second interval and is of negligible importance for OPGT. A few processes require much longer times to reach equilibrium and account for short term annealing affects; these effects are also insignificant for OPGT.

Annealing processes have two important applications for space consideration. Radiation screens can be accomplished by a cycle consisting of test, irradiation, retest, and anneal. Annealing cycles composed of temperature and/or electrical bias cycles can be used on board space vehicles to restore radiation-degraded parts.

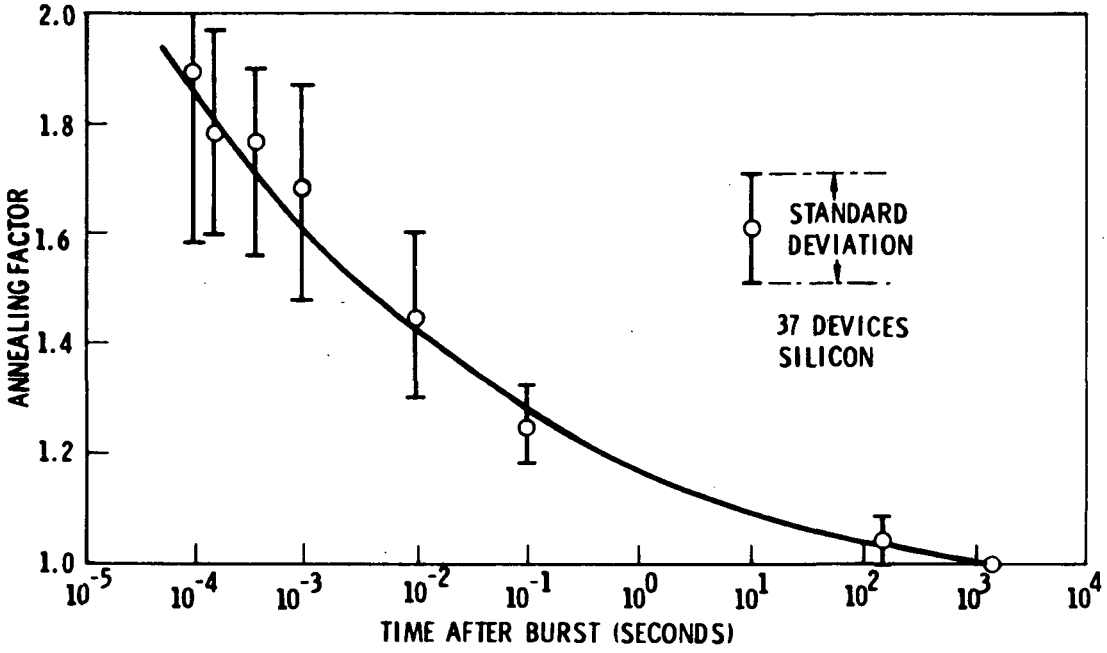

TIME DEPENDENCE OF ANNEALING FACTOR

The rapid annealing process following a neutron burst has been carefully investigated for bipolar transistors. A time-dependent annealing factor has been defined which is directly related to the damage constant:

$$AF(t) = \frac{h_{FE}^{-1}(t) - h_{FE}^{-1}(0)}{h_{FE}^{-1}(\infty) - h_{FE}^{-1}(0)}$$

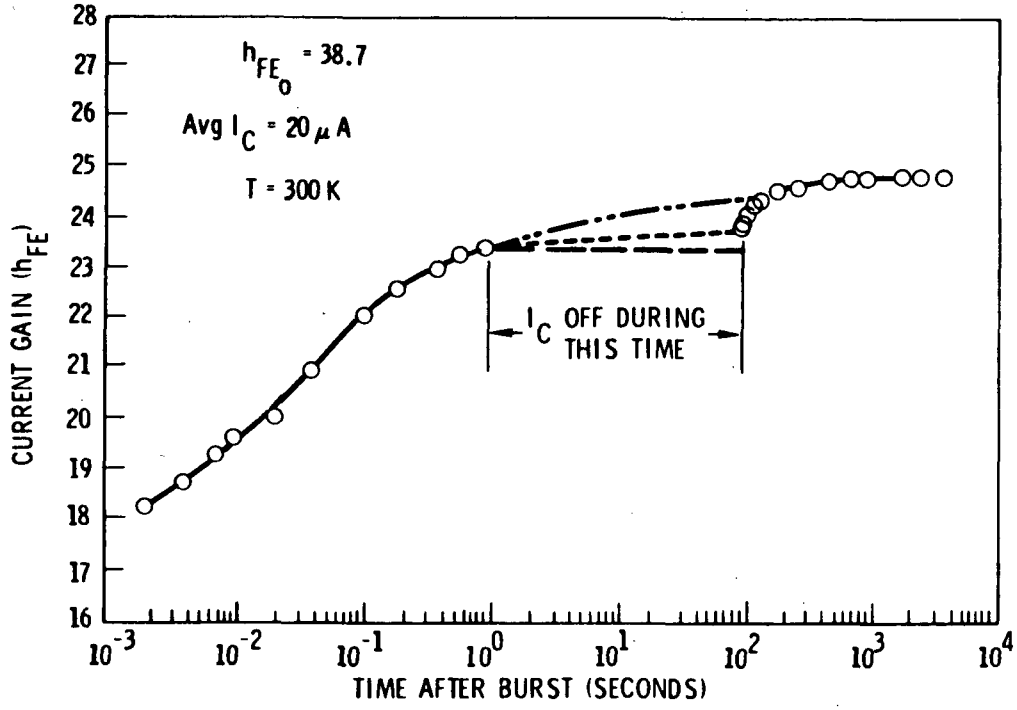

ANNEALING OF TRANSISTOR CURRENT GAIN

The rapid annealing process is strongly dependent on the bias current during the recovery period, as is shown by the off interval in the figure. A 2N914 transistor is used as an example.

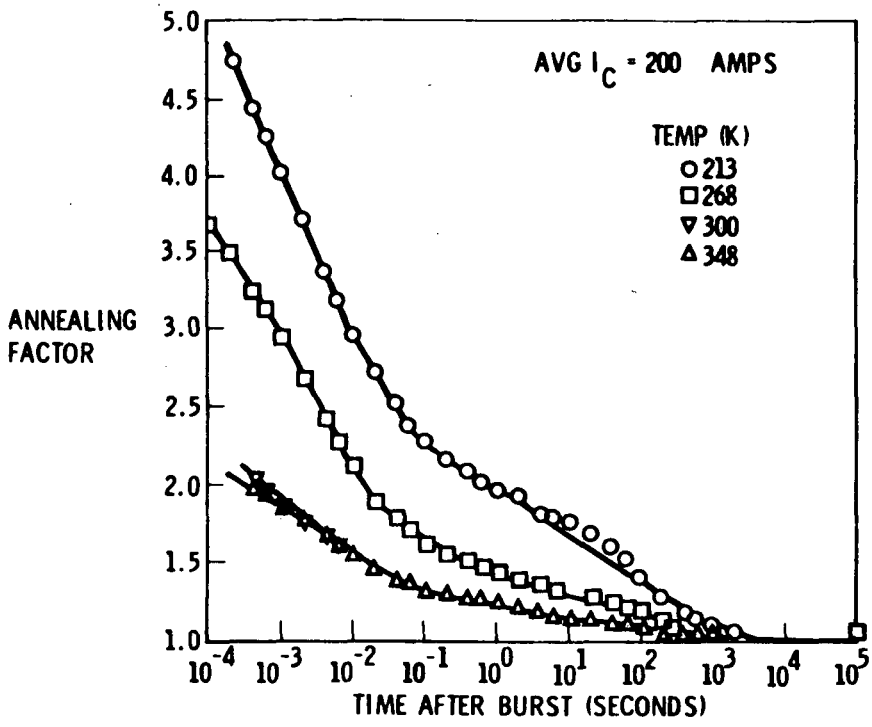

TEMPERATURE DEPENDENCE OF ANNEALING FACTOR (2N914)

The annealing process is probably dependent on the charge state of the defect as it diffuses through the semiconductor lattice. This should also lead to a temperature dependence of annealing factor. Experimental evidence gathered on the 2N914 confirms this and is typical of other transients.

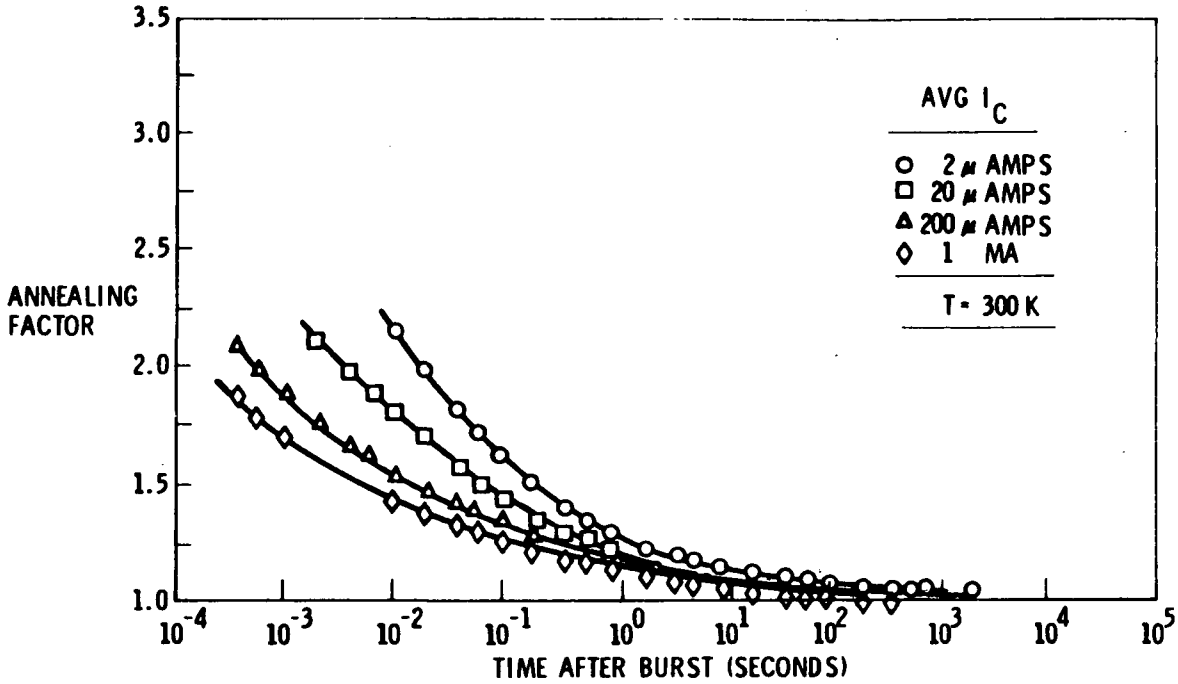

INJECTION LEVEL DEPENDENCE OF ANNEALING FACTOR (2N914)

The dependence of annealing factor on injection current has been experimentally measured for a number of devices. Annealing factor is highest at low current densities and depends somewhat on base resistivity and type. The 2N914 response shown here is typical.

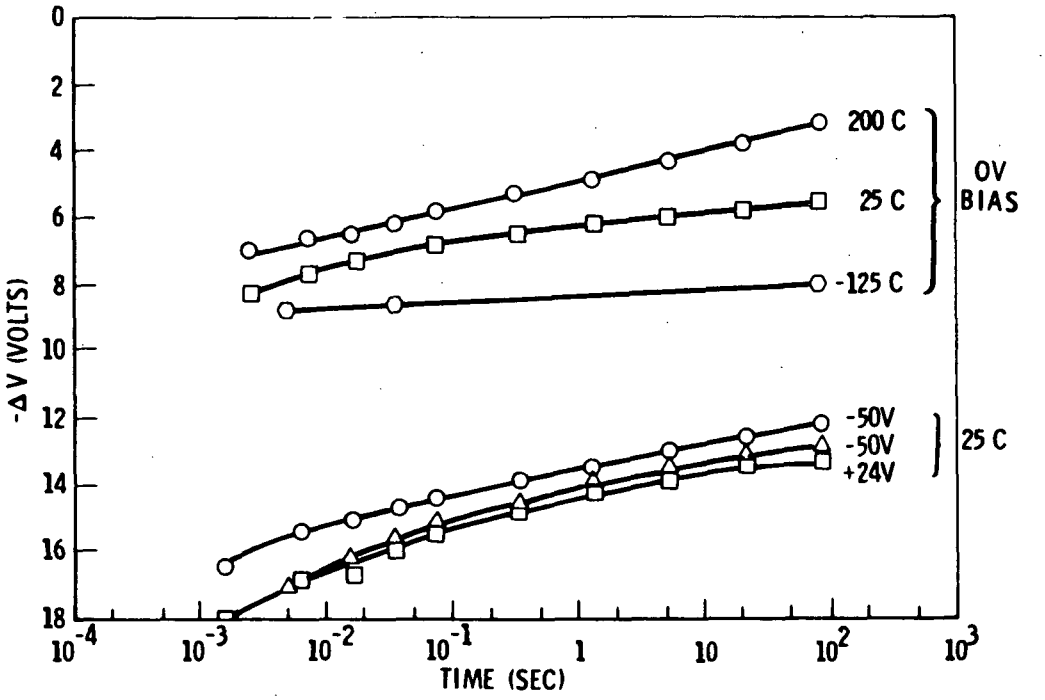

RAPID ANNEALING FACTOR FOR SURFACES

The release of trapped charges from the dielectric layer beneath the gate electrode in FET devices also leads to rapid annealing affects. The change in threshold voltage as a function of time is shown for a typical MOS FET. The dependence on temperature is small and the dependence on gate bias is insignificant. This contrasts sharply with the bulk case and is strong supporting evidence that the basic physical process is simply the release of trapped charges.

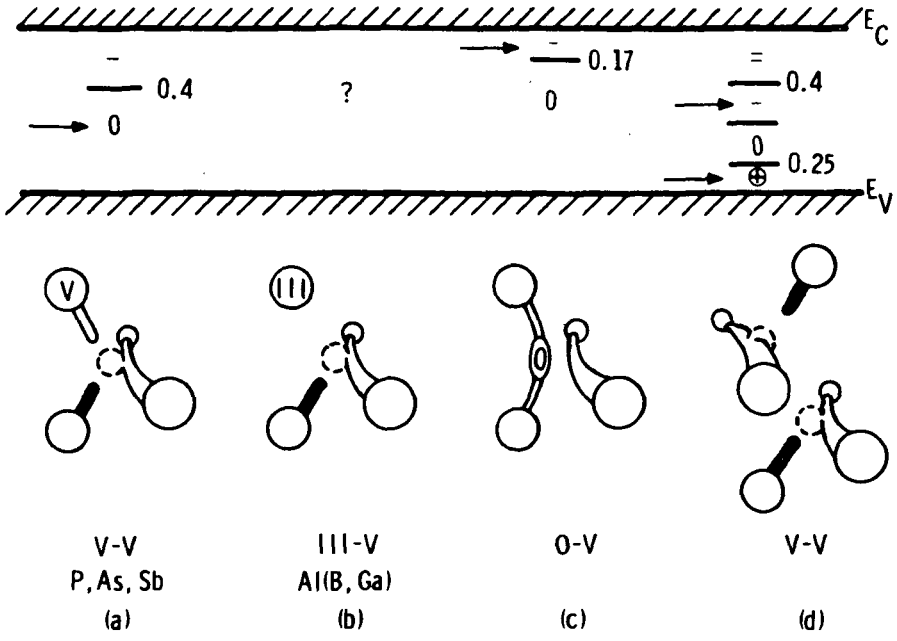

DEFECT SCHEME FOR POINT DEFECTS

Electron paramagnetic resonance (EPR) studies have identified four categories of vacancy defects stable at room temperature. The oxygen vacancy center is probably responsible for gain degradation in PNP transistors; some contribution from the down-vacancy defect is also possible. The divacancy is probably responsible for gain degradation in NPN transistors. The figure shows models of single vacancy-defect pairs as deduced from EPR studies. These include interaction with (a) substitutional Group V donors, (b) substitutional Group III acceptors, (c) interstitial oxygen, and (d) other vacancies to form divacancies. Where known, the electric level structure is indicated, the charge state shown by the arrow being that observed by EPR.

KONOPLEVA ROOM TEMPERATURE MODEL (P-SILICON)	TWO-LEVEL APPROXIMATION
$-E_c$ - 0.21	
$-E_c$ - 0.31	$-E_c$ - 0.31 'AVERAGE' LEVEL
$-E_c$ - 0.38	
$-E_c$ - 0.48	
$-E_c$ - 0.50	
$-E_c$ - 0.53	
$-E_v$ - 0.58	
$-E_v$ - 0.55	
$-E_v$ - 0.53	
$-E_v$ - 0.48	$-E_v$ + 0.35 'DOMINANT' LEVEL
$-E_v$ - 0.31	

DEFECT SCHEME FOR CLUSTERS

Neutron displacement damage produces many identifiable defect levels in the forbidden band. Some act as trapping centers, primarily influencing majority carrier concentration and resistivity; others act as recombination centers which reduce lifetime and current gain; still others have no significant electrical effect.

The table shows room temperature levels identified by Konopleva; a similarly complex picture has been determined for N-silicon. For current gain considerations, this scheme can be approximated by two recomination levels one in the upper half and the other in the lower half of the band. These levels are probably A centers and divacancies within the cluster complex.

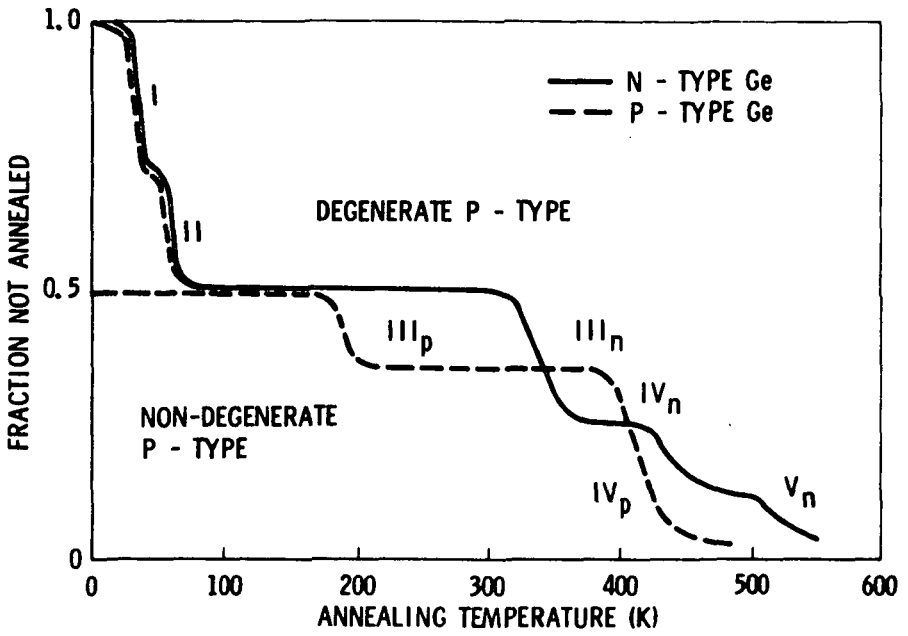

ANNEALING STAGES

The defect structure in a lattice disordered by high energy radiation is very complex. The initiating collisions between incident radiation and lattice atoms result in Frenkel defects for low-energy interaction and cluster defects for high-energy interaction processes. Subsequently, diffusion of interstitials and vacancies occurs to form defects which are stable at room temperature. The resulting defects depend on many factors: (1) type of incident radiation and its energy spectrum; (2) characteristics of the semiconductor lattice including dopants, dislocations, and trace impurities; and (3) temperature at which irradiation takes place.

Typical isochronal annealing curves indicating four or five annealing stages are shown for germanium. Annealing above 600K removes nearly all of the electrically active defects. The available data show a similar stage effect for silicon.

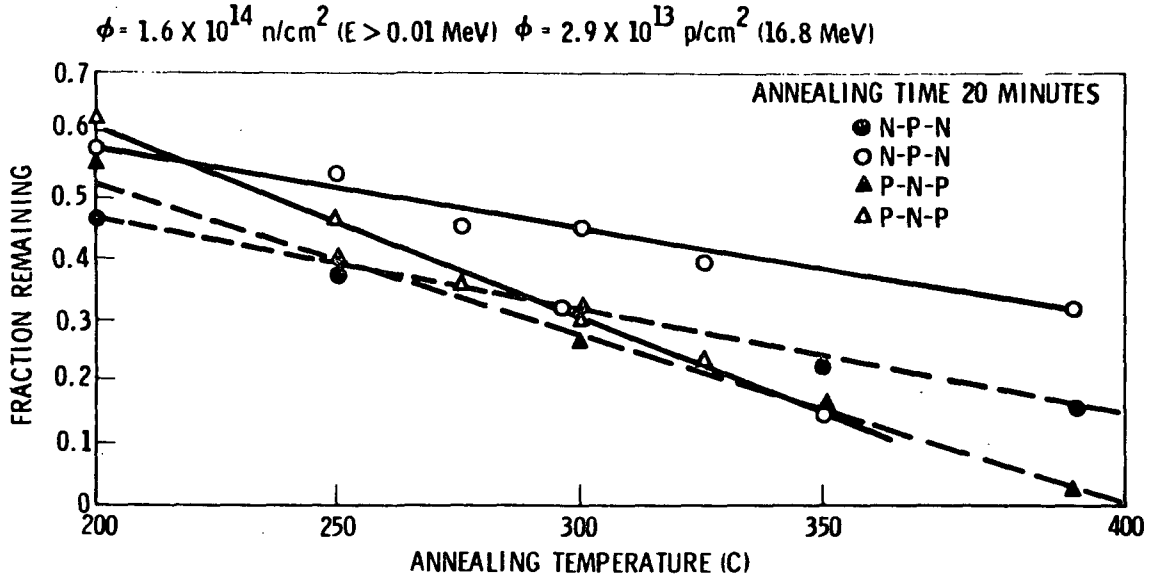

ISOCHRONAL ANNEALING CHARACTERISTICS

Cluster defects are produced by energetic protons or neutrons and they anneal in a significantly different manner as is shown above. The annealing stages are not nearly so evident as with point defects as is seen by comparison with the preceding figure. This is probably because the cluster contains many different defects with different individual stages. The composite isochronal annealing characteristics are smoothed out. This figure shows isochronal annealing curves for Lase-current recovery (I_C = 1 ma) of 2N2102 NPN and 2N1132 PNP silicon transistors damaged with 125-keV electrons followed by either 16.8-MeV protons or reactor neutrons.

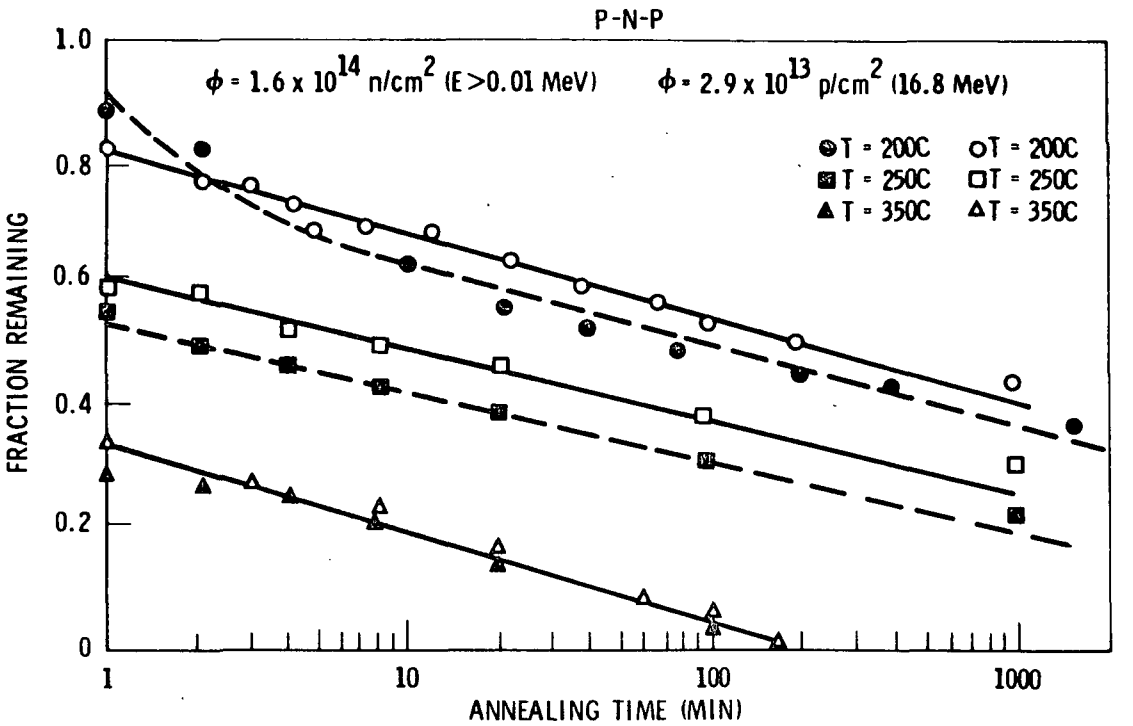

ISOTHERMAL ANNEALING CHARACTERISTICS

The 2N2102 and 2N1132 transistors have been examined using isothermal annealing cycles at 200 C, 250 C and 350 C. Again current gain recovery is used to measure the fraction of damage remaining. In this case the 125- keV electrons were followed by 16.8-MeV protons or reactor neutrons.

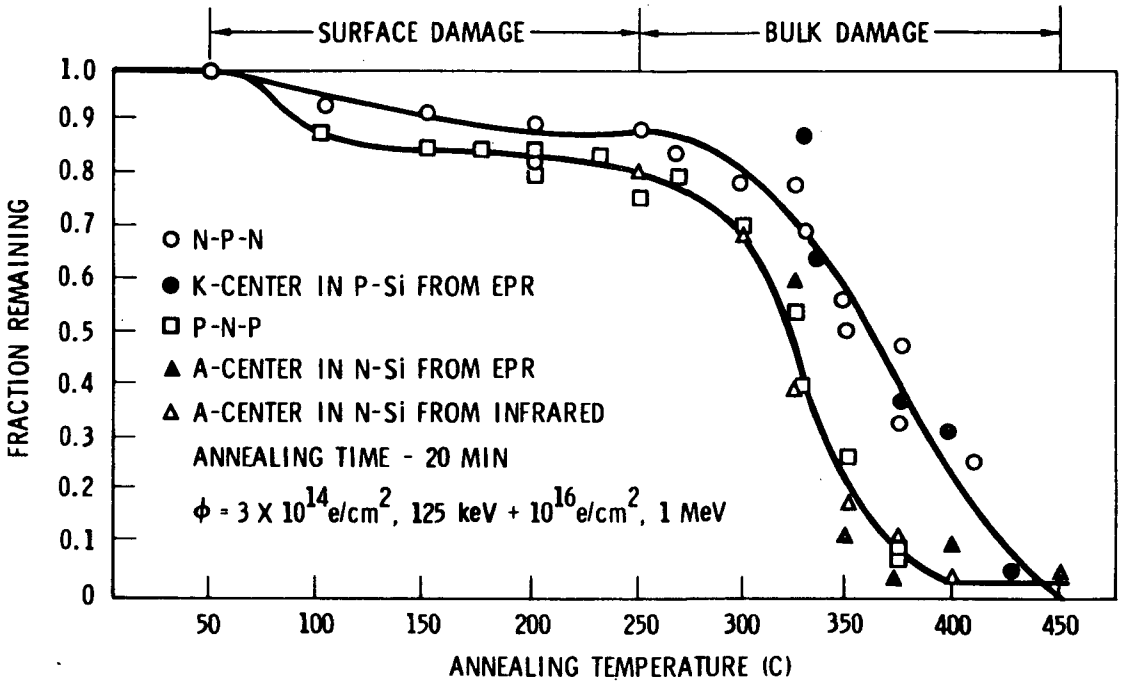

SURFACE AND BULK ANNEALING CHARACTERISTICS FOR BIPOLAR TRANSISTORS

Isochronal annealing curves for current gain recovery of 2N2102 and 2N1132 transistors show both surface and bulk annealing effects. The bulk annealing characteristic closely parallels the EPR observed annealing of A and K centers. The A center annealing characteristic deduced from infrared data is also shown. The A center is an oxygen vacancy complex stable at room temperature in silicon and the K center is a divacancy also stable at room temperature. Both defects are produced by low temperature diffusion of vacancies and their subsequent capture.

The irradiation cycle included 125-keV electrons (surface damage only) and 1-MeV electrons (bulk and surface damage).

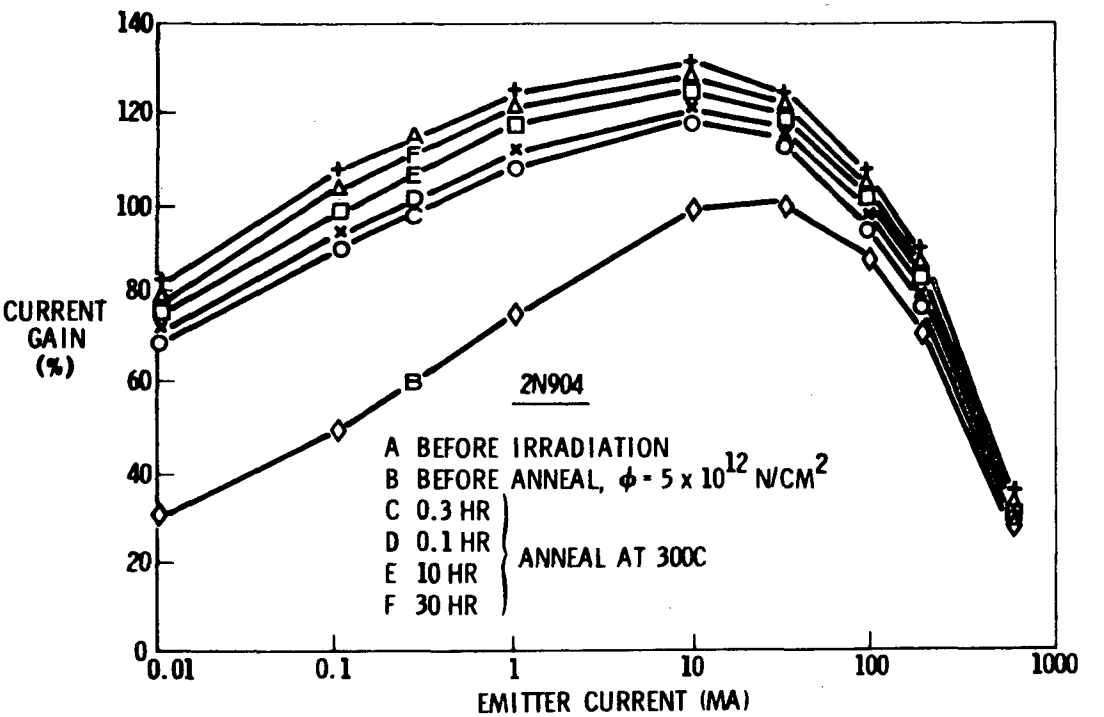

DEVICE SCREENING BY RADIATION AND ANNEALING CYCLES

High temperature annealing of "permanent" damage may be useful for initial screening of devices. Such a cycle is shown for the 2N2904. Note the almost complete recovery of the entire gain vs. collector current characteristic.

Another potential application is a pulse heating cycle during a space mission.

The annealing temperature of 300 C is as high as practical without damaging some of the device structure. This explains the rather long time for nearly complete recovery.

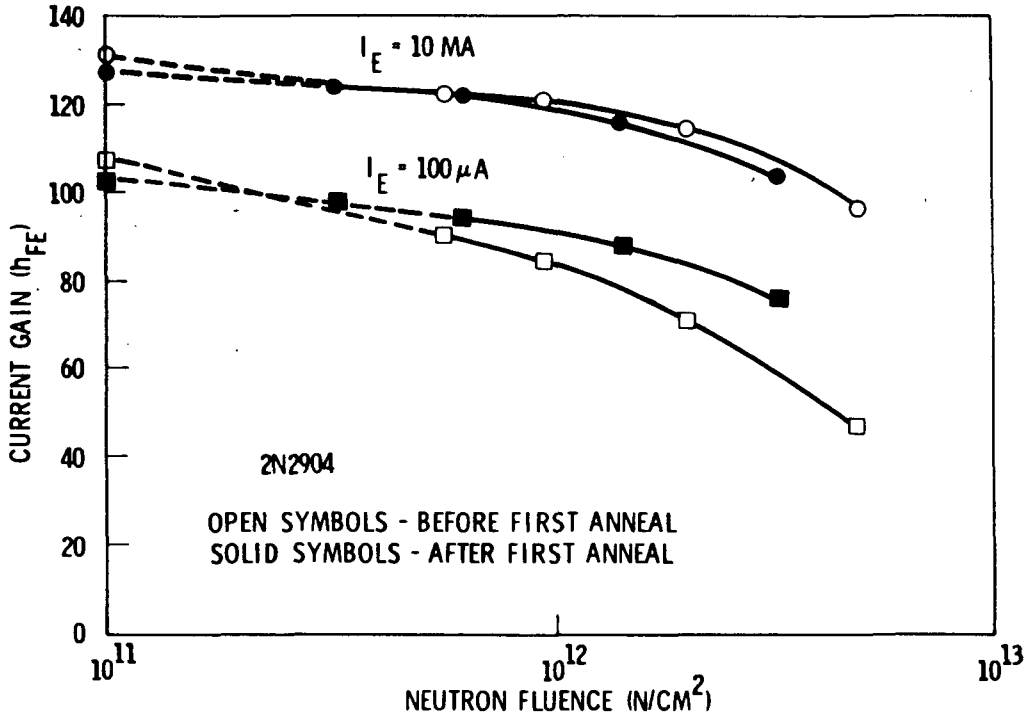

REPRODUCIBILITY OF DEVICE CHARACTERISTICS SUBSEQUENT TO SCREENING CYCLE

The use of an irradiate-and-anneal cycle requires that damage subsequent to the anneal cycle very closely follow the pre-annealing damage curve. That this is indeed the case is shown by the 2N2904 data shown above.

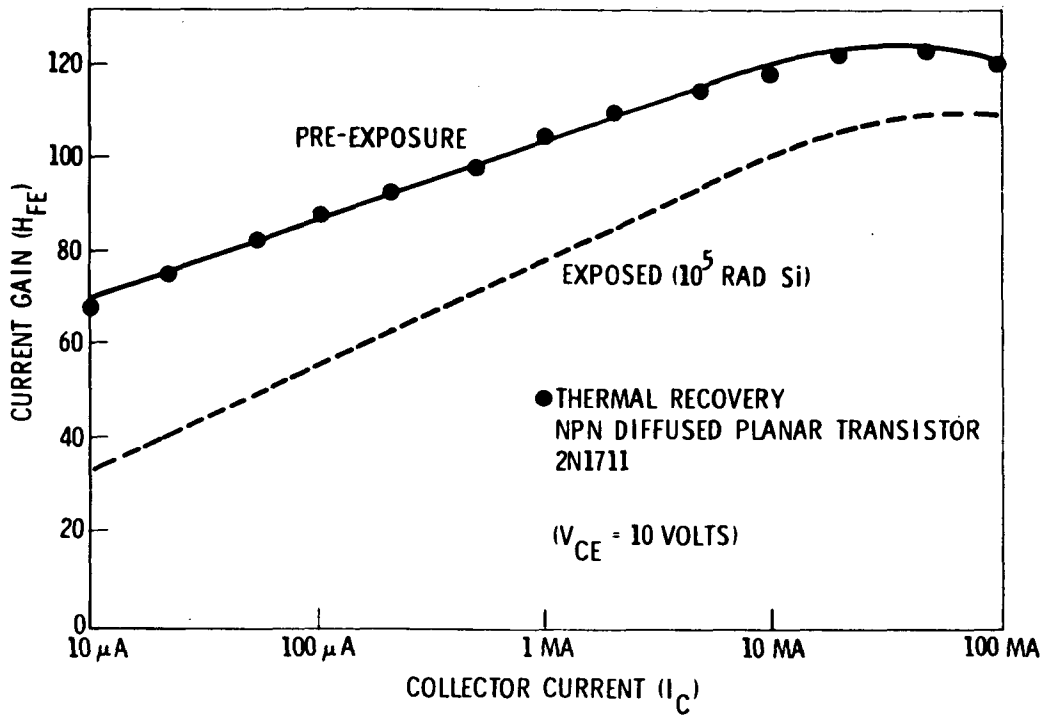

THERMAL ANNEALING OF SURFACE DAMAGE

The use of a radiation and thermal annealing cycle as a screening technique for surface damage is very promising. Required temperatures are lower (~200 C) than for annealing of bulk damage and the recovery is quite complete. Data are shown for a 2N1711 transistor. The data also show that a thermal cycling technique for recovery of degraded devices could be employed on board a spacecraft.

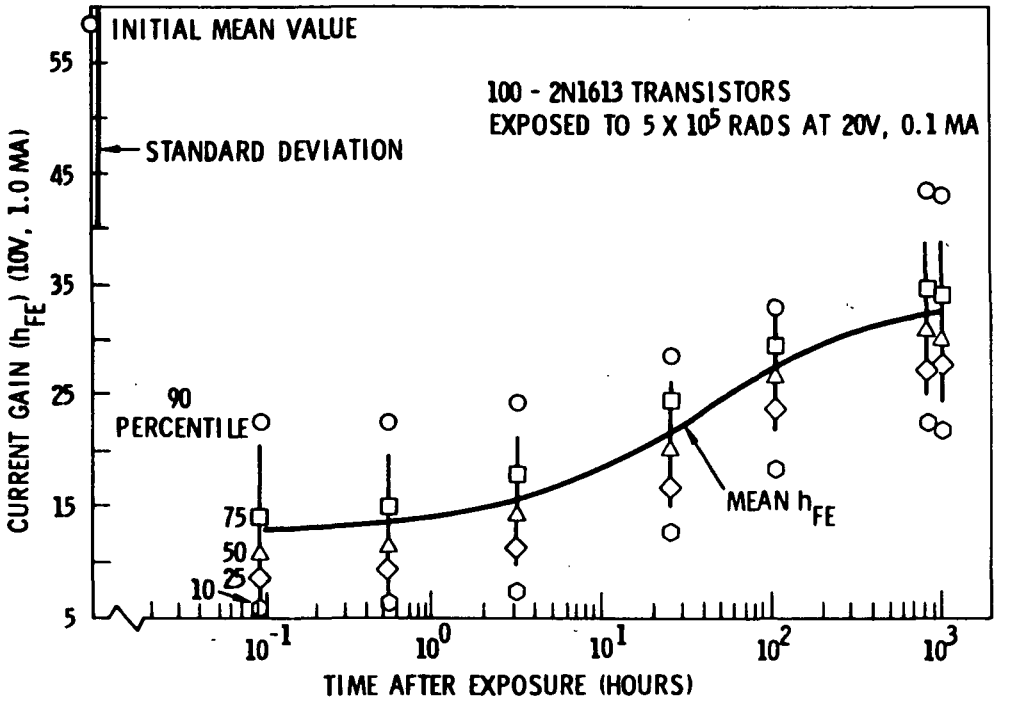

RECOVERY OF GAIN UNDER CONTINUOUS BIAS

Annealing effects can also be produced by operating biases. Gain recovery in 2N1613 transistors is shown after 5×10^5 rads. The effect of bias is to enhance the release or recombination of holes trapped in the surface oxide. Recovery is only partial at room temperature for ordinary operating biases.

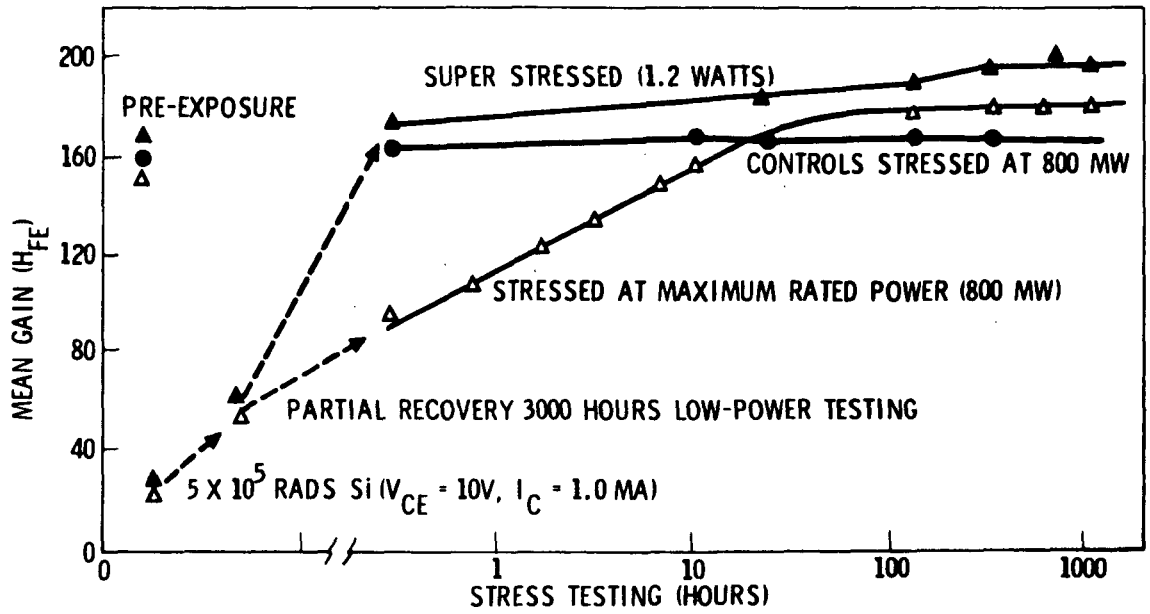

RECOVERY OF GAIN VIA OPERATING POWER STRESS

The beneficial effects of temperature and bias annealing are combined in power stressing of transistors after total dose degradation. Gain recover of 2N1711 transistors after $5X10^5$ rads exposure are shown at 800 mw (maximum rated power) and 1.2 watts (moderate overstress) and compared with control devices stressed at 800 mw. This phenomenon is readily adaptable to overload recovery of degraded units by computer controlled cycling on board the spacecraft.

(2000,000 DEVICE HOUR LIFE TESTS)

TEST CONDITION / DEVICE TYPE	PERCENT FAILURE PER 1000 HOURS* (90% CONFIDENCE LEVEL)		
	RECOVERED** FROM 5×10^5 RAD	CONTROL GROUP	JAN MIL SPEC. TX
2N1613 NPN DIFFUSED PLANAR	1.2	1.2	5.0
2N2411 PNP EXPITAXIAL PLANAR	1.2	1.2	5.0
2N1132 PNP DIFFUSED PLANAR	1.9	1.2	5.0
2N2219 NPN EXPITAXIAL PLANAR	1.9	1.9	5.0

*UNDER MAXIMUM RATED POWER
**IRRADIATED GROUPS WERE "STRESS•RECOVERED" PRIOR TO LIFE TESTING

RELIABILITY OF STRESS RECOVERED TRANSISTORS

The reliability of stress recovered units is compared with reliability of control groups and the JAN MIL specification limit. Life tests totaled 200,000 device hours under maximum rated power. No significant difference is apparent with the possible exception of the 2N1132 devices.

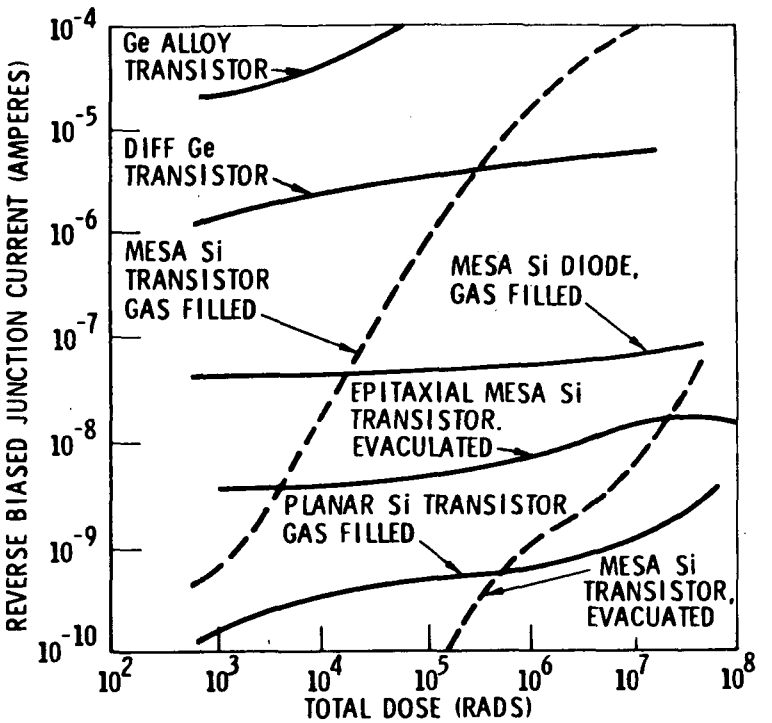

LEAKAGE CURRENTS AS A FUNCTION OF TOTAL DOSE

Surface damage depends strongly on the type of device, construction, encapsulation, and processing details. Subsequent annealing will also vary markedly due to the same variables. In addition surface control, especially on bipolar devices, is not nearly as well developed as bulk control. For field effect devices, control of the gate insulator is so vital that it has sparked considerable research and development in surface physics.

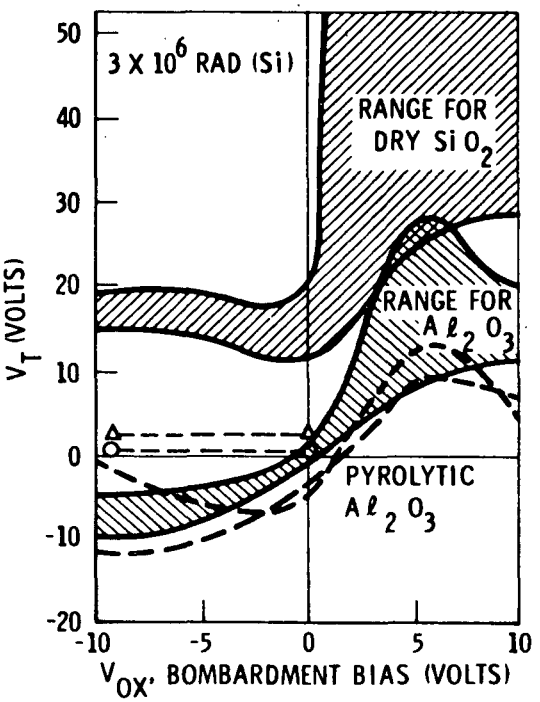

○ HARDENED SiO_2, HUGHES AIRCRAFT CO., 1 X 10^6 RAD (Si)

△ HARDENED SiO_2, AUTONETICS (CHROMIUM-DOPED), 1 X 10^6 RAD (Si)

THRESHOLD VOLTAGE SHIFT AS A FUNCTION OF OXIDE BIAS FOR MOS FETS

Unhardened MOS FETs are unsuitable for applications exceeding about 10^4 rads. The present state of the art for hardened MOS FETs is depicted here. The change for negative biases is much smaller than for positive bias since holes created by the ionizing radiation are attracted to the metal electrode and away from the oxide semiconductor interface. These properties carry over directly to the annealing results. MOS FETs anneal most rapidly under negative bias. The thermal dependence of annealing in MOS FETs is similar to transistors.

"Page missing from available version"

CIRCUIT MODELING TECHNIQUES

MODELS PREDICTING PART RESPONSE

EXAMPLES

MODELING

Circuit modeling is the mathematical representation of electrical devices and circuits so that their response to radiation effects may be predicted. Analysis of models may be by manual calculations or computer programs. A useful class of models allows prediction of response at the part level. Circuit modeling techniques are illustrated for a series regulator and an integrated circuit.

- HAND CALCULATIONS
- COMPUTER CODES

CIRCUIT MODELING METHODS

Because of the various sources of radiation damage which can be encountered in the OPGT, it is necessary to develop models for the spacecraft circuitry. These models are used to predict the effect of various components of radiation on circuit performance. The models are verified by correlation/congruence with ground radiation effects tests.

Various methods are available to model circuits for radiation effects. The first step in developing a circuit model is to obtain correspondence with electrical potentials and waveforms. Models can be developed by using simple hand calculations (equations) and by using computer codes of varying complexity.

HAND CALCULATIONS

- PERMANENT DAMAGE
- PERFORMANCE DEGRADATION
- COMPONENT STRESS
- SENSITIVITY TO RADIATION

COMPUTER CODES

- AUTOMATES HAND CALCULATIONS
  - DC BIAS/STRESS
- TRANSIENT RESPONSE
  - PERFORMANCE
  - STRESS
- AC SMALL SIGNAL
  - BANDPASS
  - STABILITY

HAND CALCULATIONS AND COMPUTER CODES

One of the most efficient ways to establish models for radiation effects is by use of hand calculations. The calculations can be formulated simply to establish component stress, effect of damage, and degradation of circuit performance. In addition, calculations can be made to determine circuit sensitivity to radiation. Such calculations can be performed on an iterative basis, or by taking the total derivative of a circuit parameter with respect to the radiation effects.

Computer codes have become increasingly useful in assisting the design and hardness specialist to prepare circuit models. Essentially, the computer codes automate many of the calculations performed in the hand analysis. They are particularly efficient in computing all biases and stresses in a circuit as a result of electrical or radiation inputs. The codes are also very useful in determining the transient and ac small-signal response of circuits. Both performance and stress calculations can be easily obtained using several available codes.

CODE ACRONYM	DEVELOPER	MACHINE
TRAC	AUTONETICS	IBM 7094, 360/65
SCEPTRE	AIR FORCE WEAPONS LABORATORY	IBM 360/65 CDC 6600
CIRCUS	BOEING CO.	IMB 360/65 CDC 6600
NET	HARRY DIAMOND LABORATORIES	IBM 360/85 CDC 6600
SYSCAP	CDC/NR	CDC 6600
MTRAC	SRI / JPL	CDC 6400 UNIVAC 1108

AVAILABLE CIRCUIT MODELING CODES

Several nationally recognized computer codes are available for use in modeling circuits. The codes are used regularly for straight-forward circuit design and evaluation as well as radiation hardening/modeling effort. In general the codes operate on the larger scientific machines: IBM 360/65, 360/85, CDC 6600, and others. Interestingly the MTRAC version of TRAC has been installed at JPL and should be operational for use.

- DAMAGE
- PHOTO CURRENT
- NONLINEAR EFFECTS

PART MODELS

In order to develop circuit models, it is necessary to use equations and data which properly characterize the piece-parts within the circuit. This characterization must include damage effects, photocurrent generation and non-linear effects. Because all parts degrade to some extent, the statistical distribution of part parameter data is necessary in order to evaluate properly the circuit probability of success for the total mission.

RESISTORS

CAPACITORS

INDUCTORS

TRANSFORMERS

RELAYS

PASSIVE PARTS

In general, the passive parts such as resistors, capacitors, inductors, transformers, relays, etc., will not be appreciably affected by radiation damage. It is necessary to characterize these parts electrically in order to properly account for the interaction between the passive parts and the more radiation-sensitive active components. Second order effects such as decreased insulation resistance, increased capacitor leakage, etc., can be modeled with parasitic resistance elements that are made a function of radiation dosage.

MINORITY CARRIER

- BIPOLAR TRANSISTOR
- RECTIFIER/DIODE
- SCRs/4-LAYER

MAJORITY CARRIER

- MOS-FET TRANSISTOR
- TUNNEL DIODE
- UNI-JUNCTION TRANSISTOR

ACTIVE PARTS

Active piece-parts are more susceptible to radiation damage than passive parts. Generally active semiconductor piece-parts fall into two categories: (a) minority carrier devices and (b) majority carrier devices. The minority carrier devices are much more susceptible to radiation damage. The bipolar transistor is often identified as the most radiation sensitive component. The damage is manifested by decreased dc current gain and increased leakage as radiation dosage is increased.

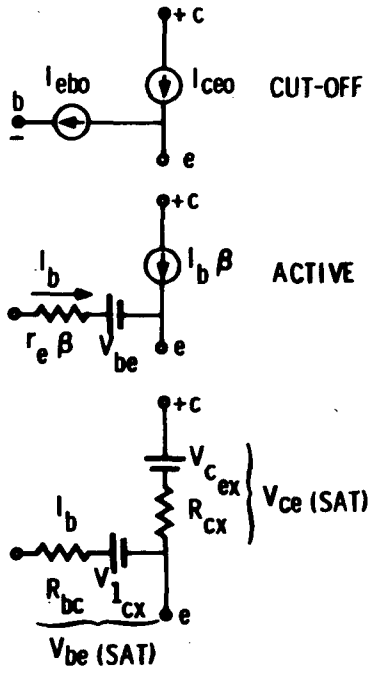

SIMPLIFIED MODELS (HAND CALCULATIONS)

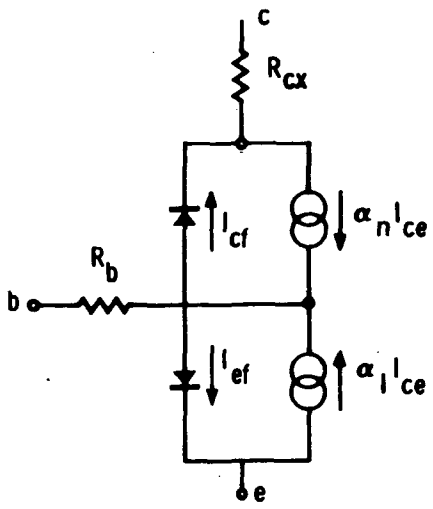

BASIC EBERS - MOLL MODEL

BIPOLAR TRANSISTOR MODELS

The bipolar transistor can be represented by two models: (a) simplified piece-wise linear and (b) nonlinear Ebers-Moll model. The former is often used in hand calculations and developing simplified functions of circuit performance. The latter is generally used in the computer codes previously mentioned. The simplified models require more knowledge of circuit states whereas the Ebers-Moll model programmed in a general purpose computer automatically determines the state.

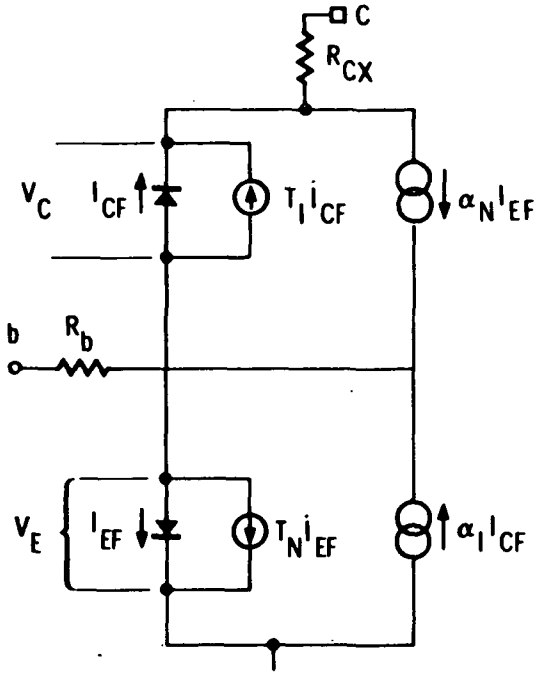

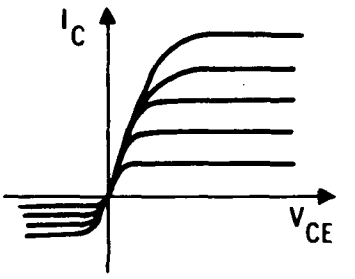

STATIC V_C-I_C

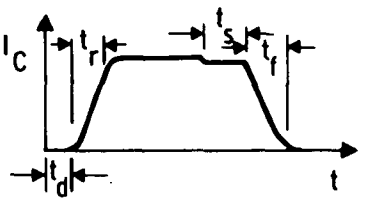

DELAY, RISE, STORAGE & FALL TIME
DYNAMIC RESPONSE

EBERS-MOLL LARGE-SIGNAL MODEL

The large-signal Ebers-Moll model accounts for the nonlinear V_C-I_C characteristics and the delay, rise, storage and fall times which characterize bipolar transistor response. More elegant improvements to this model account for (a) nonlinear beta as a function of injection level (I_E), (b) junction breakdown, (c) improved collector storage prediction, (d) conductivity modulation, (e) base-width modulation, (f) temperature effects, and (g) radiation effects. An understanding of the Ebers-Moll model is a great adjunct to improved electrical and hardness design.

- EMITTER - BASE DIFFUSION

$$I_{EF} = \frac{I_{EO}}{1 - \alpha_N \alpha_I} \left[\exp(V_E/M_E\theta) - 1\right]$$

- COLLECTOR - BASE DIFFUSION

$$I_{CF} = \frac{I_{CO}}{1 - \alpha_N \alpha_I} \left[\exp(V_C/M_C\theta) - 1\right]$$

- EMITTER-BASE DIFFUSION CAPACITANCE

$$I_{E(DIFF)} = T_N \frac{dI_{EF}}{dt} = C_e r_e \frac{dI_{EF}}{dt}$$

$$r_e = \frac{M_E\theta}{I_{EF}} = \frac{0.026}{I_{EF}} \qquad C_e = \frac{T_N I_{EF}}{M_E\theta} = \frac{T_N I_{EF}}{0.026}$$

- COLLECTOR - BASE DIFFUSION CAPACITANCE

$$I_{C(DIFF)} = T_I \frac{dI_{CF}}{dt} = C_C r_C \frac{dI_{CF}}{dt}$$

$$r_C = M_C\theta / I_{CF} = 0.04/I_{CF} \qquad C_C = T_I I_{CF}/M_C\theta = \frac{T_I \cdot I_{CF}}{0.04}$$

EQUATIONS FOR EBERS-MOLL MODEL

The basic diffusion equations for the base-emitter and base collector junctions are exponential by nature. The computer program uses a modified Newton-Raphson convergence process in order to solve these equations. The method is captured in a subroutine and permits a rapid solution for circuits with 2 to 50 transistors. More detail on the model parameters is available in the literature.

The first two equations account for the large signal dc behavior of the bipolar transistor. The remaining equations account for the dynamic small- and large-signal response of the device. Additional quantities which are not shown include: (a) depletion capacity, (b) excess phase shift in the base region, and (c) photocurrent generation.

- CURRENT GAIN

$$H_{FEN} \triangleq \alpha_N/(1-\alpha_N)$$

$$H_{FEN} = \frac{H_{FEN}(0,\ 0,\ 0)}{1 + (K_{DN} \cdot N + K_{DE} \cdot E + K_{DP} \cdot P)\, H_{FEN}(0,\ 0,\ 0)}$$

- LEAKAGE

$$I_{CBO} = I_{CBO}\left(1 + (K_{DN} \cdot N + K_{DE} \cdot E + K_{DP} \cdot P)\, K_{ICBO}\right)$$

- R_{CX}

$$R_{CX} = R_{CX}(0,0,0) / \left[1 - (a_1 N + a_2 E + a_3 P)\right]$$

DAMAGE EQUATIONS

The principal damage effect with respect to the part model causes the transistor dc current gain to decrease with increased dosage. Leakage current and collector bulk resistance also increase with increased radiation dosage, however, the effects are generally not as dramatic as the dc H_{FEN}. Each damage constant K_{DN}, K_{DE}, and K_{DP} accounts for neutron, electron, and proton dosage.

• DIODE

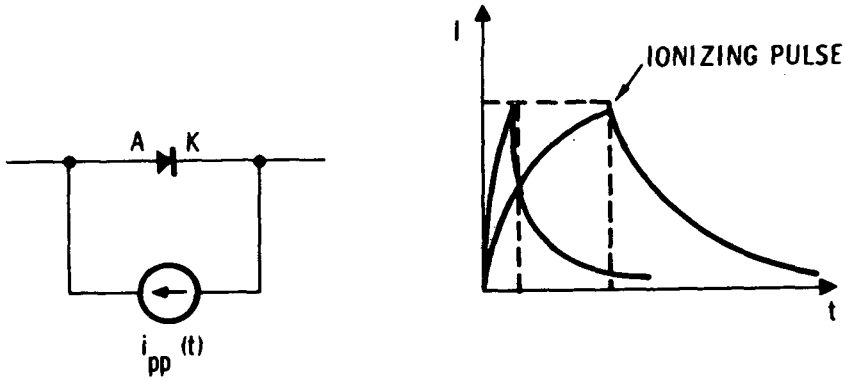

$$i_{pp}(t) = A_1 + A_2 \operatorname{erf}\sqrt{t/\tau} + A_3 \operatorname{erf}\sqrt{t/\eta}$$

τ = MINORITY CARRIER LIFETIME

η = MAJORITY CARRIER LIFETIME

PRIMARY PHOTOCURRENT

Although of secondary importance to the OPGT, photocurrent generation has been accounted for in the diffusion model. The constants represented by A_1, A_2, and A_3 represent scale factors relatable to ionizing dose rates. In general, photocurrent momentarily increases the reverse leakage current of the diode but does not appreciably affect the forward characteristics.

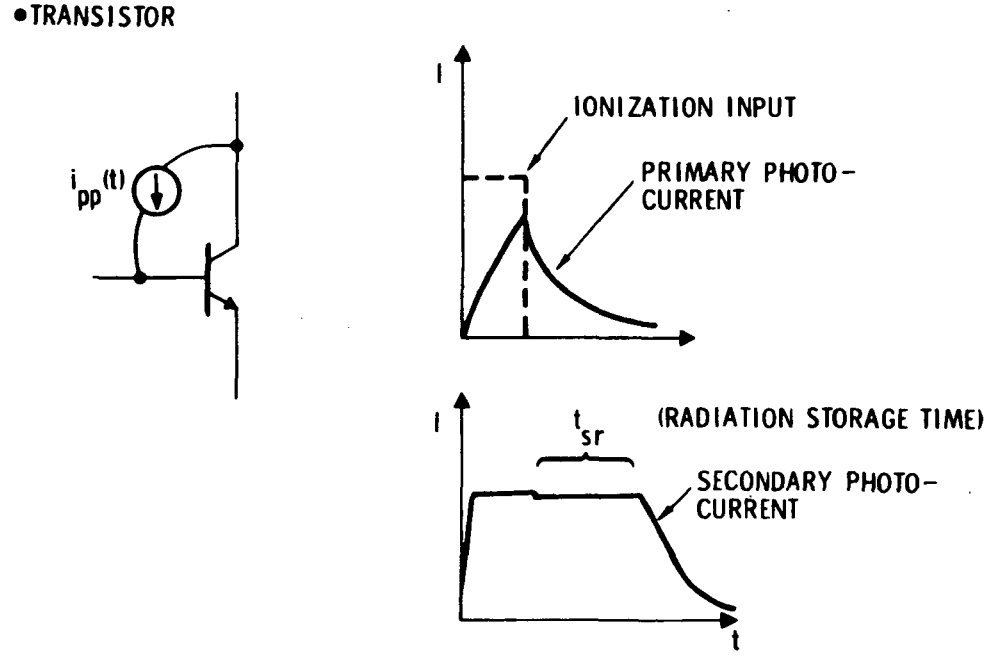

SECONDARY PHOTOCURRENT

In a bipolar transistor the primary photocurrent which flows from collector to base gives rise to a secondary photocurrent due to beta multiplication. With high gain devices (such as Darlington circuits) very high secondary photocurrents can flow for low dose rates. The ultimate result for high enough dose rates produces transistor saturation limited only by circuit resistance. The result is a radiation storage time, T_{SR}, which is indicative of device susceptibility to ionizing radiation.

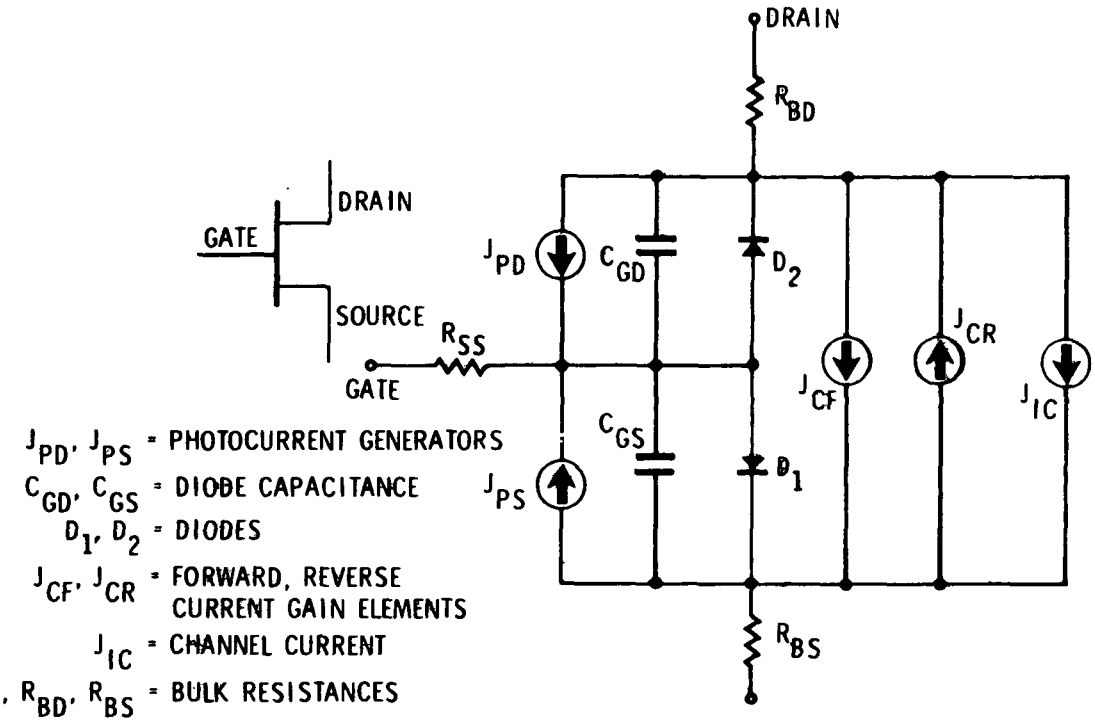

JFET MODEL

The JFET device operates on the majority carrier principle. The model accounts for forward and reverse bias conditions as well as photocurrent. Damage mechanisms are dependent on surface effects which must be obtained experimentally. These effects can be introduced empirically as fixed parameter values for pinch-off voltage and transconductance.

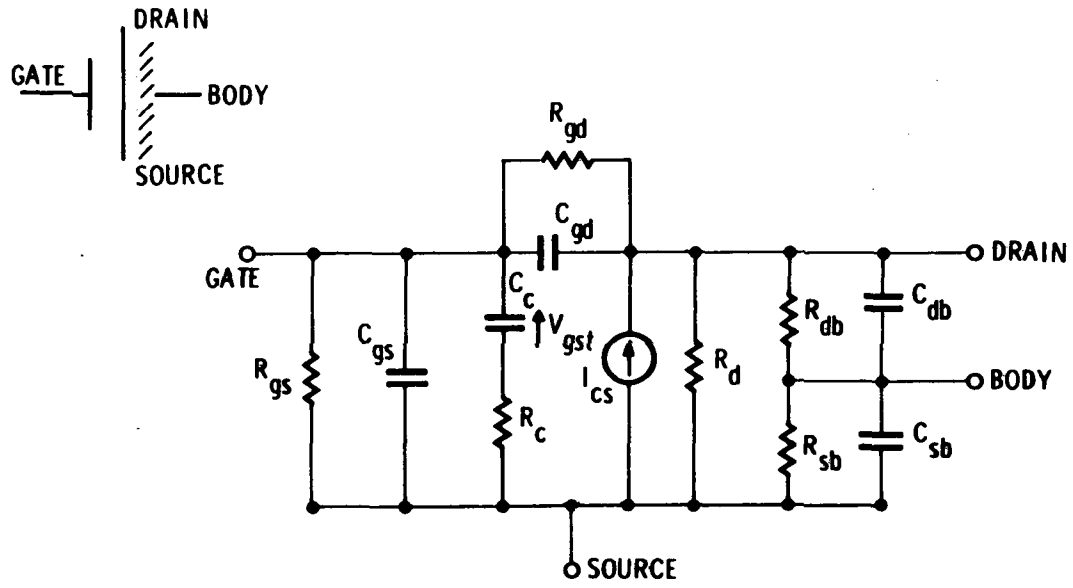

MOS FET MODEL

The MOS FET is similar to the JFET model but is characterized by improved isolation. The model illustrated is applicable to normal operation but does not account for inverse operation. Dose-dependent degradation must be inferred as fixed parameters affecting pinch-off and transconductance.

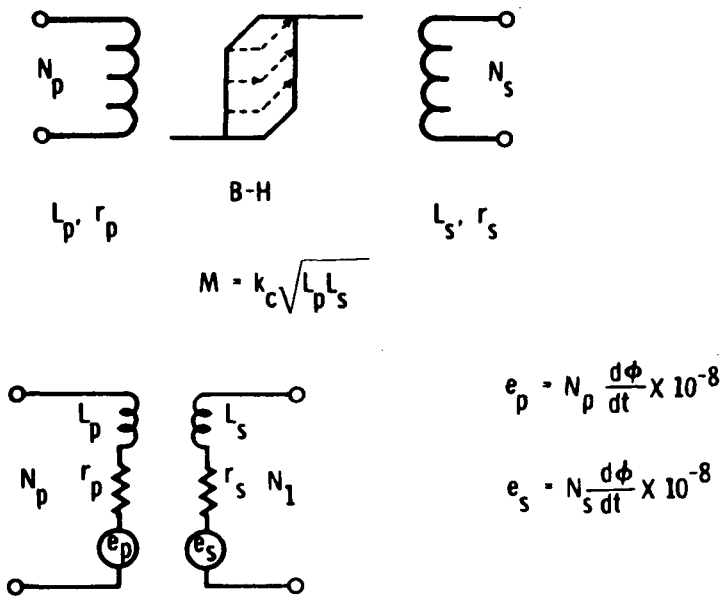

MAGNETIC MODEL

The magnetic model is often required for the analysis of power inverters, transformers, etc., when used in conjunction with semiconductors. The model accounts for the static B-H loop and simplified minor loops. The MTRAC Program contains a more elaborate magnetic model.

- SERIES REGULATOR
- INTEGRATED CIRCUIT

EXAMPLES

Two examples have been selected to demonstrate how the models can be developed and verified. One circuit is an simplified version of a series regulator. The other example is an integrated circuit. A portion of the circuit is analyzed and modeled since the total circuit is simply a repetition of the basic section chosen for modeling.

• SCHEMATIC DIAGRAM

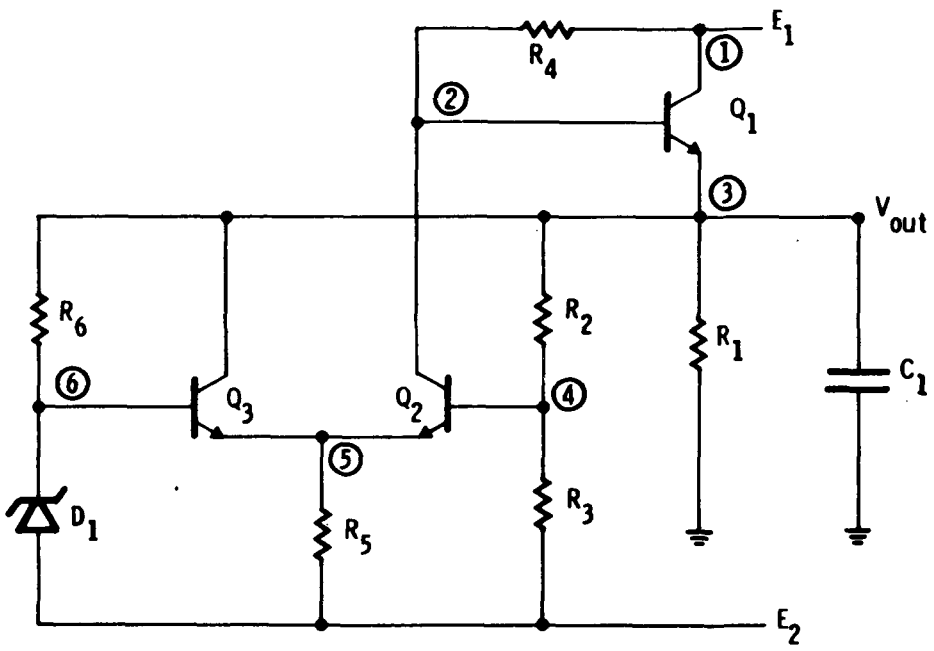

EXAMPLE 1: SERIES REGULATOR

The series regulator circuit consists of one power transistor Q_1 and two medium power transistors, Q_2 and Q_3. The circuit nodes are sequentially numbered and coded in a general purpose computer program (SYSCAP). The inputs and resultant outputs for dc and turn-on transient response are illustrated in the subsequent charts.

PART	SYMBOL	NOMINAL	MINIMUM	MAXIMUM	UNITS
RESISTORS	R_1	12	6	1200	OHMS
RESISTORS	R_2	470	465	475	OHMS
RESISTORS	R_3	3.3	3.27	3.33	K OHMS
RESISTORS	R_4	133	120	146	OHMS
RESISTORS	R_5	40	36	44	OHMS
RESISTORS	R_6	1.8	1.6	2.0	K OHMS
CAPACITOR	C_1	100	70	130	μFD
DIODE	D_1	TYPE 1N753 (DATA BANK)			
TRANSISTOR	Q_1	SPECIAL			
TRANSISTOR	$Q_{2,3}$	TYPE 2N3039			
VOLTAGE	E_1	28	24	32	VOLTS
VOLTAGE	E_2	-12	-12.1	-11.9	VOLTS

- REQUIRE VOLTAGE, CURRENT, POWER IN ALL PARTS
- ALL NODE VOLTAGES

INPUT DATA

The input for the series regulator consists of the nominal minimum and maximum values that can be expected for the circuit piece parts. The parameters for the semiconductor parts are called from the computer library. Special data are required for the power device in order to account for the beta variation including the degradation from a specified radiation damage.

In addition to part values and tolerance, interface data are required. In this example two power sources (+28V and -12V) are needed to provide raw power to the regulator.

The required output which must be calculated includes voltage current and power dissipation for all parts.

SUMMARY (BETA CHANGES ONLY)

VARIABLE	NOMINAL	MINIMUM	MAXIMUM	CRITICAL PARAMETERS
V_{OUT} (VOLTS)	12.0882	11.4541	13.3456	BETA Q_3
				BETA Q_1
				BETA Q_2
P_{Q_1} (WATTS)	16.879	16.573	17.2	SAME
P_{Q_2} (WATTS)	0.64	0.45	1.03	SAME
P_{Q_3} (WATTS)	1.8	1.357	2.022	SAME

OUTPUT (DC RESULTS)

The principal outputs calculated by the computer program indicate that the output voltage exceeds (12 + 1.0) volts by 0.3456 volts for nominal resistance values and beta variations only. The beta variations include a damage factor. The calculations for power dissipation are performed simultaneously and indicate no abrupt increase in power stress due to beta variations.

ALL PARAMETERS ARE AT NOMINAL

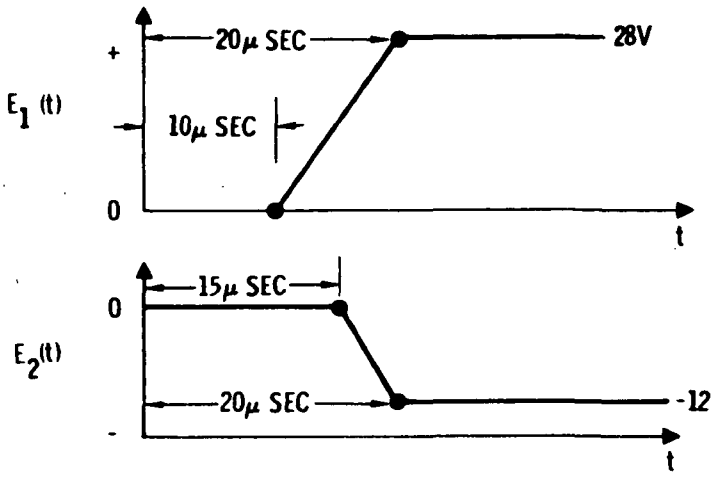

RESULT P_{Q_1} (PEAK) = 194.0 W at t = 20.3 μ SEC

TRANSIENT (TURN-ON)

Since transient effects caused by photocurrent are of secondary importance to the OPGT Mission, it is more informative to use the circuit computer model for power sequencing studies. The example series regulator can be studied for sequenced power turn-on. It should be noted that a momentary power stress of 194 watts occurred during turn-on at T = 20.3 μsec.

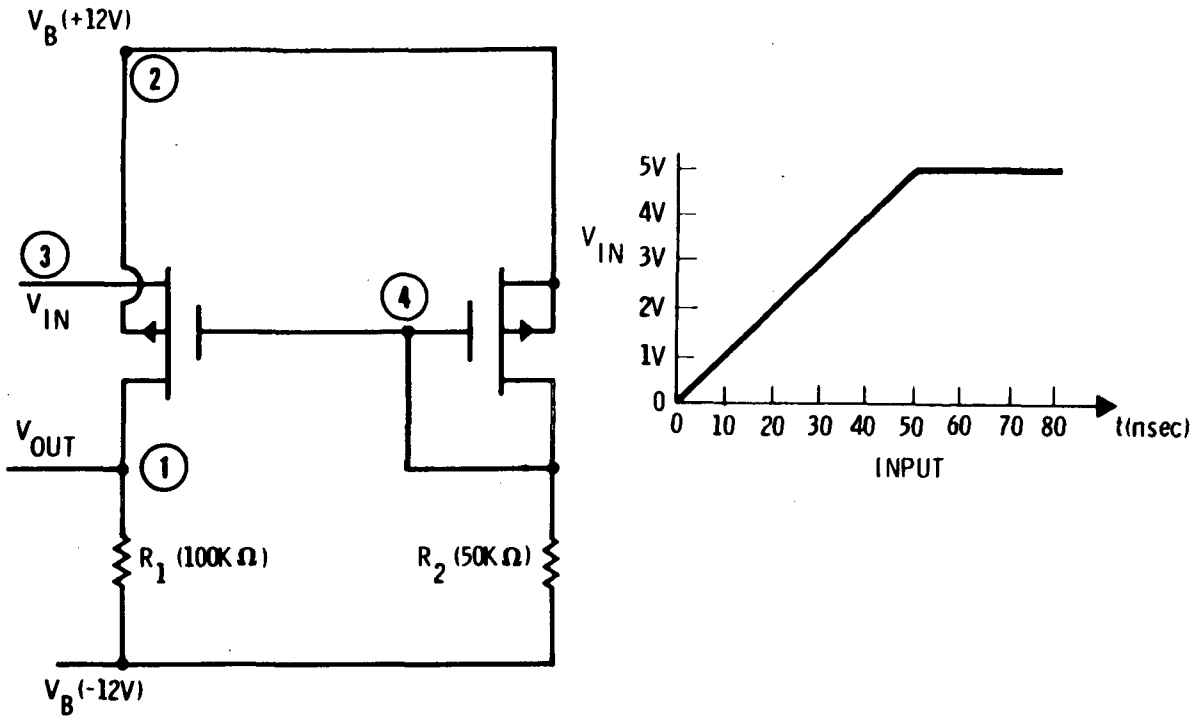

EXAMPLE 2: INTEGRATED CIRCUIT (SOS)

The integrated circuit is a portion of a special SOS designed to interface with bipolar circuitry. The computer model is used to study the variation of the circuit transfer function (V_{out} vs. V_{in}) as a function of threshold voltage V_T.

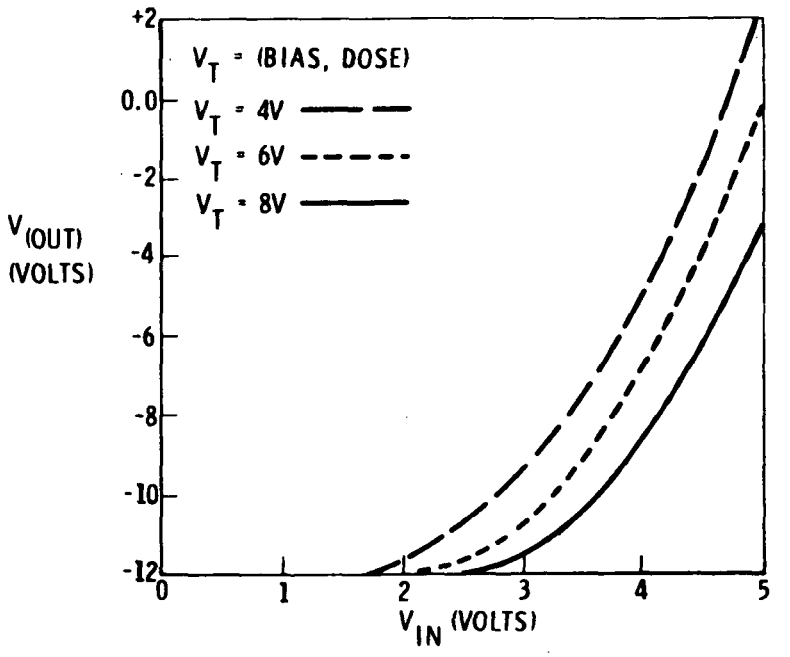

OUTPUT/INPUT VS V_T

The transfer function (V_{out} vs. V_{in}) as a function of threshold indicates a decrease in voltage swing for the available bias voltage. The incremental voltage gain remains fairly constant. The threshold voltage is affected by radiation. The amount of damage depends on the bias conditions hence:

$$V_T = V_T \text{ (Bias, Total Dose)}$$

- AMOUNT OF RADIATION (N, E, P)
- CHARACTERIZATION OF SENSITIVE PARTS
- CIRCUIT MODELS USING CHARACTERIZED PARTS
- CIRCUIT ANALYSIS USING MODELS TO VERIFY DESIGN INTEGRITY
- DEGREE OF COMPLEXITY
- DEGREE OF SOPHISTICATION

SUMMARY

The previous material has treated modeling techniques, part models, and two examples showing application of the modeling methods. The process of developing the models for circuit analysis requires: (a) quantifying the amount of radiation for each source: neutron, electron, and proton, (b) characterizing the radiation sensitive parts using part models, (c) applying the models to circuits (hand/computer), and (d) establishing the design margin required to assure mission success. The degree of sophistication required is subject to circuit complexity, criticality, and part sensitivity.

BIPOLAR DEVICES

MOS DEVICES

MICROCIRCUITS

Microcircuits allow compaction and reduced mass and power requirements in electronic subsystems. They are, therefore, of great interest in OPGT. Current microelectronic technology and associated radiation effects are described for various bipolar and metal oxide semiconductor (MOS) devices.

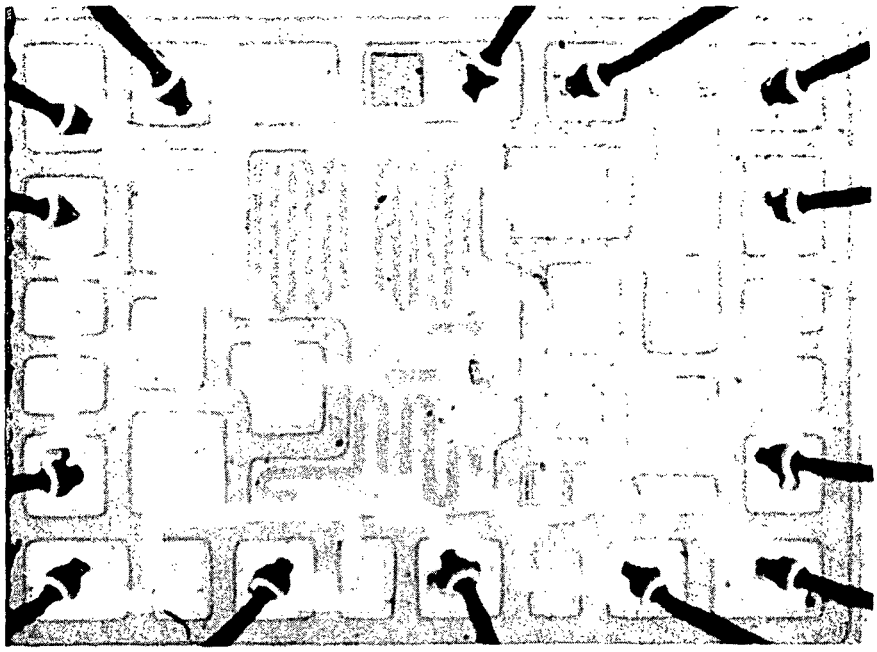

A MONOLITHIC INTEGRATED MICROCIRCUIT

The same fabrication methods which are used to build individual transistors may also be applied to the fabrication of passive components such as diodes, resistors and capacitors. All active and passive components for a circuit may be fabricated simultaneously in or on a single piece of silicon crystal. These components are then interconnected by an aluminum metallization pattern to produce monolithic microcircuits such as the one shown. Circuits such as this are now used to perform most digital and analog functions in complex electronic systems.

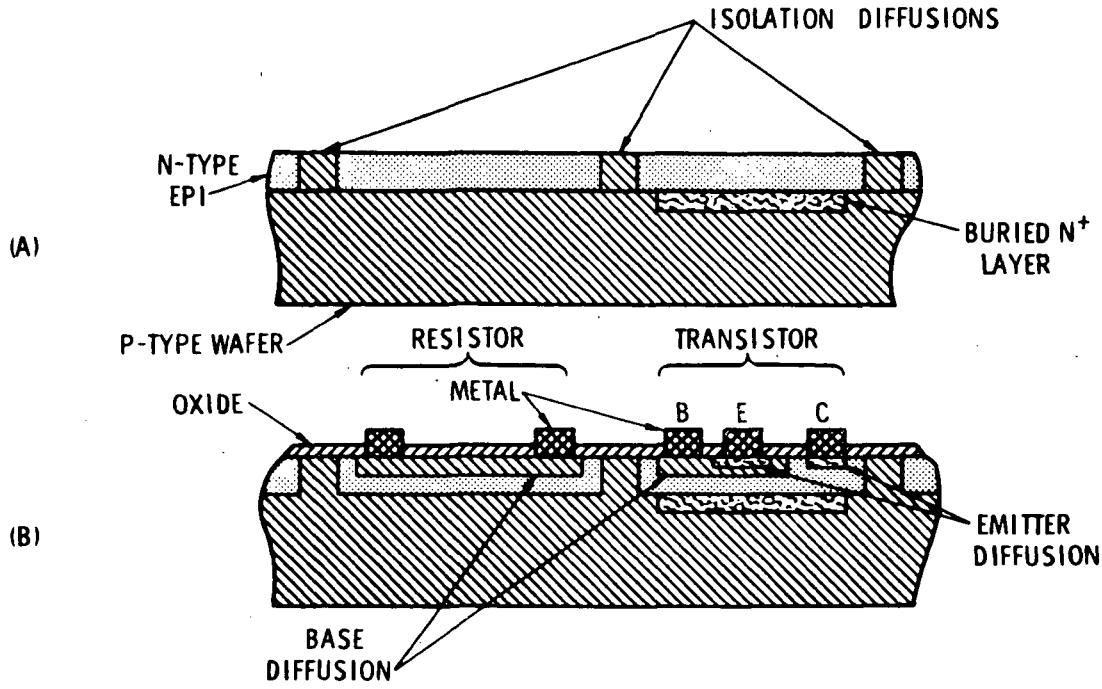

JUNCTION ISOLATED MICROCIRCUITS

The various components of a microcircuit are usually isolated from the silicon substrate by a reverse biased P-N junction. The isolation junction is formed by a combination of epitaxial growth and diffusion as shown in (a). Transistors, resistors and diodes are then formed by diffusion into the isolated N-type regions as shown in (b). A buried N^+ layer, formed by diffusion into the starting wafer before epitaxial growth, is needed to provide a low collector resistance. Capacitors may be either MOS capacitors or P-N junctions.

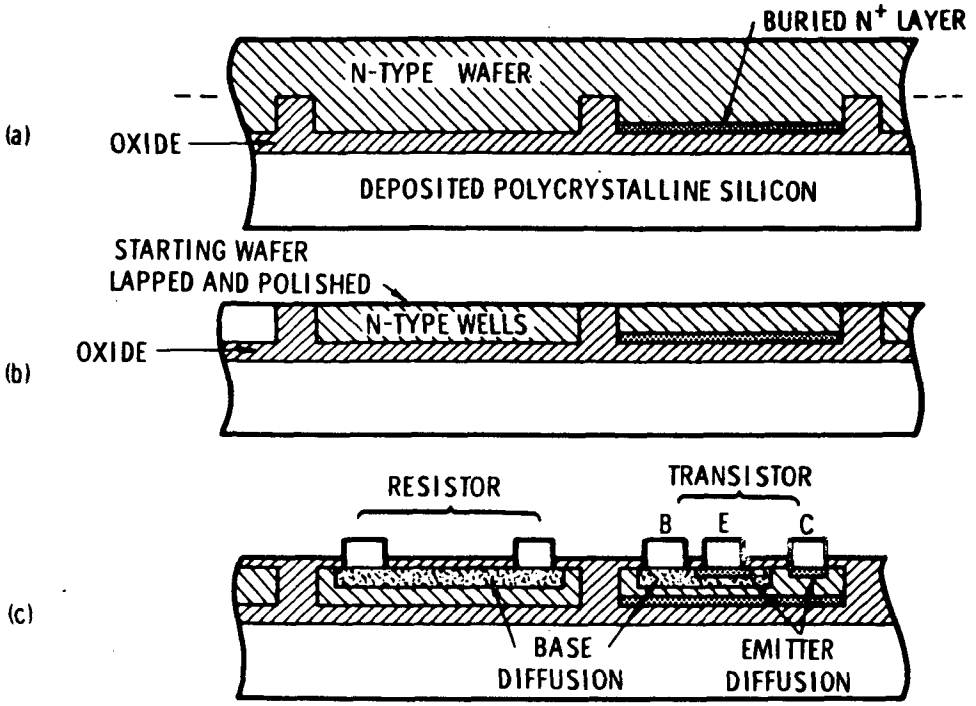

DIELECTRIC ISOLATION

Dielectric isolation is used in many radiation hardened microcircuits designed for military systems. The reason for using dielectric rather than junction isolation is to eliminate transient photocurrents generated in the isolation junctions. An outer planetary spacecraft will not encounter the high dose rates for which dielectrically-isolated (DI) circuits are needed, and junction-isolated circuits are acceptable for Grand Tour missions. Many existing radiation hardened designs do employ dielectric isolation, however, and use of an existing DI circuit type may frequently be a good design choice.

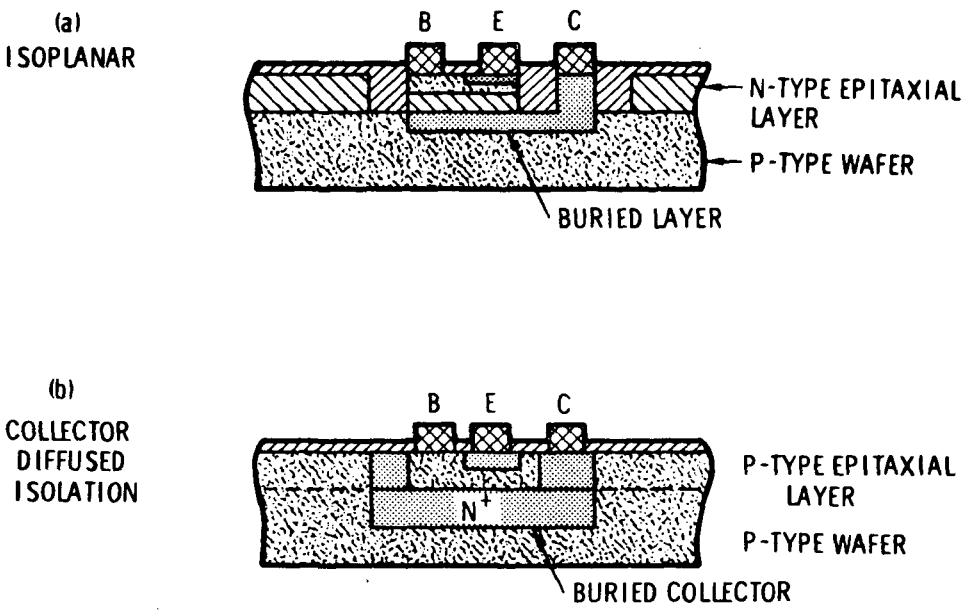

NEW FABRICATION METHODS

Two new fabrication techniques for junction isolated integrated circuits are shown above. The isoplanar technique shown in (a) replaces the isolation diffusion with a silicon etching and oxidation step which removes the silicon between N-type pockets and replaces it with silicon dioxide. The collector diffused isolation approach shown in (b) uses an N^+ diffusion to a buried N-type collector region to provide isolation. Both processes reduce the number of process steps required. They also save area on the integrated circuit chip by saving much of the space formerly required for the isolation diffusion.

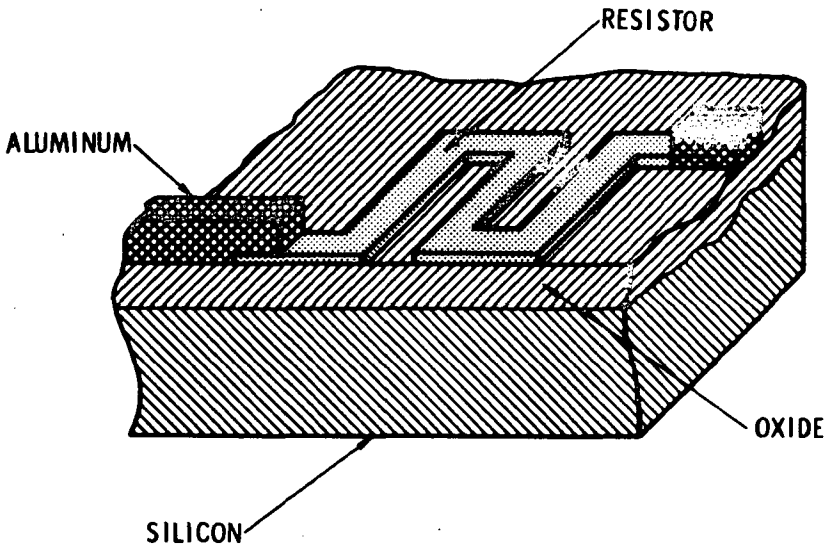

THIN-FILM RESISTORS

Another new fabrication technique for radiation hardened circuits is to substitute nichrome, chromium-silicon, molybdenum silicide, or other thin-film resistors for the diffused silicon resistors. Thin-film resistors are virtually free of any radiation damage effect at practical radiation doses, and they can also effect a saving in chip area. Before these advantages can be exploited, however, the reliability and stability of the particular fabrication process must be established. Added process steps are required for their fabrication, and this may increase production costs.

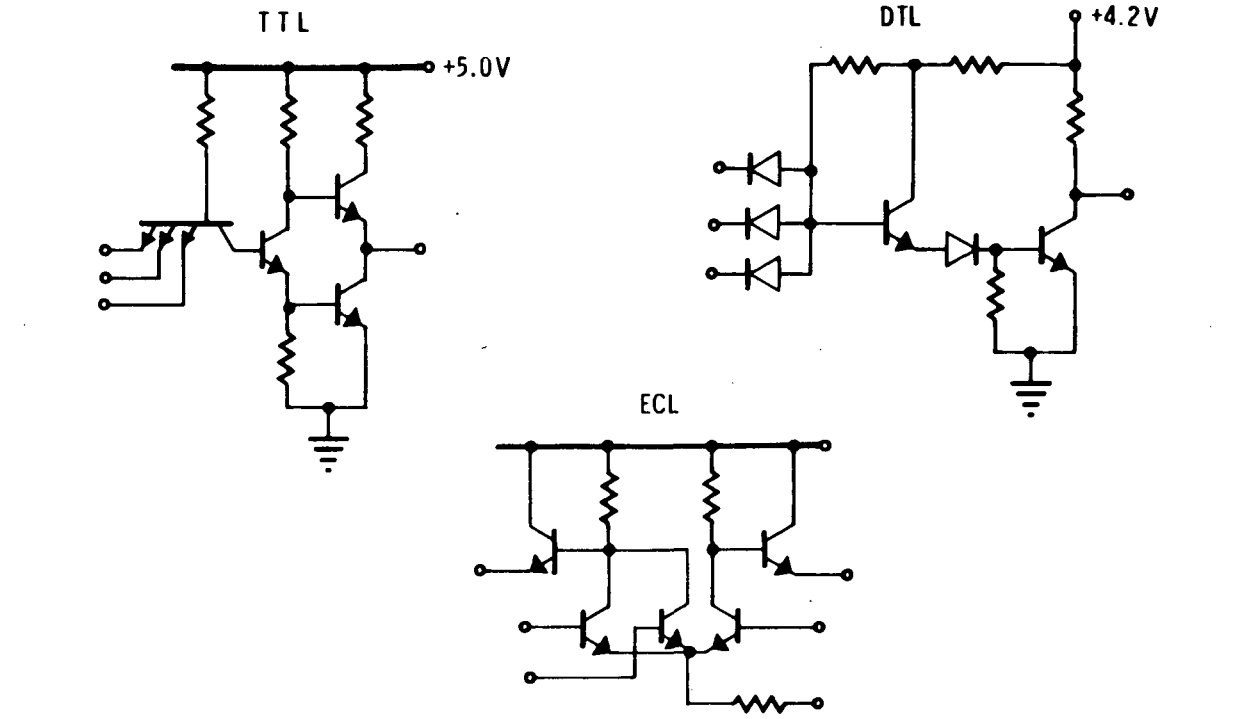

COMMON FAMILIES OF DIGITAL CIRCUITS

Digital microcircuits are available in a number of well developed families whose characteristics and specifications are nearly identical among manufacturers. Radiation hardened versions of common TTL and DTL circuits have been developed and are available from several manufacturers.

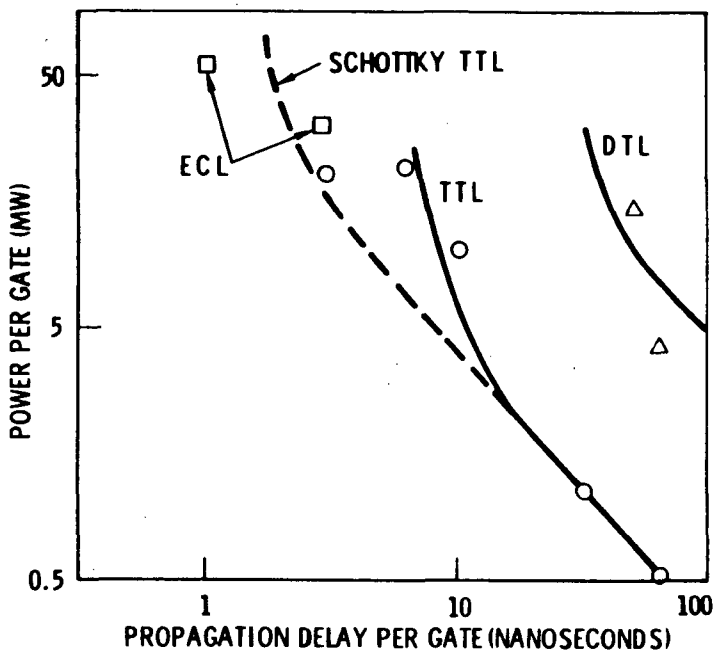

SPEED AND POWER OF COMMON LOGIC CIRCUITS

Speed and power requirements are often the most important considerations in the selection of a logic family. The range of speed and power available for each digital circuit type is shown above.

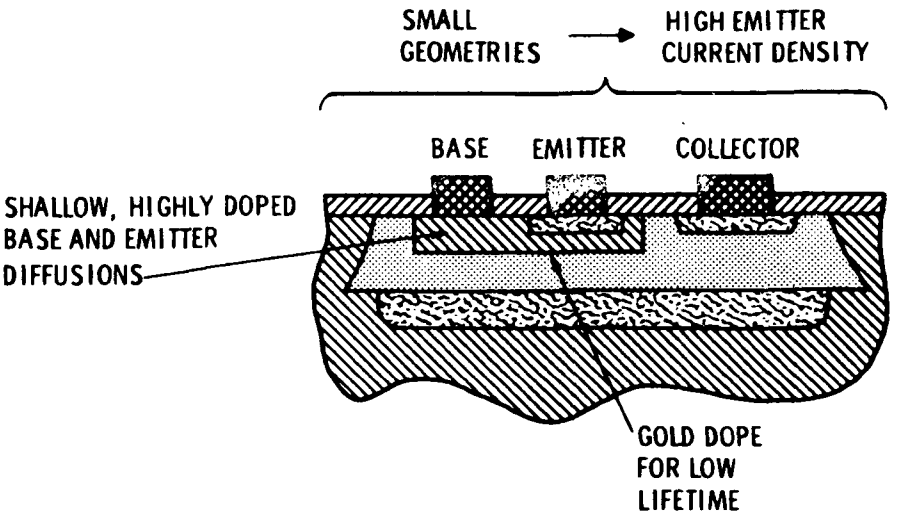

CONSTRUCTION FOR HARDENED DIGITAL CIRCUITS

The most important consideration in design and fabrication of hardened digital circuits is h_{FE} degradation in the transistors due to neutron or proton damage. h_{FE} degradation is minimized by use of shallow, highly doped emitter and base regions which result in a narrow base width and a short base-emitter space charge region. Since the effects of surface and emitter base space charge recombination are minimized by operation at high current densities, small transistor geometries are also preferred. Fortunately, these design features are also those required for high performance digital microcircuits, and major changes in device construction or performance are not required. Furthermore, fabrication techniques such as gold doping to increase switching speed also minimize photocurrent generation in a transient ionizing radiation environment.

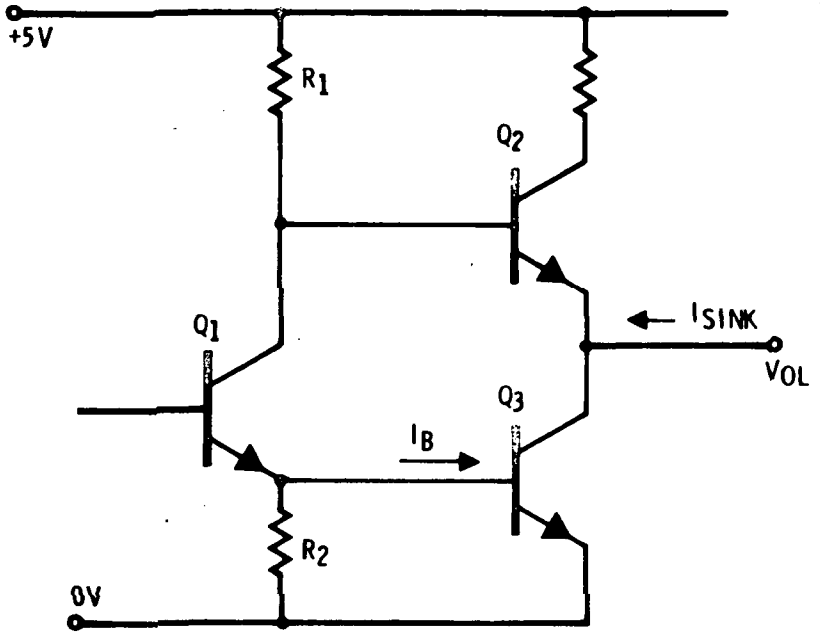

TTL OUTPUT

GAIN MARGIN IN DIGITAL CIRCUITS

Radiation induced failure in a TTL or DTL circuit is usually a result of β degradation in the output sinking transistor. In the circuit above, the base current drive on Q3 is

$$I_{B3} = \frac{5V}{R_1} - V_{BE3}\left(\frac{1}{R_1} + \frac{1}{R_2}\right).$$

This current has to be large enough that

$$h_{FE3}\ (\text{post irradiation}) \cdot I_{B3} \geq I_{SINK}$$

or Q_3 will come out of voltage saturation and allow V_{OL} to rise above the specified level.

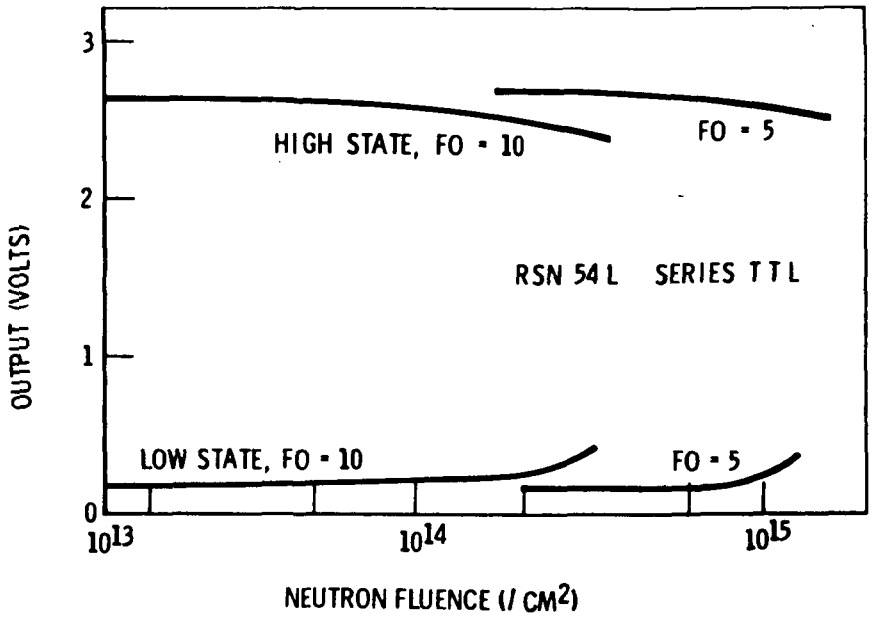

NEUTRON TOLERANCE OF HARDENED DIGITAL CIRCUITS

The neutron tolerance available in radiation hardened digital circuits is shown above. Note that reducing the required fan-out from 10 to 5 will considerably increase the radiation tolerance of the circuit. Digital microcircuits are usually among the most radiation resistant semiconductor devices in a system. See R. J. Olson, D. R. Alexander, and R. J. Antinone, Radiation Response Study of New Radiation-Hardened Low Power TTL Series, IEEE Conference on Nuclear and Space Radiation Effects, July 1971.

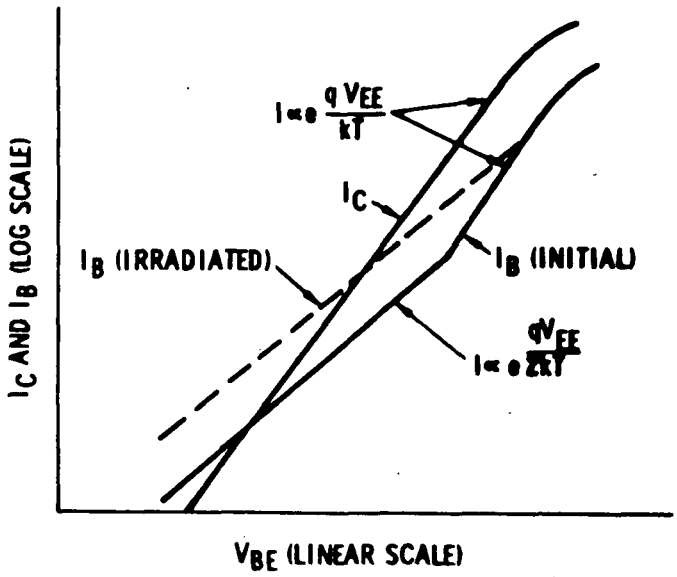

SURFACE EFFECTS ON TRANSISTOR GAIN

Degradation of bipolar devices can also be due to ionization damage at the silicon surface. The surface component of base current can be identified because it is related to V_{BE} by

$$I_{BS} = I_{SO} \exp\left(\frac{q V_{BE}}{2 kT}\right)$$

while the bulk transport component is given by

$$I_{BT} = I_{TO} \exp\left(\frac{q V_{BE}}{kT}\right)$$

This difference and the effect of ionizing radiation on the surface component are shown above. The effect on transistor h_{FE} is normally important only at low current levels.

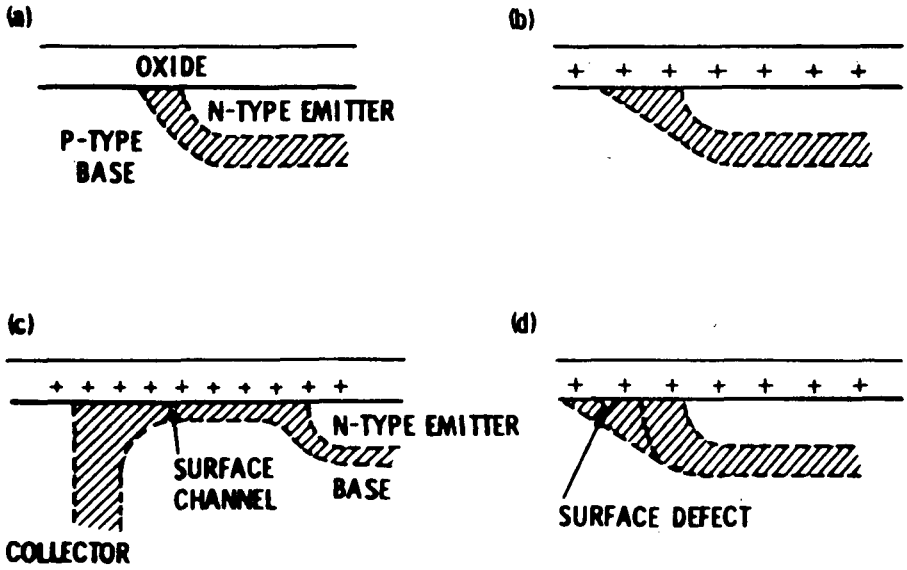

SURFACE DEPLETION AND INVERSION EFFECTS

Significant surface radiation damage in transistors operating at appreciable currents is probably due to depletion or inversion of the silicon surface over the base region. Such effects in planar devices such as microcircuits are a result of positive charge trapped in the passivating oxide. Surface depletion or inversion can be prevented by heavily doping the surface of the base region, as is done in most radiation hardened microcircuits. For a discussion of these effects, see V. J. K. Reddi and C. A. Bittman, Solid State Electronics 10, 305-334 (April 1967)

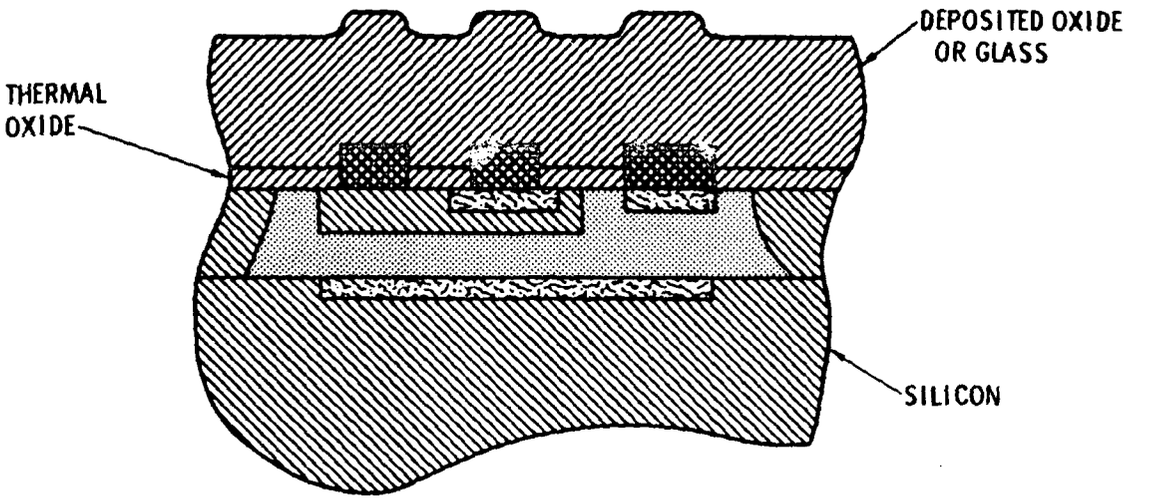

GLASSIVATION

A deposited oxide or glass layer is sometimes used as a protective coating on the top of microcircuits. This layer will prevent mechanical damage to the metallization and also helps protect against contaminants which may degrade the surface.

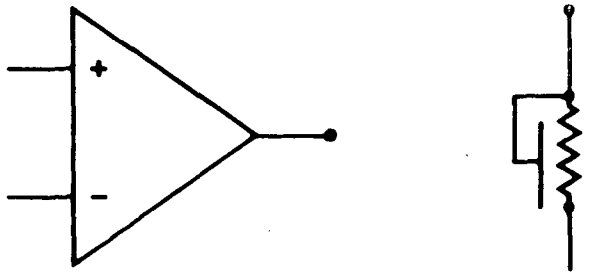

AVOID:

101PD111050
LOW CURRENT DENSITIES
SUPER β TRANSISTORS
MOS LOAD RESISTORS
CURRENT BIAS

HARDENING CONSIDERATIONS IN LINEAR CIRCUITS

Linear circuits are generally more difficult than digital circuits to harden to radiation effects. Compromises between circuit performance and radiation hardness are often required. Some linear circuit techniques which can cause problems in a radiation environment are listed above.

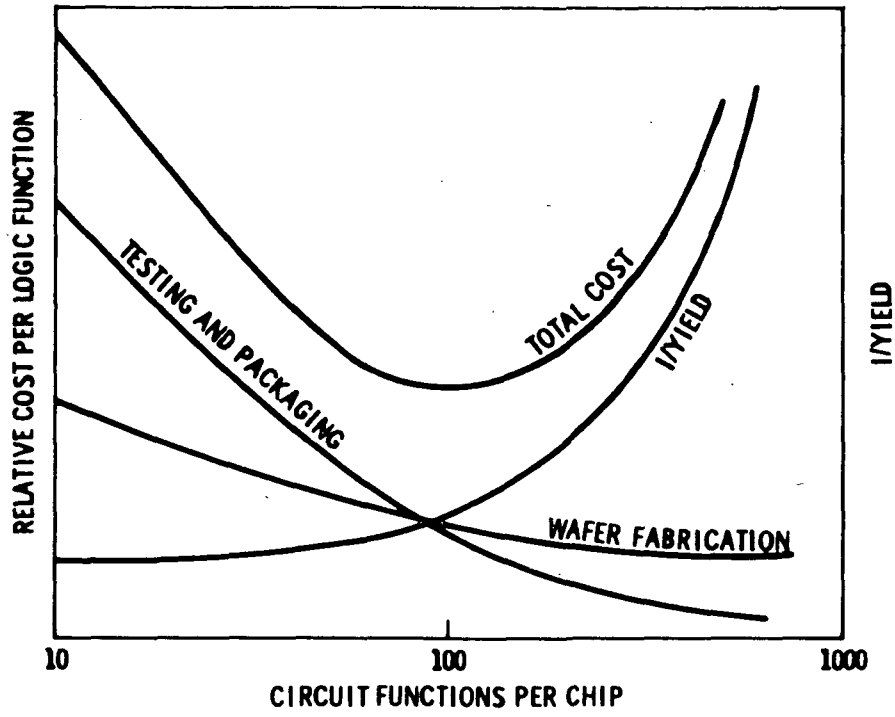

COST AND YIELD FACTORS IN MSI/LSI CIRCUITS

Microcircuits are being made increasingly larger and more complex. One of the factors in this trend is economic as shown above. Additional advantages are smaller size and lower weight for electronic systems. A major cost factor is yield, i.e., the percentage of completed circuits on a wafer which work. Yield is improved by small device geometries and simplified processing, thus the general trend is toward fabrication methods which permit high yields.

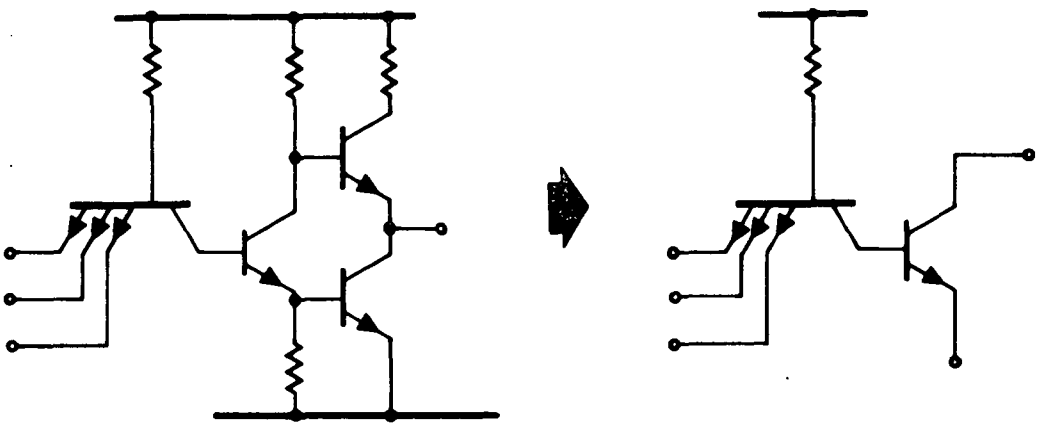

HARDNESS CONSIDERATIONS IN MSI CIRCUITS

The design of a hardened MSI circuit is somewhat changed from the design of a standard logic function. Commercial circuits take advantage of the lower capacitance and the controlled noise environment available within the confines of the circuit chip to use simplified circuit configurations as shown above. Hence, unhardened MSI circuits may prove more vulnerable to radiation effects because of the smaller noise margins that are used. To satisfy all the stringent requirements, radiation-hard designs tend to be more costly. However, they usually prove to be superior to conventional designs because individual logic gates can be tailored to a specific function.

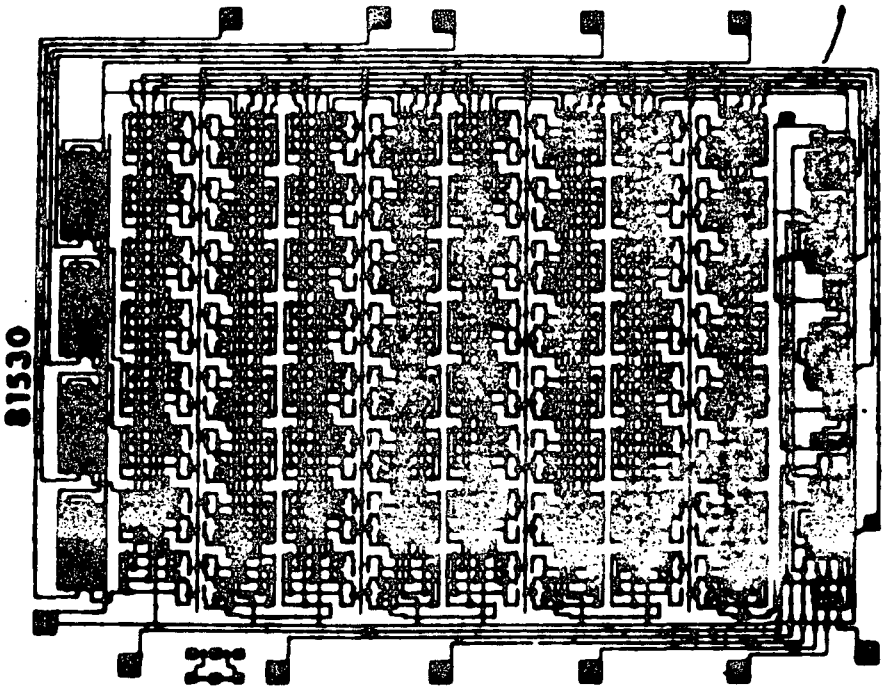

A LARGE SCALE MOS ARRAY

Microcircuits based on an MOS (metal oxide semiconductor) transistor technology are now being used in many commercial and industrial applications. The major advantages of MOS circuits are a high functional density and simple, high yield, process steps which make it practical to build highly complex circuit functions in a single chip. An attractive feature for space applications is the low power requirement of many MOS circuit types.

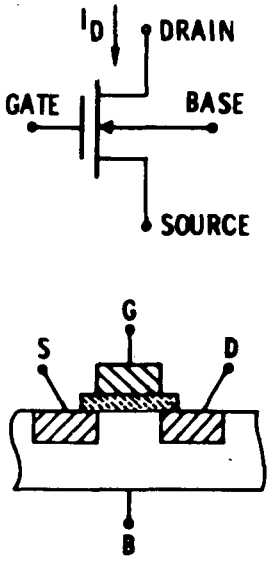

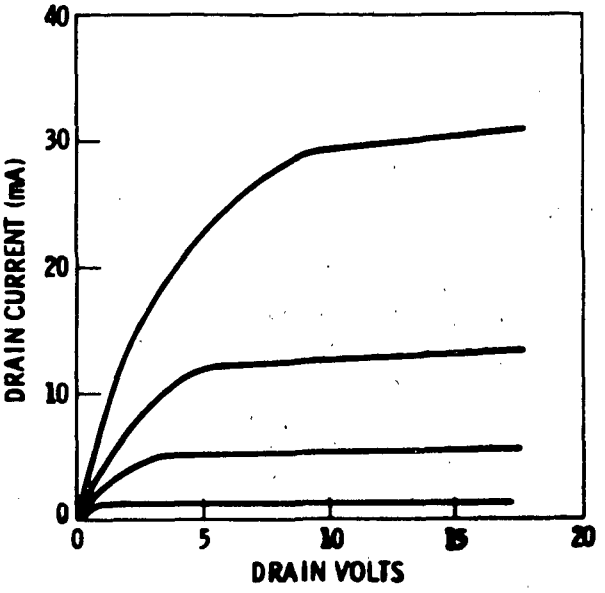

MOS DEVICE CHARACTERISTICS

MOS transistors are usually made by a single diffusion of source and drain into a substrate wafer of opposite conductivity. The construction and characteristics of a typical N-channel transistor are shown above. The active region of an MOS transistor is a surface channel between the source and drain regions. This channel is formed and controlled by the electrical effect of a voltage on the gate electrode. The gate is separated from the silicon by a thin insulating layer, usually silicon dioxide, and the properties of this insulator have a major role in transistor operation.

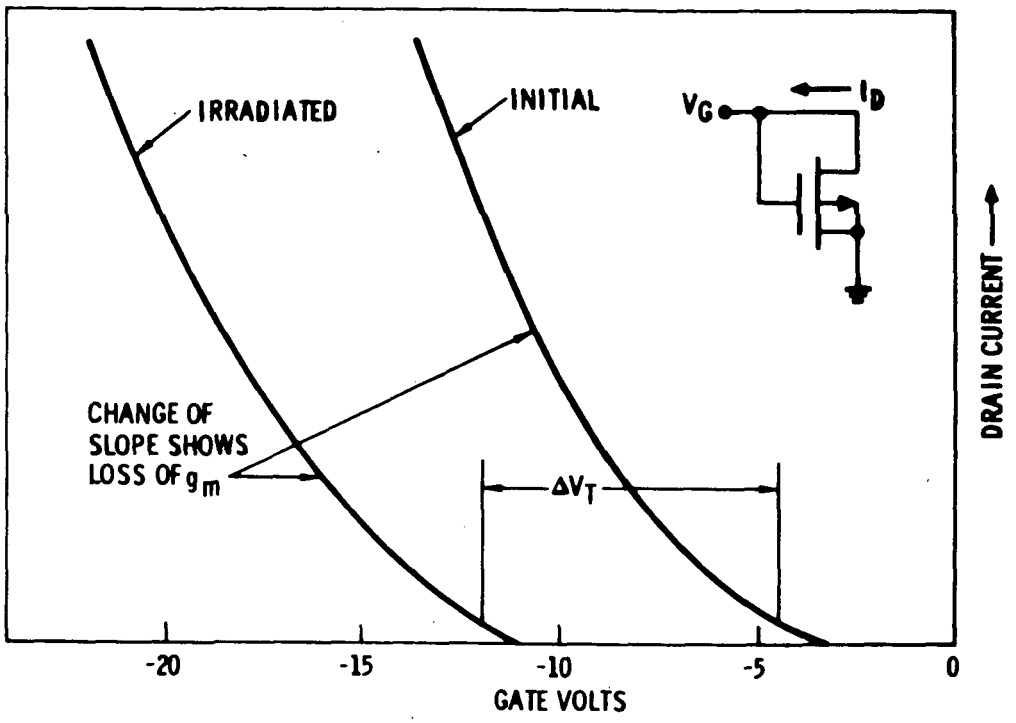

RADIATION DAMAGE TO P-CHANNEL TRANSISTORS

MOS transistors can be very sensitive to ionizing radiation. The major effect of radiation on device operation is a shift in the threshold voltage toward more negative values. This effect is shown above for a typical P-channel transistor. Secondary effects of radiation are a reduced transconductance and increased leakage currents at both source and drain junctions. The significance of the radiation damage is that a higher (more negative) gate voltage is required to turn the transistor on, and the channel current for a fixed bias condiction is reduced.

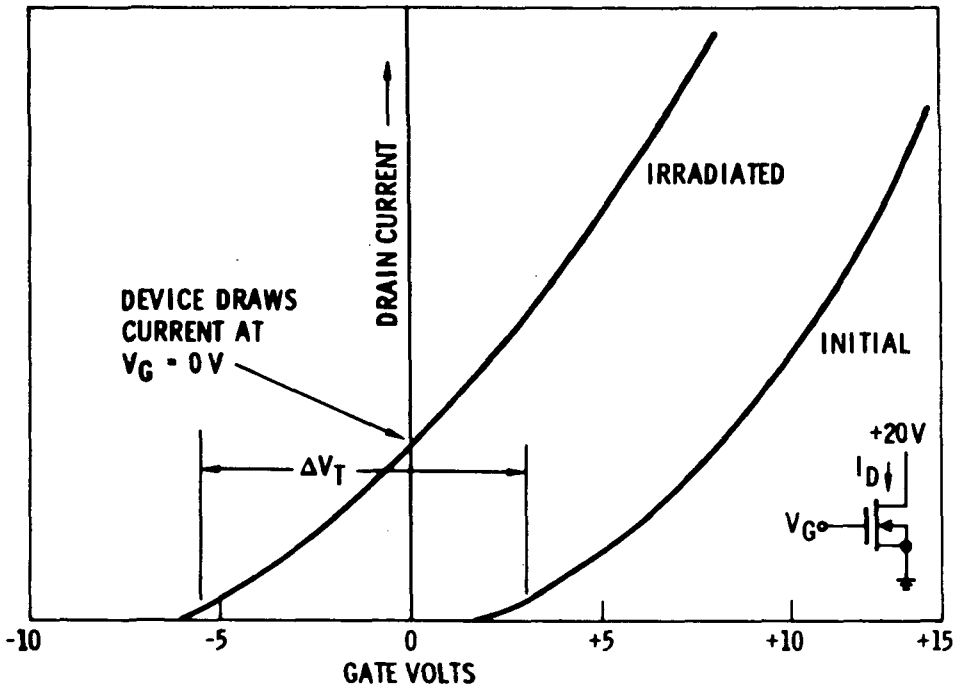

RADIATION DAMAGE TO N-CHANNEL TRANSISTORS

The threshold voltage of an N-channel transistor will also be shifted toward more negative values by exposure to ionizing radiation. A common problem is that the threshold voltage will change sign in a radiation environment and, since the transistor then conducts at zero gate volts, the transistor cannot be turned off in normal digital circuit configurations.

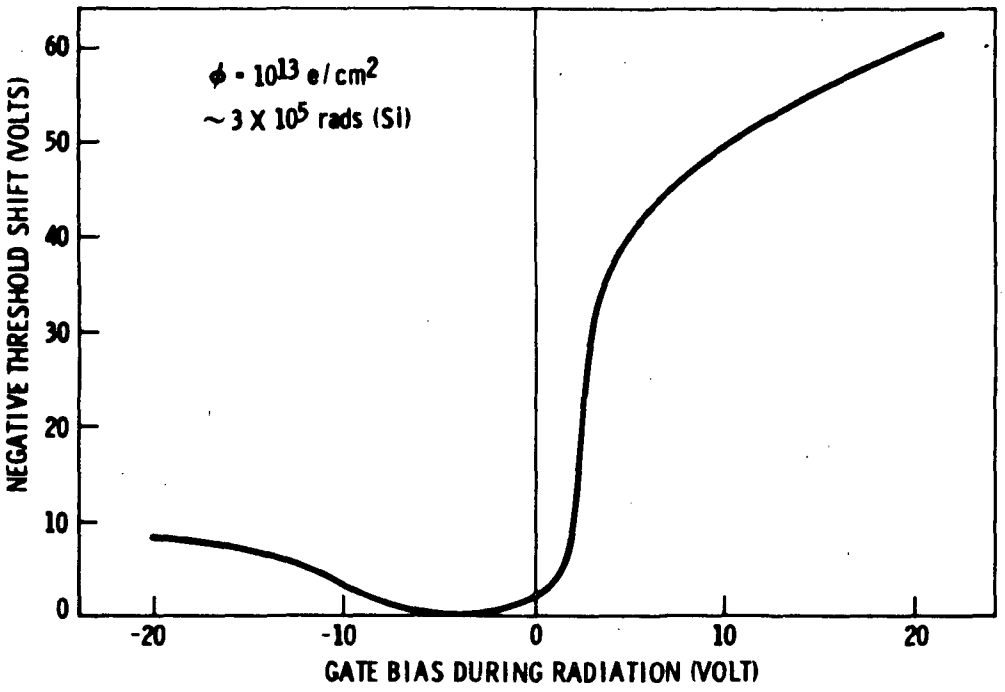

GATE BIAS DEPENDENCE OF RADIATION DAMAGE

The magnitude of the threshold voltage shift is strongly dependent on the gate bias during radiation. The greatest damage is observed if a positive gate voltage is applied during radiation. N-channel transistors, since they operate at positive voltages, are more sensitive to ionizing radiation than are P-channel transistors. MOS devices of both types will generally show less damage when irradiated unpowered; however, some of the hardened P-channel devices show less damage if power is applied during radiation.

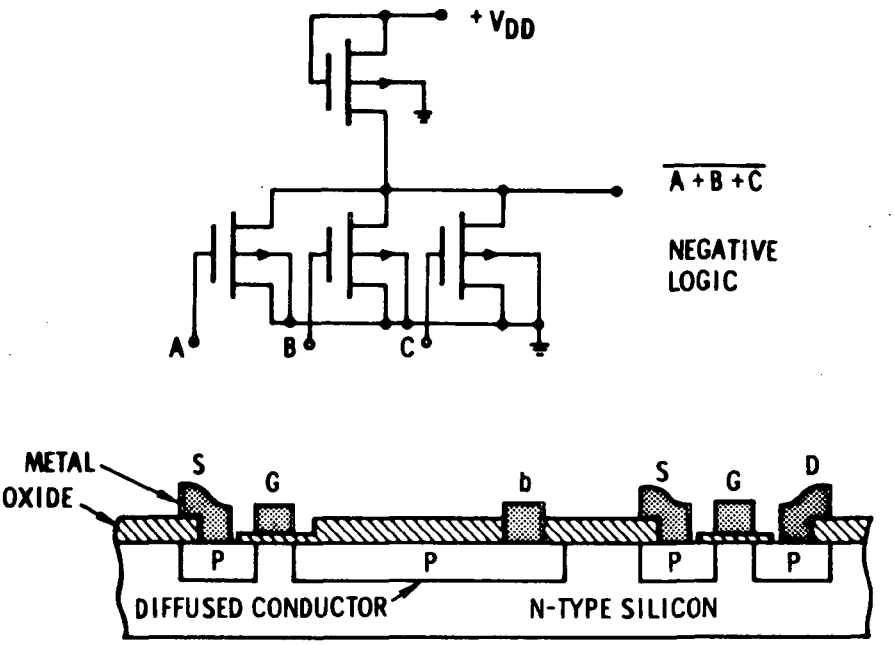

STATIC P-CHANNEL CIRCUITS

The simplest and most common type of MOS circuit uses only P-channel MOS (PMOS) transistors. MOS transistors are inherently isolated from the substrate by reversed biased source and drain junctions, so isolation diffusions are usually not required. The circuit shown is a simple static NOR gate which uses an MOS transistor as a load resistor. A common practice in all MOS circuits is the use of diffused regions in the silicon as conductors. These diffused conductors supplement the metal interconnection pattern.

Static PMOS circuits tend to be slow because the MOS load resistor is a high impedance charging path for circuit capacitance. Power requirements, while low, are often not much lower than faster bipolar circuitry. Logic delays of 100-200 ns per gate at power levels of 0.5-1 mw per gate are typical of this circuit type.

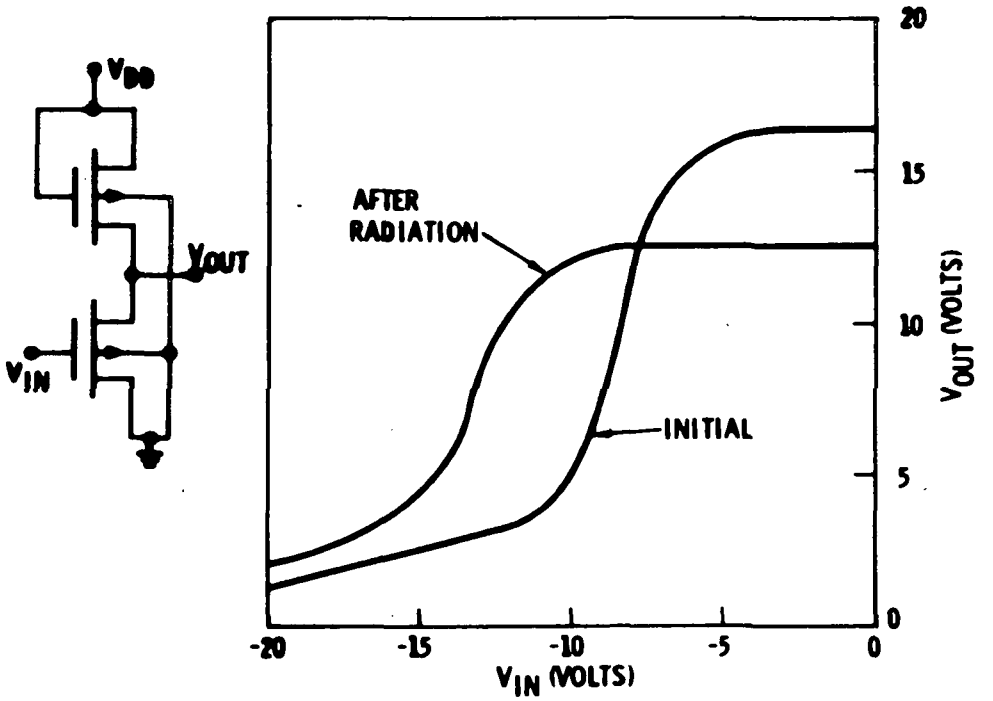

CHANGE IN STATIC PMOS CIRCUIT
OPERATION AFTER RADIATION

Static PMOS circuits are doubly affected by any radiation-induced threshold shift. First, the voltage required for a low output state is shifted to a more negative value. Second, the voltage drop across the load devices is increased so less voltage is available to drive the logic gates. Typical unhardened commercial circuits of this type will often show serious degradation at radiation doses of 10^4 rads (Si).

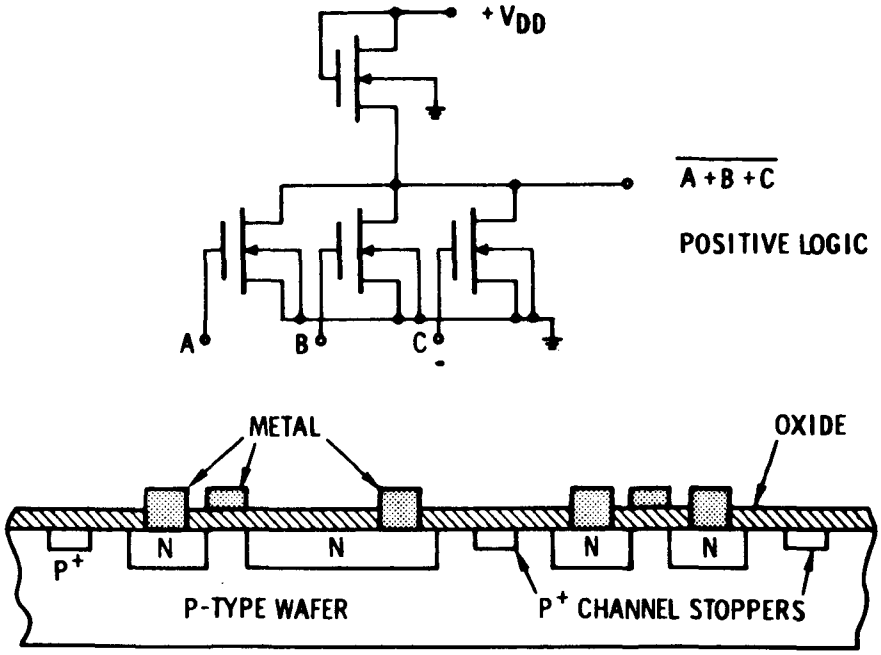

N-CHANNEL MOS CIRCUITS

Higher speeds can be obtained in N-channel MOS (NMOS) circuits because electrons have a higher mobility than holes. Circuit construction is similar to that for PMOS circuits; however, more stringent process controls are required and a second "channel stopper" diffusion step is needed to prevent unwanted surface channels. The fact that N-channel devices show greater radiation damage than P-channel devices usually prevents use of NMOS circuits in a radiation environment. The difference in sensitivity, however, is not likely to be significant at radiation doses up to about 10^4 rads.

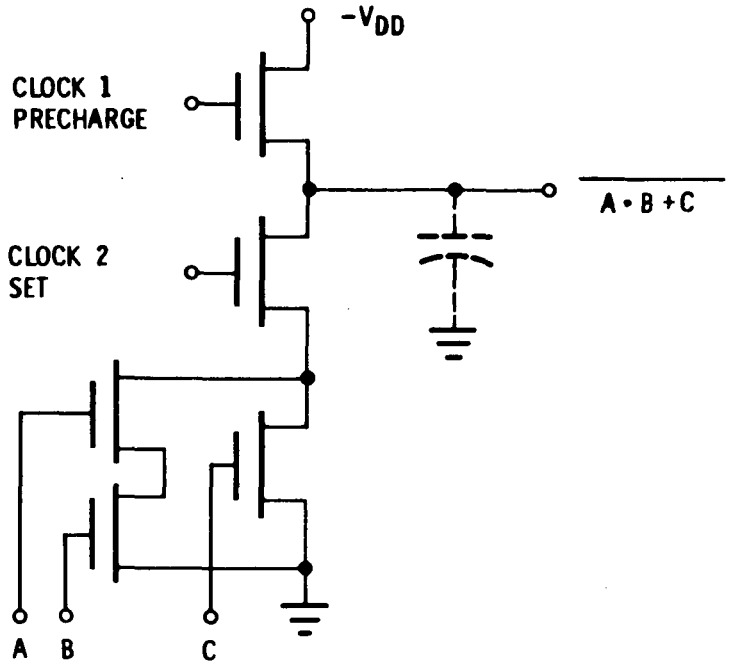

DYNAMIC CIRCUITS

Higher speed operation of MOS circuits can also be achieved by various dynamic circuit configurations. Such circuits use dynamic charge storage on circuit capacitance to hold a voltage level and require an externally generated 2-phase or 4-phase clock. Other advantages of dynamic circuits are high circuit density and a low power requirement. Direct conduction paths from the power supply to ground never occur, and only the power required to charge and discharge circuit capacitance must be supplied. Such circuits generally operate at 1- to 2-MHz clock rates and require power levels of about 0.2 mw/gate. Special circuits such as shift registers can be made to operate at 5- to 10-MHz clock rates.

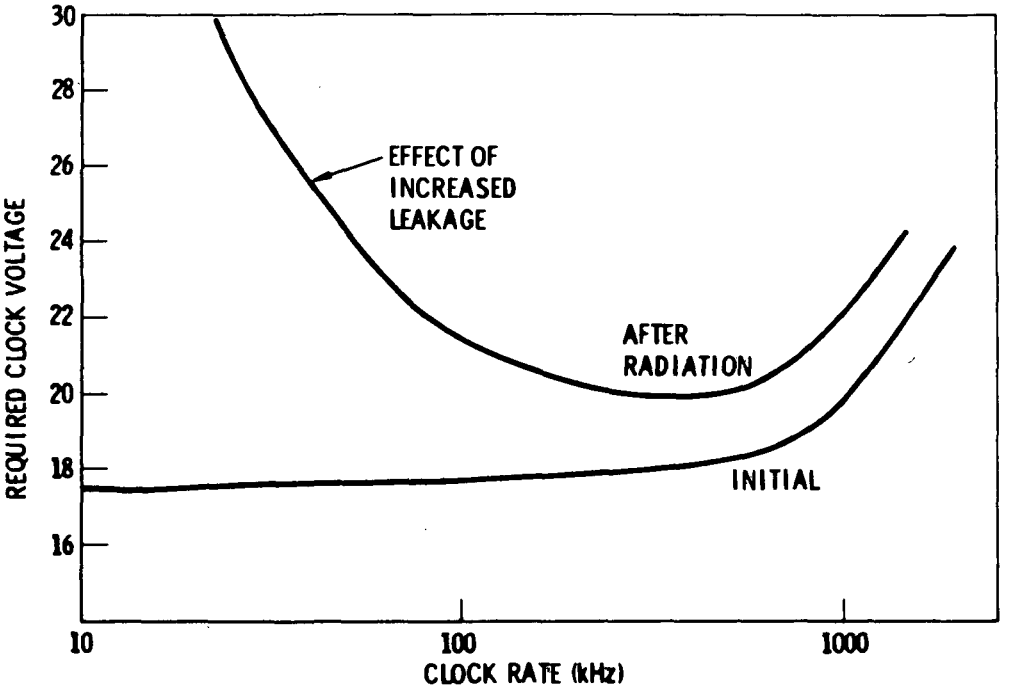

RADIATION EFFECTS IN A DYNAMIC PMOS CIRCUIT

The change in dynamic PMOS circuit operation after exposure to ionizing radiation is evidenced by a change in the minimum clock voltage required to operate the circuit. The general upward shift of the curve and the reduced high frequency capability are a result of more negative threshold voltages. The reduced ability of the circuit to operate at low frequencies is due to increased leakage currents. Loss of dynamically stored charge through leakage currents will cause a circuit malfunction, and dynamic circuits can be vulnerable to this radiation damage effect. Dynamic PMOS circuits are fairly tolerant of threshold voltage changes and commercial grade circuits will usually operate to about 10^5 rads (Si) before failing.

Dynamic NMOS circuits are also possible, but their use is not common. Also such circuits would be very sensitive to radiation-induced threshold voltage shifts.

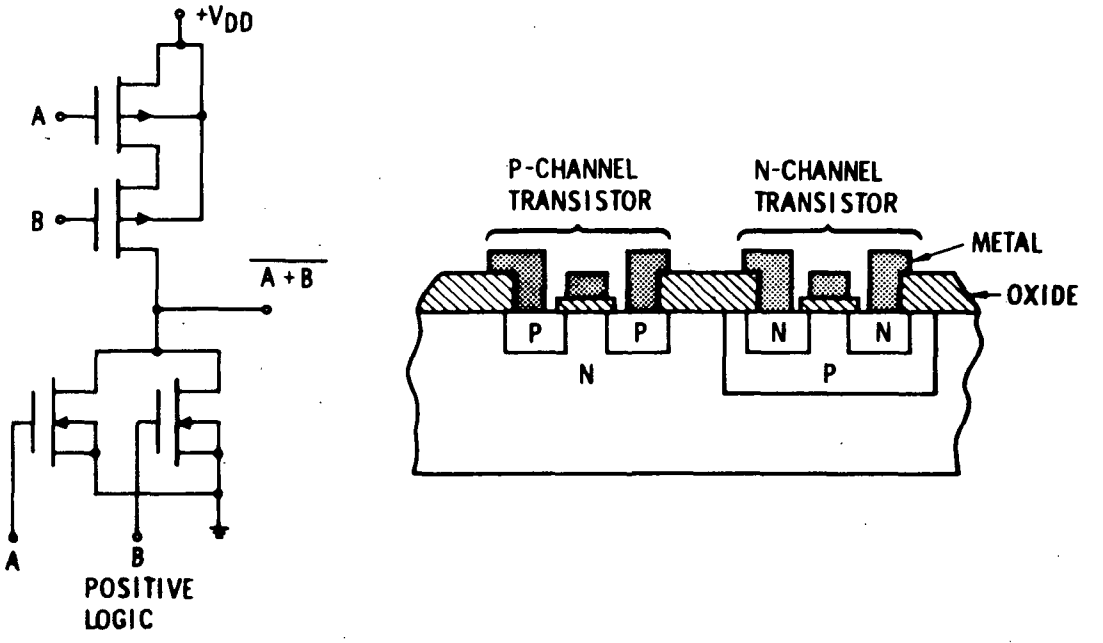

COMPLEMENTARY MOS CIRCUITS

Complementary MOS circuits require almost no standby power, and this feature is very attractive for space systems. CMOS circuits also have higher speeds than either PMOS or NMOS static circuits. Because the fabrication process is more complex, CMOS circuits are more costly than their single-channel counterparts and less suited to large scale integration. The primary use of CMOS circuits has been in applications where low power consumption is a major requirement.

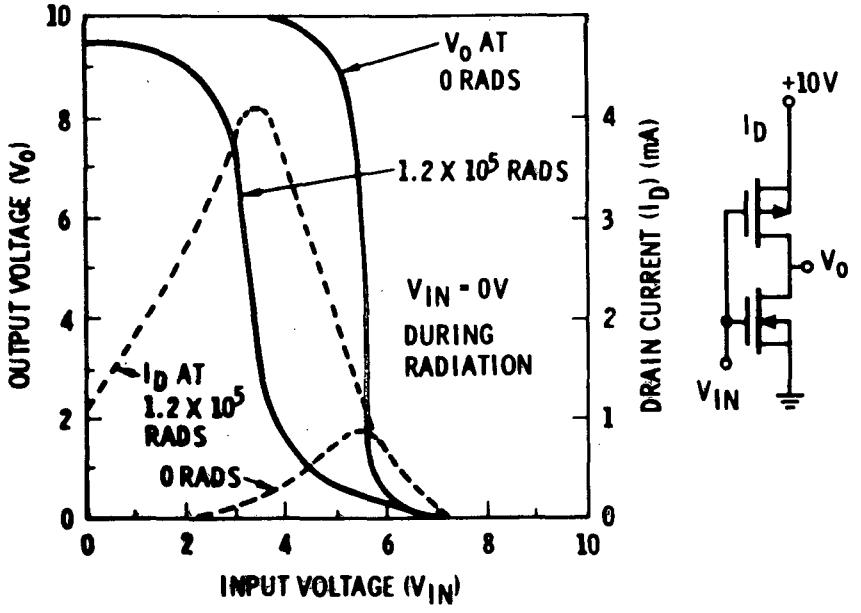

RADIATION EFFECTS IN CMOS CIRCUITS

The radiation tolerance of CMOS circuits is highly dependent upon the initial threshold voltages of the transistors and the operating voltage. Since the threshold voltage of both P and N-channel transistors shifts negative, the entire transfer curve of any logic gate will be shifted to the left as shown above. When the threshold voltages of the N-channel transistors become negative, the circuits begin to draw standby power. Increased power requirements rather than logic failure often limit use of CMOS circuits in a radiation environment. It appears that fairly conventional CMOS circuits can be made to operate to doses of about 10^5 rads (Si) before serious problems are encountered. See W. J. Poch and A. G. Holmes-Siedle, The Long Term Effects of Radiation on CMOS Logic Networks, IEEE Transactions, Vol. NS-16 (Dec. 1969).

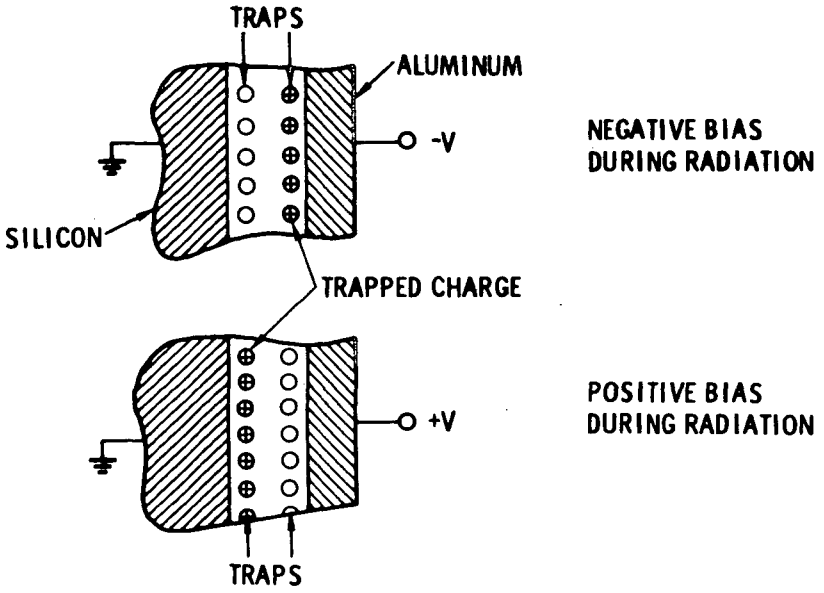

CHARGE TRAPPING IN GATE INSULATORS

Radiation causes a threshold voltage shift in MOS transistors because holes formed by ionization in the silicon dioxide insulator become trapped within the insulator. Most charge is trapped near the negative electrode and, since charge near the silicon insulator interface has the greatest effect on threshold voltage, larger threshold shifts are observed under positive bias irradiation.

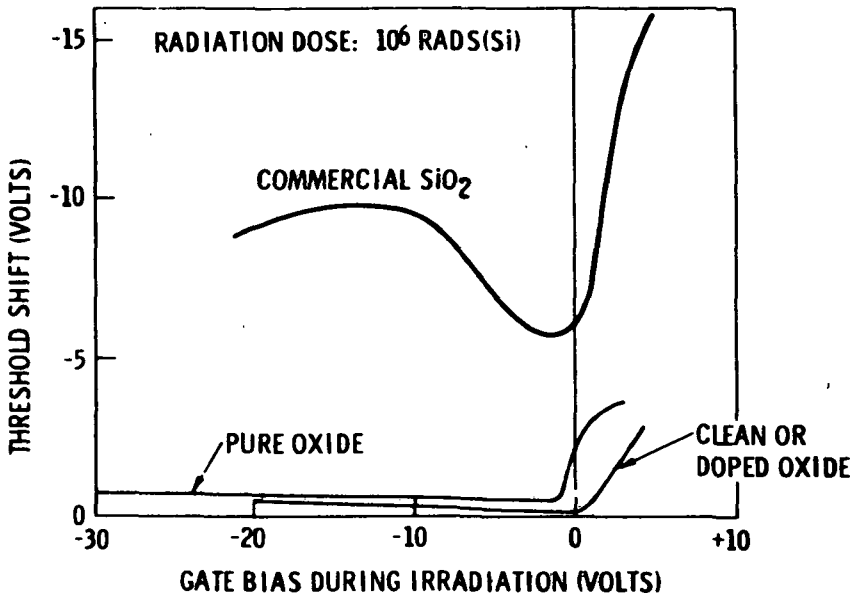

RADIATION RESISTANT SILICON DIOXIDE GATE INSULATORS

Trapping of ionized holes was originally thought to be an inherent property of the silicon dioxide insulator. Recent work by several researchers, however, has shown that most of the traps can be eliminated. Process optimization and careful control of oxidation and metallization steps alone can provide a high degree of radiation hardness. Chrome-doping the oxide has also proven helpful in reducing radiation damage and a combination of process optimization and chrome doping can be used to further improve radiation hardness as shown above. These processes are more than sufficient to harden PMOS devices to the required OPGT levels. NMOS and CMOS devices still show higher damage levels.

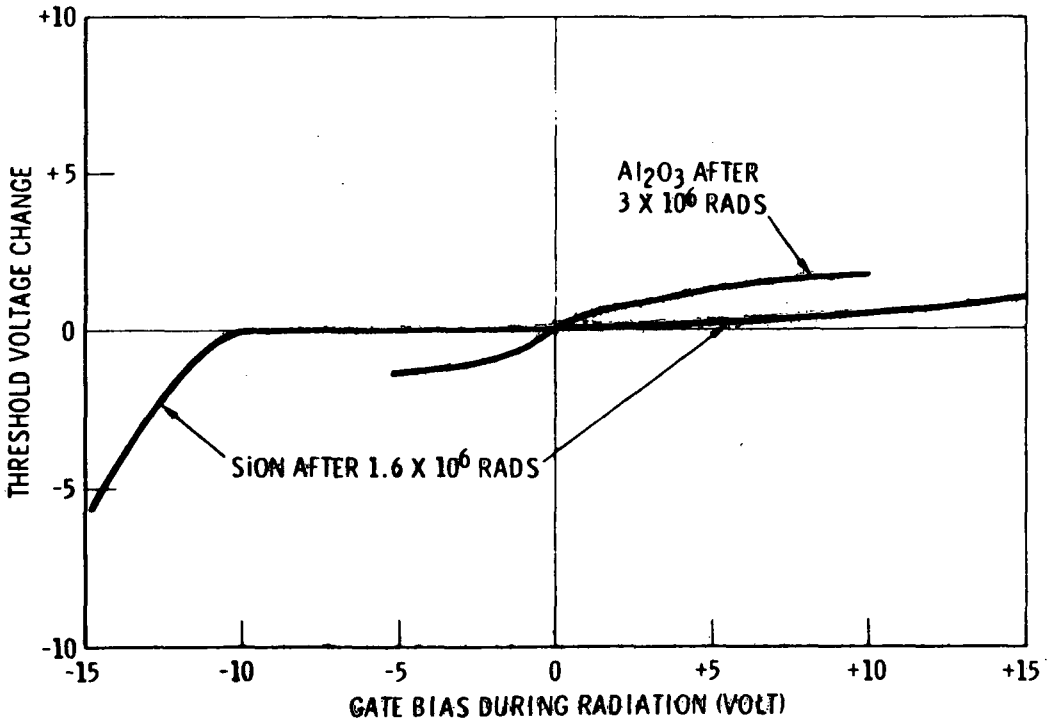

RADIATION HARDNESS WITH OTHER DIELECTRICS

Other insulators, notably silicon nitride and aluminum oxide, have also been studied as possible hardened insulators. Both have shown promise as a means of making radiation hardened NMOS and CMOS devices. Very impressive radiation resistance has indeed been shown for simple devices using these materials. Offsetting the radiation hardness has been a variety of fabrication problems and some undesirable electrical properties. These or other materials may ultimately provide an acceptable solution to MOS hardening, but the practical problems must first be solved.

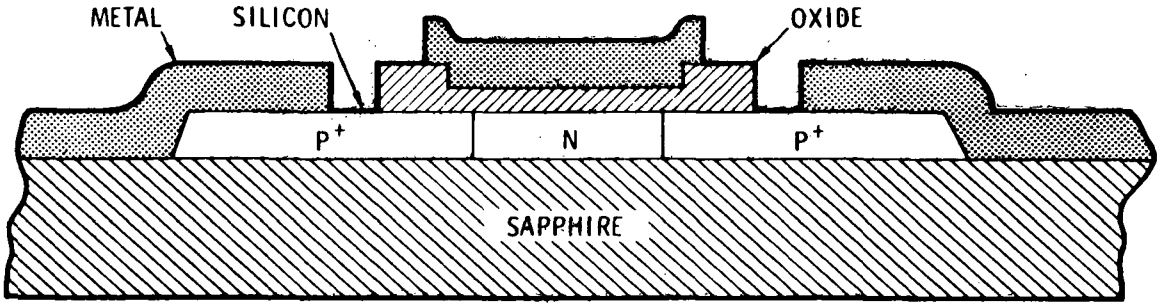

SILICON ON SAPPHIRE

Isolation for MOS circuits may be obtained by fabricating the transistors in islands of oxide crystal silicon on a sapphire substrate. Since dielectric isolation is attained by etching away all the unused silicon, this technique offers significant reductions in parasitic capacitance, junction photocurrents, and parasitic current paths over the conventional P-N junction isolation method. As in the case of bipolar circuits, dielectric isolation to prevent transient radiation effects is not required for the OPGT. Several other advantages, however, may be gained with construction on sapphire--e.g., higher speed, lower power, and a near absence of junctions which may become leaky under radiation. This fabrication process is still relatively new and has not yet been used on a production basis.

"Page missing from available version"

CIRCUIT CONSIDERATIONS

PARTS CONSIDERATIONS

SYSTEM HARDENING

HARDENING

Hardening is the design or protection of a device or equipment item to increase its radiation resistance and damage threshold. Hardening may result directly from the design, fabrication, or operating conditions of the affected device, or from shielding placed around the device. Hardening may, in general, be applied at the system, circuit, or individual part level. Radiation effects data on hardened devices are presented.

- CHOOSE PROPER DEVICE BIAS CONDITIONS TO MINIMIZE DAMAGE EFFECTS
- USE STABLE WORST CASE DESIGN METHODS
- USE ADDITIONAL SPECIAL DESIGN TECHNIQUES THAT MINIMIZE RADIATION DEGRADATION OF CIRCUITS
- AVOID PARTS THAT ARE INHERENTLY VULNERABLE TO RADIATION AND CAN PRODUCE CATASTROPHIC FAILURES

CIRCUIT HARDENING

A wide variety of techniques are available for hardening electronics systems. Among these are the choice of component and operating conditions. Special or more complex designs, or conservative designs which assure adequate design margins at worst case radiation damage and part end-of-life, will further enhance hardness.

$$\frac{1}{h_{FE}} = \frac{1}{h_{FE}}\text{(BULK CURRENTS)} + \frac{1}{h_{FE}}\text{(SURFACE CURRENT)}$$

$$\frac{1}{h_{FE}}\text{(BULK CURRENTS)} \simeq C + C' e^{-qV_{BE}/nkT}, \; n>1$$

$$\frac{1}{h_{FE}}\text{(SURFACE CURRENT)} \simeq C'' e^{-qV_{BE}/mkT}, \; m>1$$

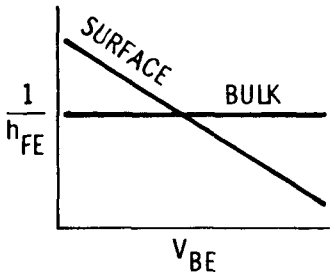

$\frac{1}{h_{FE}}$(BULK CURRENTS) AFFECTED BY BULK DISPLACEMENT DAMAGE, INCREASING C AND C', OR C BECOMES A FUNCTION OF INJECTION LEVEL

$\frac{1}{h_{FE}}$(SURFACE CURRENT) AFFECTED STRONGLY BY SURFACE IONIZATION DAMAGE, INCREASING C'' AND POSSIBLY INCREASING m

BIPOLAR BIAS CONDITIONS

The current gain of bipolar transistors is determined by both surface and bulk mechanisms. Surface phenomena are particularly sensitive to ionizing radiation dose degradation.

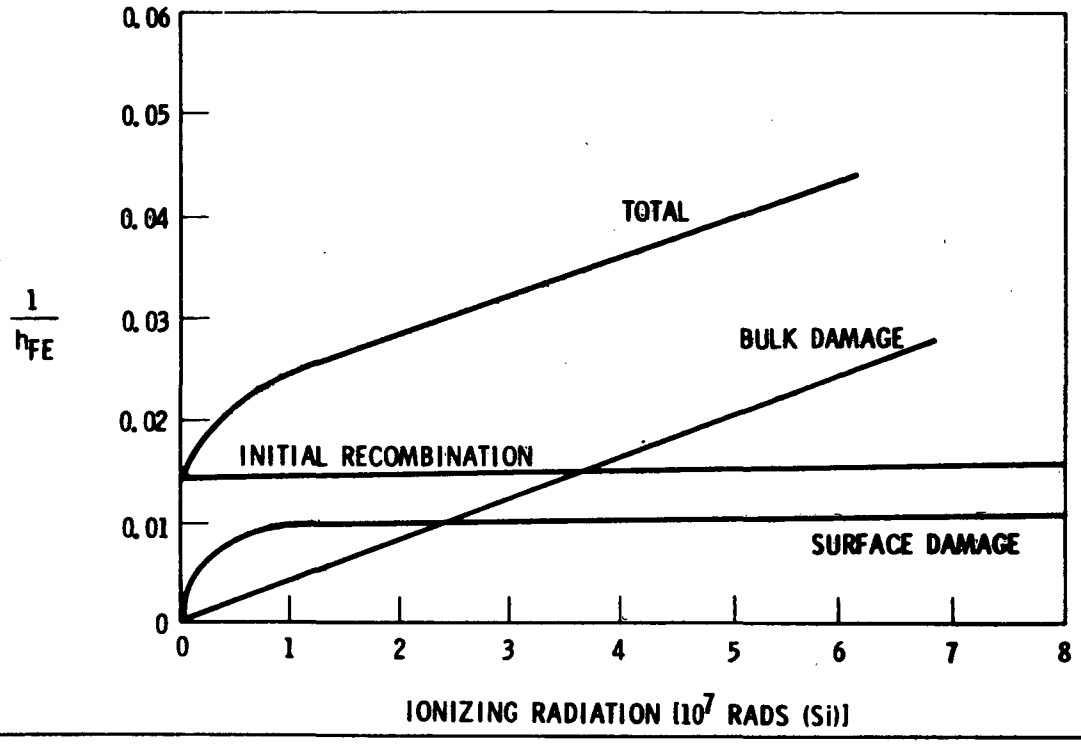

TYPICAL SURFACE AND BULK BIPOLAR TRANSISTOR DAMAGE FROM IONIZING RADIATION

A typical bipolar transistor ionizing radiation current gain degradation curve is caused by bulk and surface damage. The surface contribution often results in a rapid change in h_{FE} which saturates at about 10^7 rads (Si). Bulk damage results in a continuous decrease in h_{FE}.

	DOSE (RAD (Si))			
DEVICE	0	1×10^6	3×10^6	1×10^7
1	15.1 mA 12.8	20.5 mA 16.9	21.0 mA 17.8	21.2 mA 18.0
2	10.0 9.6	18.8 16.9	21.1 19.1	21.5 19.7
3	14.9 14.4	24.5 23.2	27.2 26.3	26.9 26.4
4	11.2 12.6	22.8 23.6	23.6 22.5	21.4 20.6
5	10.1 11.6	18.2 18.4	18.4 16.9	15.7 13.8

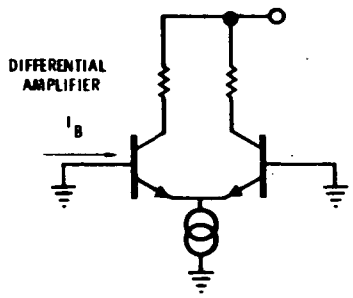

DIFFERENTIAL AMPLIFIER BIAS CURRENT VS. IONIZING DOSE

Empirical data are shown illustrating the change in bias current of a modern differential amplifier integrated circuit for ionizing Co^{60} radiation doses up to 10^7 rads (Si).

Co^{60} IONIZING DOSE				
DEVICE	NONE	1×10^6 RAD	3×10^6 RAD	1×10^7 RAD
1	+0.62 mV -2.00	+0.60 mV -2.08	+0.56 mV -2.00	+0.54 mV -2.00
2	+1.45 +1.16	+1.41 +1.01	+1.42 +1.06	+1.40 +1.14
3	+0.40 +0.06	+0.25 -0.08	+0.15 -0.05	+0.12 +0.02
4	+0.45 +0.30	+0.33 +0.07	+0.42 +0.03	+0.53 +0.09
5	-0.20 +1.05	-0.23 +0.89	+0.78 +0.80	+0.80 +0.81

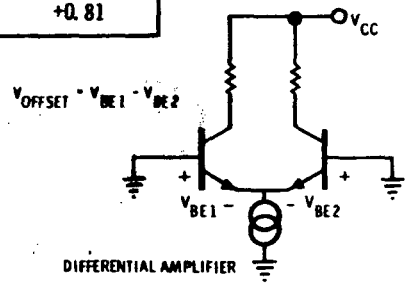

DIFFERENTIAL AMPLIFIER OFFSET VOLTAGE VS. IONIZING DOSE

Empirical data are shown illustrating the change in offset voltage of a modern differential amplifier integrated circuit for ionizing Co^{60} radiation doses up to 10^7 rads (Si).

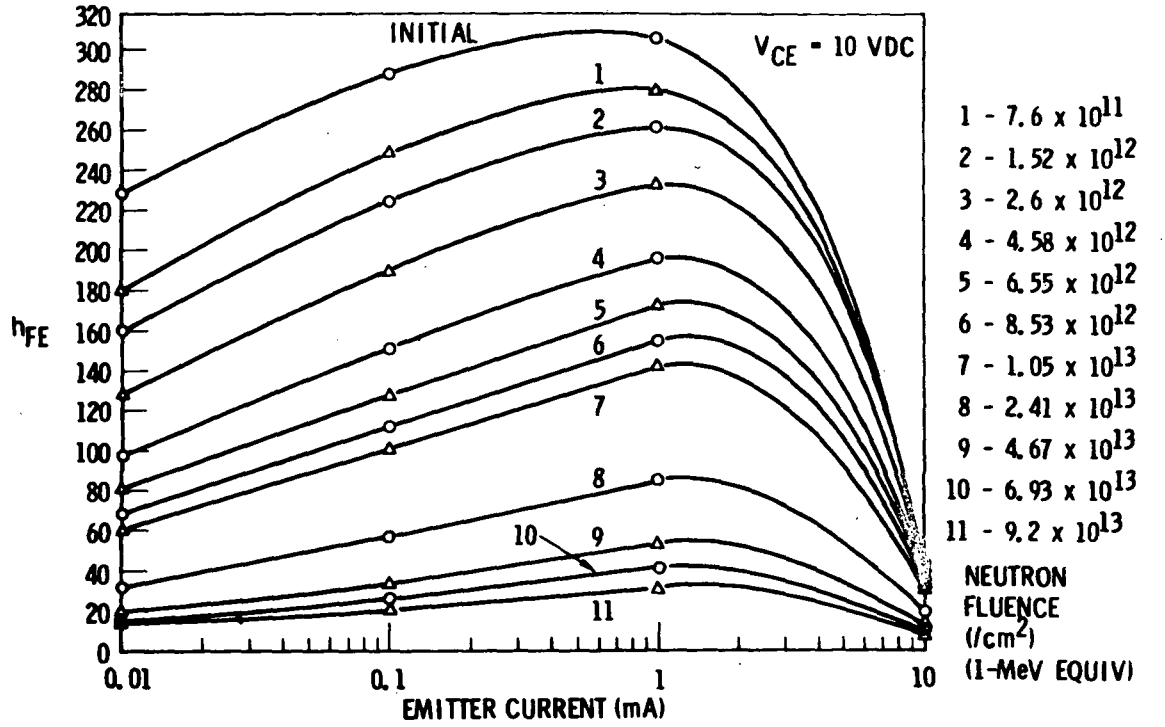

h_{FE} of 2N4042 VS. EMITTER CURRENT AND NEUTRON FLUENCE

Neutron displacement damage data are shown for a typical bipolar transistor for neutron fluences up to 10^{14} n/cm^2 (1-MeV equivalent) and for emitter currents from 10 microampéres to 10 milliamperes.

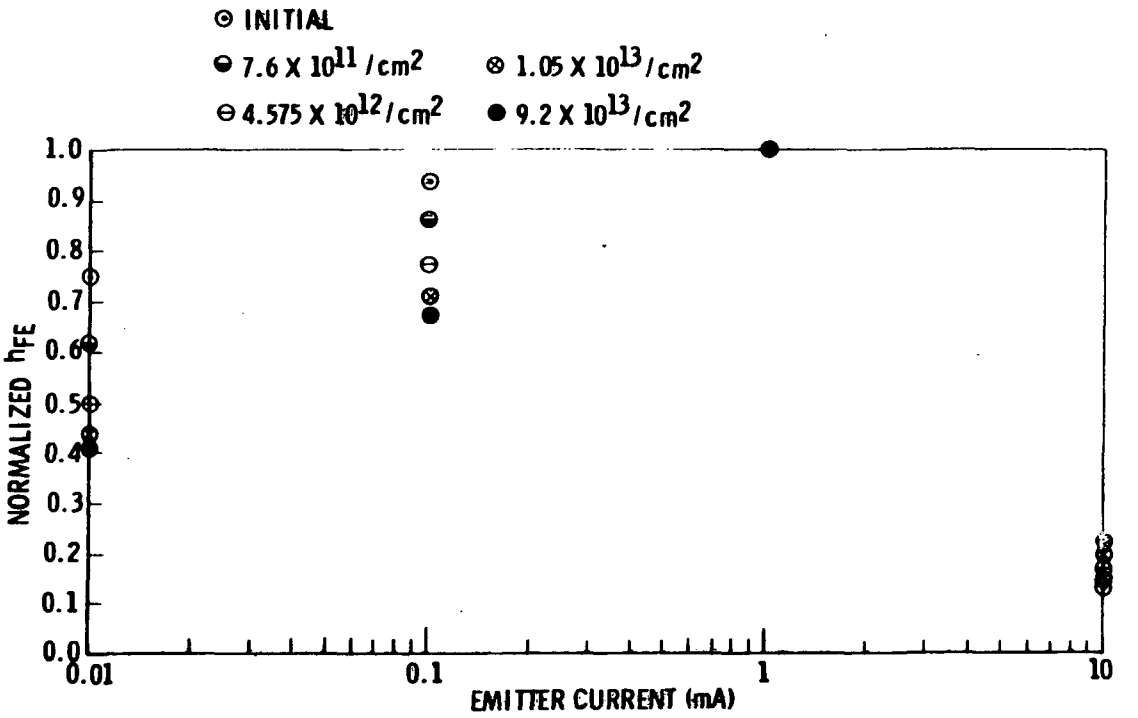

DC CURRENT GAIN OF 2N4042 FOR FIVE VALUES OF NEUTRON FLUENCE

The bias current dependence of displacement damage is illustrated by superimposing the current gain curves of a transistor at several neutron fluences. The current gain curves have been normalized to the gain value measured at an emitter current of 1 milliampere.

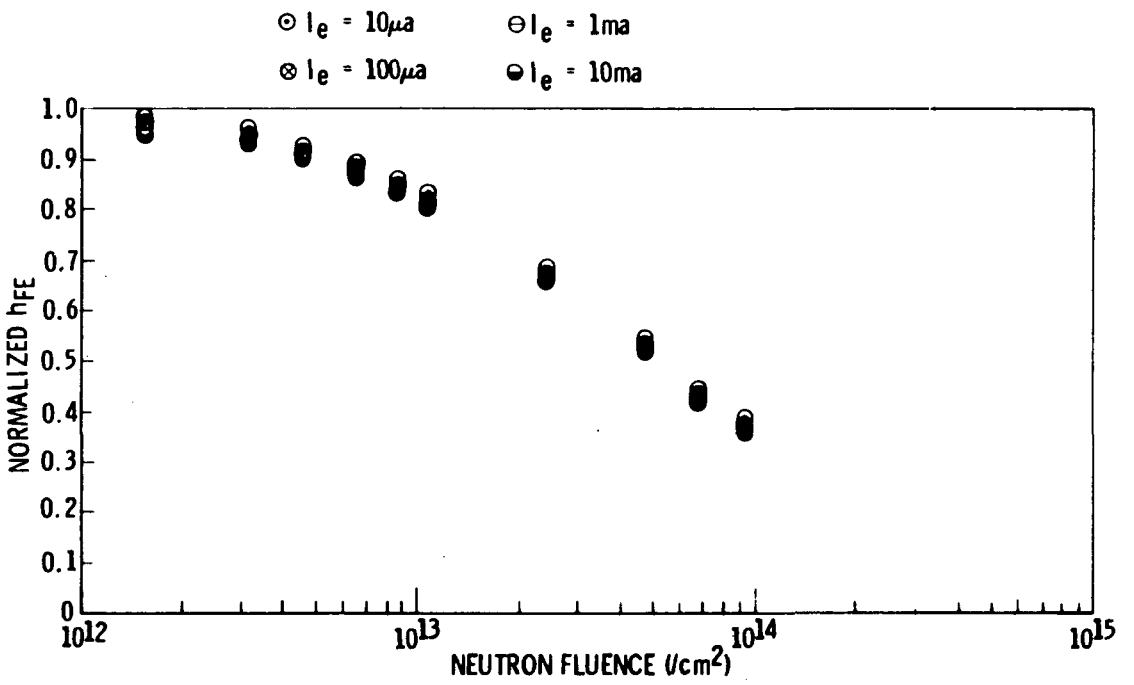

NORMALIZED DC CURRENT GAIN OF 2N709 AT FOUR EMITTER CURRENTS VS. NEUTRON FLUENCE

The normalized current gain as a function of neutron fluence for a typical 2N709 transistor is shown for several emitter currents. The apparent lack of bias current dependence indicates that only a small surface component of h_{FE} is present in the device and the emitter area is sufficiently small so that low emitter currents do not result in small injection levels.

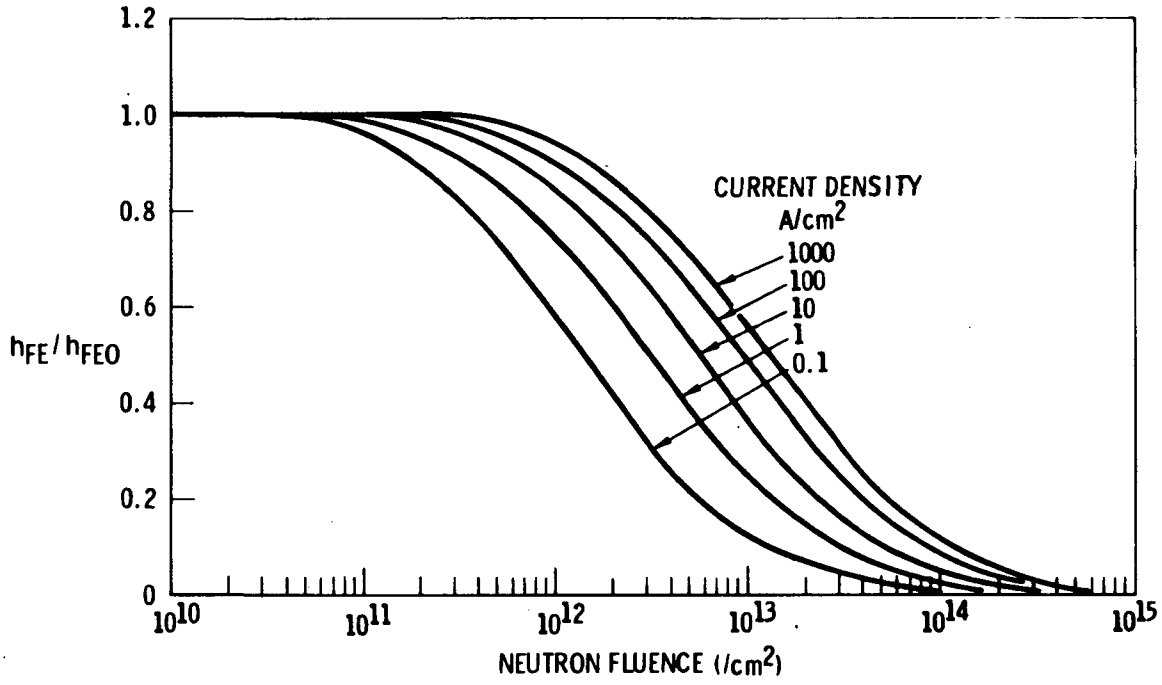

TYPICAL TRANSISTOR CURRENT GAIN AS A FUNCTION OF NEUTRON FLUENCE AND EMITTER CURRENT DENSITY

The bias current dependence of bulk damage is illustrated by the damage curves for a typical transistor at several emitter current density levels.

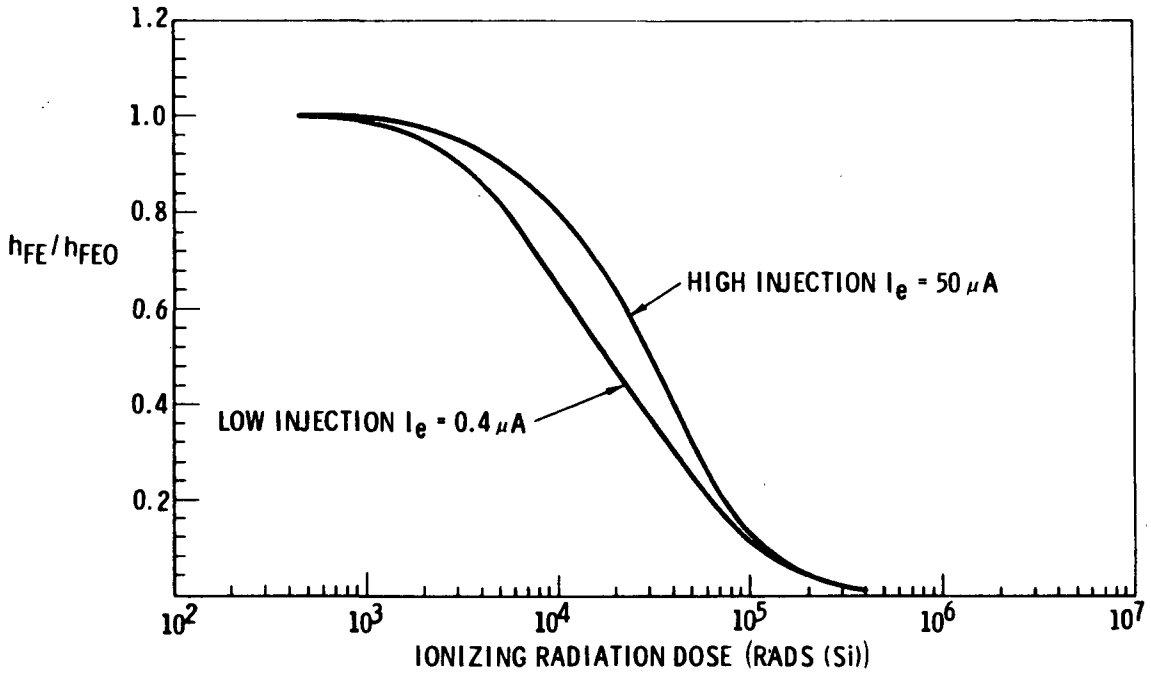

LOW-LEVEL TRANSISTOR TOTAL DOSE DAMAGE CHARACTERISTICS

The possible severity of low emitter current gain degradation is illustrated by empirical data.

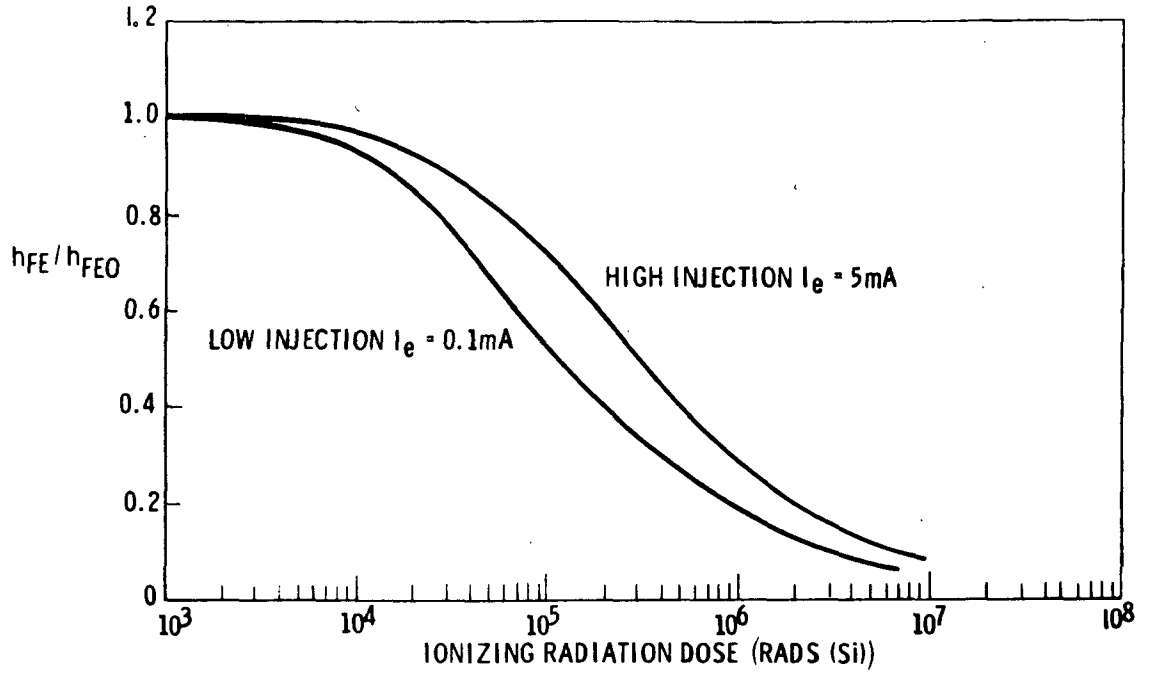

MEDIUM-LEVEL TRANSISTOR TOTAL DOSE DAMAGE CHARACTERISTICS

The current gain degradation of a medium-level transistor is illustrated for two bias current levels.

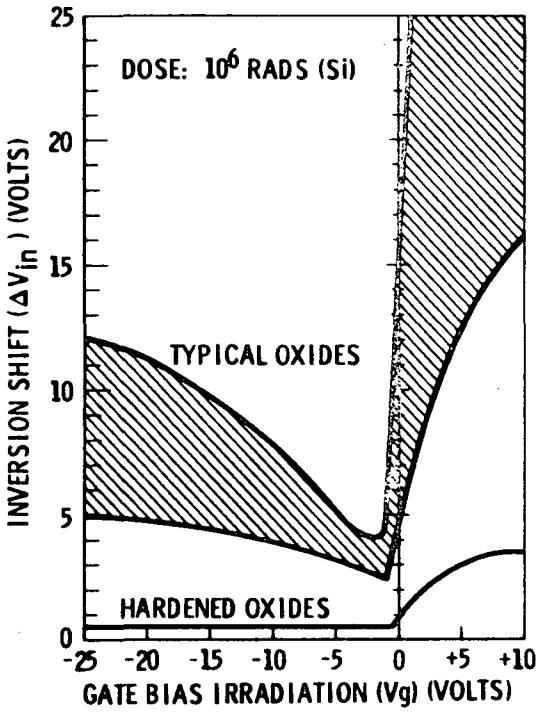

TYPICAL MOS TRANSISTOR DAMAGE CHARACTERISTICS VS. GATE BIAS DURING IRRADIATION

The high sensitivity of field effect (MOS) transistors to ionizing radiation when exposed with positive gate bias is illustrated at a total dose of 10^6 rads (Si). Typical and hard gate oxides are shown.

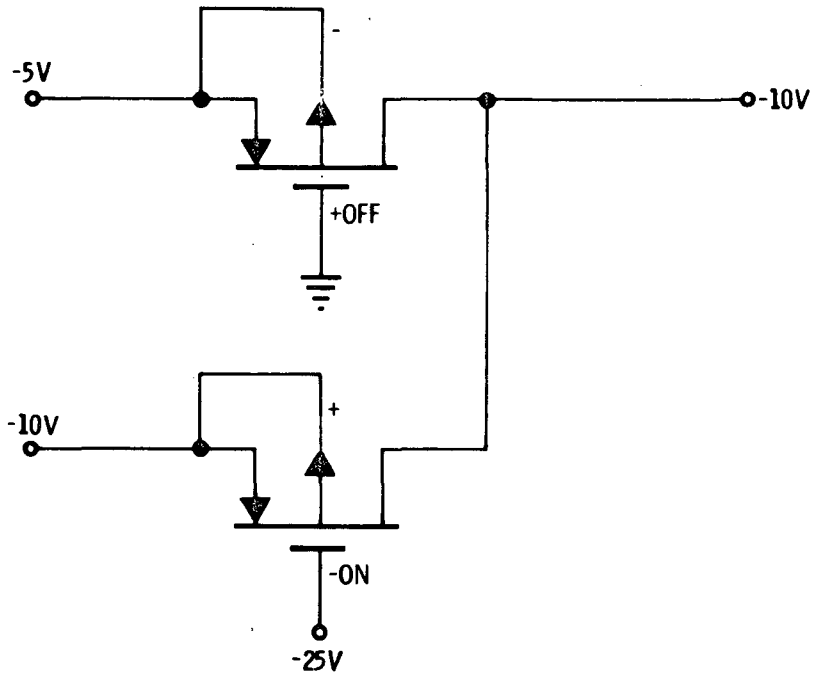

TYPICAL MULTIPLEXER CIRCUIT IN WHICH POSITIVE GATE BIAS CAN EXIST

A multiplexer circuit is shown to illustrate a design in which positive gate bias can be experienced in a MOS device. Hardening is easily achieved by returning the body of all devices to the most positive circuit potential (ground) rather than the source of each device.

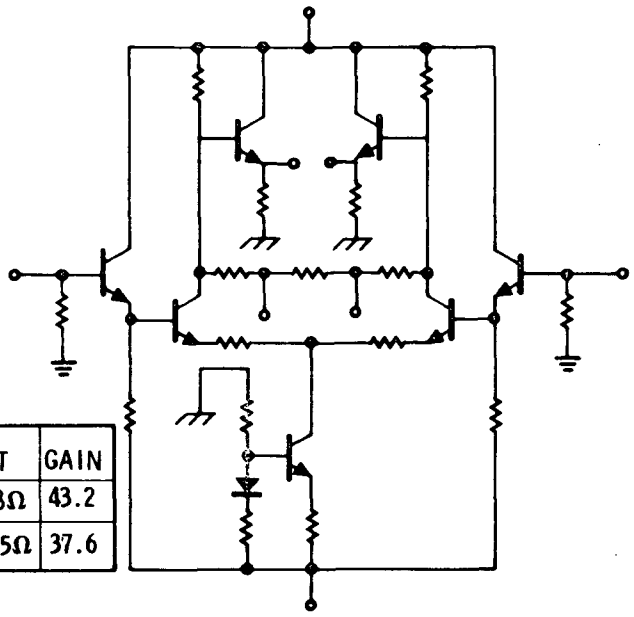

	R_{IN}	R_{OUT}	GAIN
INITIAL	>10KΩ	63.8Ω	43.2
2.4×10^{14} N/CM^2 1-MeV EQUIV	10KΩ	112.5Ω	37.6

SIMPLIFIED CIRCUIT OF A HARDENED DIFFERENTIAL AMPLIFIER

A typical hardened integrated circuit differential amplifier is shown. Impedance isolation at the input and output is provided by emitter followers and local gain degeneration or feedback is accomplished by emitter resistors. Small-geometry high-gain-bandwidth devices are used, material parameters selected, and processes controlled to enhance damage tolerance.

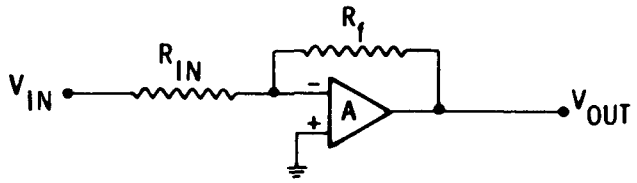

$$\frac{V_{OUT}}{V_{IN}} = -\frac{R_f}{R_{IN}}\left[\frac{1}{1+\frac{1+R_f/R_{IN}}{A}}\right]$$

$$A = \frac{(R_f/R_{IN})(100)}{\%\ \text{ERROR}} \qquad A \gg \frac{1}{1+R_{IN}/R_f}$$

R_f/R_{IN}	A		
	0.01%	0.1%	1%
100	10^6	10^5	10^4
1,000	10^7	10^6	10^5
10,000	10^8	10^7	10^6

OPEN LOOP GAIN REQUIRED TO MAINTAIN GAIN ACCURACY

Adequate gain margin must be provided in operational amplifiers to assure gain accuracy after damage. Because the open loop gain of an operational amplifier is determined by the product of the gains of several stages, the rate of open loop gain degradation is quite steep. Hardened operational amplifiers use more stages, impedance isolation between stages, and local feedback to maintain gain.

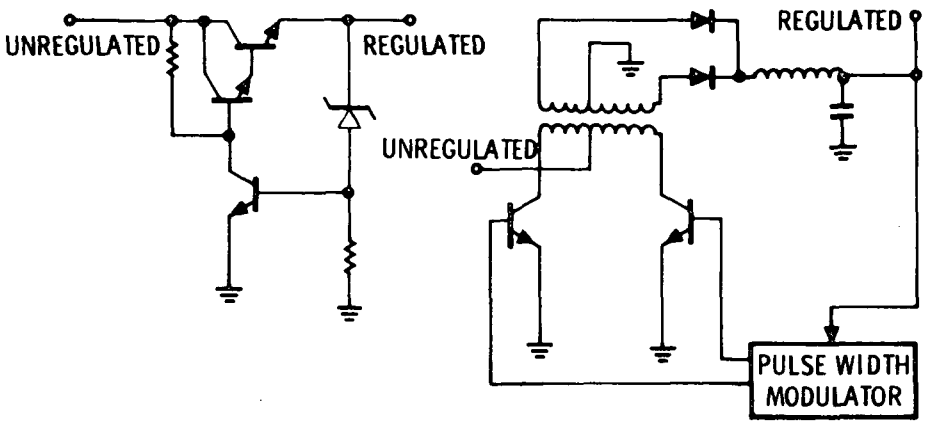

ADVANTAGES
- SIMPLE
- HIGH RELIABILITY
- FAST

DISADVANTAGES
- MODERATE EFFICIENCY
- HIGH POWER TRANSISTORS

ADVANTAGES
- HIGH EFFICIENCY
- REDUCED TRANSISTOR POWER REQUIREMENTS

DISADVANTAGES
- COMPLEX
- FILTER REQUIREMENTS

POWER SUPPLY HARDENING

High power circuits are generally sensitive to displacement damage because of the inherent characteristics of power semiconductors. The use of high gain-bandwidth transistors in power control circuits will result in greater damage tolerance at the expense of circuit complexity. High-speed devices are often more susceptible to electrical failure from second breakdown, further complicating designs.

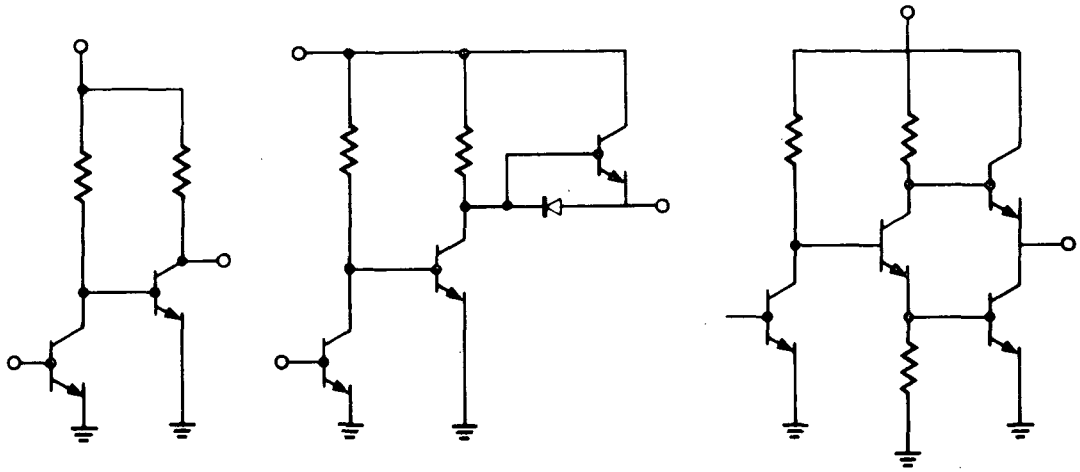

LOW FAN-OUT

HIGH FAN-OUT

TYPICAL INTEGRATED CIRCUIT LOGIC OUTPUT STAGES

Conventional modern integrated circuit logic elements can be used in moderate-damage environments at reduced fan-out levels. Alternatively, power gates can be employed in applications where standard gates would normally be used to maintain drive capability.

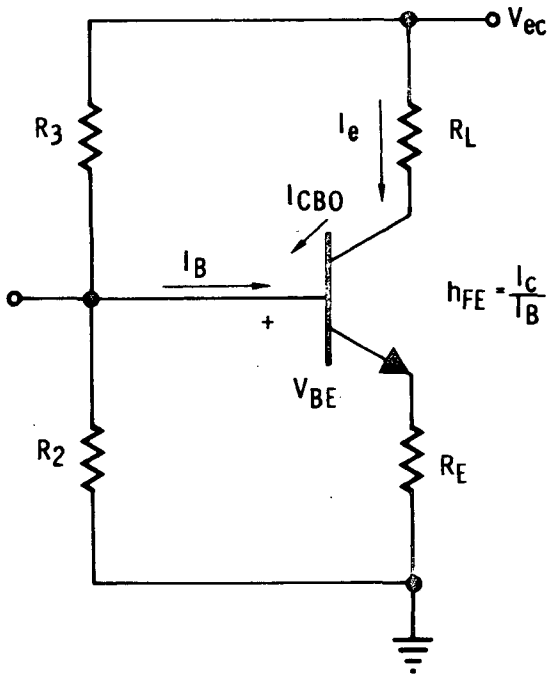

TYPICAL BIPOLAR AMPLIFIER STAGE BIAS CONDITIONS

A typical single-ended bipolar amplifier stage is illustrated. The stability of the collector current bias and, therefore, the collector voltage are functions of the values of all resistors, I_{CBO}, V_{BE}, and h_{FE}, all of which are changed by radiation.

$$S_1 = \frac{\Delta I_C}{\Delta I_{CBO}}$$

$$S_1 = (h_{FE} + 1)\frac{(R_E + R_B)}{R_B + R_E(h_{FE} + 1)}$$

$$R_B = \frac{R_2 R_3}{R_2 + R_3}$$

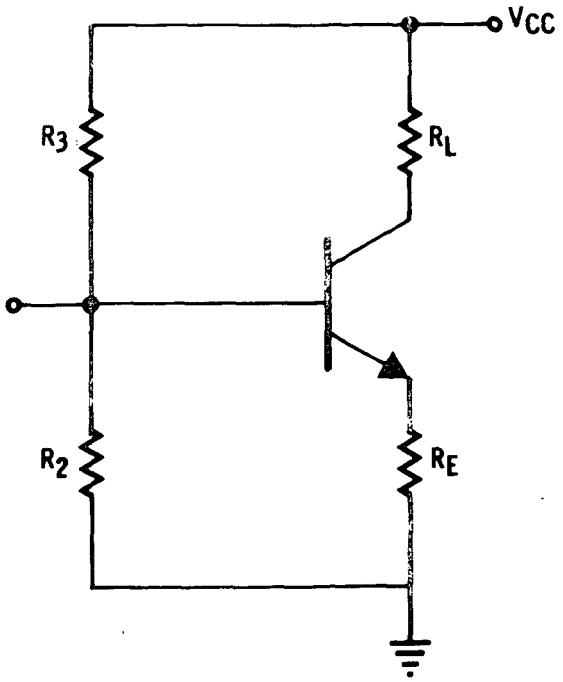

COLLECTOR CURRENT STABILITY VS. I_{CBO}

The sensitivity of an amplifier stage collector current to changes in I_{CBO} is defined. High impedance base voltage bias, high current gain, and low emitter resistor values contribute to instability.

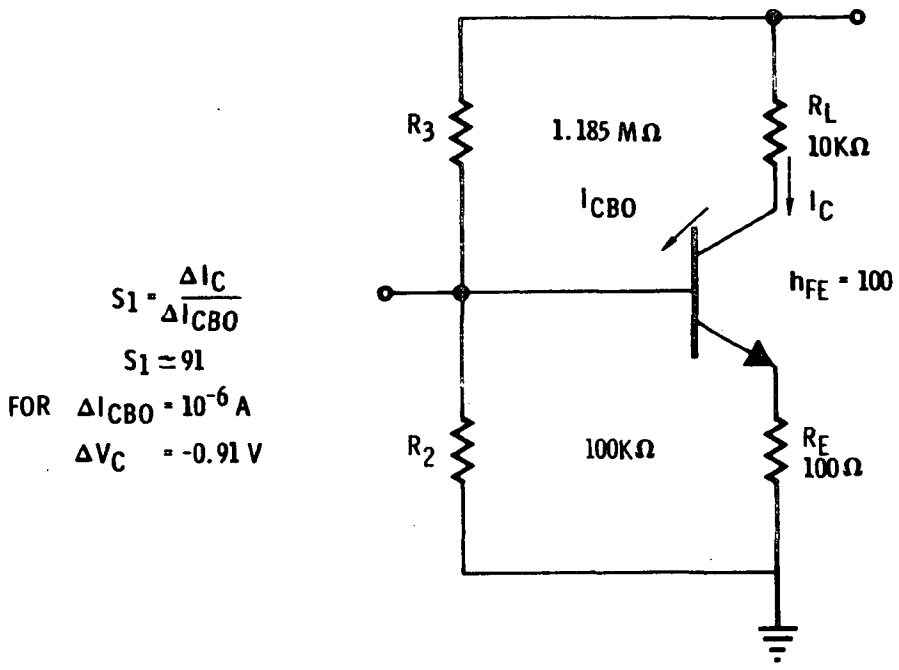

I_{CBO} BIAS STABILITY NUMERICAL EXAMPLE

The change in collector voltage for an increase in I_{CBO} of 1 microampere is derived for typical amplifier parameter values.

$$S_2 = \frac{\Delta I_C}{\Delta V_{BE}}$$

$$S_2 = \frac{-h_{FE}}{R_B + R_E (h_{FE} + 1)}$$

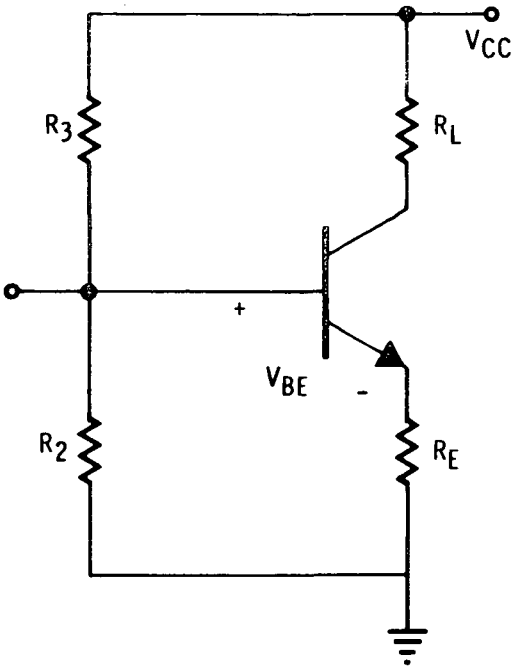

COLLECTOR CURRENT STABILITY VS. V_{BE}

The sensitivity of an amplifier stage collector current to changes in V_{BE} is defined. Low base bias resistance and low emitter resistor values contribute to instability.

$$S_2 = \frac{\Delta I_C}{\Delta V_{BE}}$$

FOR $R_B = 0$

$R_E = 0$

$$S_2 = -\frac{1}{101}$$

FOR $V_{BE} = +5$ mV

$\Delta I_C \simeq -0.05$ mA

$\Delta V_C \simeq +0.5$ VDC

ΔT FOR $V_{BE} = 5$ mV $\simeq 3.1$ C

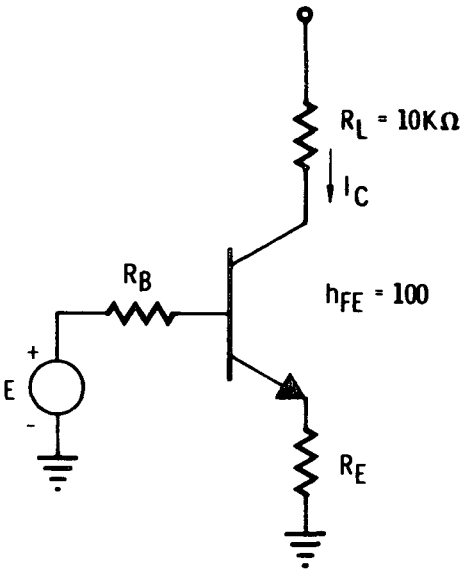

V_{BE} BIAS STABILITY NUMERICAL EXAMPLE

The change in collector voltage for a 5-millivolt increase in V_{BE} is calculated for worst-case amplifier conditions. The change in V_{BE} for large radiation damage is equivalent to a 3.1-K change in operating temperature.

$$S_3 = \frac{\Delta I_C}{\Delta h_{FE}}$$

$$S_3 = \frac{S'_1 I_{E1}}{(h_{FE1} + 1)(h_{FE2} + 1)}$$

$$S'_1 = \frac{(h_{FE2} + 1)(R_E + R_B)}{R_B + R_E (h_{FE2} + 1)}$$

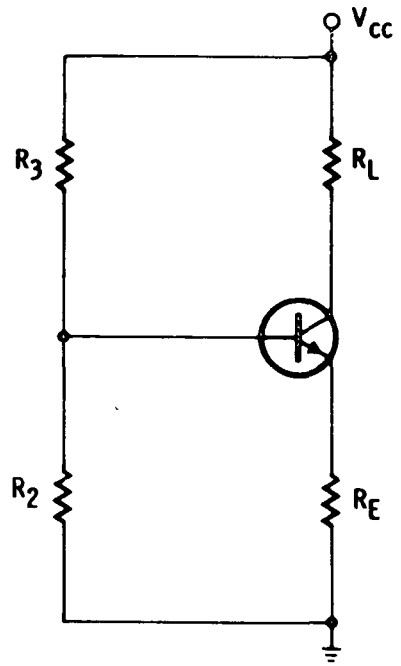

COLLECTOR CURRENT STABILITY VS. h_{FE}

The sensitivity of an amplifier stage collector current to changes in h_{FE} is defined. Low emitter resistor values and high base bias resistances contribute to instability.

$$S_3 = \frac{\Delta I_C}{\Delta h_{FE}}$$

$S_3 = 9.5 \times 10^{-6}$

$\Delta I_C = (9.5 \times 10^{-6})(-50)$

$\Delta I_C = -0.475$ mA

$\Delta V_C = +4.75$ VOLTS

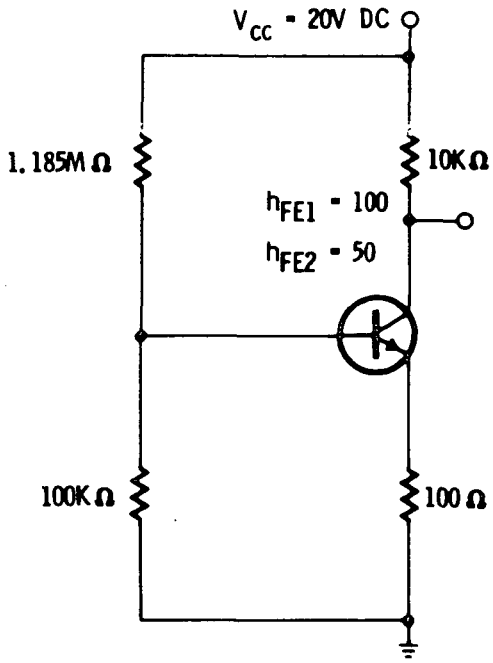

h_{FE} BIAS STABILITY NUMERICAL EXAMPLE

The change in collector voltage for a 50-per cent decrease in h_{FE} is calculated for typical amplifier parameter values.

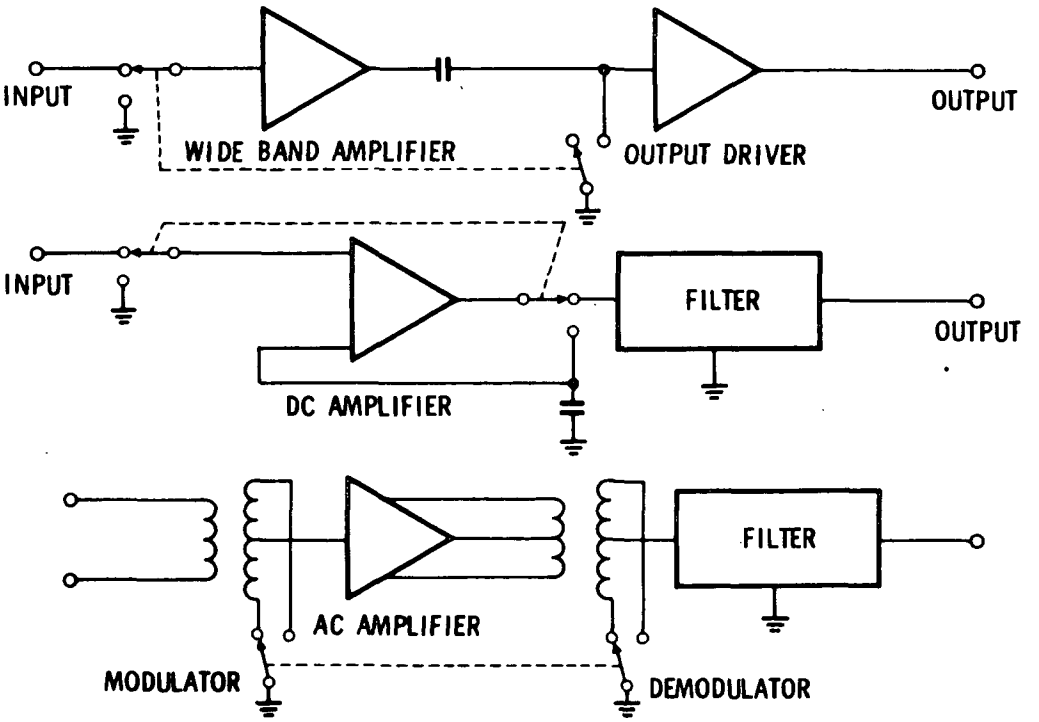

STABILIZED DC AMPLIFIERS

Three amplifier configurations are illustrated which are capable of accurate dc signal amplification with large changes in transistor parameter values.

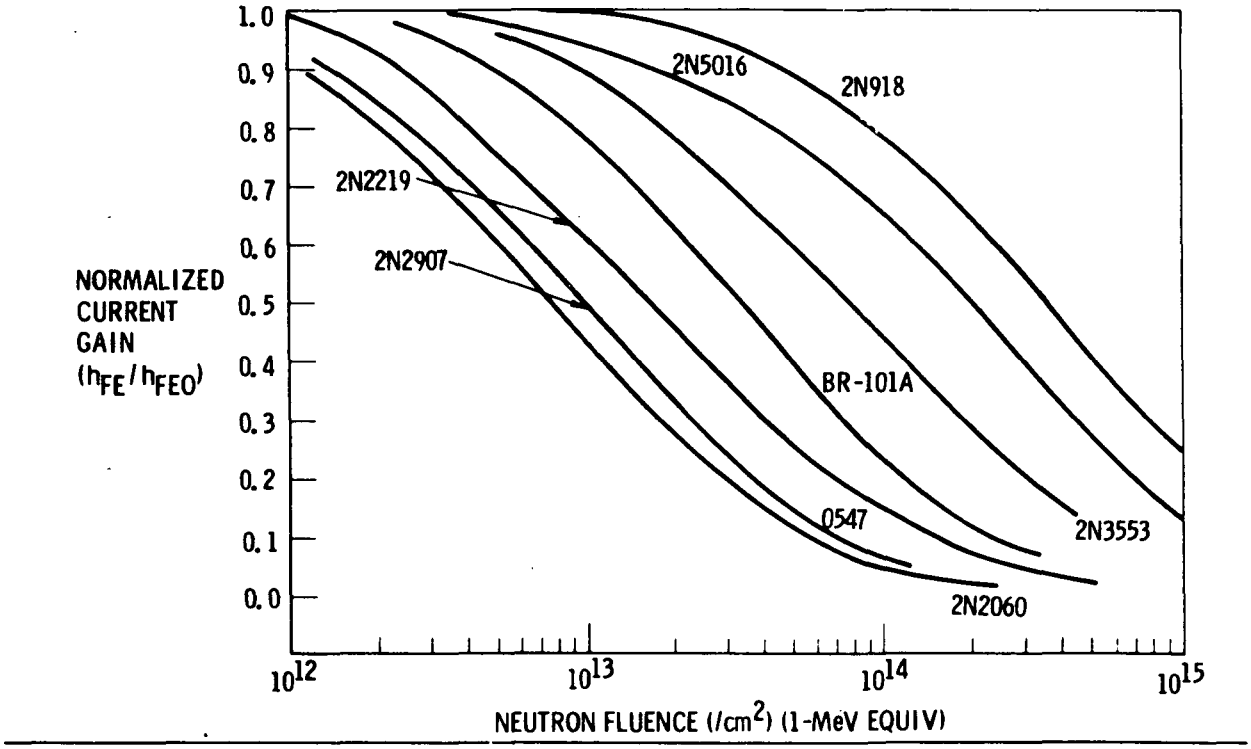

NEUTRON DEGRADATION CURVES
FOR BIPOLAR TRANSISTORS

Typical bipolar current gain damage curves are illustrated. Small-signal, rf, general purpose, power, and matched differential amplifier devices are shown.

DEVICE PAIR	NEUTRON FLUENCE (/CM^2)						
	0	4.8×10^{12}	9.9×10^{12}	3×10^{13}	9.2×10^{13}	1.92×10^{14}	3.7×10^{14}
1	1.169	1.171	1.175	1.170	1.183	1.148	1.153
2	1.100	1.105	1.112	1.124	1.130	1.109	1.114
3	0.695	0.705	0.722	0.750	0.845	0.900	0.939
4	1.437	1.416	1.383	1.331	1.182	1.110	1.064
5	0.993	0.983	0.986	0.982	1.007	1.000	1.000
6	1.059	1.062	1.050	1.047	1.062	1.039	1.020
7	0.933	0.898	0.903	0.918	0.930	1.076	0.947
8	1.085	1.089	1.084	1.078	1.036	1.033	1.025
9	1.041	1.024	1.022	1.007	1.040	1.007	1.013

CURRENT GAIN MATCHING OF INTEGRATED CIRCUIT TRANSISTOR PAIRS VS. NEUTRON FLUENCE

The current gain matching of typical integrated circuit transistor pairs is shown for several neutron fluences at 1-MeV equivalent.

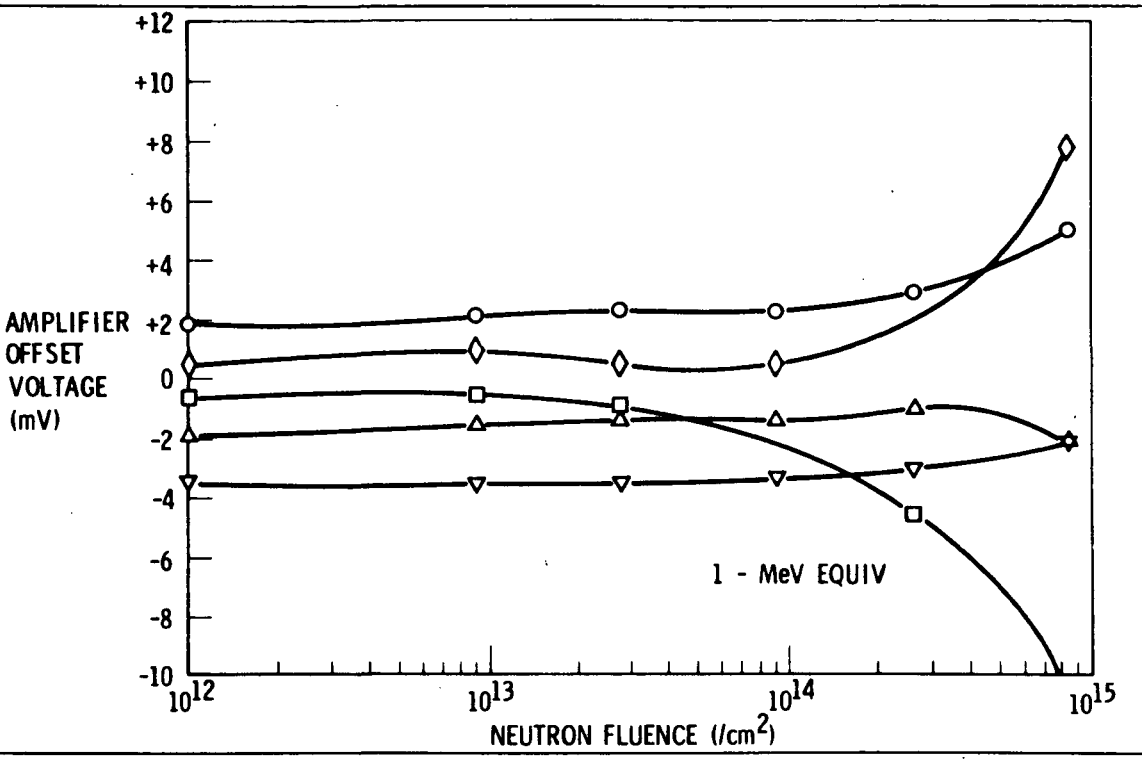

INTEGRATED CIRCUIT DIFFERENTIAL AMPLIFIER
OFFSET VOLTAGE VS. NEUTRON FLUENCE

The offset voltage of typical integrated circuit transistor pairs is shown as a function of neutron fluence.

V_{CB} = 12V BIAS	COLLECTOR-BASE PHOTOCURRENT RATIO VS. DOSE RATE (RADS (Si)/SEC)				
DEVICE PAIR	4.4×10^9	1.7×10^9	9.0×10^8	4.3×10^8	2.5×10^8
1	1.04	1.0	1.07	1.04	0.896
2	1.0	1.0	0.921	0.893	0.782
3	0.9	0.98	1.03	1.10	1.05
4	0.9	1.03	1.11	1.14	1.14
5	0.89	0.96	1.04	1.07	1.05
6	0.786	0.883	0.912	0.945	0.955
7	1.07	1.18	1.19	1.11	1.14
8	0.813	0.90	0.955	0.913	0.962
9	0.91	1.04	1.09	1.08	1.14
10	0.763	0.864	0.888	0.95	0.96
11	0.875	0.96	1.0	1.03	1.08
12	0.83	1.0	0.959	0.98	0.986
13	0.80	0.98	1.07	1.06	1.10
14	0.792	0.893	0.917	1.0	0.973
15	0.81	0.895	0.937	--	1.08
16	0.80	0.89	0.948	1.19	1.0

PHOTOCURRENT MATCHING DATA ON INTEGRATED TRANSISTOR PAIRS

The photocurrent matching of typical integrated circuit transistor pairs is shown as a function of ionizing radiation dose rate.

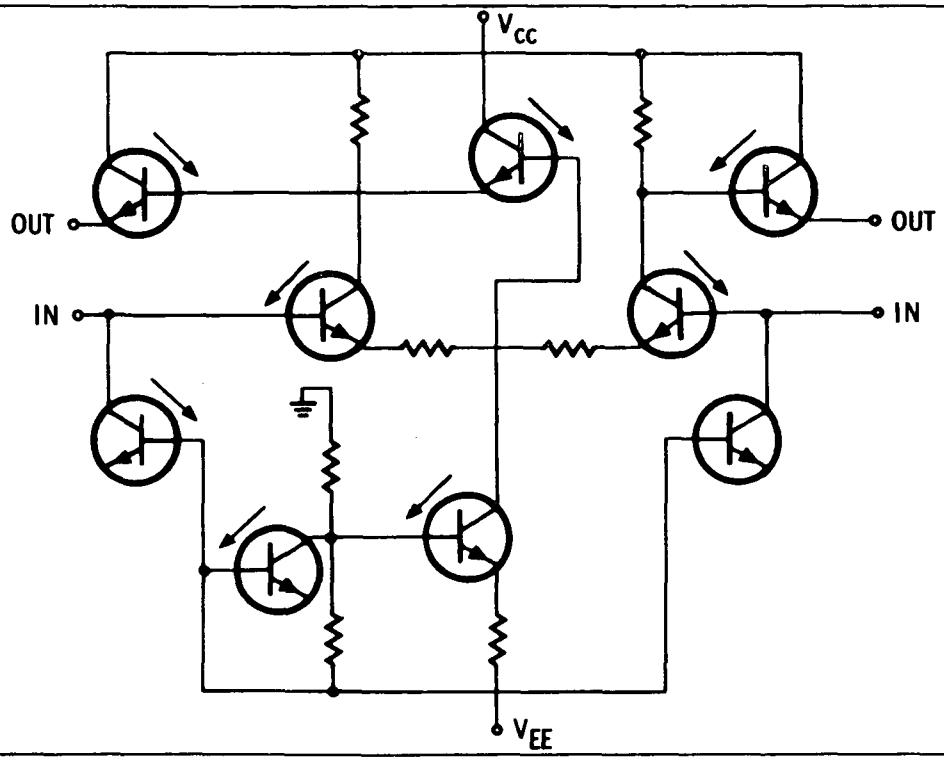

PHOTOCURRENT COMPENSATED DIFFERENTIAL AMPLIFIER

A circuit diagram of an integrated circuit differential amplifier is shown. Photocurrent compensation is employed, enabling the circuit to perform in high ionizing radiation dose rates.

DEVICE	PHOTOCURRENT GENERATION RATE (COUL/RAD)
2N709	4×10^{-13}
2N914	1.5×10^{-12}
2N2222	1.4×10^{-11}
2N697	1.1×10^{-10}
2N174	4.0×10^{-8}

TYPICAL TRANSISTOR PHOTOCURRENT GENERATION RATE

Typical collector-base primary photocurrent generation rates are listed for familiar transistors. The ionizing radiation dose rates predicted for OPGT will result in only extremely small photocurrent disturbances.

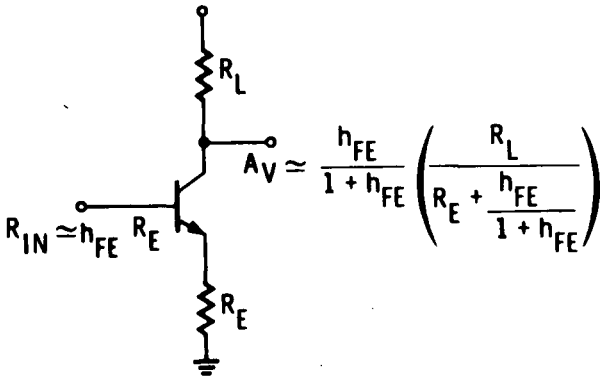

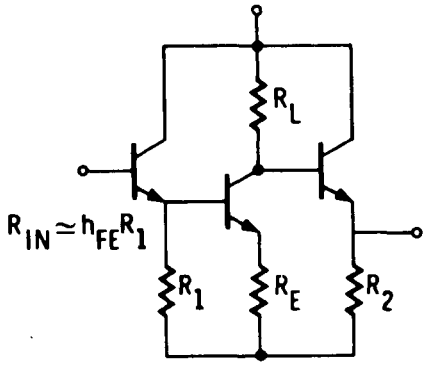

IMPEDANCE ISOLATION

The gain of simple transistor stages is often affected more severely by changes in load impedance from following stages than by degradation of the current gain of the stage transistor. Impedance isolation can be used to maintain gain with device degradation.

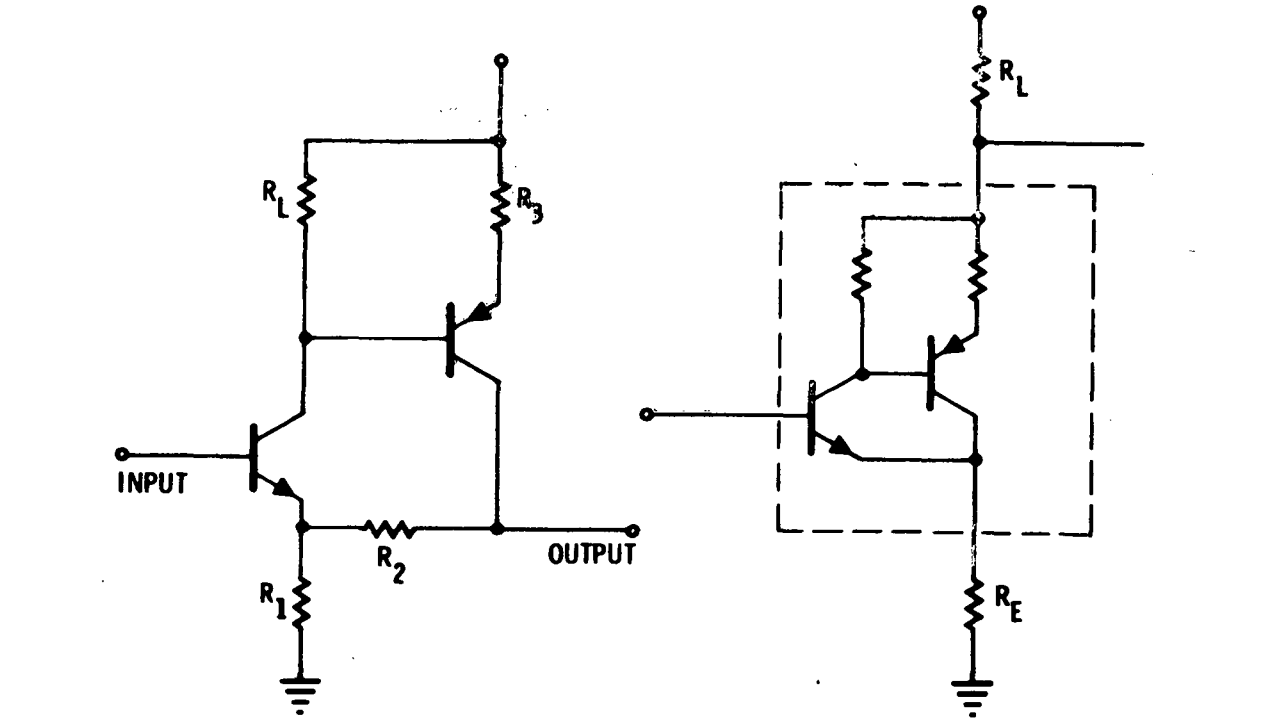

COMPOUND STAGES

The characteristics of single gain stages can be maintained over a large range of device degradation by using compound transistor gain configurations. The Darlington configuration and the feedback pair are particularly attractive.

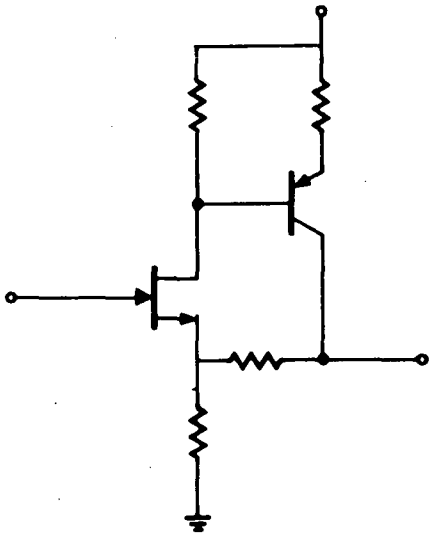

A COMPOUND STAGE USING A JUNCTION FET TO MAINTAIN HIGH INPUT IMPEDANCE

Junction field effect transistors or hardened MOS transistors can be used in hybrid bipolar - FET circuits to maintain high input impedances. Leakage currents, changes in I_{DSS}, and threshold voltage shifts (in MOS devices) compromise dc stability.

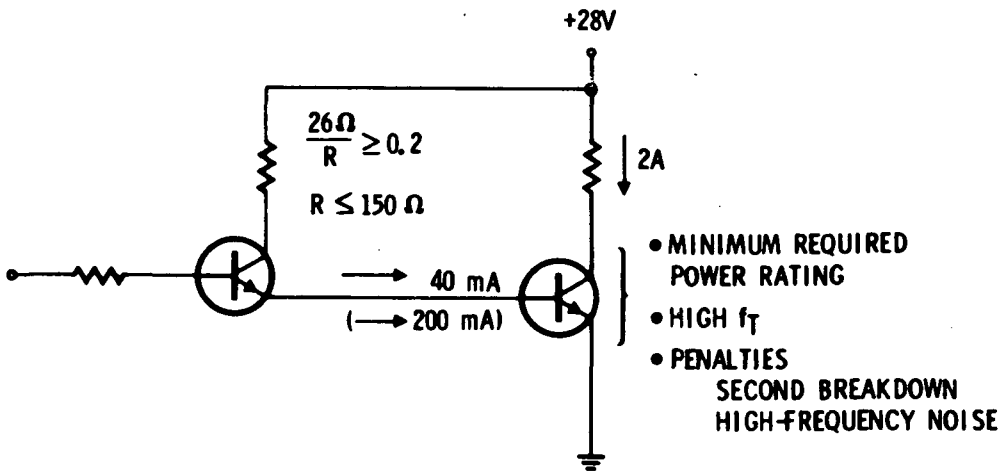

TYPICAL CONSERVATIVE POWER SWITCH DESIGN

Displacement damage in bipolar transistors often results in additional circuit complexity to achieve hardness. In the illustrated power switch, an additional stage is necessary to achieve adequate circuit current gain. Part selection to minimize device damage can be based on the speed capability of the device. However, increased speed is often accompanied by increased susceptibility to second breakdown failure. Additionally, higher-speed circuit operation can result in increased power filter requirements and electromagnetic interference.

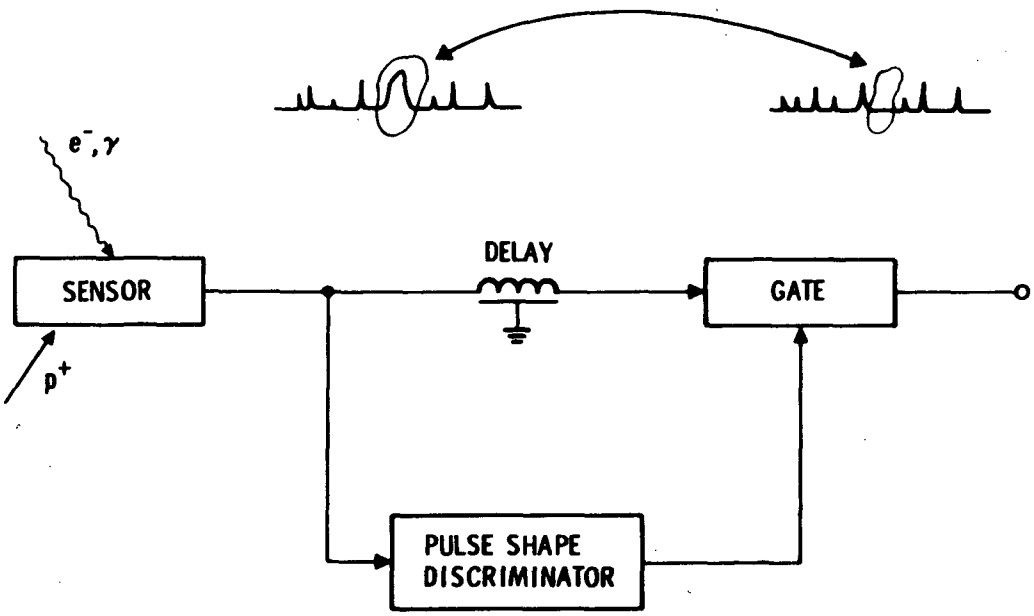

ELIMINATION OF SINGLE-PULSE IONIZATION INTERFERENCE

Pulse shape discrimination and impulse noise gating can be used to eliminate single-pulse photon or charged particle interference which may be experienced in some sensors.

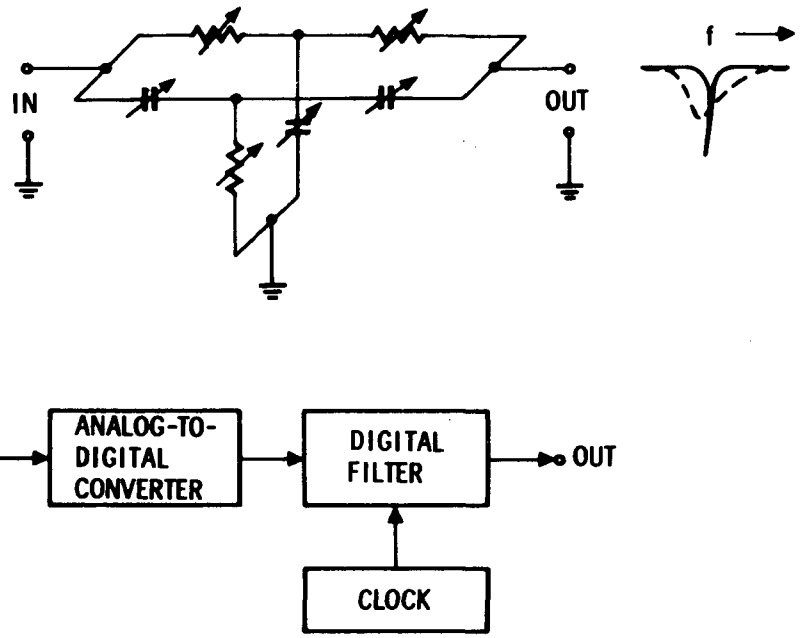

ELIMINATION OF PASSIVE COMPONENT DEGRADATION SENSITIVITY BY DIGITAL PROCESSING

Ageing and radiation damage changes in passive components can result in significant degradation of analog networks. A possible solution is the mechanization of digital data processing algorithms where sensitivities are restricted to software or clock timing functions.

$$\frac{h_{FE}}{h_{FEO}} = \frac{1}{1 + \frac{Kh_{FEO}\phi}{f_T}}$$

BIPOLAR BULK DAMAGE EQUATION

Bipolar bulk displacement damage is a function of the device initial minority carrier lifetime, base width, initial h_{FE} and gain bandwidth product. Electrical screening of devices is possible by monitoring the critical device parameters which can be related to those physical parameters that determine device damage.

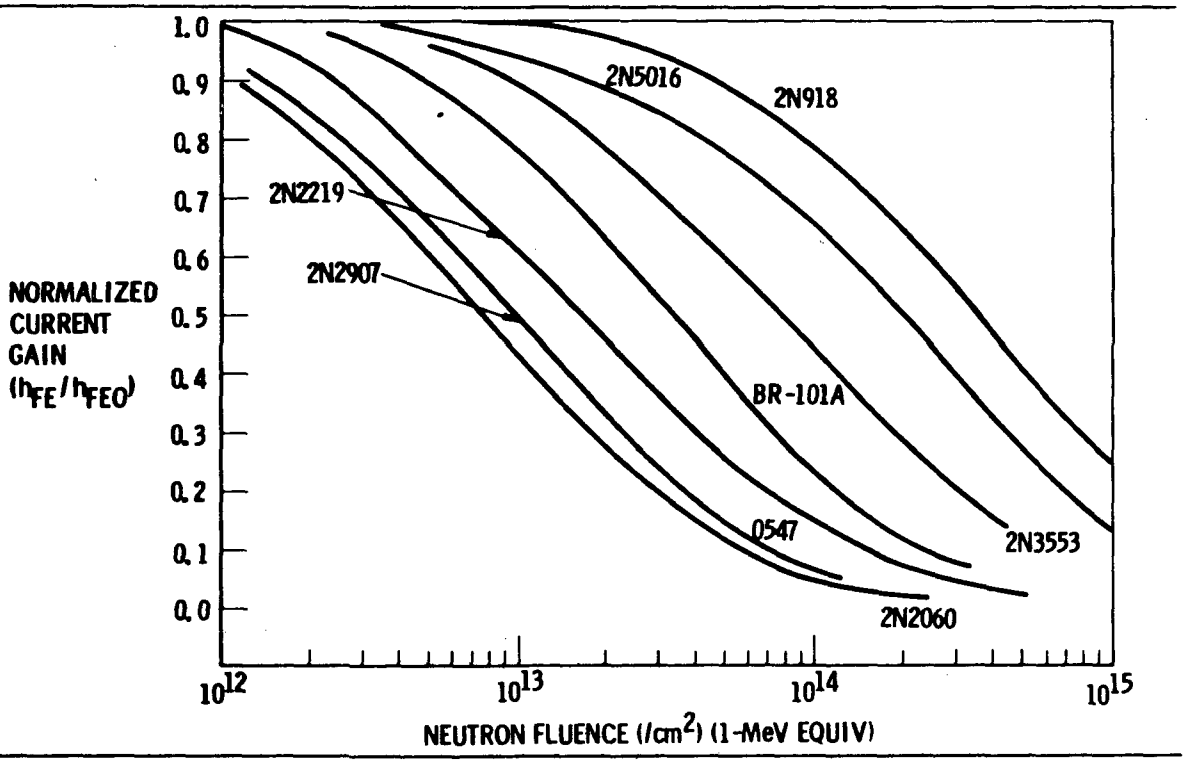

NEUTRON DEGRADATION CURVES FOR BIPOLAR TRANSISTORS

Bipolar device degradation sensitivities vary widely with the construction techniques and electrical performance of device types. Some device electrical parameters are optimized at the expense of hardness. Special design procedures or special devices may be required to achieve electrical performance and hardness.

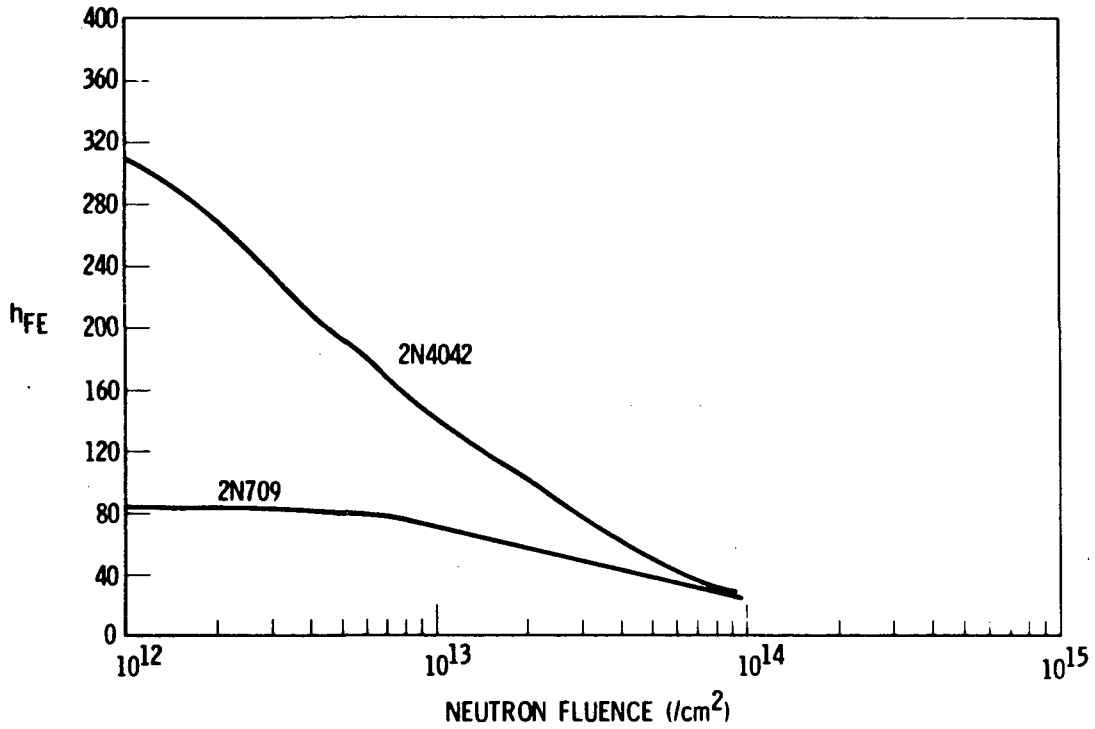

NEUTRON DEGRADATION OF 2N4042 AND 2N709 TRANSISTORS

Device selection should not be based on the gain-bandwidth product alone. For example, the initial current gain or other electrical parameters may be of major concern.

BIPOLAR

- LEAKAGE CURRENT
- SURFACE CONTRIBUTION TO GAIN
- LOW-LEVEL OPERATION

MOS FET

- LOW-FREQUENCY NOISE
- NOISE CORRELATION TO SURFACE CONDITIONS

BIPOLAR ICs

- EXTERNAL TERMINAL MEASUREMENTS
- WAFER LOT CONTROL DEVICES

ELECTRICAL SCREENS

The leakage current of low-level bipolar transistors is a good indicator of the device surface quality. The low-current damage sensitivity of transistors is often largely determined by surface characteristics. An electrical screen can therefore be developed to eliminate devices which are particularly sensitive to radiation.

Reliable MOS FET electrical screens have not been developed. However, estimates of surface characteristics can be made from low-frequency noise characteristics. Threshold voltage characteristics can also be monitored to eliminate mavericks.

The damage characteristics of integrated circuit (IC) devices can often be monitored directly from device external terminal measurements. Special test devices can also be provided at strategic locations on wafers for separate evaluation.

- MOS FET

  LOW-LEVEL IRRADIATION

  PROCESS SENSITIVITIES

- BIPOLAR

  IRRADIATE AND ANNEAL

RADIATION SCREENS

Low-level irradiation of MOS FET devices will often indicate the radiation damage susceptibility of devices at much higher radiation levels. Radiation controls can therefore be devised to eliminate fabrication lots which are particularly sensitive.

Bipolar damage characteristics can be evaluated empirically and devices annealed to provide hardness assurance. A considerable volume of experimental evidence has been compiled to verify the behavior of devices over several damage and anneal cycles.

HIGH-RELIABILITY SCREENS

- TRUNCATE PARAMETER DISTRIBUTIONS
- PROVIDE WAFER TRACEABILITY
- INSURE HERMETIC SEALING
- IMPROVE SEMICONDUCTOR SURFACE CONTROL

HIGH-RELIABILITY STRESSES

- ELIMINATE MARGINAL DEVICES

HIGH-RELIABILITY PARTS

The electrical and mechanical tests and inspections required in the production of high-reliability parts also contribute to radiation hardness. The tighter parameter distributions of high-reliability parts are amenable to accurate analysis and hardness prediction. The elimination of surface contamination by mechanical and surface process control is particularly advantageous for low-power devices operated in ionizing radiation environments.

- DEDICATED FACILITIES
- DOCUMENTED PROCESSES
- MODIFIED PROCESSES
- ADDITIONAL PROCESSES

PROCESS CONTROLS

Dedicated facilities and closely documented process procedures can materially contribute to parts hardness. Modified processes such as surface passivations or altered doping levels (or materials) can result in enhanced hardness in standard parts.

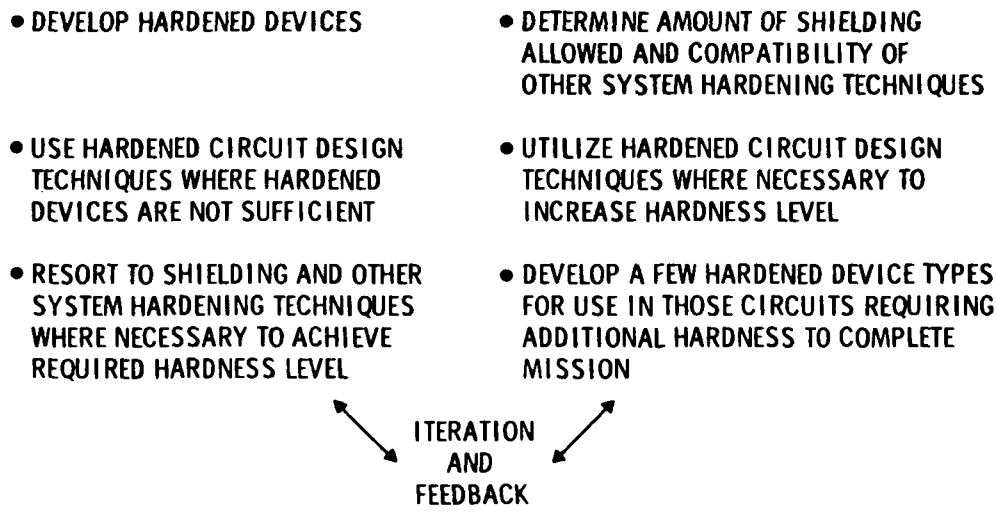

HARDENING APPROACHES

Radiation-hard systems may be developed by selecting or developing hard components and progressing through circuit and subsystem design. Alternately, subsystem and circuit designs may be performed, leading to part or device hardness specifications. Neither approach is entirely adequate. 'Soft' or vulnerable circuits and subsystems can be made from parts which offer state-of-the-art hardness. Parts requirements which are unnecessarily costly or impractical can result from unrealistic designs. A combined approach is therefore required which utilizes cost-effective hardened parts in engineering designs that are guided by a basic understanding of parts limitations and radiation effects.

- PREFERENTIAL SHIELDING
- REDUNDANCY
- SELF-REPAIR CAPABILITY
- OVERDESIGN
- SHUTDOWN/RESET

SYSTEM HARDENING CONCEPTS

Cost-effective system hardening will combine several approaches such as shielding, redundancy, and conservative design to result in a balanced program. Each of several hardening techniques must be examined in detail to determine which approach is optimum for each subsystem or circuit. Minimum costs such as weight, power, risk, and complexity are used as success criteria. Shielding is often a last resort when hardening is otherwise unfeasible. Redundancy and overdesign also carry penalties of weight and cost. Self-test and repair capability can be used to switch in redundant parts, components, or subsystems, or to shut down and reset temporarily degraded devices.

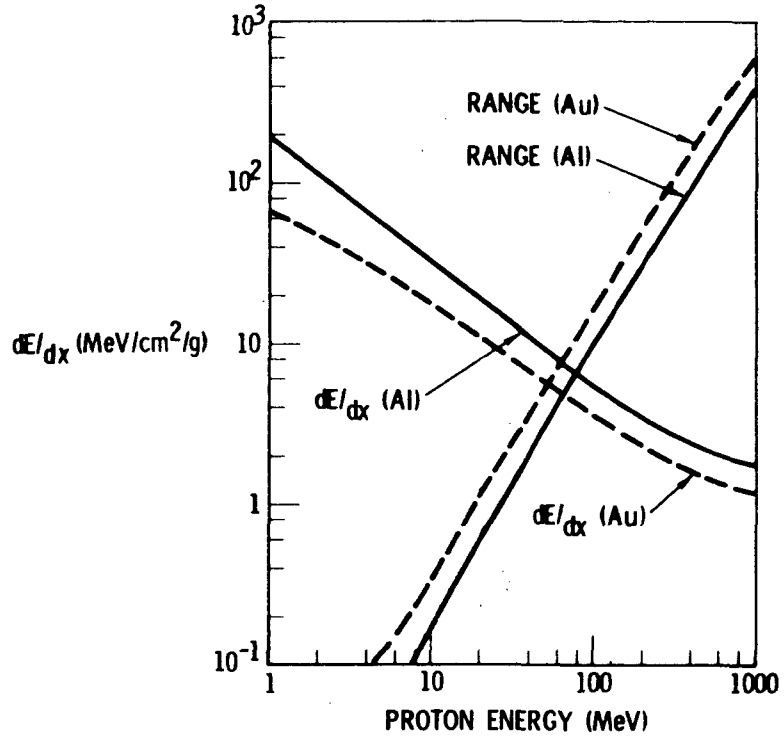

ENERGY LOSS AND RANGE OF PROTONS IN ALUMINUM AND GOLD

The range and energy loss of protons in typical spacecraft materials are strong functions of the particle energy. The shielding effectiveness of materials is therefore strongly dependent on the environment energy spectrum. A "good" shield for a distant approach to Jupiter is therefore not necessarily adequate or even desirable for a close approach trajectory.

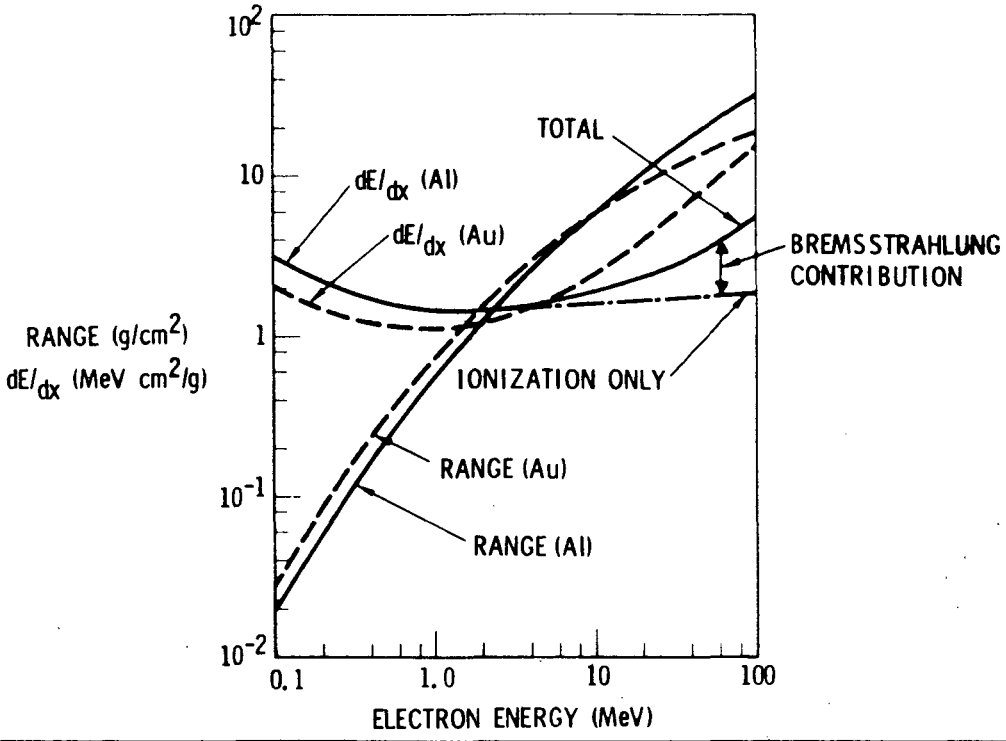

ENERGY LOSS AND RANGE OF ELECTRONS IN ALUMINUM AND GOLD

The rate of energy deposition (dE/dx) for electrons in shield materials is a moderate function of energy. The range of an energetic electron is not a strong function of the shielding material but is roughly proportional to the energy of the particle. The contribution of bremsstrahlung to the energy loss rate in aluminum is also shown.

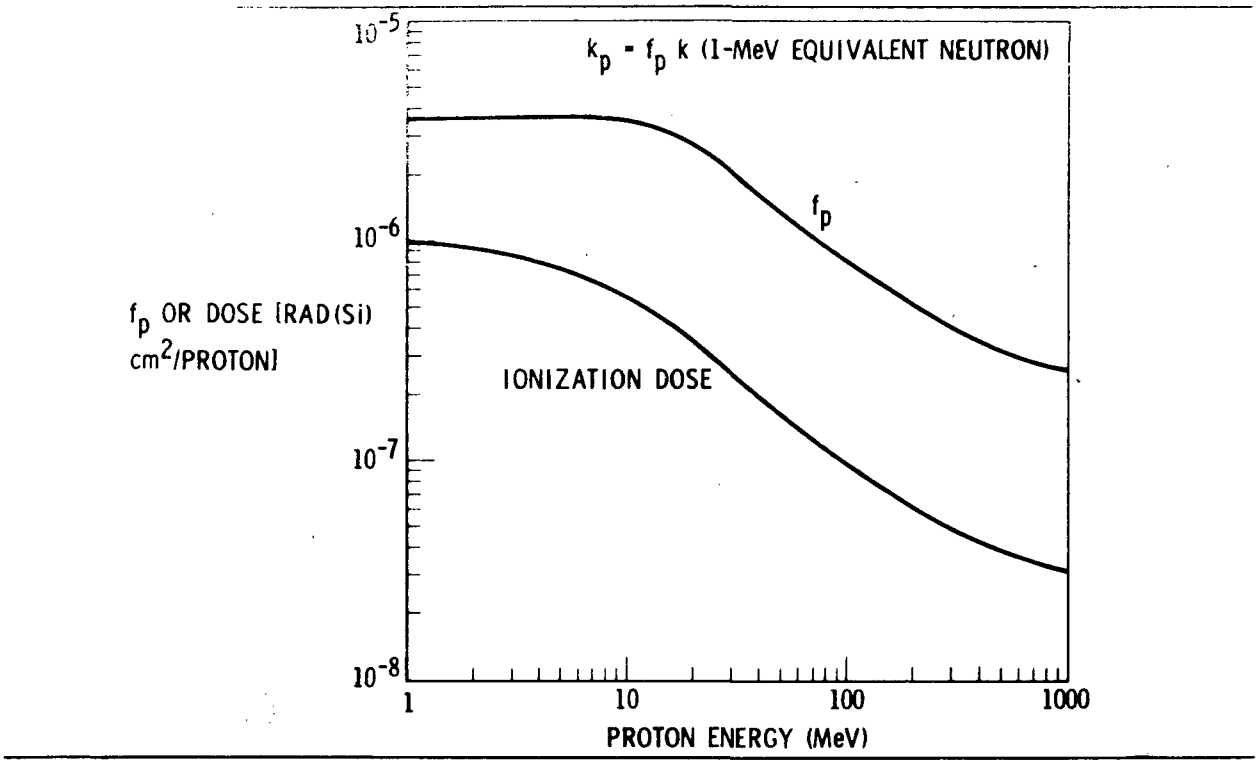

RELATIVE DISPLACEMENT DAMAGE AND IONIZATION EFFICIENCY OF PROTONS

The silicon displacement damage and ionization caused by protons is a function of the energy of the particle. Damage or ionization and shield effectiveness calculations must be carefully performed to equate fluences to familiar terms such as 1-MeV neutron damage equivalence.

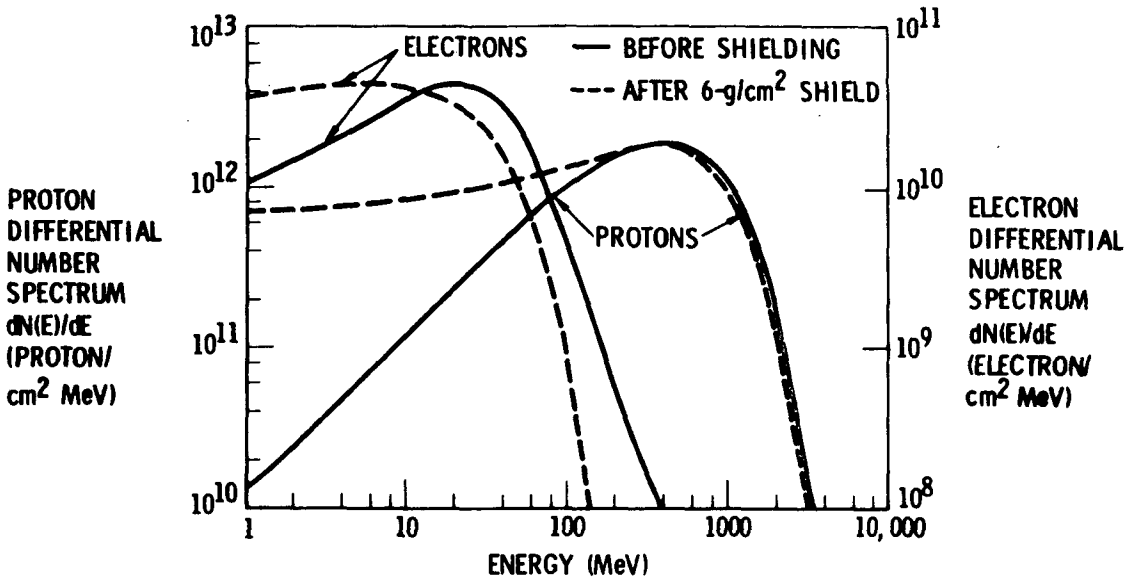

MODIFICATION OF THE DIFFERENTIAL ENERGY SPECTRUM OF PROTONS AND ELECTRONS BY A 6-G/CM^2 SHIELD

A typical electron shield can modify a high energy proton spectrum in such a manner to reduce the proton flux but also to reduce the proton energies to values where the silicon damage efficiency is greater.

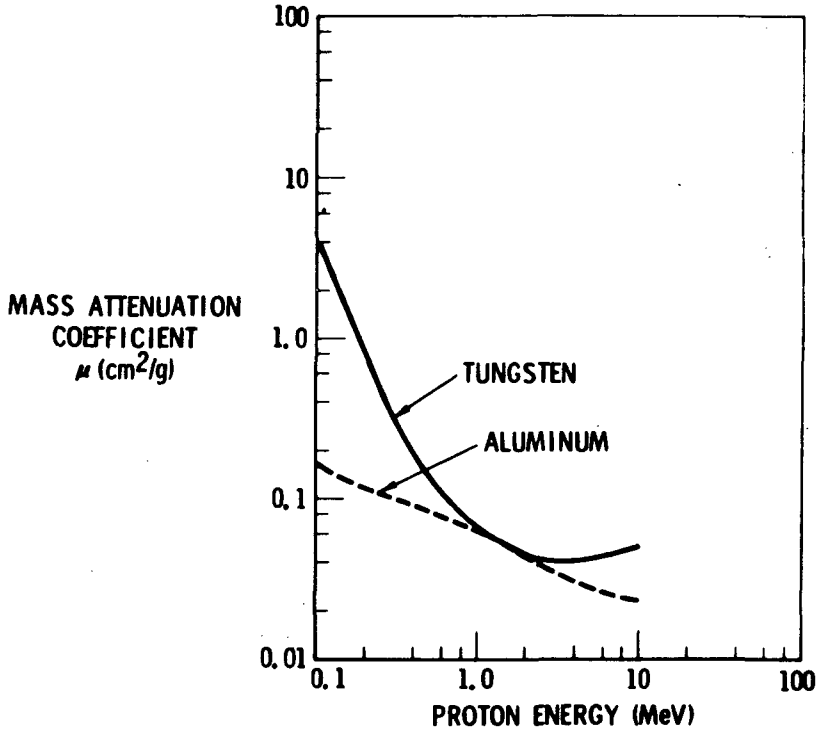

MASS ATTENUATION COEFFICIENT OF ALUMINUM AND TUNGSTEN

Photon absorption is higher in elements of high atomic number than in low-Z materials. However, the absorption in tungsten and aluminum is not significantly different for photon energies between 0.6 and 4 MeV where a large fraction of RTG radiation is found.

PARTICLE	MATERIAL	THICKNESS	ENERGY STOPPED	EFFECTIVENESS
PROTONS	Al	400 G/CM^2 (148 CM)	1000 MeV	DECREASED DAMAGE
PROTONS	Al	6 G/CM^2 (2.2 CM)	75 MeV	INCREASED DAMAGE
ELECTRONS	Al	6 G/CM^2 (2.2 CM)	10 MeV	DECREASED DAMAGE
ELECTRONS	Al	0.55 G/CM^2 (0.2 CM)	1 MeV	SAME DAMAGE
FISSION NEUTRONS	LiH	14 G/CM^2 (18.7 CM)	*	DECREASED DAMAGE
PHOTONS (10 MeV)	Al	100 G/CM^2 (37 CM)	*	DECREASED DAMAGE
PHOTONS (10 MeV)	W	46 G/CM^2 (2.4 CM)	*	DECREASED DAMAGE
PHOTONS (1 MeV)	Al	28 G/CM^2 (10.4 CM)	*	DECREASED DAMAGE
PHOTONS (1 MeV)	W	27 G/CM^2 (1.4 CM)	*	DECREASED DAMAGE
PHOTONS (0.1 MeV)	Al	14.4 G/CM^2 (5.3 CM)	*	DECREASED DAMAGE
PHOTONS (0.1 MeV)	W	0.55 G/CM^2 (0.028 CM)	*	DECREASED DAMAGE

*STOPS 90 PERCENT OF INCIDENT FLUX

SHIELDING CONSIDERATIONS

Calculations of the shielding required for large attenuations of some spacecraft environments indicate that extreme weight penalties are required for shielded volumes of only moderate size. Parts, circuit, and subsystem hardening are therefore necessary with shielding used only where other approaches result in penalties of greater significance than the required shield weight.

- MULTIPLE CHANNELS
- VOTING
- SELF-TESTING
- ERROR CODES

REDUNDANCY

Several electronic system or subsystem redundancy techniques which are used to enhance reliability or fault tolerance can also be used to increase hardness.

DISPLACEMENT EFFECTS TESTING

IONIZATION EFFECTS TESTING

SYSTEM - LEVEL TESTS

DOSIMETRY

TESTING

Radiation testing equipment and procedures are described in this section. Testing for displacement effects requires energetic neutrons or protons from reactors or particle accelerators. Ionization effects tests require electrons, gamma rays, or X-rays. In radiation tests on large OPGT systems, accelerated testing, environment simulation (of one type of radiation by another), and the sequence of exposures to various environments become important considerations. To standardize and calibrate radiation test results, dosimetry, or the measurement of radiation flux and fluence, is an essential requirement.

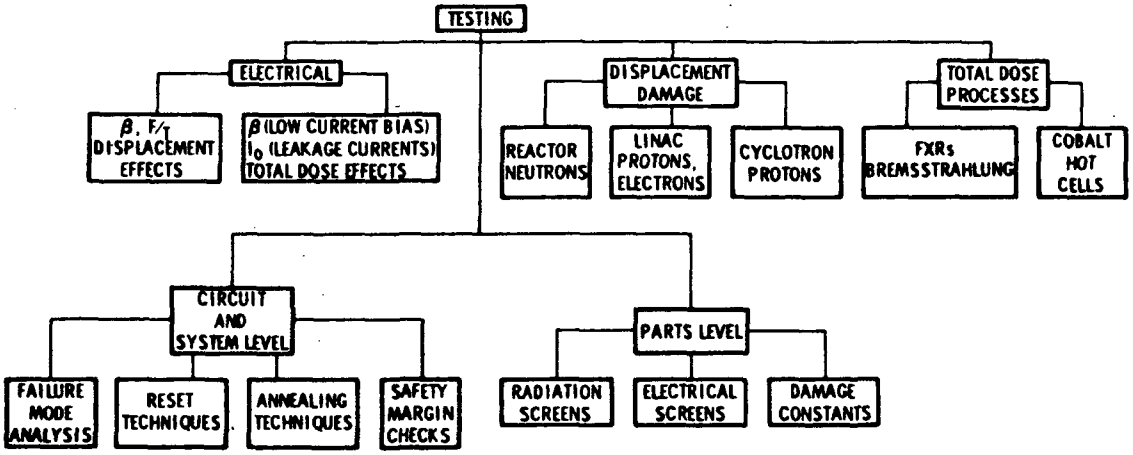

TESTING

The testing program for radiation effects involves three basic kinds of tests: electrical, displacement damage, and total dose tests. Electrical tests measure radiation related variables such as current gain, gain bandwidth product, and leakage currents which may be used to predict expected radiation response. Displacement damage tests measure circuit and system degradation and device damage constants in the proton, neutron, and electron environments. Total dose tests characterize the degradation of semiconductor circuits and devices due to ionizing radiation.

The testing program must consider the appropriate test level for various objectives. Radiation screens, electrical screens, and device radiation response are addressed at the parts level. Failure mode analysis, reset techniques, annealing cycles during operation, and safety margin measurements are done at circuit and system levels.

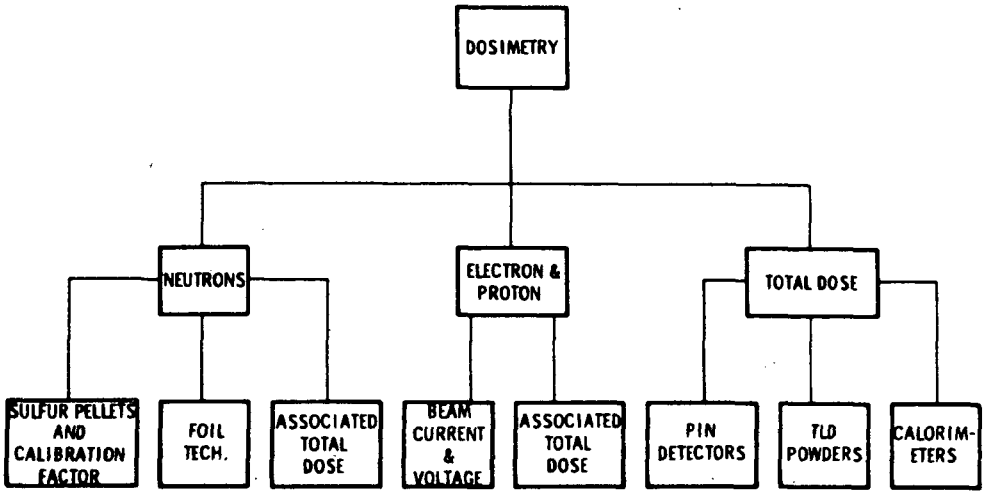

DOSIMETRY

Dosimetry must be accurately accomplished. Sulfur pellets and foil techniques are used for neutron fluence; beam current and voltage for electron and proton fluence; and PIN detectors, TLD powders, and calorimeters for total dose assessment.

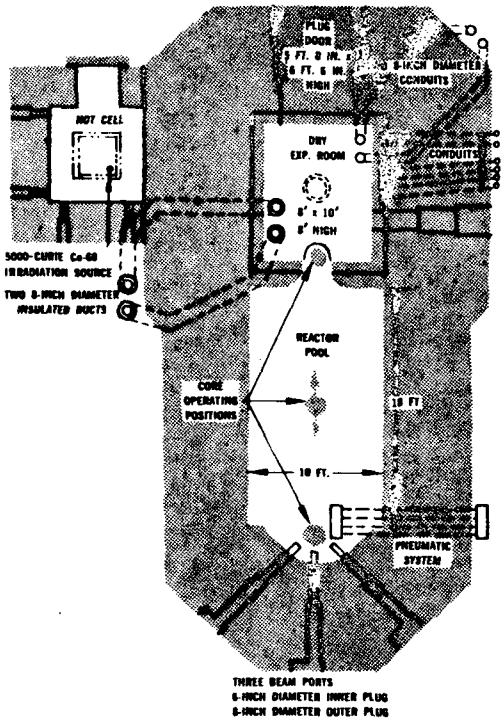

NORTHROP TRIGA REACTOR FACILITY

The Northrop TRIGA facility is a typical neutron test facility. The dry room is a convenient area for testing parts, circuits, or black boxes. Neutron spectral information has been carefully obtained for this facility so that sulfur pellet dosimetry may be combined with a facility factor to obtain the neutron fluence >10 keV. A 5,000-curie hot cell is also available for total dose experimentation.

ENERGY RANGE	1 MeV - 75 MeV
PULSE WIDTH	10 ns - 20 μs
BEAM DIAMETER	0.5 cm - 2 cm
MULTIPLE PULSES	COVERS REQUIRED FLUENCE RANGE
BREMSSTRAHLUNG MODE	TOTAL DOSE SIMULATION

ELECTRON LINEAR ACCELERATORS

The significant features of LINACs relative to their use as damage simulators are depicted here. Entirely adequate coverage of the energy range is readily available from existing LINACs. Pulse widths are adjustable from about ten nanoseconds to twenty microseconds. Pulse repetition rates and beam currents allow deposition of required electron fluences at a rate limited only by device thermal dissipation. LINACs are readily converted to γ or total dose simulators by using a tantalum target and exposing devices to the resulting bremsstrahlung.

The disadvantage of LINACs is the small beam diameter which severely limits the exposure area. Practically speaking, only individual devices may be tested; modules are too long to receive uniform exposure.

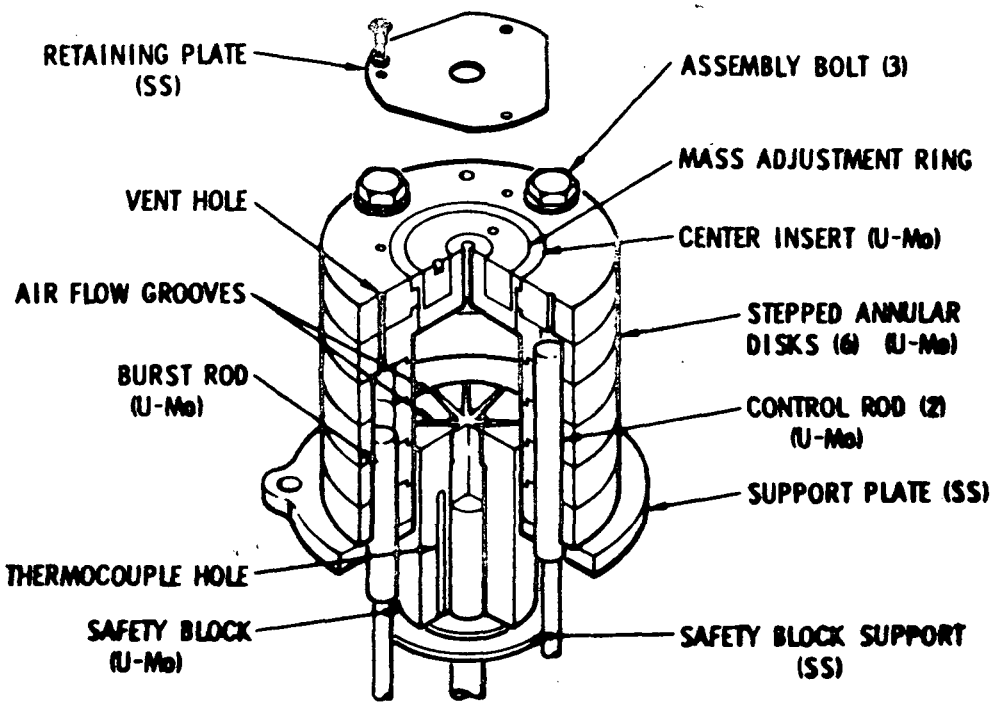

FAST BURST REACTORS

Fast burst reactors are a convenient source of pulsed neutrons and/or γ radiation. Narrow pulse widths are available (~50 μsec) which permit the study of rapid annealing effects. Cooling problems limit the number of bursts to six or eight per day. This facility can not be readily operated in the steady state. The maximum neutron fluence per pulse is about 1×10^{11} n/cm^2 on a 1-meter horizontal circle.

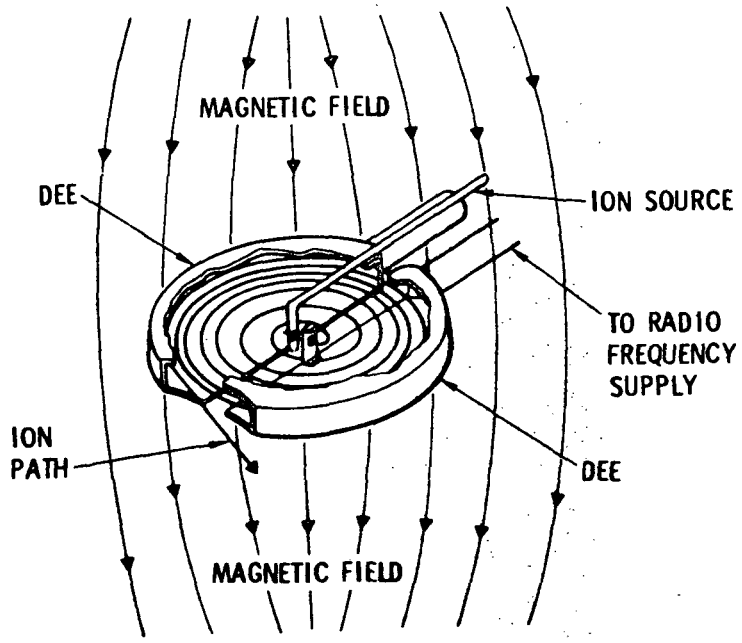

CYCLOTRON

In the basic cyclotron, particles injected at the center are bent into circular paths by traveling in a vertical magnetic field. A rapidly alternating horizontal electric field applied between hollow electrodes (dees) accelerates the particles each time they complete a half circle. The particles are extracted and aimed at an external target. The dees are enclosed in a vacuum so that air molecules will not obstruct the motion of the particles.

The cyclotron is a convenient source of protons for radiation effects testing in the 1-to 100-MeV range. Dosimetry is similar to that used for LINACs and flash X-rays.

ENERGIES	-	1.17 MeV
	-	1.33 MeV
HALF LIFE	-	5.3 YEARS
SOURCE STRENGTH	-	100,000 CURIES
PHOTON FLUX	-	10^{12} PHOTONS/CM^2 SEC

COBALT HOT CELL

Radioisotopes are convenient sources for studying ionization damage. The most popular is the Cobalt-60 hot cell characterized above.

Another example is Cesium-137 which produces 0.66-MeV photons with a 30-year half-life. Gamma rays from spent fuel elements are also used. The average energy is 0.7 MeV and the useful life is about one month after removal.

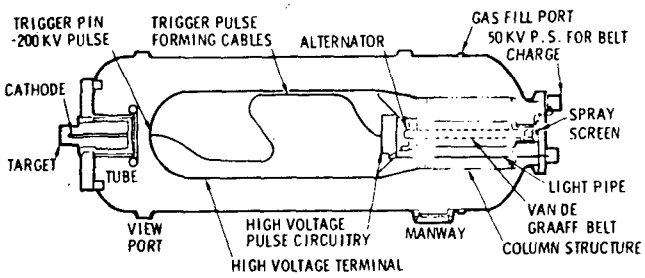

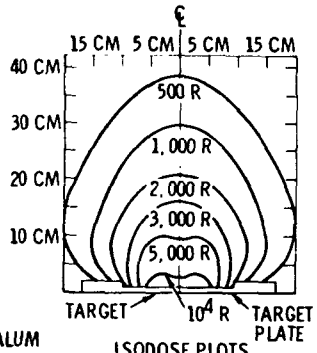

ISODOSE PLOTS

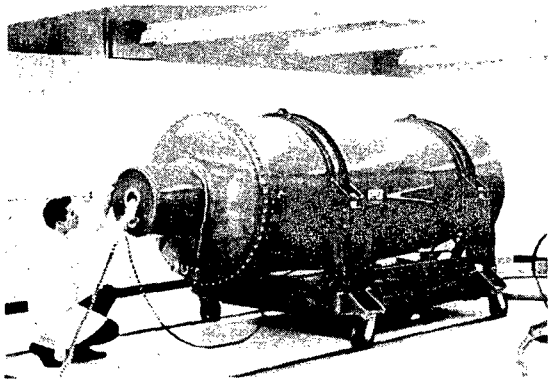

TARGET 0.020 IN. TANTALUM
FILTER 0.380 IN. ALUMINUM
SINGLE POINT CATHODE,
10-CM SPACE

STORED ENERGY	15 KJ AT 7 MV
ELECTRON CURRENT	50 KA
PULSE WIDTH	30 NSEC (FWHM)
X-RAY DOSE	100 RAD(Si) AT 1 M
	10^4 RAD(Si) AT 2 CM
X-RAY DOSE RATE	3×10^9 RAD(Si)/SEC AT 1 M
	3×10^{11} RAD(Si)/SEC AT 2 CM

UP TO 120 SHOTS/DAY

FLASH X-RAYS

Flash X-ray machines produce short bursts of bremsstrahlung by rapidly dumping a high-energy electron beam into a high-Z target. Pulse widths are typically 30 ns and are not readily adjustable. Accelerating voltages are adjustable over a narrow range. They are particularly useful in weapon effects testing and are adaptable to some testing requirements for OPGT type environments.

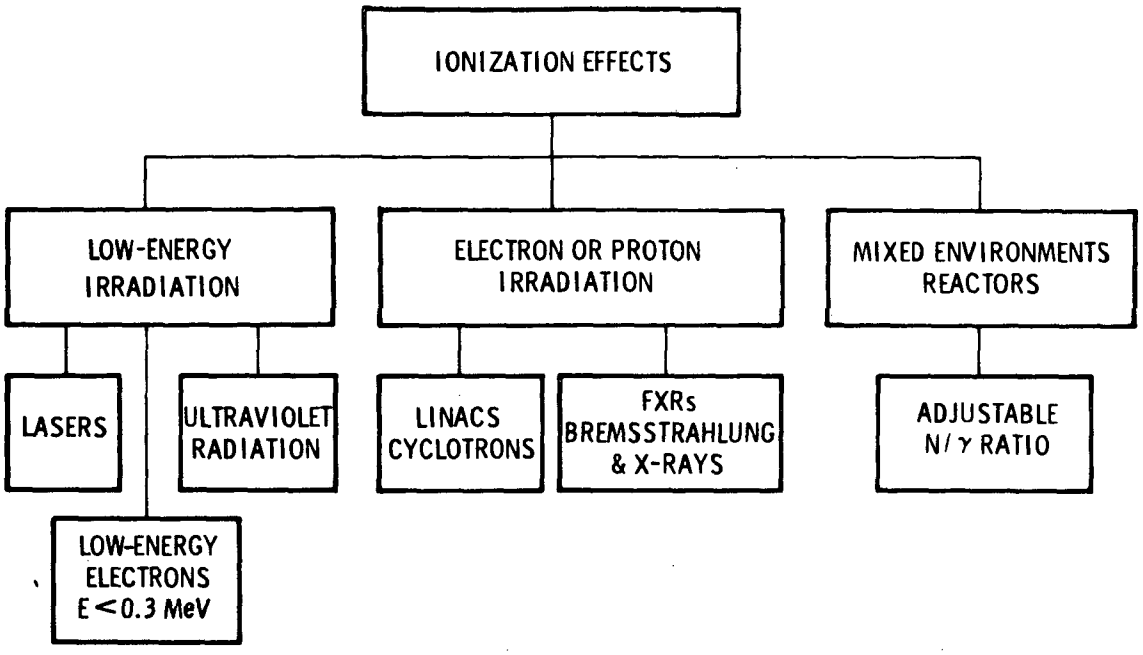

IONIZATION EFFECTS TESTING

A wide range of simulators produce ionization effects. Low-energy radiations from lasers, low-energy electrons, and ultraviolet radiation produce only ionization effects, since individual quanta or particles cannot displace lattice atoms. High-energy irradiation from electrons or protons produce mostly ionization effects coupled with some displacement damage. Use of a tantalum target to produce bremsstrahlung eliminates displacement damage. Reactors produce combined displacement and ionization damage with the mix controllable by shielding designed to select appropriate n/γ ratios. Cobalt cells provide essentially monoenergetic γ radiation which produces mostly ionization damage with a very small amount of displacement damage.

ENVIRONMENT	DISPLACEMENT DAMAGE	IONIZATION EFFECTS	REMARKS
REACTOR	UNIFORM PRODUCTION OF CLUSTER DAMAGE	ACCOMPANYING RADIATION	MOST WIDELY USED TEST FACILITIES FOR DISPLACEMENT DAMAGE
LINAC	NON-UNIFORM PRODUCTION OF POINT DEFECTS	DOMINANT EFFECT	ELECTRON DISPLACEMENT DAMAGE COMBINED ENVIRONMENT
CYCLOTRON	NON-UNIFORM PRODUCTION OF POINT DEFECTS & CLUSTERS	DOMINANT EFFECT	PROTON DISPLACEMENT DAMAGE
COBALT CELL	UNIFORM PRODUCTION OF POINT DEFECTS	DOMINANT EFFECT	GOOD SIMULATOR FOR LOW DOSE RATE IONIZATION EFFECTS

TEST FACILITIES SUMMARY

The many test facilities available allow the experimental production of point defects on both a uniform and non-uniform basis, the production of cluster defects on both a uniform and non-uniform basis, and the production of ionizing dose effects uniformly or distributed with a specific dose depth profile. Combined environments can be produced in a manner which will closely approximate actual operating conditions in a spacecraft.

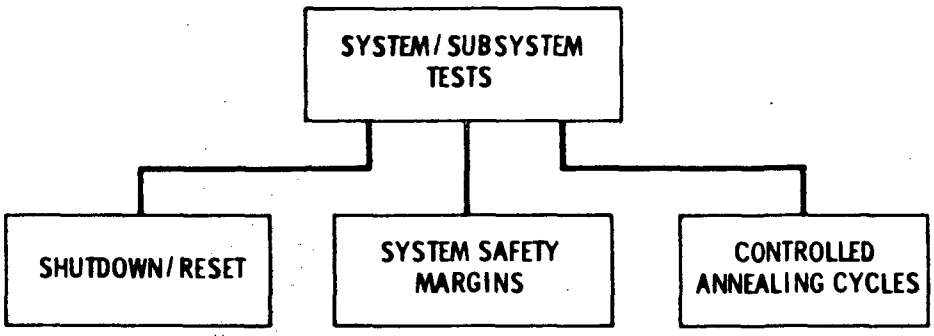

SYSTEM TESTING

The operation of systems or subsystems can be checked out in the larger radiation simulator facilities. Operations such as shutdown/reset can be checked out in a radiation environment. An example would be computer-or ground controlled switching of a redundant power supply regulator to replace a failed unit.

Subsystem safety margins can be baselined by irradiation to failure. The failure level measures safety margin, and monitoring of specific subsystem functions details characteristic responses as the subsystem approaches failure.

Controlled annealing cycles can be checked for degree of annealing, and the baseline engineering responses such as temperature rise determined in a simulated radiation environment.

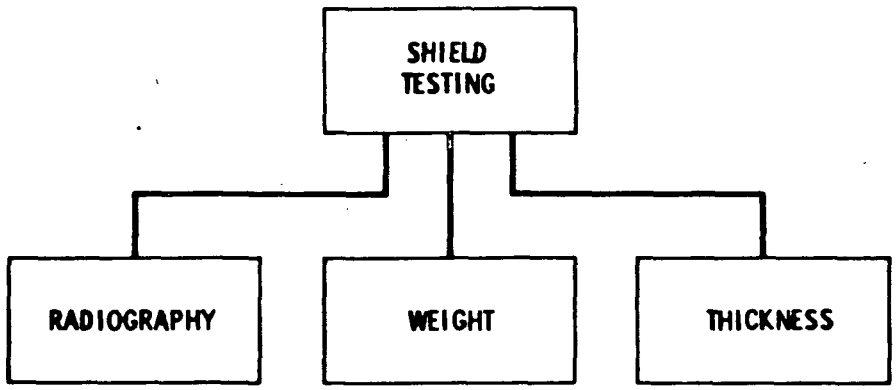

SHIELD TESTING

Radiation shields can be measured radiographically to determine the existence of defects such as thinning, line-of-sight failures, and proper positioning of baffles. Corrective action can be taken before launch. A standard wedge is irradiated simultaneously with the shield. Density is compared optically or with a densitometer to determine thickness. Other testing methods include direct measurement of thickness and weight.

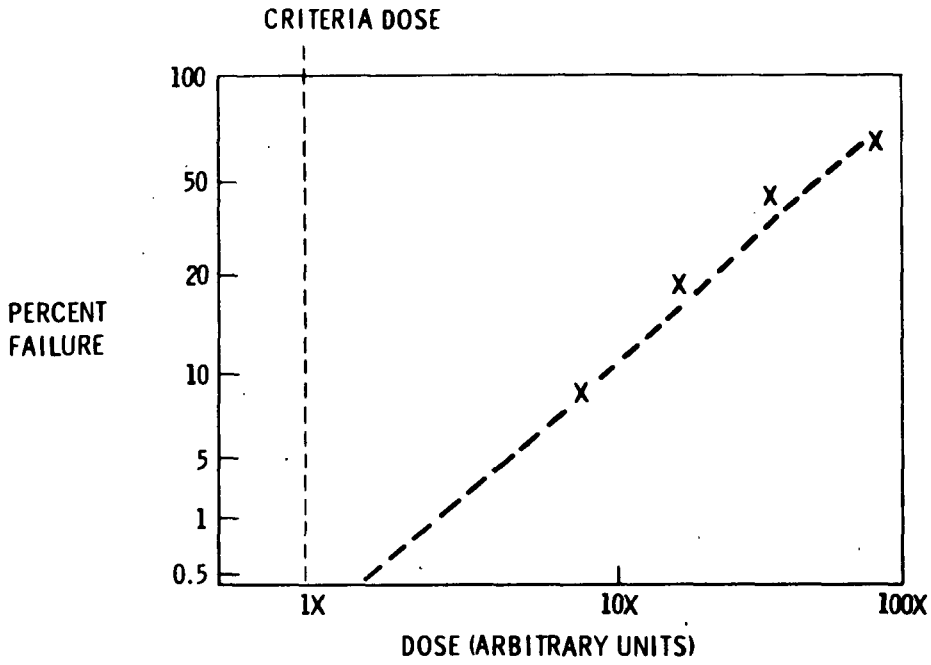

SYSTEM SAFETY MARGINS

Safety margins can be measured for dominant failure modes by irradiation to failure, compiling a cumulative failure distribution, and extrapolating to criteria dose levels. This is an important concept for establishing design confidence and provides a data base for combining reliability and radiation degradation.

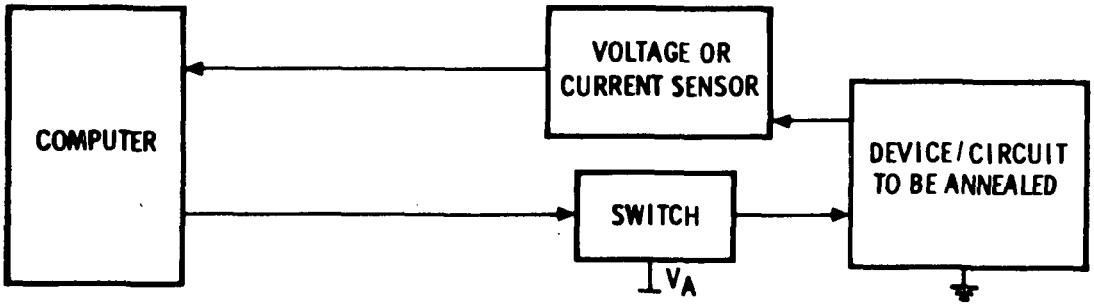

ANNEALING CYCLE

In this oversimplified annealing circuit, a computer senses low output due to accumulation of total ionizing dose and initiates a simple bias anneal cycle through a switch.

The operation and characteristics of such a cycle can be thoroughly baselined in a radiation test facility, e.g., a cobalt hot cell.

FOIL	REACTION	THRESHOLD ENERGY (E_T) MeV	CROSS SECTION ($\bar{\sigma}$) (10^{-30} cm)
GOLD	$Au^{197}(n,\gamma)Au^{198}$	THERMAL	9
PLUTONIUM-239	$Pu^{239}(n,F)$ FISSION PRODUCTS	0.01	1.7 (SURROUNDED BY 1 cm BORON-10)
NEPTUNIUM-237	$Np^{237}(n,F)$ FISSION PRODUCTS	0.600	1.6
URANIUM-238	$U^{238}(n,F)$ FISSION PRODUCTS	1.50	0.55
SULFUR	$S^{32}(n,p)P^{32}$	3.00	0.30
MAGNESIUM	$Mg^{24}(n,p)Na^{24}$	6.30	0.06
ALUMINUM	$Al^{27}(n,\alpha)Na^{24}$	8.10	0.130

$$\bar{\sigma} = \frac{\int_0^\infty \sigma(E)\,\phi(E)dE}{\int_{E_T}^\infty \phi(E)dE}$$

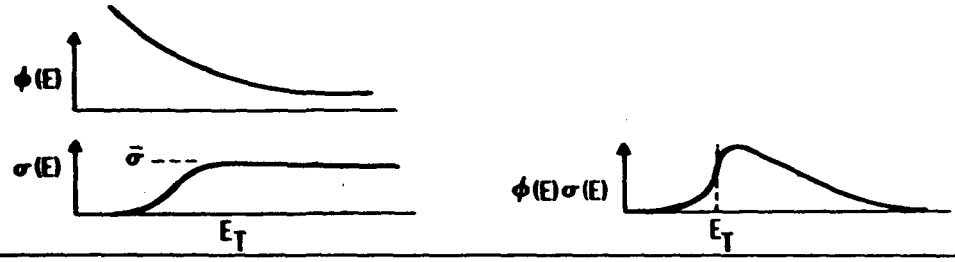

THRESHOLD REACTIONS

Neutron spectra are unfolded using foil activation techniques where the activity in each foil is proportional to

$$\int_0^\infty \sigma(E)\,\phi(E)\,dE$$

Using the definition of $\bar{\sigma}$ displayed above, the activity is proportional to

$$\bar{\sigma} \quad \int_{E_T}^\infty \phi(E)\,dE$$

A few of the common foil materials, reactions, threshold energies, and average cross sections are listed here.

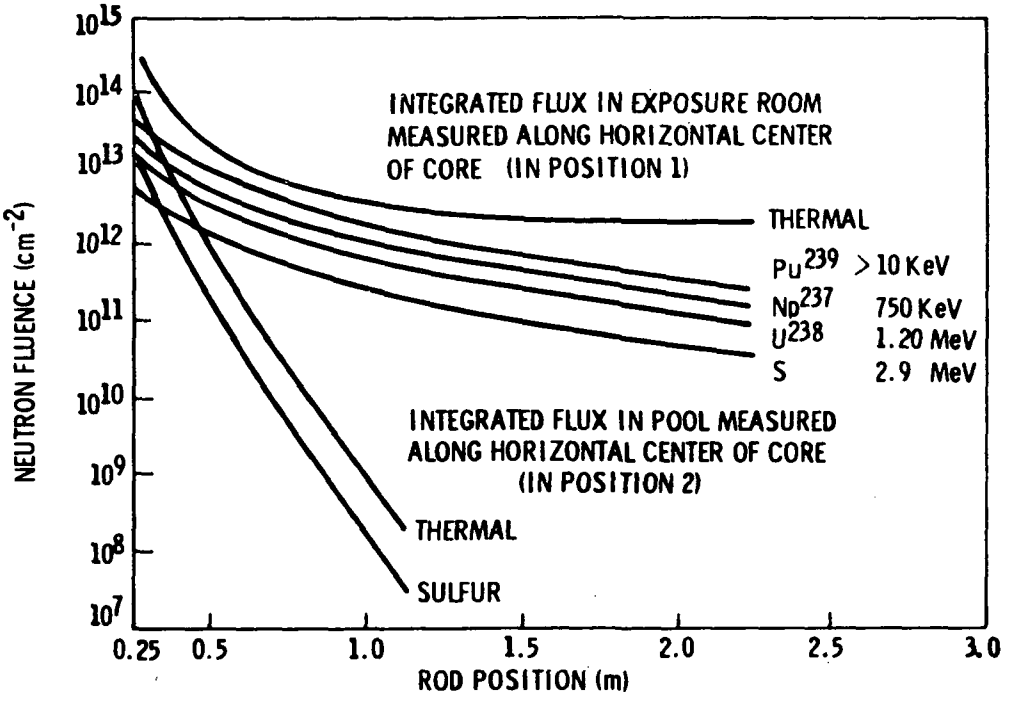

SULFUR DOSIMETRY

A set of measurements made at the Northrop TRIGA reactor are shown above. These measurements are repeatable for a given facility and a given rod placement in the core. After such a series of measurements have been carefully made to characterize an experimental facility, sulfur dosimetry only is employed and the fast neutron fluence (E >10 keV, fission spectrum) is determined by multiplying the sulfur neutrons by the sulfur-to-plutonium ratio which has been determined for the facility.

TYPE	EXAMPLE	STIMULATION	MEASURED QUANTITY	REMARKS
RPL	SILVER METAPHOSPHATE GLASS	UV	TOTAL LIGHT EMISSION	SHIELD TO SUPPRESS LOW-ENERGY RESPONSE OF SILVER
OPTICAL DENSITY DEVICE	CINEMOID	LIGHT	LIGHT TRANS-MISSION	DO NOT ANNEAL SATURATION MAY OCCUR
TLD	LiF	HEAT	TOTAL LIGHT EMISSION	REGULAR READER CALIBRATION
THIN CALORIMETER	COPPER CONSTANTAN THERMOCOUPLE ON THIN COPPER FOIL		TEMPERATURE RISE	

PASSIVE DOSIMETERS

A number of passive dosimeters have evolved to measure total dose in various materials. Probably the most useful for effects work are the LiF TLD powders. The absorption characteristics closely match silicon above photon energies of 150 keV.

DOSIMETER TYPE	MODEL NO., ETC.	GAMMA-RAY SENSITIVITY $\left(\frac{\text{coul}}{\text{R(Co}^{60})}\right)$	NEUTRON SENSITIVITY $\left(\frac{\text{coul}}{\text{n/cm}^2\text{(E)}}\right)$
SILICON PIN	004-PIN-2501E	6×10^{-9}	5×10^{-17} (14 MeV) 2×10^{-18} (FISSION)
PHOTODIODE-SCINTILLATOR (FW 114)	PILOT B	2×10^{-8}	1×10^{-18} (FISSION)
	NE 211 (XYLENE)	1×10^{-9}	1.5×10^{-19} (FISSION)
	NE 226 (C_6F_6)	$\sim 1 \times 10^{-9}$	1×10^{-21} (FISSION)
SEMIRAD TI WALL	ECON 7318	1.2×10^{-11}	3.5×10^{-20} (14 MeV) 1.5×10^{-21} (FISSION)
STAINLESS STEEL	REUTER STOKES-GAMMA SENSITIVE	$1.7\text{-}6 \times 10^{-11}$	NEGLIGIBLE (FISSION) NOT NEGLIGIBLE (FUSION)
STAINLESS STEEL U^{238}	REUTER STOKES-NEUTRON SENSITIVE	3.5×10^{-11}	3×10^{-22} (FISSION) 1×10^{-21} (14 MeV)
COMPTON DIODE	(REPRESENTATIVE MODEL, EG&G)	1.4×10^{-11}	5.3×10^{-21}
CERENKOV DETECTOR	(REPRESENTATIVE MODEL, EG&G)	2.5×10^{-10}	8×10^{-19}

GAMMA-RAY AND NEUTRON SENSITIVITY OF ACTIVE DOSIMETERS

When pulse shape is important, or when rate information is desired there are a number of choices for active dosimeters. The most useful device for radiation effects work is undoubtedly the PIN diode. It is subject to displacement damage effects and its calibration should be checked frequently. It can readily be used in an integrating circuit to estimate total dose. The combination of TLD powders and PIN diodes provides excellent dosimetry for most tests.

When dosimeters are used in a reactor, part of the response is caused directly by the neutrons. The neutron senstivity coefficient can be used to correct the reading and get γ radiation measurements.

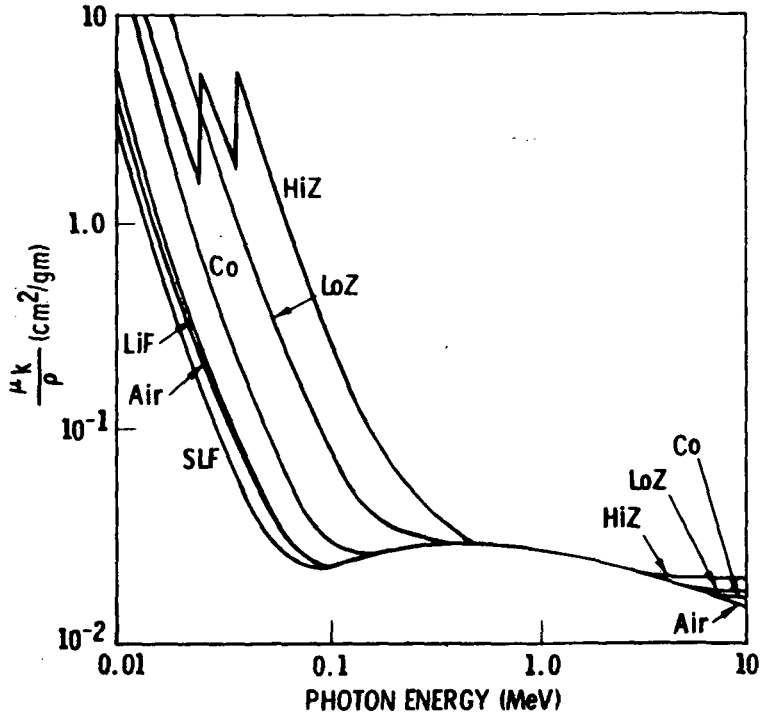

$$R = D \frac{\int R(E)\phi(E)dE}{\int D(E)\phi(E)dE}$$

R = DOSE IN RADS IN MATERIAL OF INTEREST

D = DOSE IN RADS IN DOSIMETER

LoZ } SILVER ACTIVATED
HiZ } METAPHOSPHATE GLASS

Co — COBALT GLASS

LiF — LITHIUM FLUORIDE TLD

SLF — PLASTIC FILM

SPECTRAL PROBLEMS

The attenuation factor (cm^2/gm) of most materials is nearly the same above 150 keV. However many machines below 2 MeV produce a significant photon spectrum below 150 keV and accurate dosimetry becomes quite difficult. 2-MeV machines may be shielded to eliminate the low-energy photons and reduce this problem.

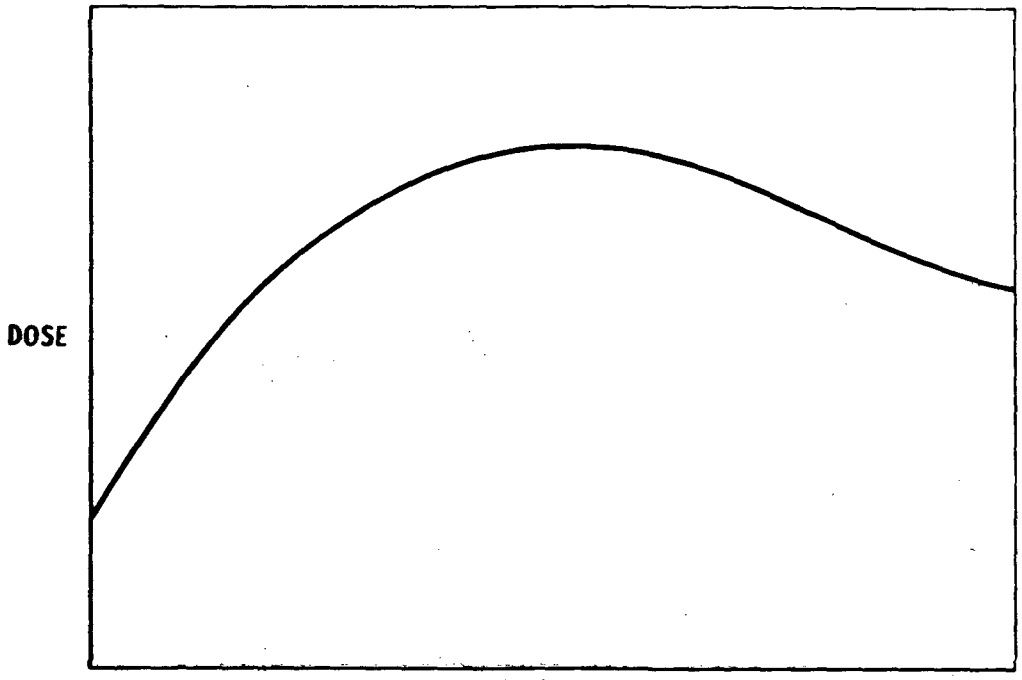

ELECTRON EQUILIBRIUM

Energy deposition from photons increases with depth in a material up to approximately the range of secondary electrons. At this point the photons and electrons are in equilibrium. Accurate dosimetry requires the interposition of a foil of appropriate atomic number and equal in thickness to the electronic range.

DISCRETE DEVICES	CIRCUITS
h_{FEF}	GAIN
h_{FEI}	COMMON-MODE REJECTION
V_{BE}	R_{IN} AND R_{OUT}
V_{SAT}	BIAS CURRENT
DIODE FORWARD/REVERSE	FAN OUT
V_{OFFSET} (PAIRS)	INPUT AND OUTPUT VOLTAGES, CURRENTS, AND IMPEDANCES

TYPICAL PARAMETERS SENSITIVE TO DISPLACEMENT DAMAGE

The chart shows several typical device parameters which are sensitive to displacement damage (e.g., from neutron or proton fluences). Since field-effect devices exhibit very little displacement damage at fluences of interest to OPGT, the parameters shown are primarily related to bipolar devices. Often, it is necessary to measure many parameters for a variety of bias (e.g., current injection) and operating conditions. If a great number of devices must be tested, then automated equipment may be required.

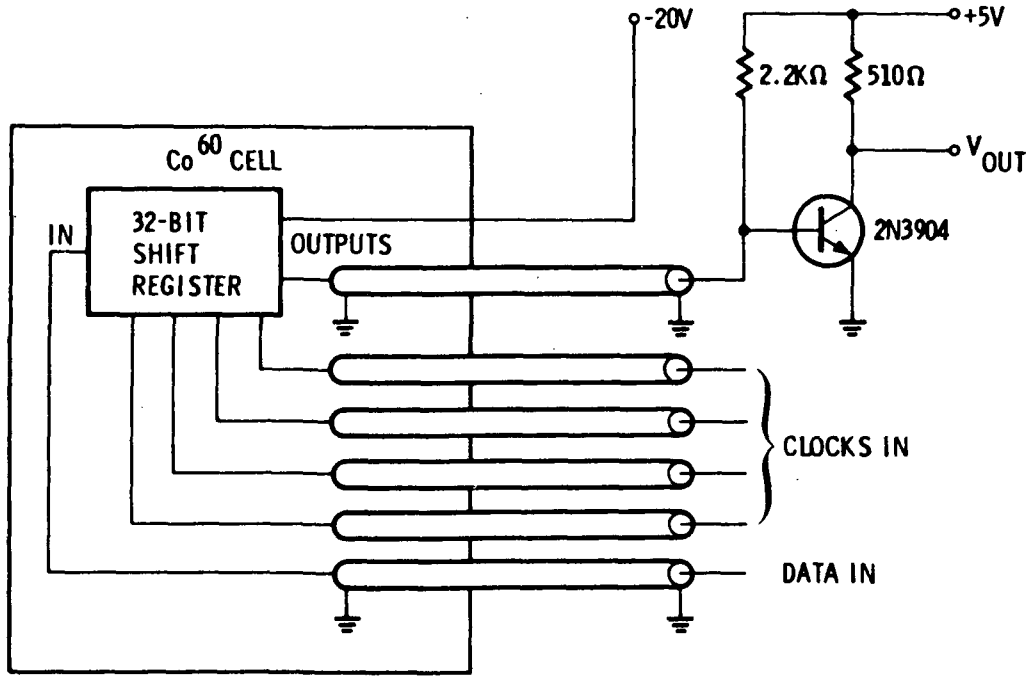

TYPICAL CIRCUIT FOR IONIZING DOSE TESTS

Since ionization damage may be dependent upon biases and operating conditions, it is often necessary to bias and exercise the test devices during irradiation. A typical test-configuration for an integrated circuit will provide for remote biases, inputs, and monitors. The remote equipment must be coupled to the test device through radiation-hard cables, which exhibit low capacitances and appropriate impedances. Terminations and buffers (e.g., emitter followers) may be necessary to insure proper loading and impedance matching over a range of frequencies.

BIPOLAR TRANSISTORS

- CURRENT GAIN
- LEAKAGE CURRENTS
- BREAKDOWN VOLTAGE
- NOISE

MOS TRANSISTORS

- THRESHOLD VOLTAGE
- TRANSCONDUCTANCE
- BREAKDOWN VOLTAGE
- NOISE

MNOS MEMORY DEVICES

- THRESHOLD VOLTAGE
- CHANNEL CONDUCTANCE
- MEMORY RETENTION
- WRITE CHARACTERISTICS

BIPOLAR INTEGRATED CIRCUITS

- DRIVE CAPABILITY/OUTPUT IMPEDANCE
- SPEED/FREQUENCY RESPONSE
- INPUT LEAKAGE/RESISTANCE
- GAIN
- POWER DISSIPATION

MOS INTEGRATED CIRCUITS

- DRIVE CAPABILITY/OUTPUT IMPEDANCE
- SPEED/FREQUENCY RESPONSE
- INPUT LEAKAGE/RESISTANCE
- GAIN
- POWER DISSIPATION

TYPICAL PARAMETERS SENSITIVE TO IONIZATION DAMAGE

Shown above are several bipolar and field-effect device characteristics which may be sensitive to ionization effects. In general, characteristic changes are due to surface effects -- degradation, charge-accumulation, etc. Hence, the changes and the degree of degradation are often dependent upon biases and operating conditions during and after exposure.

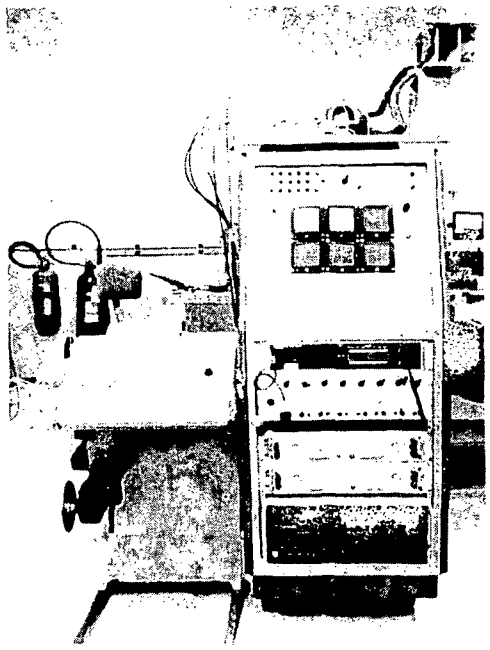

AUTOMATED DAMAGE-MEASUREMENT SYSTEM (TYPE OUT)

Automated test equipment greatly reduces the time and cost for large numbers of measurements. The illustrated instrumentation commutes up to 75 fourteen-pin device holders via coaxial cables to a test-condition console. Each holder can accommodate an IC, or six transistors with all emitters common, or 13 two-terminal devices. The total capability is 475 two-terminal devices (one lead common).

Devices with more than 14 leads can be accommodated if no more than 14 signals are required for operation. Data can be typed out or punched out and the punched tapes are compatible with computer data reduction and tabulation.

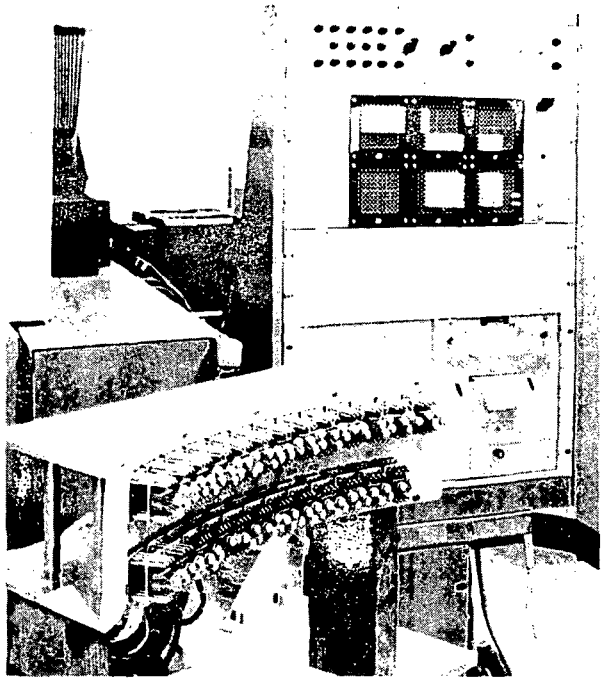

AUTOMATED DAMAGE-MEASUREMENT SYSTEM (PUNCH OUT)

Test conditions can be programmed by plug-in cards from the test console. A total of 25 different tests are possible. Separate tests can be assigned to individual devices so that mixed components can be tested. Ten to fifteen thousand on-line data points can be acquired in 8 hours at a typical TRIGA-type reactor. The resulting data can be computer-analyzed to identify failures, calculate means, standard deviations, etc., tabulate and correlate data, and plot curves and correlations.

RADIATION EQUIVALENT MODELS

FAILURE MODE ANALYSIS

CORRECTIVE ACTION

PERFORMANCE EVALUATION

Because it is not feasible to simulate the fluxes and energies of some OPGT radiations, especially at the system level, radiation equivalent models are needed to allow the application of test data to predict radiation damage modes in OPGT environments. During a mission, the nature of the damage may sometimes be inferred from the status of the damaged system or of the spacecraft. Such failure mode analysis may allow corrective action to be taken. Examples of such action are compensation for degraded performance, selection of alternate operating modes, and switching in redundant components.

- GROUND TEST SIMULATION
- OPGT ENVIRONMENT
- SYNERGISM

ENERGY LEVEL

The effect of various components of radiation (neutrons, electrons, and protons) is dependent on the amount (total flux and fluence) and the energy level. The effects of various components of radiation can be determined by ground tests. The test facility will produce the desired type of radiation but will do so with a characteristic energy band. The system must operate with different energy bands and with several inputs. The effect of simultaneous or cumulative damage effects often results in a synergism at the system level.

$$\bar{D}_i = \frac{\int_{E_i}^{E_{i+1}} \phi(E)\, D(E)\, dE}{\int_{E_i}^{E_{i+1}} \phi(E)\, dE}$$

CONVERSION FACTORS (EQUATIONS)

In order to translate facility damage effects to OPGT, the expected environment conversion factors must be used. A general expression for converting one band of damage for a given energy interval to another band of damage is illustrated. The functions $\phi(E)$ and $D(E)$ are generated by use of mathematical models of the material under bombardment (often silicon) and the result is a damage function vs. energy band.

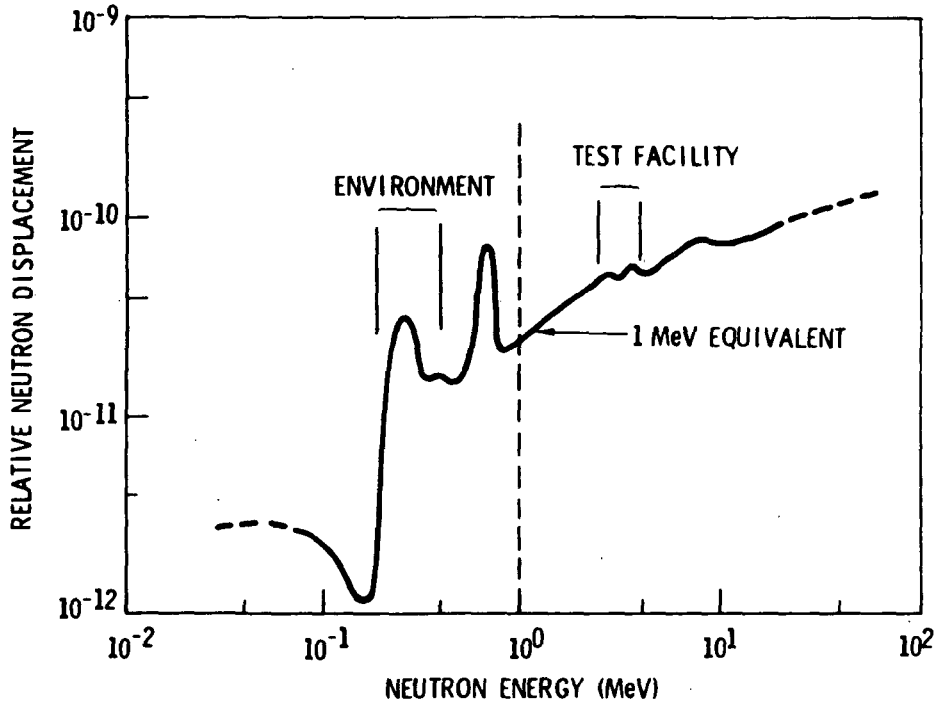

ENERGY CONVERSION FACTORS (GRAPHIC ILLUSTRATION)

The relationship between neutron energy (MeV) and equivalent neutron displacement damage is illustrated. The 1-MeV equivalent is arbitrarily selected as a reference energy, so 1 MeV corresponds to a factor of unity. The ground test facility may fall to the right (higher energy) while the actual OPGT environment energy may fall to the left. This difference is resolved by properly referencing both effects (facility and environment) to the 1-MeV energy band. A similar process can be used for protons and electrons.

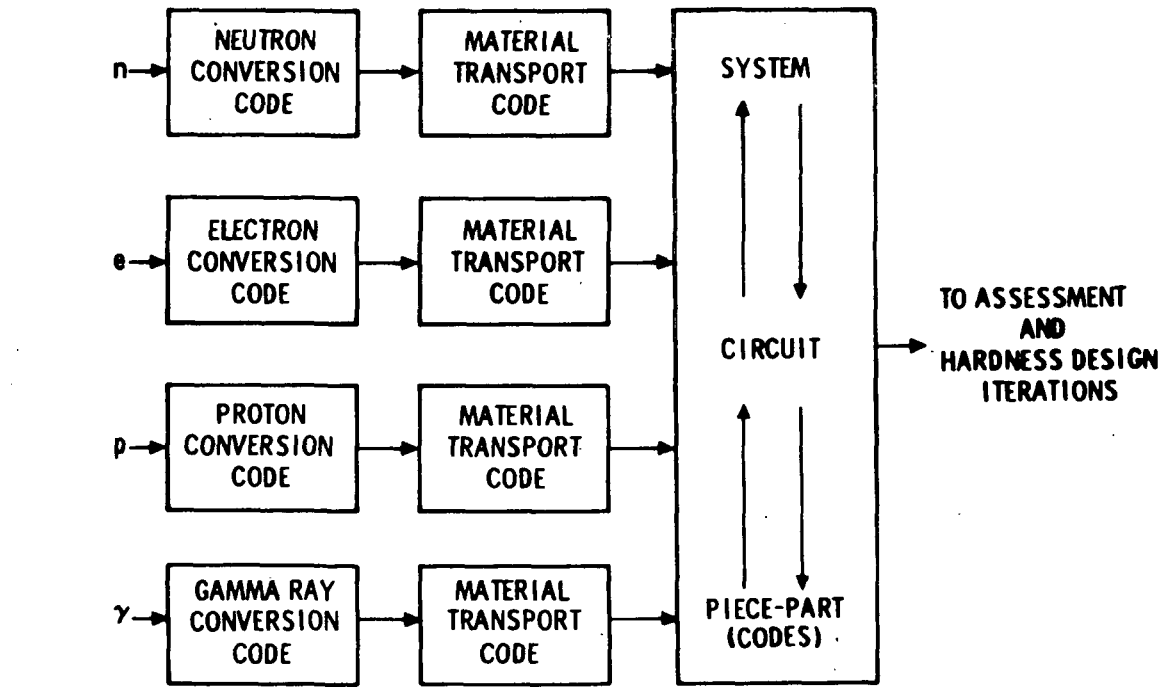

OPGT ENVIRONMENT ANALYSIS

The process of converting the OPGT environment to a form which can be used to assess the spacecraft nuclear survivability and iterate hardness designs is illustrated. The various components of radiation (neutrons, electrons, and protons) must be converted to the appropriate equivalent energy. This must be adjusted for the type of material being considered (usually silicon) and in turn, these effects must be accounted for at the piece-part, circuit, and system levels.

MIXTURE OF EFFECTS

- DAMAGE
- DEGRADATION

SYSTEM EFFECTS

- MULTI-MODE
- SELF-CHECKING/REPAIR

SYNERGISM

From the previous illustration, it should be apparent that a complex interaction between ratiation sources, materials, and hardware is possible. Some of these factors intermingle to accelerate or retard damage and/or degradation of hardware performance. The effects can be influenced by the system mode of operation including self-check and repair modes.

- SECURE
- CSMP
- VAM

APPLICABLE COMPUTER CODES

Numerous special purpose computer programs exist for energy conversion and material transport calculations. These codes often consume large amounts of computer time. As a result, simpler methods of calculations are available from charts and graphs based on extensive computer calculations. In the area of general purpose codes for system evaluation certain codes have been developed. These include SECURE (System Evaluation Code Under a Radiation Environment) and CSMP (Computer Simulation and Modeling Program). For vulnerability assessment, the VAM Program has been developed.

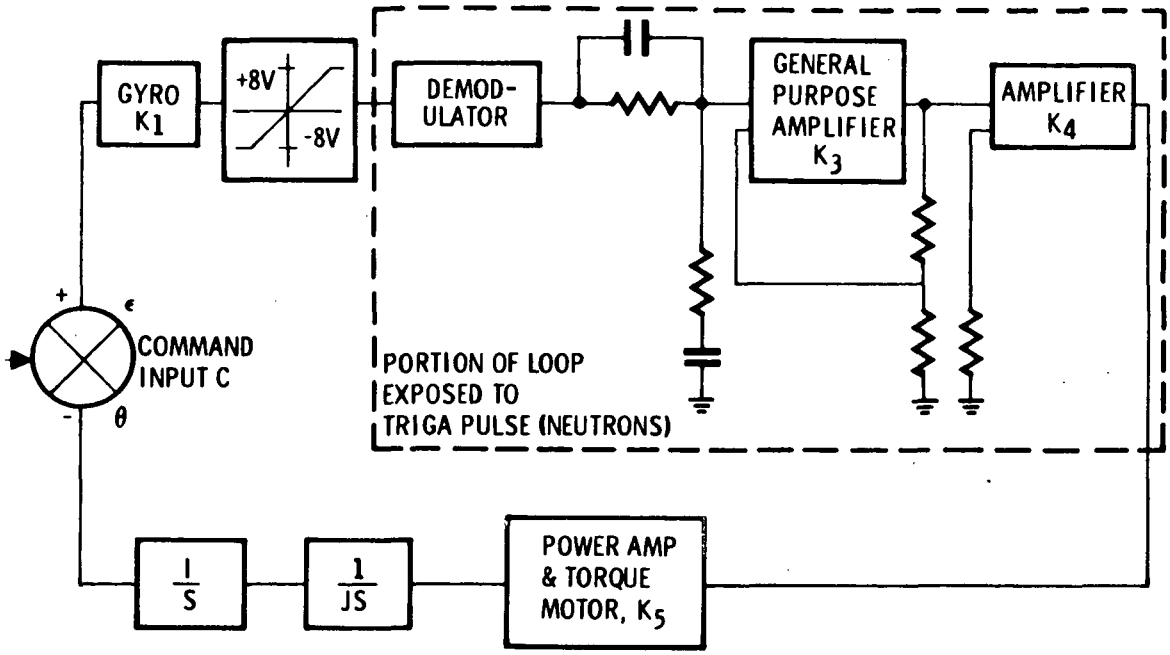

EXAMPLE (CLOSED LOOP SYSTEM)

An example of how the SECURE code is used at the system level is illustrated. The code simulates the electronic portion (control amplifier) within a closed-loop simulation of a stable platform. Effectively the response of the loop is determined as a function of neutron dose. The response is not illustrated but characteristically becomes more sluggish as the amplifier gain decreases.

- ELECTROMECHANICAL
- 3 & 6 DEGREES OF FREEDOM
- REDUNDANCY
- COMPLEX INTERRELATIONSHIPS

LARGE SYSTEMS

Large systems can be simulated by the codes previously discussed. The systems which have been simulated include (A) electromechanical control loops, (B) guidance systems involving 3-and 6-degree-of-freedom dynamics. The codes aid in understanding the effects of redundant systems (back-up) and quantify many complex interrelationships between radiation-induced part degradation and mechanical actuators.

FAILURE MODES ARE COMPLEX AND MANIFOLD

- CAN'T WRITE DOWN ALL POSSIBLE FAILURES
- FAILURES START AT SINGLE POINT AND PROPAGATE RAPIDLY
- FIRST NOTICED AS ANOMALOUS TEMPERATURES, CURRENTS, LOW VOLTAGE AND NOISY DATA
- ANOMALIES APPEAR ON SEVERAL OUTPUTS (TEMPERATURE, CURRENT, ETC.)

BOTTOM-UP ANALYSIS

- STUDY OF COMPONENT FAILURE AND EFFECTS
- SUCCESS DIAGRAMS COMPLEX AND LENGTHY
- PERFORMED FOR EXPECTED FAILURE (WEAK-LINK) PARTS ONLY

TOP-DOWN ANALYSIS

- STUDY OF FAILURES OF SUBSYSTEM AS AN INTEGRAL UNIT
- FAILURE DIAGRAMS - COMPLEX BUT SIMPLER THAN BOTTOM-UP
- PERFORMED TO POINT OUT WHAT FAILURES ARE MOST CRITICAL & HOW PREVENTED

BOTTOM-UP VERSUS TOP-DOWN FMECA

Subsystem failure modes are complex and extensive. Anomalies may begin with a single part, but can quickly spread to a number of associated parts. One should develop primarily the principal modes of failure, and specify the engineering measurements of temperature, current, voltage, etc. required to identify the causes of potential anomalies (which in general will show up on several outputs at a time).

A bottom-up Failure Mode Effect and Criticality Analysis (FMECA) starts at the part level and follows the normal operation paths for conveying information from sensor to telemetry. Bottom-up diagrams (or reliability block diagrams) are complex, but should include mainly the major failure paths, whereas the top-down study follows critical failure logic paths from the spacecraft systems level back down to the part failure level. The top-down failure diagram is still complex, but shows the interrelationships of groups of parts and subsystems and helps identify what parts should be duplicated.

MECHANISMS

- MINORITY CARRIER LIFETIME DECREASE
- REDUCED PHOTON SENSITIVITY
- RESISTIVITY - ELECTRICAL PROPERTIES CHANGED
- INCREASED DARK CURRENT
- SURFACE BLEMISHES

EFFECTS

- ON INDIVIDUAL PIXELS

  BRIGHT AND DARK BLEMISHES
  PATTERN REPEATABILITY UNCERTAIN

- OVER WHOLE FRAME

  LOSS OF CALIBRATION
  LEAKAGE OF PHOTOELECTRONS
  INCREASED DARK CURRENT
  REDUCED SENSITIVITY

- CATASTROPHIC FAILURE

  SIGNAL/NOISE RATIO UNACCEPTABLE
  DYNAMIC RANGE LOST
  VARIABLE BLEMISHES
  BIAS VOLTAGE SHORTED BY LOW RESISTIVITY

DISPLACEMENT DAMAGE OF SILICON VIDICONS

Energetic protons in Jupiter's magnetosphere may cause displacement damage in a silicon vidicon in an OPGT television camera. The damage can result in decreased minority carrier lifetime, reduced sensitivity to light, altered electrical properties, increased dark current (with reduced signal-to-noise ratio), and surface blemishes. The damage may affect individual picture elements (pixels) or the entire TV picture. Light or dark blemishes in single pixels may be permanent and hence repeatable, or transient and hence varying from frame to frame. Widespread damage leads to loss of photometric calibration and sensitivity changes that vary irregularly across the tube face. If the signal-to-noise ratio, sensitivity, resistivity, or blemish density reach unacceptable values, the vidicon fails catastrophically.

PHOTOMETRIC RECALIBRATION

- STAR FIELD COMPARISONS
- SATURN OR URANUS APPROACH PHOTOGRAPHIC COMPARISONS
- TEST IMAGE
- TEST OPTICAL PATTERN

BLEMISH CORRECTION

- RECALIBRATION OF EACH PIXEL IN MATRIX
- DATA ANALYSIS (AUTO-CORRELATION)
- ENHANCEMENT

REDUNDANT SENSORS

- OTHER TV CAMERA
- NON-TV IMAGING SENSORS
- GATLING-GUN VIDICONS
- BEAM SPLITTER/MIRRORS WITH OTHER IMAGE DETECTORS

POTENTIAL VIDICON CORRECTIVE ACTIONS

Degradation of wide areas of a vidicon may be compensated by photometric recalibration. This may be done by comparison of star field or Saturn or Uranus distance approach pictures with earth-based photometric data. Other approaches are to view a test optical pattern on the spacecraft or to transmit a stored test pattern.

Blemish compensation may be accomplished by recalibration of individual pixels, auto-correlative data analysis, or picture enhancement as was done with the Mariner Mars 1964 pictures.

If the vidicon fails catastrophically, we may use other vidicons in the same camera (turret or beam-splitting arrangement), the other TV camera, or obtain limited imagery from radiometers and photopolarimeters.

RADIATION ENVIRONMENT LIFE TESTS

- GAMMA & NEUTRON EXPOSURES COMBINED
- ELECTRON & PROTON EXPOSURES SEPARATELY
- NOISE DURING EXPOSURE
- PERMANENT DAMAGE & MECHANISMS
- RECOVERY
- THERMAL ANNEALING POSSIBILITIES
- COMPARISON WITH OTHER TV FAILURE MODES & EFFECTS

CALIBRATION STABILITY

- TIME OVER WHICH CALIBRATION CHANGES SIGNIFICANTLY DURING GAMMA & NEUTRON EXPOSURE
- CALIBRATION OF EXPECTED RESPONSES TO RADIATION
  - LONG TERM
  - SHORT TERM
  - NOISE AT JUPITER

SILICON VIDICON TEST DATA REQUIREMENTS

In order to identify vidicon vulnerability and failure modes and to quantify corrective actions, radiation environment life tests are needed. These tests may involve combined gamma ray and neutron irradiation and separate electron and proton exposures, with measurements of noise, permanent damage effects on the picture quality, recovery, and thermal annealing. Other TV camera failure modes should be identified. Another area of test requirements is the rate of calibration drift during exposure to simulated RTG radiation. We also need to calibrate the permanent and transient response of vidicons to the expected OPGT environments.

MECHANISMS	EFFECTS
OPTICS & GLASS TUBE FACE DARKENING, LOSS OF FILTER OR REFLECTIVE COATINGS	LOWER S/N, LOSS OF SENSITIVITY
LOSS OF PROTECTIVE COATINGS	TEMPERATURE INSTABILITIES
SIGNAL PROCESSOR FAILURE	THRESHOLD & GATING FAILURE
LOGIC FAILURE	AUTOMATIC MODE CONTROL FAILURE, LOCK ON WRONG STAR
DARK CURRENT INCREASE	LOWER S/N
TUBE ELECTRONICS FAILURE	LOSS OF LINEARITY
PHOTOEMISSIVE SURFACE DAMAGE	LOSS OF RESOLUTIONS & ELECTRON EMISSION, LOWER S/N

IMAGE DISSECTOR START TRACKER DAMAGE

Radiation can damage either temporarily or permanently any semiconductor electronics. Additionally it can darken the glass of the lens or the face plate of the tube. Optics darkening can result in lower signal-to-noise (S/N) ratio and loss of sensitivity. Darkening also can change the response of filter coatings or the transmission or reflectivity of optics coatings. Damage to protective coatings can change the effects of thermal radiation on the tube or components. Photocathode and electronics failures affect the tube gating, thresholding, and automatic logic. The potential effects is to lock on the wrong star or star pattern. Radiation also increases the dark current, lowering S/N and affecting the linearity of the tube output.

NON-CATASTROPHIC FAILURE

- LOGIC FAILURE

  COMMAND MODE CONTROL

- GATING & PHOTOCATHODE DAMAGE

  CALIBRATION

  CHANGE IN POINTING ANGLE OR ALIGNMENT WITH APERTURE

CATASTROPHIC FAILURE

- REDUNDANT SENSORS

  ADDITIONAL IMAGE DISSECTOR

- USE OTHER SENSOR

  APPROACH GUIDANCE SENSOR OR SCIENCE SENSOR

POTENTIAL CORRECTIVE ACTIONS (STAR TRACKER)

Corrective actions which can be taken include redundancy in instruments and circuits in the event of catastrophic failure. Additionally, other sensors such as the approach guidance or science image tubes could be used for tracking if the scan platform is pointed. Loss of logic in the automatic mode could be corrected by command.

RADIATION ENVIRONMENT LIFE TESTS

EXPOSURES OF:

- OPTICS
- TUBE
- ELECTRONICS
- DEFLECTION ELECTRONICS

DETERMINE EFFECTS ON:

- LIFE
- SENSITIVITY
- S/N RATIO
- DISTORTION
- LINEARITY

STAR TRACKER TEST DATA REQUIREMENTS

Radiation testing should be conducted to determine the effects of exposure on the star tracker components in terms of life, sensitivity, S/N ratio, distribution, and output linearity. The extent of shielding, optics type and coatings, and effects on logic remain to be determined.

"Page missing from available version"

305 - 308

ACRONYMS

ac	Alternating current
AMU	Atomic mass unit (1.6×10^{-24} gram)
CMOS	Complementary metal oxide semiconductor
dc	Direct current
DI	Dielectrically isolated
DTL	Diode transistor logic
ECL	Emitter-coupled logic
EPR	Electron paramagnetic resonance
eV	Electron volt (1.6×10^{-12} erg)
FET	Field effect transistor
FMECA	Failure mode, effect, and criticality analysis
IC	Integrated circuit
IG	Insulated gate
JFET	Junction field effect transistor
JPL	Jet Propulsion Laboratory
keV	Kilo-electron volt (10^3 eV)
LSI	Large-scale integrated (circuit)
MeV	Mega-electron volt (10^6 eV)
MOS	Metal oxide semiconductor
MSI	Medium-scale integrated (circuit)
N	Negative

N	Negative
NMOS	Negative metal oxide semiconductor
NPN	Negative-positive-negative
OPGT	Outer Planets Grand Tour
P	Positive
PMOS	Positive metal oxide semiconductor
PN	Positive-negative
PNP	Positive-negative-positive
RBE	Relative biological effectiveness
REM	Roentgen-equivalent-man
REP	Roentgen-equivalent-physical
rf	Radio frequency
RPL	Radiophotoluminescence
RTG	Radioisotope thermoelectric generator
SCR	Silicon controlled rectifier
S/N	Signal-to-noise (ratio)
TLD	Thermoluminescent dosimetry
TOPS	Thermoelectric Outer Planet Spacecraft
TREE	Transient Radiation Effects on Electronics
TTL	Transistor-transistor logic